2021

Mechanisms of movement in meroplankton: A primer for dispersal

James, Molly Kendall

http://dx.doi.org/10.24382/753
University of Plymouth

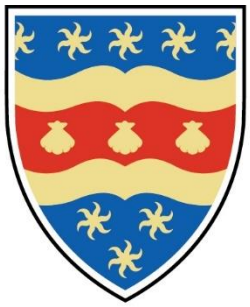

UNIVERSITY OF PLYMOUTH

Mechanisms of movement in meroplankton: A primer for dispersal

by

Molly Kendall James

A thesis submitted to the University of Plymouth in partial fulfilment for the degree of

DOCTOR OF PHILOSOPHY

School of Biological and Marine Sciences

February 2021

This thesis is dedicated to Pampa

ACKNOWLEDGEMENTS

Before I started this journey, I had heard that doing a PhD can be a solitary experience. I'm so glad I can say that this wasn't the case for me, and I'm so grateful to have this section of my thesis to be able to give thanks to all the wonderful people in my life who have supported me down this path.

First and foremost, I would like to thank my director of studies for this project, Tony Knights. Tony, I would like to thank you for your confidence in me (or at least not showing it if that confidence ever waivered), and for pushing me to come up with my own ideas, reach conclusions independently and take ownership of my work. Since starting the project, I have gained an unexpected (rather geeky) new love for the command line and all things code, and I have you to thank for that! You have become a good friend to me over the last few years and I am grateful that your office door has always been open to me whether it be to ask technical questions, or to watch twitter clips of outrageous dump tackles during the rugby world cup.

Second, I would like to give thanks to my supervisory team: Jeff Polton, Kerry Howell and Alex Nimmo-Smith for their collective support and guidance. Jeff, thank you for welcoming me into the masses up at NOC and being patient with me when my modelling terminology didn't match up with yours (on account of my terminology being made-up, and typically incorrect – the model/simulation confusion took a while to get my head around). Our skype sessions have been invaluable at keeping me on track. Additionally, I would like to thank GaBy Mayorga-Adame and Ash Brereton for their guidance, input and advice, for always being on the receiving end of an email when

needed, and for taking me out in Liverpool and making me feel welcome on my visit to NOC.

Thank you to the University of Plymouth and the School of Marine and Biological Sciences for providing the funding to make this project possible. MBERC is a fantastic facility to undertake a PhD, and I am grateful to have been able to work in such a supportive environment over the last few years. Thank you to the technical staff for their help and time in setting up and undertaking both lab and fieldwork and to the undergraduate volunteers who helped me with my boat work, I'm sorry you got seasick!

Thank you to placement students Jananee Prakesh and Alexandra Constrasas for their plankton taxonomy skills. Thank you to the skippers of the university fleet: Sean Marshall, Dave Uren, Chris Lowe and Jon Frary for getting me out on the water and collecting samples and to Jonathan Coe for providing technical knowledge and advice regarding ocean science tech. Although the weather was seldom in our favour we persevered, and chapter 3 would not have been possible without you. Thank you to the people of MBERC for keeping me full of caffeine and biscuits, for offering advice when needed and for always being counted on to lower the tone of the coffee-time chats. In particular I would like to thank Imogen Napper and Poppy Best who have instilled in me a love of bouldering, Stan Butt for treating every day like Christmas, Chris Dwane, for bringing some level of sanity to bay 618, and Amelia Bridges for always being there for me at 5pm on a Friday.

I wouldn't be where I am today without the unwavering support of my family and friends. I am so lucky to have you all in my life. Special thankyous to Thorndogg and the muskies for always making me smile, and to Sarah Crosby for being the best big

sister I never had. Thank you to all the girls at Newton Abbot Ladies RFC, in particular Gunnings, for your support and friendship.

Thank you to my large and loud family have had who always will have my back. To my aunties and uncles, my cousins – especially Josie who has been by my side for the most part of my Devonian adventures, my Dad, my Grandad and my brothers… I love you all.

Finally, I would like to give thanks to two of the most important people in my life: my Mum, and my Pampa. You two are by far the best fan club anyone could wish for! Thank you both eternally for your never-ending faith in me – it has undoubtedly made me the person I am today.

AUTHOR'S DECLARATION

At no time during the registration for the degree of Doctor of Philosophy has the author been registered for any other University award without prior agreement of the Doctoral College Quality Sub-Committee. Work submitted for this research degree at the University of Plymouth has not formed part of any other degree either at the University of Plymouth or at another establishment. This study was financed with the aid of a studentship from the University of Plymouth and carried out in collaboration with the National Oceanography Centre, Liverpool.

Publications:

James, M.K., Polton, J.A., Brereton, A.R., Howell, K.L., Nimmo-Smith, W.A.M., Knights, A.M., 2019. Reverse engineering field-derived vertical distribution profiles to infer larval swimming behaviors. Proceedings of the National Academy of Sciences of the USA. 116(24) 11818-11823. https://doi.org/10.1073/pnas.1900238116

Visits to external institutions:

- National Oceanography Centre, Liverpool, UK
- Monash University, Melbourne, Australia
- Melbourne University, Melbourne, Australia

Presentations at conferences/invited seminars:

- **International Marine Connectivity (iMARCO) Conference** (Oral presentation) – University of Aveiro, Aveiro, Portugal. September 2019
- **Invited seminar** (Oral presentation) – Melbourne University, Melbourne, Australia. August 2019 (*invited by Prof. Steve Swearer*).
- **Invited seminar** (Oral presentation) – Monash University, Melbourne, Australia. August 2019 (*invited by Prof. Dustin Marshall*).
- **Invited seminar** (Oral presentation) – National Oceanography Centre, Liverpool, UK. February 2019. (*Invited by Dr Jeff Polton*).
- **Plymouth Marine Science and Education Foundation (PlyMSEF) Conference** (Oral Presentation) – Plymouth Marine Laboratory, Plymouth, UK. February 2019.
- **Marine Biological Association of the UK Postgraduate Conference** (Poster Presentation) – Plymouth Marine Station, Plymouth, UK. May 2018

Word count of main body of thesis: 30926

Signed 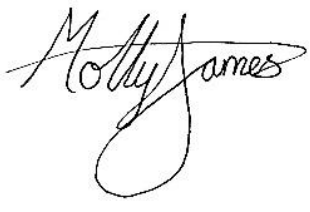

Date: 22nd February 2021

ABSTRACT

MECHANISMS OF MOVEMENT IN MEROPLANKTON: A PRIMER FOR DISPERSAL

MOLLY KENDALL JAMES

Biophysical models have become the 'go-to' tool for predicting the dispersive trajectories of planktic marine organisms, and are used to design Marine Protected Areas (MPAs), identify pathways of invasion, and understand metapopulation dynamics and biogeography. Yet, despite this relatively long history of development, continued technological advancement and increased usage, models continue to often fail to predict patterns in nature.

As biophysical models are able to accurately predict the dispersal of abiotic particles, it is argued that it is how we incorporate larval behaviour (*sensu* vertical swimming) in models that may be decoupling predictions of dispersal and species distribution patterns. Yet, despite the recognised importance of vertical distribution/position to dispersal by advection, especially in smaller organisms, there is currently no general consensus of how, what, and when behaviours can and should be included in models, perhaps because the drivers of larval behaviour are inherently complex and as yet, not fully understood (Chapter 1). The typical approach is to parameterise behaviours as 'rules' based on laboratory observed responses to cues, but it this approach appropriate given the complexity of larval decision-making in the presence of multiple cues in

nature in comparison to single cue responses in controlled environments? In Chapter 2 I explored the movements larvae must undertake to achieve the vertical distribution patterns observed in nature. Results suggest that behaviours are not consistent with those described under the Tidal Vertical Migration (TVM) hypothesis, instead, showing a need for swimming speed and direction to vary over the tidal cycle -- with upward swimming needing to be 2.5x faster than downwards swimming and a change in direction from upwards to downwards needing to occur around the midpoint of the flood tide - and low model compatibility during the ebb tide. Next, I looked to identify the environmental drivers of larval vertical distribution during the ebb tide, where the model compatibility of Chapter 2 was low. Explored external drivers (density, salinity, temperature, turbulence) explained very little of the vertical distribution patterns of the larvae, however, results suggest differential usage of environmental cues based on ontogenetic stage, and vertical distribution patterns observed differed from previous observations of a similar species at a different location. Finally, I presented a framework for assessing how behavioural parameterisation can influence dispersal trajectories in marine systems (Chapter 4), comparing a novel approach of reverse engineering larval swimming from in-situ observations (Chapter 2: REVM behaviours) against simulations adopting passive dispersal, and particles attributed a tidal vertical migration (TVM) signature. Results highlight how the implementation of behaviour within biophysical models can lead to fundamentally different dispersal outcomes, and specifically, that the inclusion of vertical migration behaviour is a mechanism that significantly reduces dispersal distances, but depending on the approach to implementation can lead to fundamental differences in dispersal direction.

This thesis makes significant steps towards improving the parameterisation of behaviour within dispersal models by considering larval movement as a manifestation of behaviour influenced by the larva's *in-situ* environment. The methodologies and analytical techniques designed and applied within the data chapters can be applied to any species with a planktonic dispersal phase in any location, and provide an important step towards improving the biological 'realism' of behavioural parameterisation in dispersal models in the absence of an understanding of the complex drivers of active larval movement.

TABLE OF CONTENTS

List of Tables

LIST OF FIGURES

1 INTRODUCTION

The majority of marine species (approximately 80%) spend at least some part of their life history as a member of the plankton (Milekovsky,1971). For many, their life history is bi-phasic, whereby relatively sessile adults release larvae into the pelagic environment. This is the predominant developmental strategy for most marine phyla, with only 4 of the estimated 30 phyla present in the ocean not exhibiting a larval development stage (Strathmann, 1985; Pechenik, 1999). The planktic larval stage is therefore the only ‘free-living’ period in an organism's life history, but a crucially important stage as it is the mechanism through which an organism can disperse and is therefore a key determinant in the ecology and evolution of species (Levin, 2006; Cowen and Sponaugle, 2009; Lowe & McPeek 2014).

Larval dispersal has been the focus of marine studies for over 120 years. Cleve (1900) was perhaps one of the first to consider pelagic life-histories and the role of water currents in the dispersal of marine animals, although his early observations were unable to distinguish between geographic and biological groups (Gran, 1902). In 1928, Astrid Cleve-Euler - Cleve's daughter who was a botanist, geologist, chemist, and the first woman in Sweden to obtain a Doctorate in science - continued her father's early work and went on to state:

> *"regular biological analysis of the oceans and of the coastal waters would no doubt give a more thorough knowledge of the sea currents, their movements and their intermingling, than could be expected from hydrographic observations only".*

In the years surrounding that statement, dispersal research had become driven by applied interests, and especially effort to understand the distribution of fish larvae and

their importance for commercial fish stocks (e.g. Hjort, 1926; Walford 1938; Johnson 1939). Today, scientific interest in the mechanisms of larval dispersal remains unabated (see Swearer et al. 2019 for review). The link between physics and biology is clearly recognised and technological advances in molecular tools, electronic tagging, hydrodynamic modelling and computing have undoubtedly improved our understanding of dispersal., yet many questions and uncertainties still remain.

1.1 The need to understand the dispersal process

Despite the ever-burgeoning literature, understanding larval dispersal and the ecological linkages of populations remains a key challenge in marine ecology (Treml and Haplin, 2015). In part, this is due to the dynamic nature of the marine environment, leading to constant change in the geographic distribution of marine species worldwide in response to stressors including rising sea temperatures and ocean acidification (Parmesan and Yohe, 2003; Burrows et al., 2011). Profound changes in the biogeography of species have occurred in recent years, particularly as previously unsuitable environments have become suitable with respect to an organism's physiological tolerances (Kimball et al., 2004; Hare et al., 2012). For some species, this has manifested as a poleward shift in distribution (Neumann et al., 2013; Hiddink et al., 2015) but in others, no shifts are reported (Doak & Morris 2010, Firth et al. in review), or are counter to predictions of net poleward movement (e.g., Lenoir et al. 2010). Larval dispersal may underlie some of these idiosyncratic responses. For instance, warmer oceans can elicit physiological stress and mortality (Laubier, 2001), increase larval development rates (see O'Connor et al. 2007 for a review of 72 species across 6 phyla including fish and invertebrates), or reduce plankton duration and exposure to ocean currents, thereby altering population and community dynamics as connectivity patterns change (Lockwood et al., 2005). Given that dispersal is a key mechanism that shapes the distribution of marine species

(Piñeda et al., 2007; Lowe & McPeek, 2014), understanding how and where species disperse is imperative to understanding the structure and functioning of marine ecosystems today and in the future.

1.2 Quantifying larval dispersal

Larval dispersal is often defined as the movement of larvae between their spawning source and their settlement site (Cowen and Sponaugle, 2009; Piñeda et al., 2007), although it can be argued that this should technically be referred to as propagule dispersal., as the dispersal process can also encompass pre-fertilisation dispersal of gametes. For the purpose of continuity and in this thesis, I shall consider movement from the spawning source to settlement site, including the movement of free-living gametes, as ‘larval dispersal’.

Larval dispersal can be described as a probability distribution function away from a starting location (Neubert and Caswell, 2000), or statistically, a probability density function or 'kernel' (PDF) describing the frequency of individuals at a distance from their source (Werner et al., 2007). For many organisms, this kernel can be described as being 'long-tailed'; a large number of organisms remain ‘close to home’, while a smaller proportion undergo 'long-distance' dispersal with large variation observed in the distance travelled by those who travel further afield (Mayr, 1963; Endler, 1977). From an evolutionary and ecological perspective, high concentrations close to home are unsurprising and likely attributable to the high energetic cost and risks associated with dispersal (Lowe and McPeek, 2004, Nathan et al., 2012).

Quantifying dispersal of large marine mammals, fish and seabirds can be relatively straight-forward using technologies including GPS and satellite imagery (e.g. Carter et al., 2017; Doherty et al., 2019; Cox et al., 2016). In contrast, tracking the movement of

typically microscopic larvae is considerably more challenging due to their small size. Nevertheless, a number of direct and indirect methodologies have been developed to quantify and/or predict larval dispersal.

1.2.1 Direct approaches

Direct approaches used to examine larval transport *in-situ* include the use of trace-elemental fingerprinting to determine source locations (Becker et al., 2007; DiBacco and Levin, 2000), the use of artificial markers (tracers) such as dyes (Dabrowski and Tsukamoto, 1986), or natural (physiological) markers such as thermal stress marks to 'tag' larvae (Volk et al., 1999). These methods, however, have some drawbacks. Larval tracking by trace-elemental fingerprinting requires knowledge of the sources that lead to certain fingerprints to be able to trace the origin of the larvae (DiBacco and Levin, 2000). In artificial marking studies, larval mortality and the typical dilution of larvae in the ocean limits the number of tagged individuals that are recaptured in mark-recapture efforts (Cowen et al., 2000).

1.2.2 Indirect approaches

Genetic tools can be used to infer connectivity between marine populations (see reviews by Hedgecock et al., 2007 & Hellberg, 2007), providing indirect insights into the movement of propagules between populations (Hellberg et al., 2002). These approaches have been used for a range of taxa including crustaceans (Britto et al., 2018; Silva et al., 2019), fish (Pinsky et al., 2017; Hirase et al., 2020), and bivalves (Silliman, 2019; Van Wyngarden et al., 2017). For instance, an Isolation By Distance (IBD) model (Wright, 1943) that determines gene frequency distribution over a geographic region (Rohlf & Schnell, 1971) and associated divergence between populations can be correlated with distance to infer dispersal (Palumbi, 2003). Genotyping is typically undertaken using either microsatellite markers, or single nucleotide polymorphisms (SNPs).

Microsatellite analysis is achieved by identifying short repeats in regions of non-coding DNA (Vieira et al., 2016), whereas SNPs are regions of the genome where two strains differ by one nucleotide, or base pair (Morin et al., 2009). Genetic measures also allow indirect estimation of long-term trends in larval dispersal (Buonaccorsi et al., 2004) and provide a means to empirically quantify marine connectivity (Christie et al., 2017).

These approaches, however, share one significant limitation. While they can provide insights into population connectivity, they cannot forecast dispersal., which for instance, can limit their value for answering questions related to changes in species distribution patterns under future climatic scenarios, or in the design of Marine Protected Areas. Given rates of global environmental change, biodiversity loss, and need for action to protect biodiversity and natural resources, being able to predict dispersal and understanding ecological connectivity is paramount to addressing these challenges. Connectivity is now frequently considered in the design of coherent Marine Protected Areas (Le Quesne and Codling, 2007; Botsford et al., 2009; Christie et al., 2010; Andrello et al., 2013; Krueck et al., 2017; Ross et al., 2017; Costello and Connor, 2019; Manel et al., 2019; Moksnes and Jonsson, 2020); efforts to monitor biological invasions (Occhipinti-Ambrogi, 2007; Elith, 2017) and fisheries (Morgan and Botsford, 2001; Krueck et al., 2017; Whomersley et al., 2018; Criales et al., 2019;); and, to understand the influence of climate change on patterns of species distribution (Occhipinti-Ambrogi, 2007; Wilson et al., 2016).

Biophysical modelling provides a solution to this limitation and is regularly used to predict the dispersal of abiotic (e.g. oil spills, see Spaulding 2017 for review), and biotic, propagules including marine, freshwater and terrestrial flora and fauna (e.g. Harding and Trites, 1988; Brickman and Frank, 2000; Allain et al., 2007; Banas et al., 2009; Nicolle et al., 2013; Ross et al., 2017; Ludsin et al., 2014; Kinlan and Gaines,

2003). Biophysical models combine 3 components: a hydrodynamic model that describes the physical properties of an environment, a Lagrangian model which calculates particles movement, and biological behaviour (an Individual Based Model, or IBM). Typically, hydrodynamic fields are provided by a General Ocean Circulation Model (OGCM) that describe velocity fields based on resolving Navier-Stokes equations (Aiken et al., 2011; Banas et al., 2009; Donahue et al., 2015; Wood et al., 2014, 2016 - see Swearer et al., 2019 for review), however, other velocity field sources, such as advection diffusion models, may also be used (e.g. Cowen et al., 2000; Gaylord and Gaines, 2000; Hill, 1990; Richards et al., 1996; Treml et al., 2008). By combining these components, researchers can trace the trajectories of individual particles under modelled hydrodynamic conditions (Siegal et al., 2003).

1.3 Ocean General Circulation Models (OGCMs)

The Oceanic General Circulation Models (OGCMs) that underpin biophysical models were originally developed by researchers at the NOAA Geophysical Fluid Dynamics Laboratory in New Jersey (Bryan, 1969) following the successful development of a mathematical model of atmospheric circulation in the 1950s (Phillips, 1956) to numerically describe the circulation of water within the world's oceans. OGCMs calculate velocities, turbulence, temperature, salinity and density by resolving 'primitive' equations, discretised over space and time, and it is the different techniques used to discretise these parameters that gives rise to different types of hydrodynamic models (Jones et al., 2002; North et al. 2009; Swearer et al. 2019). These differences are summarised for a number of open-source readily available ocean models in Table 1.1.

OGCMs are discretised in the horizontal plane by grids applied to the coordinate system of the study area using either a structured (e.g. NEMO, Madec, 2008); or unstructured grid (e.g. FVCOM, Chen et al., 2003). In some instances, for example, in study areas

where the flow regime is consistently well-mixed, it may be appropriate to run the model using only this 2D (horizontal only) grid (e.g. Ellein et al., 2000). However, studies have identified that marine larvae exhibit differential depth distributions of over their life-history (Aiken et al., 2011; Knights et al., 2006), and are therefore not 'passive'. These studies indicate that consideration of heterogeneous advective flow regimes across the water column and the relationship between an organism and its vertical position within that column is likely important to outcome of model predictions, especially those applied to simulate the dispersal of biological propagules. Should propagules be incorrectly 'placed' in their vertical position, horizontal advection distances could be erroneous.

To account for this vertical heterogeneity in advection, a more complex model is required that includes a z-axis component, i.e. one that converts a model from 2D (horizontal only) to 3D (e.g. Fig. 1.1). This z-axis is usually parameterised in one of three ways. (1) Using a fixed number of vertical layers (Fig. 1.1a), known as ‘z’-levels (i.e. the Advanced Circulation Model (ADCRIC): Leuttich et al. 1992; The Hamburg Ocean Primitive Equation General Circulation Model (HOPE): Wolff et al. 1997); (2) using local topography to define sigma-levels (Fig. 1.1b)(i.e. the Regional Ocean Modelling System (ROMS): Shchepetkin & McWilliams (2005) within a Finite Volume Community Ocean Model (FVCOM) framework (e.g. Chen et al. 2003; M.I.T. General Circulation Model (MitGCM); Marshall et al. (1997)); or (3) using density-dependent depth divisions (Fig. 1.1c) (e.g. isopycnal models; OPYC - Oberhuber, 1993).

Ideally, ocean models should be able to resolve water mass characteristics over large timeframes, effectively resolve mixing in the surface layers at an appropriate resolution and be able to maintain effectiveness in shallower waters near the coasts. As such, models with hybridised vertical discretisation schemes have been developed as to take

advantage of each of the different methods, for example NEMO (z-level/sigma-level hybrid: Madec, 2008) and HYCOM (z-level/sigma-level/isopycnal hybrid: Wallcraft et al., 2009) (see Table 1.1).

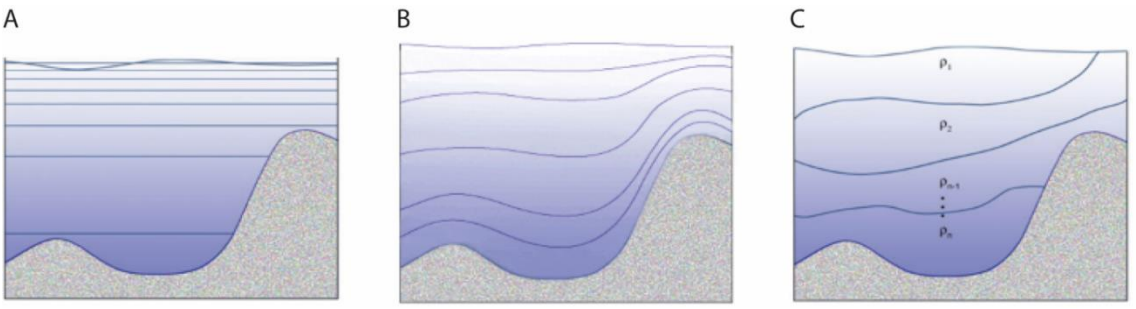

Figure 1.1: A visual representation of a) z-level, b) sigma-level (terrain following) and c) isopycnal vertical discretization methods. Redrawn from the Naval Postgraduate School: (https://www.oc.nps.edu/nom/modeling/vertical_grids.html

Table 1.1: An overview of the methods of discretisation used by Ocean General Circulation Models (OGCMs) and open-source particles trackers coupled with OGCMs.

Hydrodynamic Model	Horizontal Grid	Horizontal Discretisation Method	Vertical Grid	Scale	Citation	Coupled particle trackers	Example applications
Advanced Circulation Model (ADCRIC)	unstructured	space: finite element method; time: finite difference method	z-levels	regional	Leuttich et al. (1992)	Unnamed particle tracker (Hill, 2007)	Tang (2010)
CCSR (Centre for Climate Research) Ocean Component Model (COCO)	structured	finite-difference method	sigma-levels	unspecified	Hasumi (2015)	Unnamed particle tracker (Hsuing et al., 2018)	Hsiung et al (2018)
Coupled Hydrodynamical Ecological Model for Regional Shelf Seas (COHERENS)	structured	finite-difference method	sigma-levels	regional	Luyten et al. (2006)	SEDLAG (Luyten et al., 1999)	Savina et al. (2010)
Finite Volume Community Ocean Model (FVCOM)	unstructured	combination of finite element and finite difference methods	sigma-levels	regional	Chen et al. (2003)	FVCOM Lagrangian particle-tracking module (Chen et al., 2003)	Rowe et al. (2016)

Hydrodynamic Model	Horizontal Grid	Horizontal Discretisation Method	Vertical Grid	Scale	Citation	Coupled particle trackers	Example applications
AWI Finite-Element/Volume Sea Ice-Ocean Model (FESOM)	unstructured	finite-volume method	z-level; z-level/sigma-level hybrids	multi-scale	Wang et al. (2014)	FESOM-C drift (Wang et al., 2014)	Sprong et al. (2020)
The Hamburg Ocean Primitive Equation General Circulation Model (HOPE)	structured	finite-difference method	z-levels	basin-scale (Pacific)	Wolff et al. (1997)	Unnamed particle tracler (Kasai et al., 2008)	Kasai et al.(2008)
Hybrid Coordinate Ocean Model (HYCOM)	structured	finite-difference method	z-level/sigma-level/isopycnal hybrid	global and basin-scale	Wallcraft et al. (2009)	CMS (Paris et al., 2013) Pol3DD (Lebreton et al., 2012)	Ross et al. (2016) Zhang et al.(2020)
The Hamburg Large Scale Geostrophic Ocean General Circulation Model (LSG)	structured	finite-difference method	z-levels	global	Maier-Reimer et al. (1993)	Unnamed particle tracker (Drijfhout et al., 1996)	Drijfhout et al. (1996)

Hydrodynamic Model	Horizontal Grid	Horizontal Discretisation Method	Vertical Grid	Scale	Citation	Coupled particle trackers	Example applications
Miami Isopycnic Coordinate Ocean Model (MICOM)	structured	finite-difference method	isopycnal	global	Bleck et al. (1992)	Unnamed particle tracker (Cowen et al., 2003)	Cowen et al. (2003)
M.I.T. General Circultion Model (MitGCM)	structured	finite-volume method	sigma-levels	global to regional	Marshall et al. (1997)	PaTATO (Fredj et al., 2006) TrackMPD (Jalón-Rojas et al., 2019)	Berenshtein et al. (2018) No examples
Modelo Hidrodinâmico (MOHID)	structured	finite-volume method	z-levels	local to regional	Leitão et al. (2008)	Unnamed particle tracker (Pinto et al., 2016)	Pinto et al. (2016)
GFDL Modular Ocean Model (MOM)	structured	finite-volume method	z-levels or simga-levels	global	Pacanowski et al. (1991)	Unnamed particle tracker (Iida et al., 2010)	Iida et al. (2010)

Hydrodynamic Model	Horizontal Grid	Horizontal Discretisation Method	Vertical Grid	Scale	Citation	Coupled particle trackers	Example applications
Nucleus for European Modelling of the Ocean (NEMO)	Structured	Finite-difference method	z-level/sigma-level hybrid	global to regional	Madec (2008)	ARIANE (Blanke and Raynaud, 1997) Parcels (Delendmeter and van Sebille, 2019) LTRANS (Schlag and North, 2012)	Wagner et al. (2019) Le Gouvello et al. (2020) Mayorga-Adame et al. (2017a)
The Ocean Isopyncal General Circulation Model (OPYC)	structured	finite-difference method	isopycnal	global and basin-scale	Oberhuber (1993)	No examples	No examples
Princeton Ocean Model (POM)	structured	finite-difference method	sigma-levels	local to global	Blumberg & Mellor (1987)	PaTATO (Fredj et al., 2006) TrackMPD (Jalón-Rojas et al., 2019)	Hayes et al. (2019) No examples
The Parallel Ocean Program (POP)	structured	finite-difference method	sigma-levels	global	Smith et al. (2010)	No examples	No examples

Hydrodynamic Model	Horizontal Grid	Horizontal Discretisation Method	Vertical Grid	Scale	Citation	Coupled particle trackers	Example applications
The Regional Ocean Modelling System (ROMS)	structured	finite-difference method	sigma-levels	Regional	Shchepetkin & McWilliams (2005)	PaTATO (Fredj et al., 2006) TrackMPD (Jalón-Rojas et al., 2019) LTRANS (Schlag and North, 2012)	Carlson et al. (2017) No examples McManus et al. (2020)
Second-generation Louvain-la-Neuve Ice-Ocean Model (SLIM-Ocean Model)	unstructured	finite-element method	unspecified	regional	Comblen et al. (2010)	No examples	No examples

1.4 Choosing an appropriate model for larval dispersal research

Following rapid advancement in computing power and technological understanding, OGCMs are able to depict ocean circulation at spatial and temporal resolutions relevant to larval dispersal., for example, ocean currents, tides, freshwater inputs, fronts and turbulence. However, effective estimates of larval dispersal using biophysical models rely on selecting an appropriate underlying hydrodynamic model in terms of its spatial and temporal scale and resolution in order to effectively capture the physical processes that the organism is exposed to during its larval phase (North et al., 2009). Hence, the

choice of the velocity field source used in dispersal estimates is dependent on the model's ability to resolve parameters relevant to the question being asked by the study.

Readily available open-source OGCMs (e.g. ROMS, HYCOM, MITgcm, NEMO), however, are typically not 'built' with ecology in mind, where the importance of oceanographic variability and its features likely occur over very small spatio-temporal scales, rather than the more broad-scale conditions generated by most OGCMs. For instance, where velocity values are averaged over time, the output of the OGCM may not be applicable to the scale over which biological/ecological processes operate. For example, an OGCM that produces monthly average current speeds would not be sufficiently resolved enough to study larval dispersal in tidally influenced coastal regions. Recent research has highlighted that the choice of hydrodynamic model can produce marked differences in dispersal predictions (Ross et al., 2020), therefore ecologists must consider the parameters of the hydrodynamic model and the suitability of its outputs with regard to their study objectives.

For simplicity, the choice of the hydrodynamic model is often determined by the particle tracker component, which are frequently built to be coupled with certain OGCMs (see Table 1.1), however, this may result in 'unsuitable' hydrodynamic models being used. The open-source availability of many particle trackers has allowed researchers to address this, creating modified versions of Lagrangian models that can be coupled to whatever hydrodynamic model best represents their study area and best captures the temporal and spatial resolution and model complexity required for answering the study questions (e.g. Mayorga-Adame et al., 2017b).

1.5 Lagrangian particle tracking

To simulate larval behaviour within models, a Lagrangian particle tracking module is a key component. These modules can track virtual ‘particles’ in space and time; the trajectory of each particle is determined by two general inputs: (i) current velocities and diffusivity fields derived from an OGCM (van Sebille et al., 2018) and, (ii) biological parameters describing traits of the larva/simulated particle. Originally, this technique was used to track virtual water particles in order to study current pathways (Awaji et al., 1980; Imasato et al., 1980), and has since been applied to a number of different applications such as tracking plastics (Lebreton et al., 2012), oil spills (Paris et al., 2012; Haza et al., 2016), sand grains (Soulsby et al., 2007), volcanic rock (Jutzeler et al., 2014), icebergs (Marsh et al., 2015) and planktonic larvae (Siegal et al., 2003; Allain et el, 2007; North et al., 2008; Banas et al., 2009; Kim et al., 2010; Robins et al., 2012; 2013; Nicolle et al., 2013;; Phelps et al., 2015; Ross et al., 2017; Wood et al., 2014, 2016, Corell and Nissling, 2019).

There are numerous open-source Lagrangian particle trackers available (Table 1.1). Some (i.e. PartTracker, SandTrack, Ariane, TrackMPD) were designed to track abiotic particles, such that particle movement within these models is governed solely by hydrodynamic advective and diffusive processes. These models are well validated (Soulsby et al., 2007) and have shown that they and their associated OGCMs are an appropriate tool for predicting abiotic particle dispersal. However, for biotic particles such as marine invertebrate larvae, dispersal and distribution is also influenced by biological traits (Treml et al., 2015: Figure 1.2).

Larval behaviour (biological traits) has the potential to decouple model predictions from patterns in nature if incorrectly prescribed. Behaviours, however, are complex responses to a range of physiological and environmental cues (Rittschof et al., 1998; Kingsford et

al., 2002; Wahab et al., 2011; Tosches et al., 2014), and current understanding of how behaviours are stimulated (cues) and manifested in nature remains limited. Despite behavioural drivers either being poorly or simplistically described, a common response has been to increase the complexity of biophysical models in an effort to make them more 'realistic' (see a recent review by Treml et al. (2015) highlighting the complexity of modelling biological traits), to address the argument that the lack of model complexity to capture biological and behavioural traits undermines predictive efficacy. The Lagrangian TRANSport model (LTRANS; Schlag and North, 2012), for example, contains specific modules that allow the user to account for a number of biological parameters, such as settlement based on reaching appropriate habitat within a settlement competency window, the age at which a particle dies, scaled swimming speeds based on the particles age, and active swimming behaviours (i.e. Diel Vertical Migration, or behaviour in response to hydrographic features such as haloclines (e.g. North et al. 2008)). Connectivity Modelling System (CMS; Paris et al., 2013) includes modules that account for egg buoyancy, vertical migration behaviour, mortality, and through the different particle attributes module, can assign variation within the population based on a probability density function and minimum and maximum values. Yet, despite the increased complexity of the 'bio' component of biophysical models over the years, model predictions of larval dispersal are likely overestimated (Shanks et al., 2003; Shanks, 2009).

This disparity between patterns of genetic differentiation in nature and model predictions of dispersal (as suggested by Marshall et al, 2019) suggest we are currently failing to fully understand how to best incorporate dispersal-relevant biological traits within model frameworks. Similarly, can we be confident that when we do get match between model predictions and patterns in nature, is it because behavioural traits have been are correctly parameterised within the model?

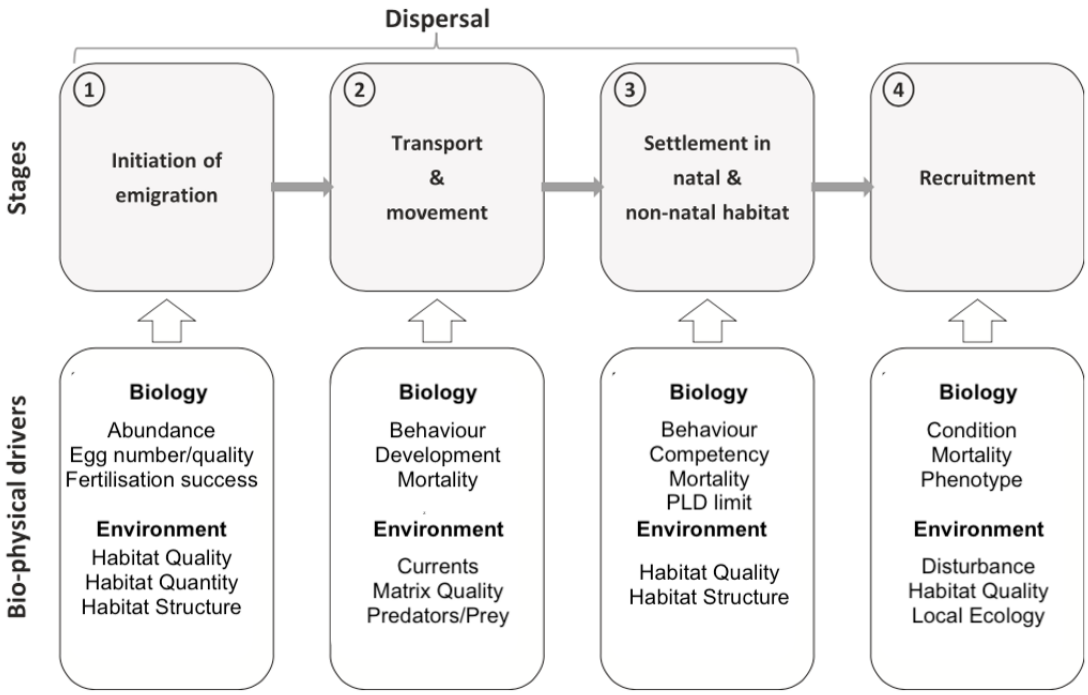

Figure 1.2: The stages of dispersal and population connectivity in benthic marine organisms and the biophysical drivers of at each stage. Redrawn after (Treml et al., 2015 and Swearer et al., 2019).

1.6 Larval behaviour: the great decoupler?

1.6.1 Hydrodynamics and larval behaviour

Due to their small size and relatively slow swimming speeds, larvae have often been considered as passive (*sensu* abiotic) objects with respect to advective ocean currents. This is perhaps reasonable given that velocities can be orders of magnitude greater than the swimming speed of planktonic organisms (Thorpe, 2005), and thus, the expectation that net transport in the horizontal plane is primarily mediated by advective flow (e.g. Mayorga-Adame et al., 2017b; Adams & Mullineaux, 2008). However, vertical current speeds associated with vertical mixing are often much slower than horizontal advection and are equal to or less than larval swimming speeds (Chia et al., 1984; Thorpe, 2005) allowing even small-bodied organisms such as larvae to manipulate their vertical

position in the water column (e.g. Raby et al., 1994; Shanks and Brink, 2005; Knights et al. 2006; Lloyd et al., 2012; Bonicelli et al., 2016; McIntyre et al., 2020).

This capacity to modify vertical position, even in microorganisms, has the potential to greatly affect dispersal projections. Horizontal (advective) flow in the ocean can change with depth in both direction and magnitude (Ekman, 1905) dependant on shear stress at the surface (wind) and bottom (friction) and stratification of the water column. Consequently, manifestation of vertical movement, irrespective of stimulus (James et al. 2019), can lead to differential exposure to advective currents of different velocity (i.e. magnitude and direction). Much research argues that vertical migration by the early-life histories of marine organisms represents an 'active' dispersal mechanism allowing species to exert some control over their horizontal movement through selection of specific advective conditions (Knights et al., 2006; Marta-Almeida et al., 2006; North et al., 2008; Robins et al., 2013; Phelps et al., 2015).

1.6.2 Laval behaviour and biophysical models

Despite the general appreciation that larval behaviour plays a key role in larval transport (Kingsford et al., 2002; Levin, 2006; Phelps et al., 2013; Gary et al., 2020), the majority of biophysical modelling studies assume passive larval transport (Swearer et al., 2019). A number of recent studies justified the exclusion of behaviour for different reasons. Assis et al (2015) argued the omission of behaviours, such as larval swimming, was appropriate because the behaviour only influences a larvae’s position at the scale of metres and was not applicable at the large spatial scale of their study. Wood et al (2016) stated that: 1) their model was designed to provide estimates of dispersal potential of an undefined positively buoyant species, and so the study did not set out to achieve biological realism, and 2) observations from the field indicated that positively buoyant larvae were restricted to the surface layers, thus it was assumed that in conditions where

the larvae became mixed into deeper waters, the energy that caused the mixing would also homogenise the water column. In fact, it is only relatively recently (in comparison to larval dispersal research in general e.g. Cleve 1900) that incorporation of larval behaviour within biophysical models has gained traction (Garland et al., 2002; Marta-Almeida et al., 2006; Nicolle et al., 2013; North et al., 2008; Phelps et al., 2015), however as the drivers of larval behaviour are inherently complex (Figure 1.3), there is currently no general consensus of how, what, and when behaviours can and should be included (Swearer et al., 2019).

The aim of this thesis is to consider how we parameterise larval behaviour within model frameworks, explore whether there are behavioural signals that can be generalised, and determine the impact of adopting different behavioural rules within models on dispersal predictions.

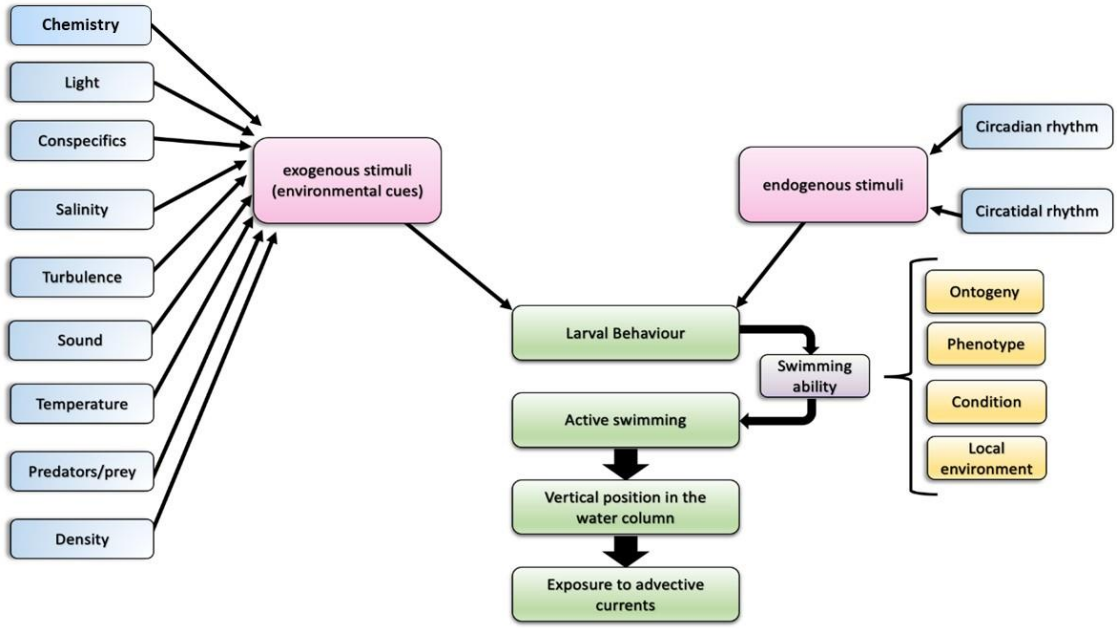

Figure 1.3: Schematic of the cues influencing larval behaviour, and the manifestation of behaviour and its influence on larval dispersal.

1.7 The duality of larval behaviour: linking the biology to the environment

1.7.1 'Rule-based' behaviours

In the context of biophysical modelling, "larval behaviour" typically refers to applying an active swimming response (speed/direction) by a model propagule (larvae) to an exogenous (i.e. external stimuli) or endogenous cue (e.g. circadian rhythm) (North et al., 2008; Banas et al., 2009; Butler et al., 2011, Daigle et al., 2016) (Figure 1.3). Behaviours can be incorporated in biophysical models by the use of simple 'rules' based on laboratory observations. For example, to simulate diel vertical migration, particles can be programmed to swim down during daylight hours and up during the night (negative phototaxis, e.g. Phelps et al., 2015). Similar rule-based approaches have been adopted in biophysical models of dispersal to parameterise larval behaviour in relation to ontogeny (Puckett et al., 2014), temperature (Civelek et al., 2013; Daigle et al., 2016), salinity (North et al., 2008), chlorophyll gradients (Cowen et al., 2003), and tidal (tidal vertical migration) cycles (Moksnes et al., 2014). However, it remains unclear if rules based on laboratory-made observations are appropriate. Studies have shown that swimming behaviours observed in lab-based settings can be absent from field observations (Maldonado et al., 2003; 2006), thus parameterising behaviours within dispersal models based on laboratory observations should be undertaken with caution. This decoupling of lab and field-based observations may be due to the fact that in nature organisms are likely exposed to multiple, rather than single cues, which may alter their responses (Welch and Forward, 2001). Moreover, the scale and/or intensity of cues may be masked in nature, such that behaviours observed in a laboratory are not always expressed in the field (Ettinger-Epstein et al., 2008), and local conditions may prevent behavioural responses from manifesting (Wheeler et al., 2016). As such, lab-observed

behaviours in response to a single stimulus in a controlled environment may not be reflective of the in-situ movements of larvae.

1.7.2 How to respond? Dealing with multiple cues

Hierarchal responses to stimuli have been shown to influence the vertical migration of a range of taxa including larval sponges (Ettinger-Epstein et al., 2008; Whalan et al., 2008), crustaceans (Welch and Forward, 2001), polychaetes (Verasztó et al., 2018) and larval fish (Teodósio et al., 2016). Laboratory studies have clearly shown that larvae can exhibit behavioural responses and directed movement in response to external cues resulting in phototaxis (Forward, 1974; Jékely et al., 2008; Butler et al., 2011), rheotaxis (Oteiza et al., 2017), geotaxis (Rius et al., 2010; Cohen et al., 2015), chemotaxis (Dumas et al., 2014), phonotaxis (Lillis et al., 2016; Egglestone et al., 2016) and thermotaxis (Yokogawa et al., 2014; Goodman et al., 2018) (see Kingsford et al., 2002 for an in-depth review on larval cue responses and their implications for dispersal). However, how multiple cues amalgamate in nature i.e. what is the relative strength/importance of cue(s) in the manifestation of a behavioural response (e.g. movement), remains unclear and consequently, how to account for behaviours governed by multifaceted cue responses is currently a significant knowledge gap.

1.7.3 The manifestation of behaviour

Active swimming can be considered the emergent or manifested behaviour of marine larvae in response to one/multiple cues that is important to larval dispersal. Active larval swimming behaviours have been observed in the laboratory for a range of taxa including bivalves (Sprung et al., 1984; Jonsson et al., 1991; Troost et al., 2008; Fuchs and DiBacco, 2011; Fuchs et al., 2013), echinoderms (Roy et al., 2012; Strathmann and Grünbaum, 2006; Gilpin et al., 2017), gastropods (Fuchs et al., 2004), and crustaceans (Walker, 2004; Møller et al., 2007; López-Duarte and Tankersley, 2007; Gravinese et

al., 2018). Invertebrate larval vertical swimming speeds are suggested to range from between 0.08 - 4.2 cm s^{-1} (Chai et al., 1984). Leis (2020) recently considered how larval swimming speed is incorporated in biophysical dispersal models, and found that most studies use a critical swimming speed (i.e. the maximum speed of flow at which larvae are able to maintain their position). Realising that larvae are unlikely to consistently maintain this critical swimming speed, Fisher and Wilson (2004) argue that 50% of the critical swimming speed was an adequate approximation for a maintainable swimming speed. This approximation has been used in modelling studies (Kobayashi 2006; Chang et al., 2018), however, later Fisher and Leis (2009) claimed that such an approximation is not appropriate for use in dispersal modelling. Indeed, Leis (2020) suggests that critical swimming speed and *in-situ* swimming speed are in fact not well correlated, and may lead to significant model prediction errors. This raises a number of questions: (1) should active swimming be incorporated within model frameworks, and if so, (2) how should that be done, and (3) what swimming speeds should be included?

1.7.4 Larval behaviour is complex

To address these questions, and to move toward ensuring best predictions of larval dispersal., we must consider the environment in which a larva exists, and the extent to which it may influence its behaviour/movement (Metaxas and Saunders, 2009; Swearer et al., 2019). Yet, much of the effort into incorporating behavioural algorithms into dispersal models has considered behaviour to be independent of the physical state of the larva i.e. the rules applied to particles to not consider context specificity, notwithstanding increasing evidence that behavioural decisions are governed by responses to the local environment (Swearer et al., 2019), and that behavioural manifestation is mediated by a larva's surroundings (i.e. hierarchal responses to complex cues (Kingsford et al., 2002), or limitations to swimming ability (Wheeler et

al., 2016; Leis, 2020)). As discussed earlier, the link between cue detection and behavioural manifestation in the field remains unresolved. We argue that behavioural ‘rules’ within dispersal models (which are typically a set of 'additive' rules) are unlikely to capture behavioural complexity, leading to incorrect representation of active swimming, and thus, inaccurate representations of larval vertical distribution patterns affecting horizontal dispersal predictions. Logically, these errors are likely to propagate over time (Firth et al., 2016), and as a consequence, the incorrect incorporation of behavioural parameters that inaccurately reflect *in-situ* vertical distribution profiles is of particular concern, especially when considering species with long planktonic duration periods.

A new approach is therefore needed in modelling studies that consider active swimming, and ideally, one that is not focussed on individual responses to individual cues, but instead considers the mechanisms of movement required to accurately reflect the vertical distribution patterns we see in nature so that organisms are exposed to the ‘correct’ advective currents for dispersal (i.e. the horizontal velocities that match what they would be exposed to in the natural environment due to their vertical position in the water column).

1.8 The aims of this thesis

The chapters that make up this thesis focus on two objectives: (1) improving current understanding into how larval behaviours manifest in nature (Chapters 2 and 3), and (2) refining behavioural parameterisation methods within biophysical models of dispersal with illustrations of how differences in behavioural parameterisation affect dispersal predictions (Chapter 4). Chapter 2 described an approach to *reverse-engineer* larval swimming based on *in-situ* observations of larval vertical distribution patterns. We test a range of swimming velocities within a model environment to examine if vertical

(active) swimming could feasibly be the mechanism that results in patterns observed *in-situ*, and if so, generate a **single active swimming behaviour** that can replace a suite of complex behavioural rules. In Chapter 3, we undertook a high spatial and temporal resolution sampling regime to assess whether change in larval vertical distribution patterns can be attributed to *in-situ* environmental drivers, and compared vertical distribution profiles of the same species in different regions to assess the influence of locality. Finally, based on the outcomes of Chapters 2 and 3, Chapter 4 undertakes simulations to predict dispersal using the Irish Sea as a case study. Here, we explore how vertical distribution profile error propagates through larval dispersal predictions made by a biophysical model, with a formal comparison of three 'behaviours'; passive dispersal., a tidal vertical migration (TVM) ‘rule-based’ behaviour, and a reverse-engineered active swimming behaviour (after Chapter 2), and consider the effect of these behavioural parameterisations on larval biogeography.

2 REVERSE ENGINEERING FIELD-DERIVED VERTICAL DISTRIBUTION PROFILES TO INFER LARVAL BEHAVIOURS

A version of this chapter has been published at: James MK, Polton JA, Brereton AR, Howell KL, Nimmo-Smith WA & Knights AM (2019) Reverse engineering field-derived vertical distribution profiles to infer larval swimming behaviors. Proceedings of the National Academy of Sciences. 116 (24):11818-23. (see: Publications)

2.1 Abstract

Biophysical models are well-used tools for predicting the dispersal of marine larvae. Larval behaviour has been shown to influence dispersal., but how to incorporate behaviour effectively within dispersal models remains a challenge. Mechanisms of behaviour are often derived from lab-based studies, and so may not reflect behaviour in-situ. Here, using state-of-the-art models, we explore the movements larvae must undertake to achieve the vertical distribution patterns observed in nature. Results suggest that behaviours are not consistent with those described under the Tidal Vertical Migration (TVM) hypothesis. Instead, we show (i) a need for swimming speed and direction to vary over the tidal cycle, and (ii) in some instances, larval swimming cannot explain observed vertical patterns. We argue that current methods of behavioural parameterisation are limited in their capacity to replicate in-situ observations of vertical distribution, which may cause dispersal error to propagate over time, due to advective differences over depth, and demonstrate an alternative to lab-based behavioural parameterisation that encompasses the range of environmental cues that may be acting upon planktic organisms.

2.2 Introduction

Larval dispersal is a primary factor shaping the distribution of marine species and influencing the structure of marine communities (Cowen and Sponagule, 2009). Understanding mechanisms of dispersal is therefore imperative to predicting species distributions (Levin, 2006). Biophysical modelling – the tracking of particles assigned biological parameters (‘behaviours’) within ocean models – has become a ubiquitous tool for predicting propagule dispersal in the marine environment (Banas et al., 2009; Nicolle et al., 2013; Ross et al., 2017). Models have become increasingly complex to enhance ‘realism’, yet despite these efforts, simulation outcomes often do not match the

patterns observed in nature identified by genetic studies (Marshall et al., 2010). As biophysical models are able to accurately predict the trajectories of abiotic particles (Soulsby et al., 2007), the decoupling of modelled and observed distributions is frequently attributed to poorly-defined larval behaviour mechanisms, and a limited understanding of how to incorporate behaviours within dispersal models (Marshall et al., 2010; Metaxas and Saunders, 2009).

In the context of biophysical modelling, 'behaviour' refers to applying an active swimming response, typically in the z-dimension, to a model propagule (larvae). Planktic organisms generally swim at relatively slow speeds (mm-cms-1) in comparison to horizontal currents, which can be orders of magnitude faster (i.e. ms-1). As such, active horizontal movement, especially for the early life-history stages of many marine organisms (which tend to be small), can be assumed passive. Swimming speeds can, however, exceed the vertical mixing velocities in the ocean (Thorpe, 2005), providing individuals with a mechanism by which they can alter their vertical position in the water column. When considered in conjunction with depth-related differences in horizontal velocity, vertical migration is argued to provide a mechanism through which weak-swimming individuals can manipulate their horizontal trajectory (e.g. Porch, 1998; Knights et al., 2006). Such depth-related differences can be generated by Ekman processes, which can be significant in both tidal (Polton et al., 2013a) and open ocean environments (Polton et al., 2013b), and tidally induced vertical shear (Uncles and Stephens, 1990).

Vertical swimming is often modelled in response to exogenous (i.e. external stimuli) or endogenous cues (e.g. circadian rhythm) (Banas et al., 2009; North et al., 2008). This seems sensible as laboratory studies have clearly shown that larvae can exhibit behavioural responses and directed movement in response to stimuli (e.g. Kingsford et

al., 2002). In nature, however, organisms are likely exposed to multiple, rather than single cues, which may alter their responses (Welch and Forward, 2001). Moreover, the scale and/or intensity of cues may be masked in nature, such that behaviours observed in a laboratory are not always expressed in the field (Ettinger-Epstein et al., 2008). As such, lab-observed behaviours in response to a single stimulus in a controlled environment may not be reflective of the in-situ movements of larvae.

A number of field-based studies have highlighted changes in larval vertical distribution patterns that correlate with the tidal cycle, for instance, where larvae occupy surface waters during the flooding tide, and remain in close proximity to the seabed during the ebbing tide, or vice versa. Such tidally synchronised vertical migration (TVM) has been documented for a range of taxa (Knights et al., 2006; Kimmerer et al., 1998; Criales et al., 2011; Ueda et al., 2010) across a range of larval ages (North et al., 2008; Lutz and Kennish, 1992) and observations have been made in both estuarine (Kunze et al., 2013; Peterio and Shanks, 2015) and coastal (Knights et al., 2006; Weinstock et al., 2018) environments. Active occupation of different depths during alternate tidal states (flood/ebb), often referred to as Selective Tidal Stream Transport (STST) (Criales et al., 2011; Forward and Tankersley, 2001), allows organisms to exploit depth-related current differences. These observations are often interpreted as evidence of larval behaviour and specifically, an energy-efficient tactic to facilitate migration over long distances or promote retention close to coastal areas. However, the mechanisms that govern tidally timed movements of marine larvae remain poorly resolved (Forward and Tankersley, 2001). Synchronisation of movement with the tide suggests the presence of (i) cue(s), and (ii) behavioural decision-making (Gibson, 2003).

Research has suggested salinity gradients may act as a cue to vertical migration (North et al., 2008). Salinity gradients associated with tidal state would be expected in

estuaries, however, in coastal environments where tidally correlated distribution profiles have also been observed, these signals would be much weaker and thus more difficult for larvae to detect. At coastal sites, one could assume that there would be an absence of strong tidal signals, except in velocity. Otezia et al. (2017) recently showed that some larval fish can detect flow velocity using their lateral line, providing a navigational signal in the absence of visual or chemical cues, but it is unclear if non-fish larvae can perceive changes in the magnitude and direction of the current due to their small size and the lack of focal points in the marine environment (McManus and Woodson, 2012). There is, however, increasing evidence to suggest that they can respond to turbulence (Welch and Forward, 2001), either acting as a cue for larval behaviour (Fuchs and DiBacco, 2011; Fuchs et al., 2013), or alternatively, by hindering a larva's motion strategy (Michalec et al., 2015) due to disorientation preventing expression of a behavioural response (Bradley et al., 2013). Weinstock et al. (2018) suggest that TVM patterns may be passive, caused by vertical advection resulting from the tidal flow over a sloping shelf, however Knights et al. (2006) observed a shift in abundance from the surface waters during the flood tide to deeper waters at high water (Fig. 2.1) that contradicts this theory. It was suggested that larvae may be responding to tidal conditions to facilitate transport, but the exact mechanism could not be resolved.

Larval behaviour can be applied in biophysical models through the application of simple 'rules' e.g. TVM can be simulated by programming 'larvae' to swim up during the flood, and down during the ebb (or vice versa). This approach has been implemented in numerous studies (e.g. North et al., 2008; Paris et al., 2013; Robins et al., 2012). But is it appropriate to apply these rules, and if so, does our current understanding of larval movement allow accurate replication of in-situ patterns? Although distribution profiles in Knights et al. (2006) correlated to tidal state, the patterns observed were not analogous STST theory, in which larval abundances would be expected to be greatest in

the surface waters during mid-flood and high water to promote advection towards the coast, and greatest near the bed during mid-ebb and low water to limit offshore transport (Forward and Tankersley, 2001). Instead, larvae were most closely associated with the sea-bed during both slack water periods, with the middle and bed during the ebb tide. Despite these observations, Knights et al. (2006) has been heavily cited as evidence of STST, and specifically used as justification for TVM in dispersal models (Robins et al., 2013). We argue that this is inaccurate and will lead to erroneous predictions of dispersal. Here, using a combination of empirical data and state-of-the-art modelling, we explore the active movements that bivalve larvae would need to undertake in order to create the patterns observed in nature over the course of a tidal cycle. We test a range of swimming velocities within a model environment to examine if vertical swimming could feasibly be the mechanism that facilitates the patterns observed in-situ, given what we know about the swimming speed of early life-history stages of bivalves.

2.3 Methods

2.3.1 Observations of vertical distribution profiles

To determine the extent of vertical migration in a coastal environment, we used data collected for a previous study (Knights et al., 2006) from two 100 m × 100 m sites (Site 1: 52° 19.542’ N, 6° 15.538 W; Site 2: 52° 20.036’ N, 6° 15.344’ W) within a 4 km2 area with a mean depth of 24m in the Southern Irish Sea off the coast of County Wexford, Ireland. The waters at this location are well-mixed (Brown et al., 2003); with mean horizontal advection of up to 1ms-1 (Knights et al., 2006), and vertical mixing at rates of up to 0.1m2s-1 (Fig. 2.2), which can result in turbulent velocities that are orders of magnitude greater than the swimming speeds of larvae. These conditions therefore provide a challenging test for the effectiveness of larval behaviour (e.g. swimming) to influence vertical distribution. Replicate samples (n=5) were collected from three depth

zones (surface, 0-8m; mid-water, 8-16m; bottom, 16-24m) during four consecutive tidal states (low water slack; flood; high water slack; ebb) over a full tidal cycle (12.1 hours). Replicate sampling was undertaken in May/June and July/August in order to capture early and late stage larvae respectively, and to encompass variation associated with differences in the tidal amplitude cycle (spring/neap). Previous analyses of the data have shown that larval vertical distribution profiles correlate to a change in the tidal state (flood, high water slack; ebb; low water slack), but not the tidal phase (spring/neap), nor with ontogenetic larval stage or sampling location. In the present study, we take a numerical approach using a realistic modelled hydrodynamic environment to explore whether vertical swimming could feasibly be the mechanism that facilitates the observed changes in distribution over a tidal cycle.

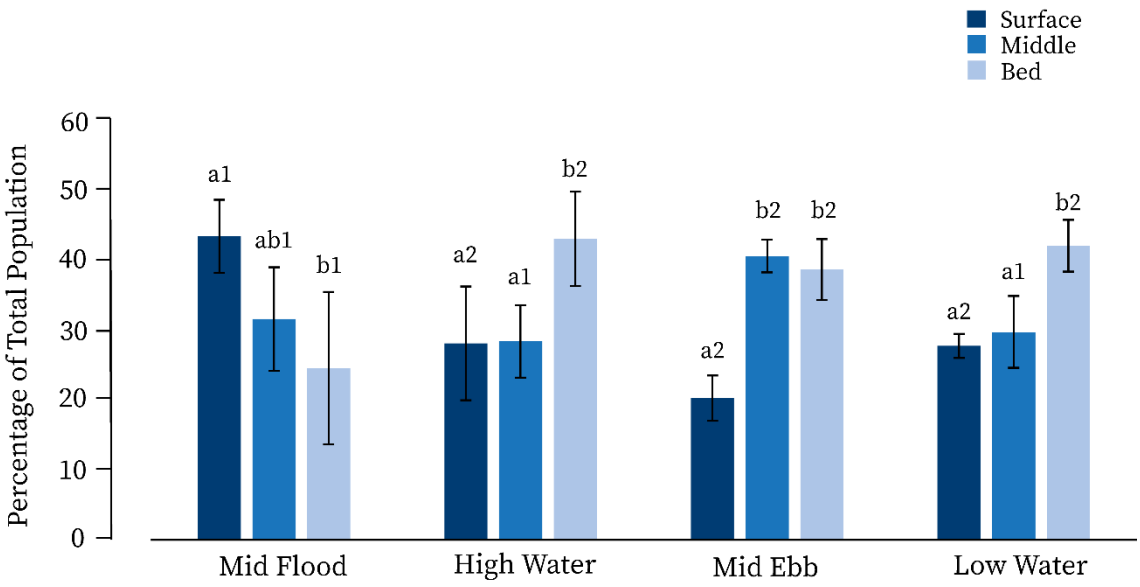

Figure 2.1: Observed proportional abundance (% ± SD) of *Mytilus* spp. larvae within each depth zone during four tidal states (Mid Flood; High Water; Mid Ebb; Low Water). Multiple comparison outcomes are shown above each bar, where different letters and numbers indicate a significant difference ($p < 0.05$) in (a-b) larval proportions between depth zones within a tidal state and (1-2) between tidal states within a depth zone (Tukey's HSD).

2.3.2 The hydrodynamic model

A large-eddy simulation (LES) of an unstratified tidal boundary layer was used to generate a time and depth varying diffusivity coefficient. The purpose of the LES was to create a diffusivity matrix that represented the hydrodynamic environment at the time/location of sampling. The LES configuration was set-up to be forced by time series profiles of 'filtered' horizontal velocities obtained from an ADCP record and solved for the turbulent 'perturbation' flow (Brereton et al., 2019). The LES domain was nominally 50m x 50m x 25m with a lateral grid size of 0.4m and a stretched vertical grid sizes 0.07 m - 0.17m. This method is validated against independent measurements of turbulence dissipation. The advantage of this method over a direct 3D turbulent simulation of particles comes from the fact that online Lagrangian simulations are computationally demanding. This method undertakes trajectory analysis offline using the output from the LES, reducing the computational demand of the simulation, allowing many experiments to be run to seek statistical convergence (see 'the particle-tracking model'). In this simulation the background tidal flow, U, was assumed to be oscillating in one direction. The direction of the flow had no influence on the resultant diffusivity coefficient. From these resolved turbulent fluctuations, an effective eddy-diffusivity (Fig. 2.2) can be derived from the following relationship:

$$K = \left(\frac{< u'w' >}{\frac{\delta U}{\delta z}} \right) \cdot Prt$$

where K is the eddy diffusivity (in m^2s^{-1}), $<u'w'>$ is a resolved Reynolds stress averaged horizontally over the domain (calculated by the LES), $\partial U/\partial z$ is the prescribed vertical mean (tidal) shear, and *Prt* is the turbulent Prandtl number of seawater, taken as one. As this statistic is not well defined when the vertical mean is near zero, a cubic

spline was used to smooth K in time, with 2-minute intervals (de Boor, 1978). This has no discernible effect on K away from the slack tide.

A velocity depth profile was fitted assuming a log-layer approximation with a roughness length of z_0 = 0.001 m, though eddy-diffusivity was not sensitive to the choice of z_0. As the Irish Sea tends to be well-mixed with no known hydrographic features during the spring and summer months when field samples were collected (Brown et al., 2003), it was deemed appropriate to use a constant density LES. The mid-points of the flood and ebb tide were determined from the depth-averaged current velocities when maximum positive and maximum negative flows occurred. Similarly, the slack tide mid points were identified as the times when the associated depth-averaged current velocities were nearest to zero.

It should be noted that, as is the case with all models, the parameterised diffusivity output of the LES may not necessarily be a perfect match for what the real organisms experienced in the field. However, direct calculation of the diffusivities using an LES seems preferable to simply taking a constant value or estimating diffusivity from either a hydrostatic model or scaling arguments. Furthermore, the LES is validated to simulate realistic levels of dissipation (which represents processes at the scale of the organisms (Metaxas, 2001). Such, it was considered an appropriate trade-off between hydrodynamic complexity and physical accuracy, whilst also permitting investigation into larval movement through offline particle tracking.

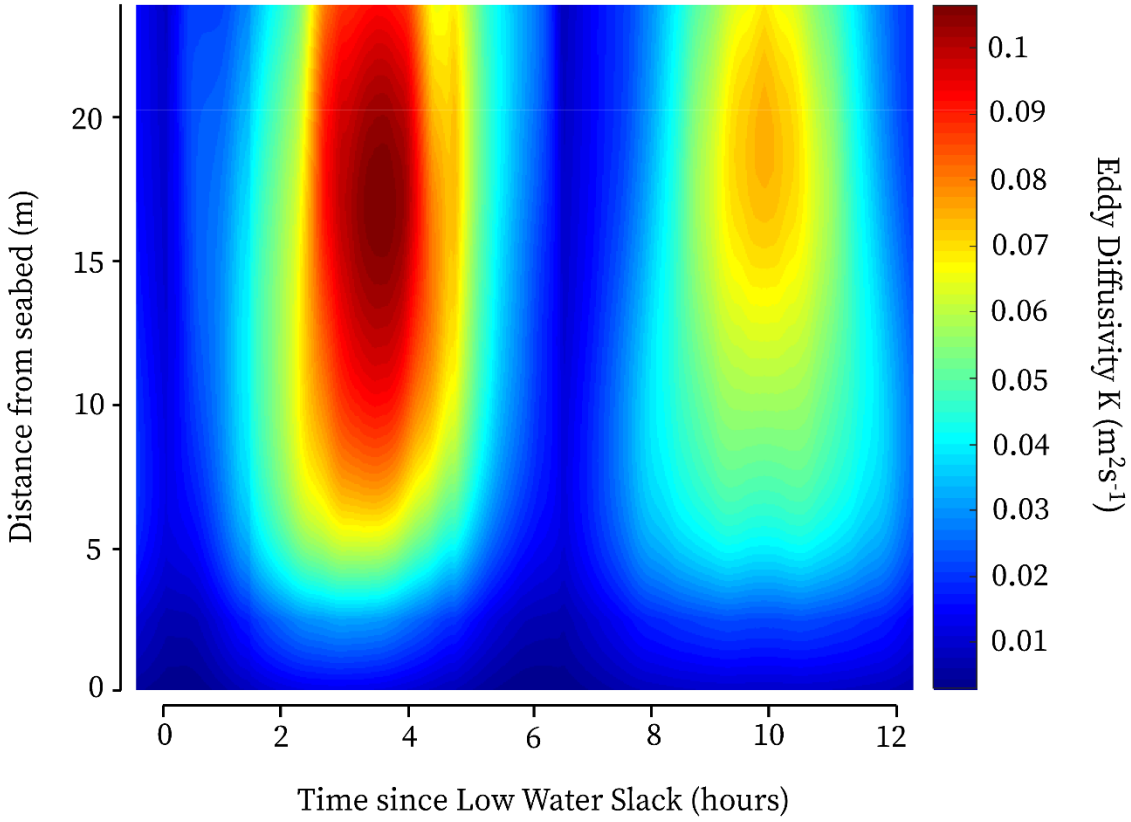

Figure 2.2: Visualisation of the eddy diffusivity field (K) created by the Large Eddy Simulation over a 12.1 hour tidal period from low water $slack_1$ to low water $slack_2$ forced by time series profiles of 'filtered' horizontal velocities, and solved for the turbulent 'perturbation' flow. See Brereton et al. (2019) for full details.

2.3.3 The particle tracking model

To test the potential of larvae to undergo vertical migration, a 1-D Lagrangian particle-tracking algorithm was built in MATLAB (Version 2017b) to follow the vertical trajectories of virtual larvae within the filtered eddy-diffusivity flow field as generated by the LES (see Appendix 1). The 1-D definition of the particle tracker is due to the exclusion of horizontal movement within the simulation (i.e. eddy-diffusivity can only move particles upwards or downwards). Preliminary tests using 100, 10,000 and 100,000 seed particles indicated convergence of the relative vertical distribution

profiles. As such, it was deemed appropriate to use 100 particles in each simulation in order to minimise computational effort without influencing results (see Appendix 2).

The hydrodynamic environment was prescribed using the horizontally averaged output of the LES, K, which was coupled with a particle movement component implemented using a random walk approach (as described in Ross and Sharples, 2004), and larval active swimming (ω) behaviour (described in detail below). The model timestep, δt, was set at 60s. This was deemed sufficiently small enough so that the diffusivity profile was locally well approximated by the first-order Taylor expansion. Particle movement was calculated for δt by:

$$z_{n+1} = z_n + K'(z_n)\delta t + R\left[\frac{2K(z_n + \frac{1}{2}K'(z_n)\delta t)\delta t)}{r}\right] + w_n\delta t$$

where z_n is the depth of a particle at the nth timestep, K′ is the diffusivity gradient at the particle location (δK/δz), R is a random number from a continuous distribution between 1 and -1 (with variance r = 0.33), and ω_n is the vertical swimming velocity of a particle at timestep n.

A Mersenne-Twister algorithm was applied to the random number generator to ensure that values of R were sufficiently random. The inclusion of the deterministic component $K'(z_n)\delta t$ ensures that particles are always advected in the direction of higher diffusivity, thus preventing artificial accumulation in low diffusion areas. It was assumed that the rate of larval diffusivity was equal to the rate of eddy diffusivity calculated by the LES. This was considered appropriate as larval transport by eddies is not affected by inertial and crossing trajectories effects due to their small size (Ross and Sharples, 2004).

Larval vertical movement was explored from each tidal state to the next consecutive state (Flood to High Water, High Water to Ebb, Ebb to Low Water, Low Water to

Flood) using a 'mixed-model' approach. Prior to each simulation, the model water column was seeded with particles in a probabilistic vertical distribution profile based on the observed vertical distribution for the defined starting tidal state. To achieve this, the model particles (n=100) were distributed so that the percentage of particles in each bin matched the percentage of the total population of larvae observed in the field for that bin/tidal state. Additionally, particles were randomly assigned depths within each depth bin using a random number generator. Particles were then assigned 'behavioural rules', explained in further detail below.

2.3.4 Parameterising swimming behaviour

To assess the influence of larval swimming on vertical distribution profiles, multiple simulations were run using a range of swimming velocities (N=2525). Although bivalve larvae have been observed to swim in a helical pattern (Jonsson et al., 1991), swimming in the model was confined to one-dimension, and as such, swimming velocities represent the absolute swimming velocity (the vertical distance travelled by an organism), rather than the linear velocity (the velocity of a larva along its swimming path). Swimming velocities explored ranged from -2.5mms-1 to 5mms-1, justified by an in-depth literature review (e.g. Fuchs and DiBacco, 2011; Sprung, 1984). Particles were considered neutrally buoyant (i.e. downward movement was an active response), and swam constantly at the swimming velocity given by the model parameters.

Each simulation ran from the midpoint of the defined starting tidal state to the midpoint of the next consecutive state. Simulation duration was variable: 174 model minutes between low water and mid-flood, 176 minutes between mid-flood and high water, 198 minutes between high water and mid-ebb, and 182 minutes between mid-ebb and low water. Variation matched that at the survey location, where local bathymetry can act to distort the pattern of the tide, generating tidal asymmetry (Dronkers, 1986).

Furthermore, around the British Isles the M2 and M4 tides can combine to give differences in the flood and ebb tidal streams (Pingree and Griffiths, 1979). Tidal asymmetry has been demonstrated in the Irish Sea (Moore et al., 2009) and was observed by Knights et al. (2006) at the study site. Such patterns were replicated by the LES.

Following each simulation, the proportional abundance of particles within each depth bin was calculated (where the proportion is the number of particles in each bin divided by the total number of seeded model particles) and compared to the observed proportional abundance of particles for the end tidal state of the model run.

2.3.5 Analysis

2.3.5.1 Larval vertical velocity as a predictor of in-situ distribution profiles

A bootstrap approach was used to assess the error between the modelled and observed profiles for each tested vertical velocity at each tidal state, given the variation in the sampled (modelled and observed) populations. We generated 100 new estimates of the observed distribution profile, using the mean and standard deviation of the observed proportional abundances in each depth bin (n=5). We then used the same method to bootstrap 100 distribution profiles for each tested swimming velocity, using the modelled proportional abundances in each depth bin as the sample data (n=25). Pairwise comparisons were used to determine the sum of squares of the proportional difference between the simulated and observed profiles for each depth bin, and the overall difference between the observed and simulated profiles was demonstrated by the total of the sum of squares of the difference for all three bins (SStotal). The mean square error (MSE) and 95% confidence intervals were calculated for each tested velocity. SStotal (n=7600 for each tidal period: 100 pairwise comparisons x 76 tested swimming velocities) and MSE (n=76) were plotted against swimming velocity. Best fitting curves

were constructed in R, using ANOVA to justify the order of the polynomial. The equation of each curve was then solved for the smallest value of y to determine the swimming velocity where the likelihood of difference between the simulated and observed profiles was lowest, and as such, the quality of that velocity as a predictor of in-situ distribution patterns was greatest.

2.3.5.2 Assessing model compatibility

Two-way ANOVA and planned F-test comparisons were used to compare proportions of larvae recorded from in-situ observations (n=5) and proportions of virtual larvae from model simulations (n=5) (Sokal and Rohlf, 1995). For each tested velocity, the number of simulation runs was fixed to match the number of replicates observed. As proportional distribution data were in percentages, data were transformed by the angular (arc-sine of square root) transformation prior to statistical analysis in order to satisfy the assumptions of the ANOVA. The simulation was replicated five times for each scenario, to generate variance estimates around the mean diffusivity based on the random walk. Stouffer's transformed z method (Stouffer et al., 1949) was used to combine the p-values of the interaction term of the 5 independently run tests to provide a quantifiable continuous measure of compatibility between the observed data and the model outcome - Model Predictive Capability (MPC) - ranging from 0 (complete incompatibility) to 1 (perfect compatibility) (Greenland et al., 2016). In addition to the continuous measure of compatibility, the combined p-value was used at the significance level of 0.01 (Bonferroni correction: $\alpha = 0.05/5$ tests) to accept or reject the null hypothesis that there was no difference between the simulated and observed distribution profiles.

2.4 Results

The success of the model at predicting the distribution profiles observed in nature was highly variable, dependent on tidal period modelled, and swimming velocity assigned to the particles, as demonstrated by the Model Predictive Capability (Fig. 2.3: bars). When particles were passive, the modelled distribution profile was significantly different to the observed profile for all tidal states (Stouffers $p<0.01$). On the flood tide, modelled distribution profiles did not significantly differ from those observed in nature when particles were assigned swimming velocities ranging from 0.8mms^{-1} to 3.3mms^{-1} (Stouffer's $p>0.01$), and maximum MPC (MPC_{max}) was achieved at 2.2mms^{-1} (Stouffer's $p = 0.997$) (Fig. 2.3a). MPC_{max} at high water was achieved when particles were assigned a swimming velocity of -0.8mms^{-1} (Stouffer's $p = 0.883$) and velocities between -0.4mms^{-1} and -1.5mms^{-1} produced profiles that did not significantly differ from the observations (Stouffer's $p>0.01$), with the exception of -1.4mms^{-1} (Stouffer's $p<0.01$) (Fig. 2.3b). The model predicted distributions that were not significantly different to those observed at low water when particles were assigned swimming velocities of -0.7,-0.8 and -1mms^{-1} tide (Stouffer's $p>0.01$), with MPC_{max} at -0.7 and -0.8mms^{-1} tide (Stouffer's $p = 0.23$ for both) (Fig. 2.3d). Combined p-values suggest significant differences between the modelled and observed distribution profiles on the ebb tide for all tested swimming velocities (Fig. 3c), and so a value for MPC_{max} on the ebb tide could not be determined.

Minimum $SS_{total.}$, as predicted by the fitted curves correlated well to MPC_{max} (Fig. 2.3), with the lowest values predicted within 2mms^{-1} of the swimming velocities related to MPC_{max} for: a) the flood tide ($VelocityMin.SS_{total} = 2.4mms^{-1}$; $MPC_{max} = 2.2mms^{-1}$), b) high water ($VelocityMin.SS_{total} = -1mms^{-1}$; $MPC_{max} = -0.8mms^{-1}$), and d) low water

(VelocityMin.SS_{total} = -0.8mms^{-1}; MPC_{max} = -0.7/-0.8mms^{-1}). The velocity at which the lowest SS_{total} was predicted on c) the ebb tide was -1.1mms^{-1}.

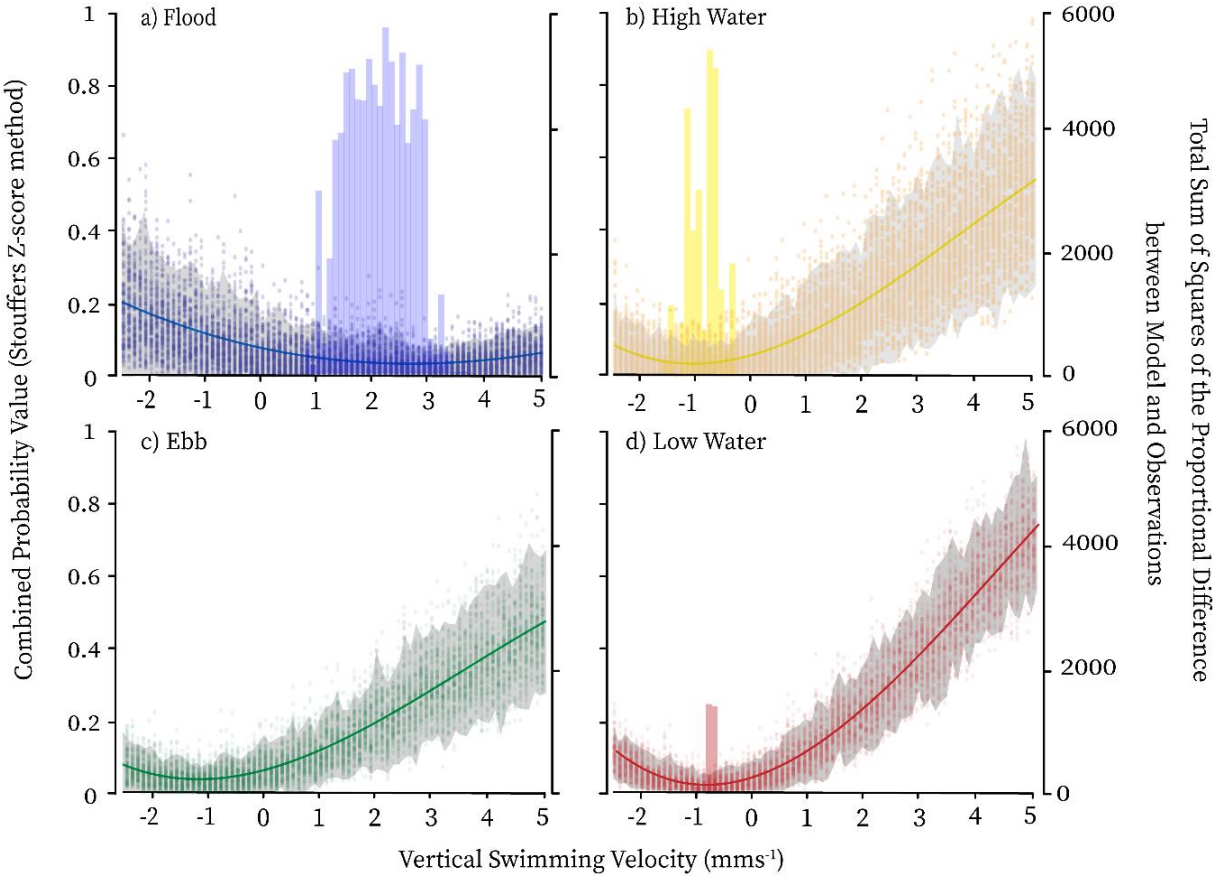

Figure 2.3: Compatibility of the model at predicting the distribution profiles observed in nature during each a) the flood tide, b) high water slack, c) the ebb tide, and d) low water slack, after a ~3hr simulation period, and the quality of vertical swimming velocity as an estimator of observed profiles. Vertical swimming velocity (mms-1) is shown against Model Predictive Capability (Stouffer's Combined p-value: coloured bars) (left axis), and Total Sum of squares of the difference between 100 pairwise comparisons of modelled and observed distribution profiles generated using a bootstrap approach (right axis). Data points indicate individual pairwise comparisons (n=7600) and grey bands demonstrate 95% confidence intervals. Mean Square Error (MSE) is represented by coloured lines. Curves of best fit are calculated using 3rd order polynomials: a) Flood: y = -1.18x3 + 43x2 – 193.16x + 448.48, r2 = 0.39 (SS_{total}), r2 = 0.97 (Mean Squared Error); b) High Water: y = -9.95x3 + 122.25x2 + 276.62x + 363.19, r2 = 0.75 (SS_{total}), r2 = 0.99 (MSE); c) Ebb: y = -9.05x3 + 91.61x2 + 252.34x + 379.60, r2 = 0.82 (SS_{total}), r2 = 0.99 (MSE); d) Low Water: y = -13.49x3 + 170.38x2 + 335.67x + 251.78, r2 = 0.93 (SS_{total}), r2 = 0.99 (MSE).

2.5 Discussion

Behaviour is often included in biophysical models using relatively simple rules based on laboratory-based observations of larval responses to cues (North et al., 2008; Robins et al., 2013). Here, we argue that this approach may not be appropriate. Our results suggest that current methods of behavioural parameterisation used in biophysical modelling studies are limited in their capacity to 'match' in-situ observations of vertical distribution profiles. Using a bootstrap approach, we identified the swimming velocities that best reduced the likelihood of difference between observed distributions and those predicted by the model, even in instances where the model predictive capability was low (i.e. the ebb tide).

We simulated change in the vertical distribution of virtual larvae by assigning 'behaviours' to particles within a novel high-resolution tidal boundary layer Lagrangian model. To our knowledge, there is no study that has attempted to reverse-engineer model simulations to determine larval behavioural parameters in this way. In addition to showing that the likelihood of difference between model and nature is reduced when particles are assigned some sort of active movement compared to passive particles, our results are the first to indicate when larvae change their swimming 'behaviour' in response to changes in tidal state. We showed that a shift from positive (upward) to negative (downward) movement around the mid-flood point of the circatidal cycle was necessary for larvae to achieve the distribution patterns observed in nature (Knights et al., 2006). This is counter to the selective tidal stream transport hypothesis, which argues that organisms swim upwards for the duration of one tidal state and downward during the opposing state (e.g. (Civelek et al., 2013), and contradicts Weinstock et al.'s (2018) theory of passive vertical advective movement by tidal straining, as this mechanism would result in the direction of vertical movement being consistent during

the flooding tide. Consequently, the implementation of TVM in a dispersal model using this 'rule' (e.g. Robins et al., 2013) may be ineffective at generating vertical profiles that accurately represent nature. Even over relatively short time periods, such as the 3-hour period between mid-flood and high water, inaccurate vertical distributions in biophysical models will influence dispersal estimates, and such errors will accumulate and propagate over time (consider species with long planktic larval durations). This effect was recently hypothesized by Firth et al. (2016). Looking forward, future research should explore how the results of this study propagate through the larval dispersal estimated by a biophysical model, and how behavioural parameters derived from the reverse-engineering of in-situ vertical distribution profiles influence both dispersal and connectivity predictions when compared to estimates made using alternative approaches to vertical distribution (i.e. 'rule-based' behaviours (e.g. Robins et al., 2013) and/or probabilistic larval vertical distribution profiles (e.g. Paris et al., 2007).

All velocities resulting in the smallest error between model and observations fell between the boundaries of larval swimming reported in the literature suggesting that swimming is an important mechanism. Reported swimming speeds and sinking velocity estimates are typically highly variable both within and across taxa; although are typically in the range of 1 to 10mms^{-1} and rarely exceed 20mms^{-1} (4.2 cms^{-1} in Cancer magister megalopa) (Chia et al., 1984). Our study showed that, for our data, upwards swimming must be 2.5x faster than downwards swimming in order to best match the observed profiles. This demonstrates the need for swimming speed to be a variable parameter in dispersal modelling studies, and highlights that the speed of upwards and downwards movement is not always consistent, however we acknowledge that any difference in optimum swimming speed among tidal states will be most marked in slower swimming species, such as bivalves, and effects will likely be less pronounced for stronger swimmers (Huntley and Zhou, 2004).

The model-generated distribution profiles on the ebb tide were significantly different to those observed for all tested velocities leading to low model compatibility (HW to mid-ebb; mid-ebb to LW). This is in marked contrast to the flood tide where compatibility was high. Our approach was able to identify the optimum vertical velocities that give the 'best fit' to the observed patterns when larval behaviour is parameterized by constant swimming in one direction; however, the low compatibility between the modelled data and observed profiles suggests that we do not fully understand the behavioural responses of the larvae and their relationship with the physical characteristics of the ocean during this particular tidal state. For instance, it is possible that spatially and/or temporally inconsistent behavioural responses *in-situ* may cause larval swimming to differ among depths over even shorter timescales. One possible solution to this problem might be to use higher spatio-temporal resolution in-situ sampling coupled with a short model internal time-step in an effort to improve model compatibility. This process alone may provide further insights into the relationship between manifestation of larval behaviours in response to their environment, whilst simultaneously supporting improved model compatibility and better characterisation of larval behaviour within model frameworks.

Due to the sampling regime of the original study, our model was only able to reverse-engineer optimum swimming speeds during daylight hours. Diel vertical migration (DVM) occurs when organisms synchronize their vertical movement to the day/night cycle. Such behaviour, thought to be a predation-avoidance response (Lampert, 1994), has been documented for a number of taxa (Romero et al., 2012; Breckenridge et al., 2011; Raby et al., 1994). Whether bivalve larvae exhibit DVM remains unclear; there is conflicting evidence in the literature (Raby et al., 1994; Bonicelli et al., 2016), and differences may well be location specific. Future research would benefit from sampling programmes that encompass the 24-hour diel cycle in order to encapsulate potential

variation in the vertical distribution of larvae within the study domain due to the day/night cycle.

The model system of this study assumes a well-mixed open coastal environment with a flat bathymetry and laterally homogenous spatially averaged velocities. Given this, and the fact that the LES model could be directly forced by observed velocities suggests that the LES data broadly described the hydrodynamic conditions that the larvae would experience throughout the study domain. It must be noted, however, that in environments with high spatial heterogeneity (for example over sloping bathymetry, or across lateral or vertical frontal systems) differential vertical mixing may influence larval ability to regulate depth as expected. Stratification of the water column has been shown to alter the vertical migration of marine organisms (Raby et al., 1994; Lougee et al., 2002) by acting as a barrier to vertical movement (Daigle and Metaxas, 2011). Should our approach be undertaken to infer larval swimming in a more heterogeneous environment, such as an estuary, the underlying hydrodynamic model should be designed as to adequately represent realistic conditions.

The cues which govern larval swimming responses in-situ remain unclear and were beyond the scope of this study. It has been previously suggested that some larvae may respond to a hierarchy of cues, indeed, many have the sensory ability to do so (Kingsford et al., 2002; Otezia et al., 2017). Hierarchical responses to stimuli have been shown to influence the vertical migration of a range of taxa including the larvae of sponges (Ettinger-Epstein et al., 2008), and fish (Teodosio et al., 2016), and so it is possible that a similar response exists in other organisms, for example, bivalves. If cues do influence the vertical migration of larvae in a hierarchical manner, their order of importance to the organism must be determined if behaviours are to be parameterised using a rule-based approach in dispersal models so that behaviours accurately depict

responses in nature. This order may change over space and time and in relation to other cues and so rule-based models must account for this. Failure to do so could greatly contribute to model error.

With this in mind, accurately parameterising larval behaviour using a rule-based approach is clearly a complex endeavour that requires an in-depth understanding of a multitude of potential drivers of larval movement, and knowledge of how these drivers influence both larvae and each other. Using field-derived vertical distribution data to set the goal posts, our approach allows larval behaviour to be based on real-life changes in the vertical distribution patterns of larvae. By focusing on the active movements particles would be required to undertake within the model domain to achieve a distribution profile that is the least different from that observed in nature, we effectively bypass the need for a complex understanding of the mechanisms of planktic swimming and larval responses to behavioural stimuli, instead focusing on the end goal: achieving a modelled distribution profile that accurately replicates nature.

Dispersal is a key mechanism that shapes the distribution of marine species, and thus an understanding of how and why species disperse is imperative to the success of marine conservation agendas, fisheries management efforts and attempts to minimise the risk of invasive species spread (Levin, 2006; Botsford et al., 2003; Palumbi, 2003). Biophysical modelling provides a cost-effective tool to estimate dispersal in the marine environment, however, inaccuracies within these models can misguide those using them, and consequently decisions made off the back of inaccurate model estimations may be ineffective (Botsford et al., 2009). This study demonstrates that active movement changes over the course of the tidal cycle at temporal scales typically not modelled. Our approach has reverse-engineered model simulations to identify the larval swimming speeds and directions that generate the smallest error between modelled and

observed distribution patterns. These estimates are not perfect, but as error is reduced compared to the passive model when particles are given active movement, we can conclude that larval swimming is an important mechanism in accurate depictions of vertical distribution. This approach will allow future research to determine the best fitting behaviours of a range of taxa, where *in-situ* vertical distribution data is/can be made available.

This study highlights that over a period as short as 12 hours, differences in behaviour (i.e. speed/direction) required to replicate observed vertical distribution profiles are great. Our results indicate that current 'rule-based' approaches to behavioural parameterisation, for example, assigning a constant swimming speed to particles and/or assuming vertical direction with respect to tidal direction (i.e. Robins et al., 2013), may lead to significant over- or under-estimates of dispersal. For larvae swimming outside optimum speeds, modelled predictions of dispersal will become increasingly divergent over time in terms of match to in-situ observations due to depth-related differences in current velocity, especially for species with PLDs longer than 1 day. This study offers an alternative method of behavioural parameterisation, where behaviour is inferred from the field rather than the laboratory, which will aid in minimising the error associated with inaccurate vertical distribution profiles in biophysical models.

3 ASSESSING ENVIRONMENTAL DRIVERS OF VERTICAL DISTRIBUTION IN A TIDALLY INFLUENCED COASTAL SYSTEM

A version of this chapter is currently in preparation as: James, MK, Polton, JA, Howell, KL & Knights, AM. Assessing environmental drivers of vertical distribution in a tidally influenced coastal system, for publication in a marine ecology and ecosystem research journal., such as Marine Ecology Progress Series.

3.1 Abstract

Identifying the drivers of larval behaviour remains a significant challenge in marine ecology. Larvae have the ability to alter their vertical position in the water column, exposing them to depth-differentiated which can influence their dispersal trajectory. However, the drivers of larval vertical migration remain unclear. Variations in the *in-situ* vertical distribution profiles of early and late stage bivalve larvae collected from the English Channel in 2018 were investigated and compared to distribution profiles of bivalves collected from the Irish Sea. Generalised Additive Models (GAMs) were used to reveal the influences of density, temperature, salinity and eddy diffusivity on the distribution profiles. External drivers explained very little of the vertical distribution patterns of the larvae, however, results suggest differential usage of environmental cues based on ontogenetic stage. Vertical distribution patterns observed differed from previous observations of a similar species at a different location, suggesting that it may not be appropriate to generalise larval behaviours as a function of temperature, salinity, density, diffusivity, tidal state or larval age.

3.2 Introduction

Larval dispersal - the movement of individuals or gametes away from their areas of origin or from centres of high population density - plays a critical role in shaping the distribution patterns of species in the marine environment (Clobert et al. 2001; Wright, 1951). Many marine species are sessile or display limited movement as adults, relying on a ‘free flowing’ larval life-history stage as the mechanism for dispersal. This ‘larval dispersal’ phase is an essential connectivity mechanism that links discrete populations that can offset disturbance, ensure gene flow and facilitate stability (Bernhardt and Leslie, 2013). Dispersal is therefore an important process in the evolution and adaptive

capacity of marine organisms and understanding connectivity a key aspect of understanding species biogeographic patterns.

During their planktonic life-history stage, larvae are exposed to oceanographic processes that can act to transport individuals from one location to another (Pineda et al., 2007). For many years, marine larvae were considered as passive particles at the mercy of ocean currents, and their dispersal - the geographic distance travelled from spawning to settlement - determined solely by hydrodynamics (Pineda et al., 2007). Coupled with the idea that oceans were open with no barriers to dispersal., the assumption was dispersal and distribution was widespread (e.g. Lessios et al., 1998). The influential paper by Cowen et al. (2000) challenged this paradigm, suggesting that marine populations may not be as 'open' as once thought. Observations of breaks in the distribution patterns of marine organisms with the capacity for long distance dispersal (LDD) indicate limits to the transport of larvae (Barber et al., 2002; Waters et al., 2005). Subsequently, hydrodynamic features such as fronts (Gilg and Hilbish, 2003; Thornhill et al., 2008), eddies (Mann and Lazier, 2006); Sanvicente-Anorve et al., 2018) and upwelling (Rocha et al., 2005) are now recognised as potential barriers to dispersal.

Concomitantly, there has been increased consideration of the role of larval behaviour on dispersal. Historically, larval behaviour was not considered important in dispersal estimates, largely because the small size of larvae (and limited swimming ability in comparison to advection velocities; Huntley and Zhou, 2004) suggested no capacity to manipulate their horizontal position. However, increasingly larvae are now thought to modify their horizontal advection through manipulation of their vertical position in the water column by actively swimming and/or by altering their buoyancy (Garrison, 1999; Szmant and Meadows, 2006; Shanks, 2009; Stanley, 2012; Daigle et al., 2016; McVeigh et al., 2017). This is achievable as larvae are able to overcome vertical mixing

in marine systems as their swimming speeds are greater than the velocities associated with vertical mixing (Yamazaki and Squires, 1996; Thorpe, 2005; Scheuch and Menden-Deuer, 2014).

A combination of physical oceanography and larval behaviours likely play a role in the idiosyncratic biogeographic patterns of biodiversity often observed in nature. It is argued that larval vertical migration in response to environmental cues provides planktic organisms with a mechanism by which they are able to take advantage of changing flow speeds and directions characteristic of coastal environments despite their limited horizontal swimming capacity (*sensu* Selective Tidal Stream Transport (STST); Forward and Tankersley, 2001) and to some extent, govern their dispersal trajectory. For example, by occupying deeper waters during the ebbing tide larvae minimise transport offshore during tidal oscillations, which promotes self-recruitment (Rowe and Epifanio, 1994; Kimmerer et al., 2014; Teodosio and Garel, 2015). Conversely, larvae that occupy surface waters during the ebb tide will facilitate offshore transport, carrying them to regions that potentially have more food/less predation risks, and/or less competition for suitable habitat (Forward and Tankersley, 2001).

Coastal systems are highly dynamic with fluctuations in tidal activity, wave action, and surface heating from the sun that can result in strong environmental gradients forming over short-term (hours: high-low water cycles), mid-term (weeks: spring-neap cycles) and long-term (months: seasons) temporal scales (Krumme and Liang, 2004), and over spatial scales ranging from kilometres (ocean-basins) to millimetres (eddy diffusivity gradients). Given that marine larvae have been shown to exhibit behavioural responses to a number of environmental cues in lab-based experiments that reflect conditions in coastal systems, it is reasonable to assume that the movement of larvae is to some extent governed by detection of their environment. For example, in laboratory experiments,

vertical profiles of marine larvae have been observed to be influenced by light (Ettinger-Epstein et al., 2008; Cisewski et al., 2010; Wahab et al., 2014; Andres-Bragado et al., 2018), the presence of conspecifics (Ettinger Epstein et al., 2008;), temperature (Gardner et al., 2004; Fouzai et al., 2015), salinity (Crosbie et al., 2019) food availability (Bianco et al., 2011; Fouzai et al., 2015), familiar soundscapes (Lillis et al., 2018), turbulence (Fuchs et al., 2004; Fuchs and DiBacco, 2011; Wheeler et al., 2016) and welling events (DiBacco et al., 2011) suggesting at the potential for phototactic, chemotactic, gravitactic, visual., auditory, and olfactory behavioural responses.

Yet, little is known about the mechanisms by which larvae perform vertical migration in the water column. In marine environments, larvae are consistently exposed to a plethora of cues of which laboratory experiments indicate that they have the ability to respond to (see above). It is unclear, however, which of these they respond to in nature when cues are presented simultaneously. We have only recently shed light on what larvae might be doing to achieve changes in their vertical distribution (James et al., 2019; Chapter 2), but how they are interacting with their environment remains unknown, and a significant missing piece of the puzzle in larval dispersal modelling (Swearer et al., 2019). It has been suggested that cue response may be hierarchal (Kingsford et al., 2002; Woodson et al., 2007 Fuchs et al., 2010; Huijbers et al., 2012; Teodosio et al., 2016). For instance, megalopae of the blue crab, *Callinectes sapidus*, have been shown to mediate their vertical migratory behaviour in response to a hierarchy of salinity and turbulence levels (Welch and Forward, 2001). Furthermore, conflicting cues can lead to mixed behavioural responses (Fouzai et al., 2015; Morello and Yung, 2016), decoupling predictions of behaviour made through observations of single-cue responses under relatively artificial laboratory conditions. Consequently, our understanding of the environmental cues that larvae use to signal vertical migratory behavioural responses is

limited, due to both our lack of knowledge surrounding decision-making by larvae, coupled with the inherent complexity of their surrounding environment.

Zooplankton are known to respond rapidly to changing conditions (David et al., 2005), so it is likely that behavioural responses to the environment influence the vertical distribution profiles of organisms over time periods even as short as a few hours. In tidally-influenced systems, change in the vertical distribution of larvae over these types of temporal scales has the potential to significantly influence the dispersal of organisms due to tidal flow. Many studies have been published that correlate observed vertical distribution patterns to the tide (Carriker 1951,1961; Kunkle, 1957; Wood and Hargis, 1971; Booth, 1972; Maru et al., 1973; Andrews, 1983; Gregg, 2002; Baker and Mann, 2003; Knights et al., 2006; Peteiro and Shanks, 2015), yet the mechanisms that drive the formation of these profiles in nature remain unresolved. Furthermore, there is limited information available on the relationships between multiple tidally-influenced environmental variables and larval vertical distribution in-situ. Given biophysical models typically accurately predict the trajectories of abiotic particles (Soulsby et al., 2007), the decoupling of observed distributions and those predicted by dispersal studies is frequently attributed to poorly defined larval behavioural mechanisms and a limited understanding of how to incorporate behaviours within dispersal models (Metaxas and Saunders, 2009). Such, understanding how and when larval behaviours manifest in nature is paramount to effective biophysical modelling that better predicts connectivity patterns in the marine environment.

Here, we explored changing patterns of larval vertical distribution to reveal potential drivers of larval behaviour. We observed change over time and space in both larval density and proportional abundance of bivalve larvae in a macro-tidal coastal environment to answer the questions: What are the main environmental drivers of

change of larval vertical distribution, and how do the patterns of vertical distribution observed in our samples compare to previous observations of vertical distribution in a different location for the same taxa?

3.3 Methods

3.3.1 Data collection

Sampling was undertaken in Bigbury Bay, off the Coast of South Devon, UK, (50° 17' 20"N to 50° 17' 29"N, 4° 0' 24"W to 4° 0' 30"W) during September 2018 (Fig. 3.1). This location is characterised by a large tidal range (~4-5m) and experiences a semi-diurnal tide. Timing of sampling was chosen to coincide with the autumnal peak in zooplankton abundance observed on this coast, in which bivalves make a significant contribution to the total zooplankton abundance (Eloire et al., 2010). Plankton samples were collected over a 6-hour period to capture the change from low flow (high water slack) to high flow (ebb tide). This period of the tide was specifically chosen for detailed exploration as recent research revealed that the behaviours of blue mussel larvae inferred from *in-situ* vertical distribution profiles could not be explained for the period between high water slack and the mid-point of the ebb tide (James et al., 2019; Chapter 2). This modelling study explored whether observed patterns could be 'matched' in a model environment through the implementation of a uni-directional constant swimming behaviour. Results demonstrated low model compatibility during the high water → mid-ebb period and suggested that behavioural manifestation may be more complex than the tested method of behavioural implementation. As such, this study endeavoured to explore the factors that may cause complex behavioural responses to arise.

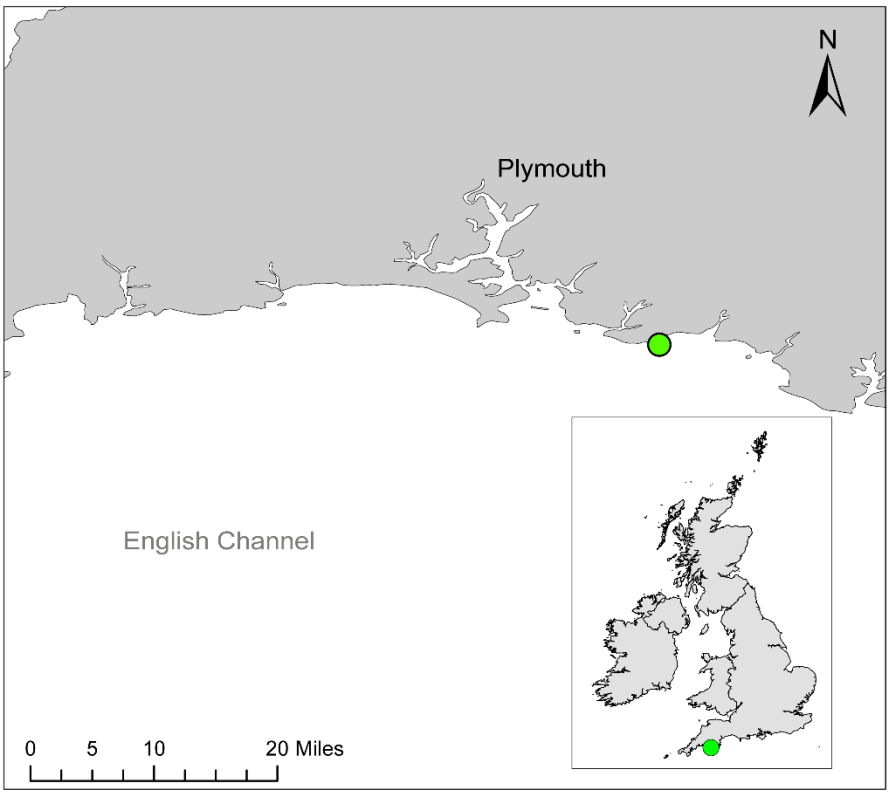

Figure 3.1: Bigbury Bay, off the coast of South Devon in the English Channel (inset, the location of Bigbury Bay in relation to the UK). Study site is marked by the green circle.

Samples were collected from within a 200m^2 area (with a water depth of ~25 m chart datum and a tidal range of 5m at the time of sampling (anyTide, National Oceanography Centre). Both sites had similar topography and seabed composition, which was predominantly stony circa-littoral reef in both locations (Gaches and Cork, 2008). Water depth was first measured *in-situ* by echo sounder (Airmar P79 transducer 200KHz: Raymarine) to the nearest 0.1m before dividing the column into 3 equal depth bins (following Knights et al., 2006), calculated as 1/3rd of the total water column depth at the time of sample collection.

Plankton nets with mouth diameter of 250mm and a mesh size of 100µm were suspended in each depth bin by attaching them to a vertical rope tied to a 25kg weight placed on the sea bed and suspended using a surface buoy (25 kN) (this setup is

hereafter referred to in the paper as ‘strings’). Each 3-hour tidal period (HWS +/- 1.5hrs and mid ebb +/- 1.5 hours) was divided into three 1 hour ‘windows’ and strings were deployed for the duration of each window (see Fig 3.2). To account for spatial variation and ‘patchiness’ within the plankton, duplicate strings were deployed within the sampling area for each 1-hour sampling period. Following deployment, nets were washed into 250ml PDFE bottles and the contents stored in 70% industrial denatured alcohol (IDA) to fix plankton. Current data was obtained by Acoustic Doppler Current Profiler (Nortek AWAC 400kHz, Norway) mounted on a bedframe (Nortek Ocean Science Sea Spider, Norway). Current speed and direction were recorded at 1 metre depth intervals every minute for the duration of the study (360 minutes). CTD casts (SBE 19plus V2 SeaCAT profiler CTD, Seabird Electronics, USA) were taken at the midpoint of each hourly sampling window to provide water column profiles of temperature, salinity and density.

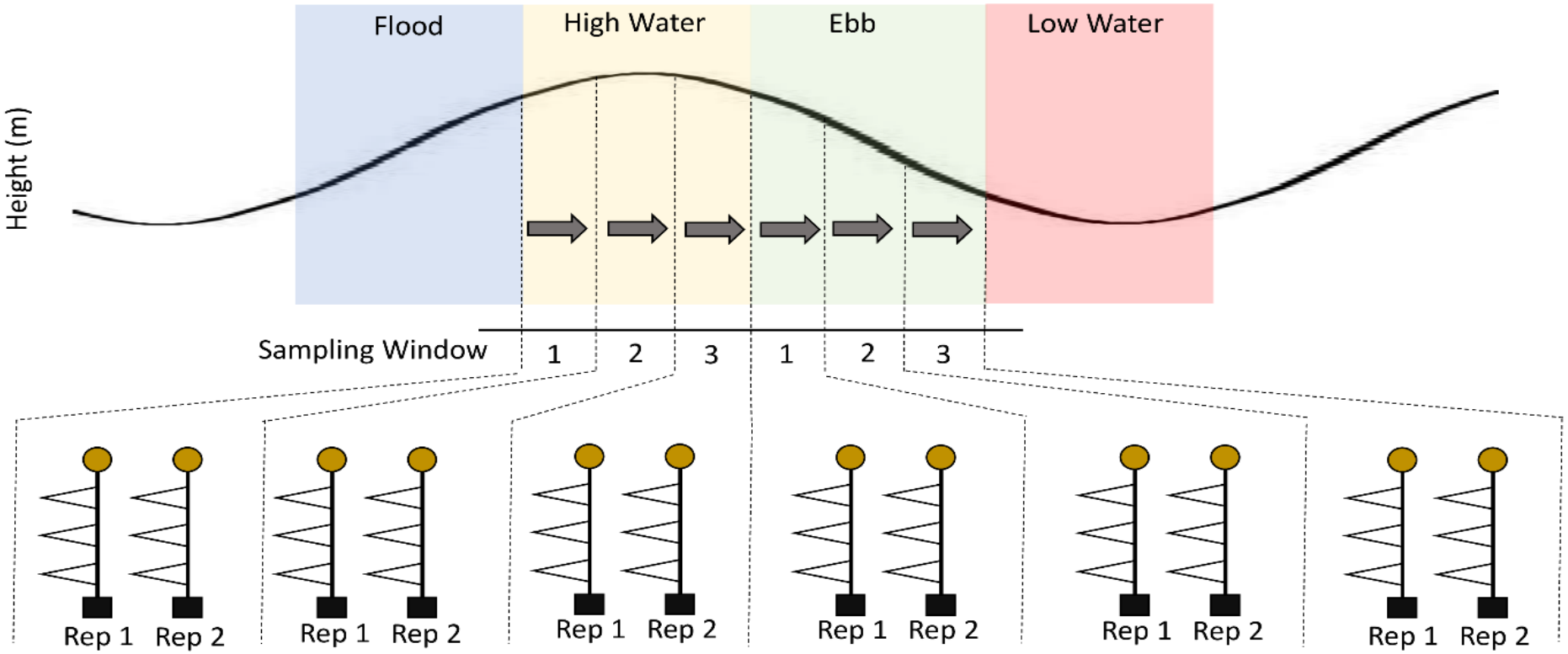

Figure 3.2: Schematic of the sampling regime. Replicate plankton strings deployed for hour long 'windows' during high water (+/- 1.5 hours from High Water Slack) and ebb tide (+/- 1.5 hours from mid-ebb: calculated as the halfway point between high water and low water).

3.3.2 Processing the oceanographic data

ADCP data were processed using MATLAB (2018b) and mean current speed (ms^{-1}) per hour in each 1m depth bin was calculated. Eddy diffusivity (m^2s^2) was fitted to the current speed profile using a scaled output of a Large Eddy Simulation (LES) (see Brereton et al. 2019 and James et al. 2019; Chapter 2 Fig 2.2) by determining coefficients between the current speeds used to force the original LES and those collected by the AWAC, and then multiplying the original eddy diffusivity by the calculated coefficient for each time step/depth bin. This process generated mean hourly eddy diffusivity records (to match the timeframe of each sampling window) with a vertical spatial resolution of 1m.

3.3.3 Plankton Taxonomy

In the laboratory, *Mytilus* larvae were identified then enumerated using the identification keys of Newell and Newell (1977) and Conway (2012). Bivalve larvae were chosen as the study species as: 1) they are known to be dominant members of the zooplankton community during the Autumn (the time of sampling); 2) they are known to have the capacity for active swimming (Sprung, 1984; Fuchs and DiBacco, 2011); and 3) previous research has examined the *in-situ* vertical distribution profiles of this taxa over the course of tidal cycles (Knights et al., 2006) allowing for direct comparison between the profiles obtained during this study and those obtained from other study sites. Identified larvae were grouped into one of two ontogenetic stages based on size and morphological features: (i) early stage (D-veliger; <210µm and no foot present), and (ii) late stage (pediveliger; >210µm and foot present). Density (number per m^3) was quantified by determining the volume of water sampled by each net during the sampling window using:

$$\pi r^2 * u$$

Where r is the radius of the net opening, and u is the cumulative velocity of the passing current over the sampling window as provided by the ADCP.

Larval densities in each depth-bin*tidal state combination (n = 6; 2 reps per hour, 3 hours per tidal state) were then bootstrapped using a normal distribution around the mean and standard deviation for each sample to improve estimates of the confidence intervals. This process was replicated so that 1350 observations were recorded in total for each depth-bin × tidal state combination.

The calculated distributions of density values for each depth bin were used to randomly assign larval density. For example, the bottom depth bin covered 7 metres of the water column and thus 7 values for eddy diffusivity, temperature, salinity, and water density (temporally averaged over each sampling window), were obtained within this depth bin for each timestep, collected at 1 metre intervals. To assign larval densities at 1 metre intervals within the bottom bin, a random larval density was chosen based on a normal distribution around the mean and standard deviation of larval density for the bottom bin for each timestep. Current velocity was not selected as a factor due to lack of evidence that it can be directly sensed by invertebrate larvae. Given plankton density differences can occur between states due to patchiness, proportional abundances of larvae in each depth bin in relation to the total abundance of larvae in the water column were considered instead of raw density to compare vertical distribution profiles between states.

3.3.4 Comparing larval densities and vertical distribution profiles

Statistical analyses were performed using R (Version 3.4.1, R Core Team, 2018). Larval densities and proportional abundances were compared using a three-factor ANOVA

design: (1) tidal state (2 levels: high water slack, ebb tide); (2) Depth Bin (3 levels: surface, middle, bed); and (3) Larval age (2 levels: early, late), and interactions among factors were also considered. Assumptions of ANOVA were tested using Levene's test for homogeneity of variances at the significance level of $\alpha = 0.05$. When assumptions of the ANOVA were not met, data were square root (x+1) transformed prior to analysis. Differences between the means of groups were assessed at the significance level of $\alpha = 0.05$. For terms that were significant, Tukey's Honestly Significant Difference (HSD) testing was used to identify which means were different and mean differences as percentages were calculated.

Additionally, larval vertical distribution profiles of proportional abundance were compared to previous data describing changes in the vertical distribution profile of bivalve larvae over a tidal cycle in the Southern Irish Sea. This study was undertaken in a well-mixed open coastal (shelf sea) environment where means currents speeds are of a similar magnitude to those in the English Channel (anyTide, National Oceanography Centre), and sampling was undertaken in water of a similar depth to this study (~25metres). Comparative analysis was done using the same factorial design as above but replacing the 'larval age' variable with a new integrative factor: 'group', in which larvae were classified as early stage, late stage or Irish. As the Irish Sea bivalve larval population exhibited no significant differences in vertical distribution patterns with respect to ontogeny (Knights et al., 2006), larval age of the Irish Sea population was not considered in this model. Furthermore, in order to assess behavioural manifestation in terms of vertical movement of the population, we looked at shifts in the vertical distribution profiles for early, late stage and Irish larvae between the two sampled tidal states and calculated the mean percentage change in the proportional abundance of larvae in each depth bin between the two states.

3.3.5 Assessing the drivers of vertical distribution

To assess which environmental variables may be driving the observed changes in the vertical distribution patterns of bivalve larvae, General Additive Models (GAMs) were implemented using the 'mgcv' package in R (Wood, 2012). A step-wise approach was used to determine the best fitting GAM to predict proportional abundance, with four environmental variables with distinct ecological effects, namely: water density (kg/m^3), temperature (°C), salinity (PSU) and eddy diffusivity (m^2s^1) used as covariates. This was done by fitting a 'thin plate' smoothing spline to each of the covariates where appropriate, and reducing the equation through the removal of non-significant variables where necessary to improve model fit. Prior to analysis, variables were tested for correlation and significant correlates were removed. Model fit was assessed using the generalised cross-validation (GCV) score of the model, with the model with the lowest GCV score indicating lowest prediction error. The relative importance of each of the covariates to the final model outcome was determined using the VarImp function from the 'caret' package in R (Khun, 2012).

3.4 Results

3.4.1 Water column features

The water column exhibited slight stratification during the high-water slack tide, with maximum differences in temperature, salinity and density throughout the water column of 0.2°C, 1.2 PSU, and 0. 9 kg/m^3 respectively (Fig. 3.3). These differences all occurred during the slack high-water period. During the ebb tide, the water column was well-mixed with no significant features (Fig. 3.3). A temporal lag of approximately 1 hour was observed between current speed intensity and the intensity of the eddy diffusivity predicted by the LES model (Fig. 3.4). Surface peaks observed for all

variables are artefacts of the sampling equipment, caused by calibration of the CTD as it enters the water.

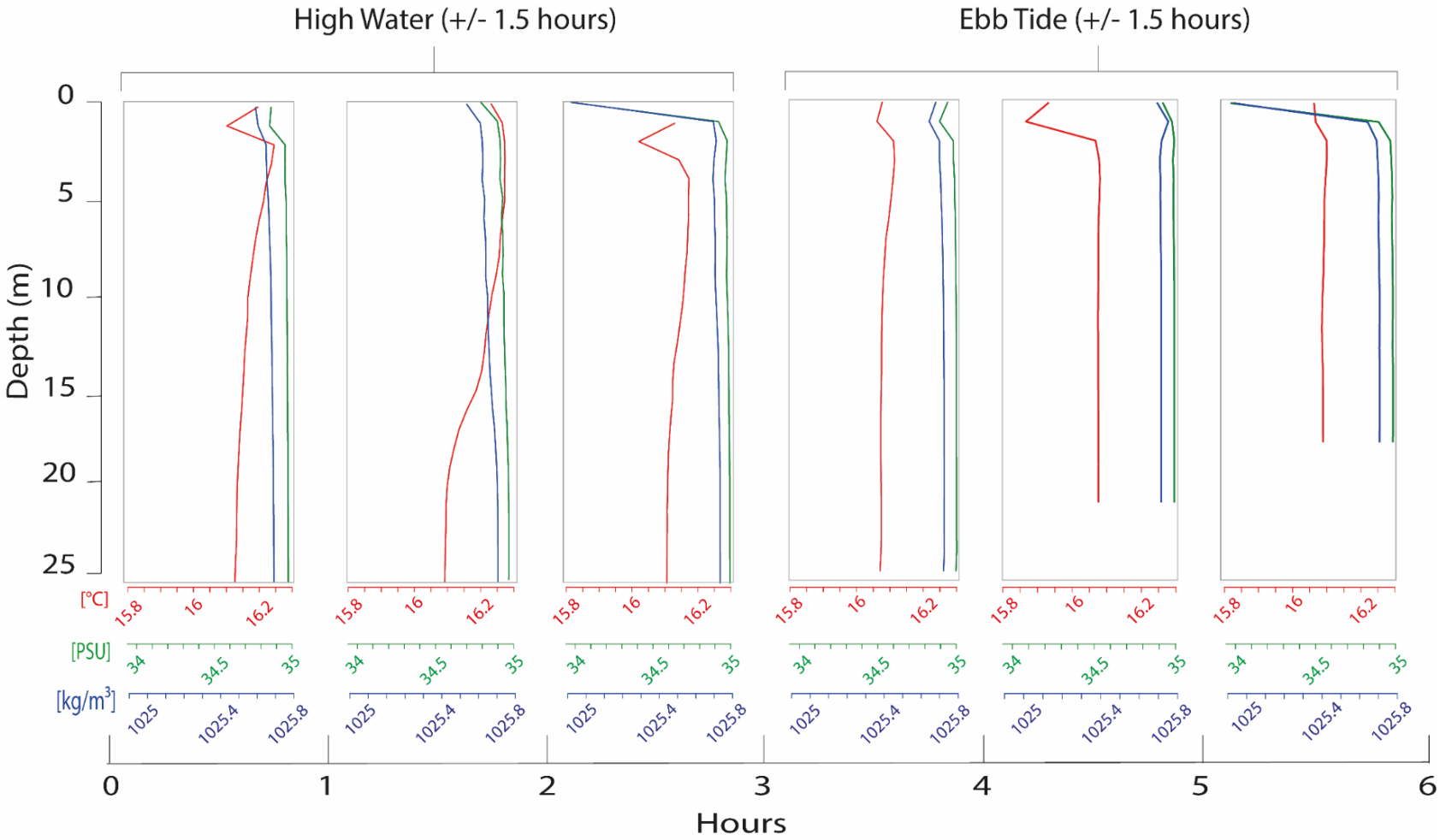

Figure 3.3: Time series of CTD casts of temperature (red), salinity (green) and density (blue) taken from Bigbury Bay, South Devon UK in September 2018 alongside a plankton sampling agenda. Profiles collected at the midpoint of each 1-hour sample collection window

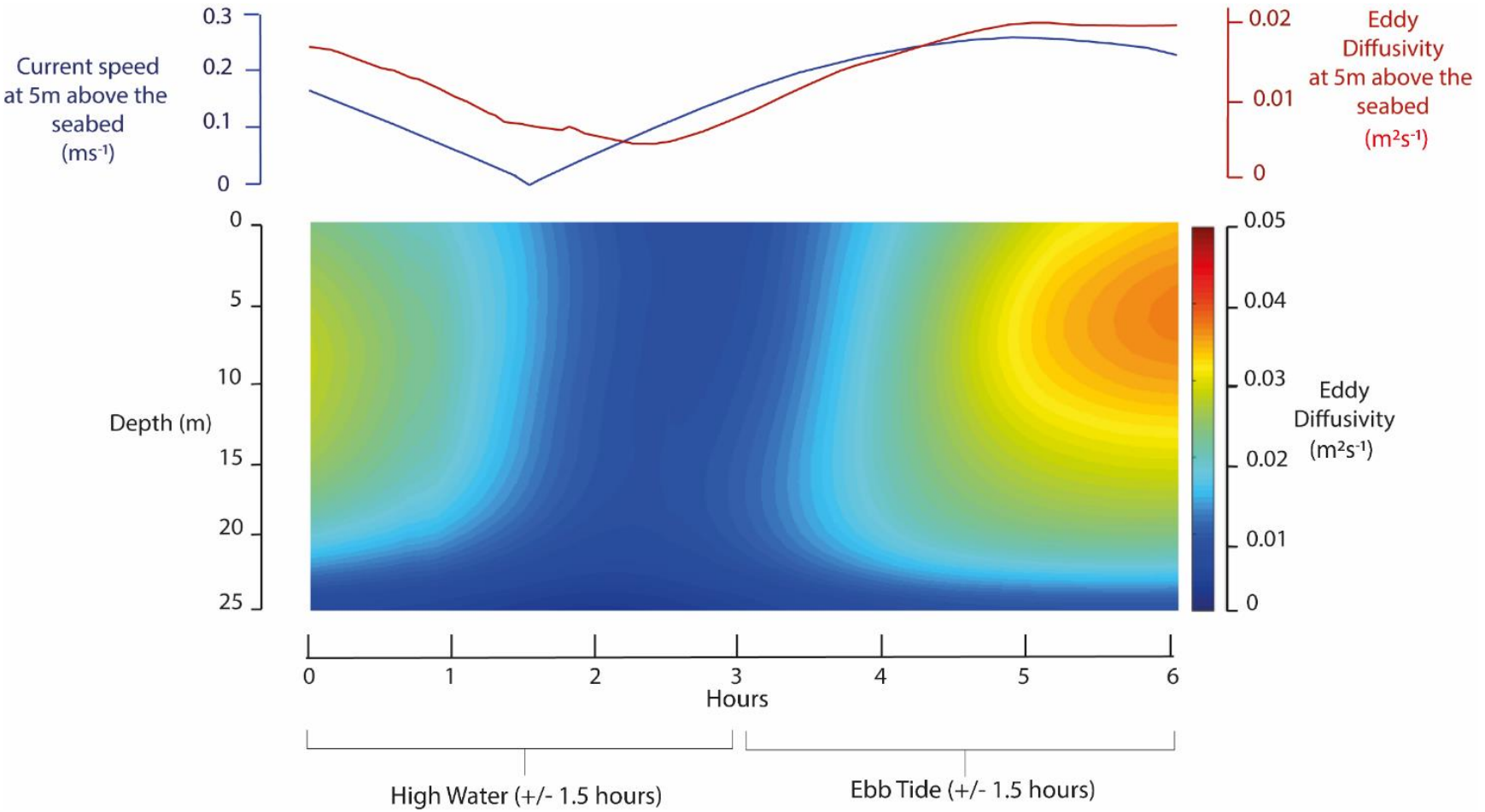

Figure 3.4: Eddy Diffusivity Profile fitted to current speeds collected by an Acoustic Doppler Current Profiler in Bigbury Bay, South Devon, UK in September 2018. Upper graph shows the current speed (taken from the ADCP) at 5m from the bed (blue) and the fitted eddy diffusivity at 5m from the bed (red). Lower graph shows the fitted eddy diffusivity profile over the water column over the sampling period. The x-axis (Time in hours) is shared between both graphs.

3.4.2 Larval abundances

The mean density of bivalves in the samples was 26.8 ± 19.8 m^{-3}. The density of early stage larvae was significantly higher than that of late stage larvae (9.55 more early stage larvae per m^3: $F_{1,2688} = 591.93$, $p < 0.001$) (Fig. 3.5), and the mean density significantly higher during slack high water than during the ebb tide (6.64 more larvae per m^3 at high water: $F_{1,2688} = 284.90$, $p < 0.001$) (Fig. 3.5). There was a significant interaction between larval stage, tidal state and depth bin. There was also a significant interaction between larval stage, tidal state and depth bin for the proportional abundances of larvae ($F_{2,2688}$, $p < 0.001$) (Fig. 3.6).

3.4.3 Comparisons of vertical distribution profiles

At high water slack, no significant differences were observed between the mean proportions of early stage larvae in the surface (36% of all larvae in the water column) and middle waters (40% of all larvae in the water column) (Tukey's HS, $p = 0.052$), but significantly fewer larvae occurred nearer the bed (24% of all larvae in the water column - 12% fewer than at the surface, 16% fewer than in the middle bin: Tukey's HS, $p < 0.001$). During the ebb tide, there were no significant differences in the mean proportions of early stage larvae in the middle and lower depth bins (middle bin 21%, bed bin 21%: Tukey's HSD, $p = 0.998$), and a significantly higher proportion of early stage larvae nearer the surface (58%: Tukey's HSD, $p < 0.001$). The mean proportion of early stage larvae in the surface waters was 22% greater on the ebb tide than at high water (Tukey's HSD: $p < 0.001$), and the mean proportion of early stage larvae in the middle of the water column was 19% greater at high water than on the ebb tide (Tukey's HSD, $p < 0.001$). The proportion of early stage larvae near the bed did not change significantly between tidal states (Tukey's HSD, $p = 0.111$).

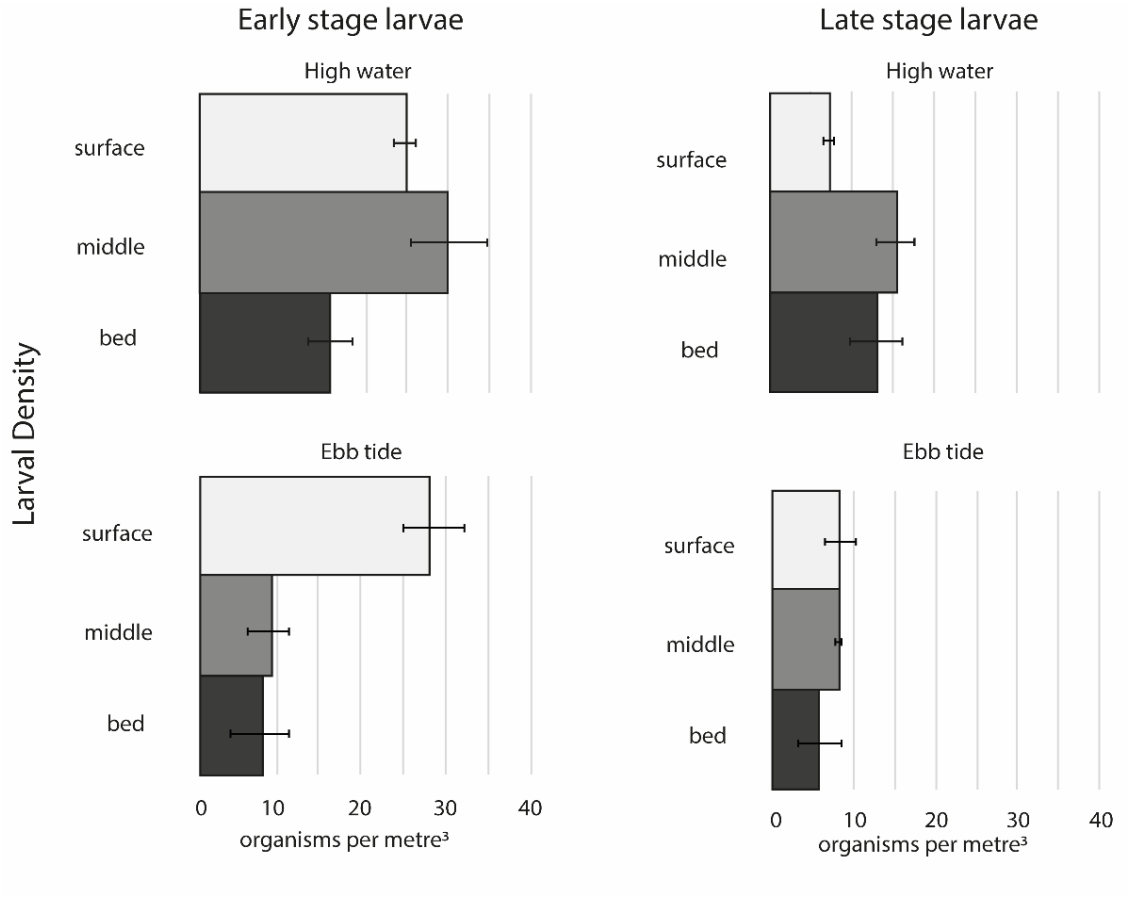

Figure 3.5: Vertical profiles of densities (organisms per metre^3) of early and late stage *Mytilus spp.* larvae at two tidal states: high water and ebb tide. Plots show mean densities (n=6) and error bars show the standard error.

The mean proportion of late stage bivalves was significantly lower in the surface waters than in the middle of the water column (21% fewer larvae: Tukey's HSD, $p < 0.001$) and near the bed (15%: Tukey's HSD, $p < 0.001$) during high water. During this tidal state, the greatest proportion of late stage larvae were found in the middle of the water column 42% of all the larvae in the water column), where the mean proportion of late stage larvae was 21% greater than at the surface, and 6% greater than near the bed (Tukey's HSD, $p < 0.001$). During the ebb tide, the greatest proportion of late stage larvae remained in the middle of the water column (44%), however, in contrast with the high-water distribution, the proportion of late stage larvae near the surface was greater than near the bed (9% more larvae near the surface than near the bed: Tukey's HSD, p <

0.001). No significant differences were observed in the proportional abundances of late stage larvae in the middle depth bin between tidal states (Tukey's HSD, $p = 0.902$), however a significantly greater proportion of late stage larvae were present in the surface waters during the ebb tide when compared to high water (11% more larvae in relation to the total number of larvae in the water column observed at the surface during the ebb tide) (Tukey's HSD, $p < 0.001$), and a greater number of late stage larvae were present near the bed during high water compared to the ebb tide (13% more larvae in relation to the total number of larvae in the water column observed near the bed during high water: Tukey's HSD, $p < 0.001$).

The proportion of early stage larvae in the surface waters relative to the total abundance of early stage larvae in the water column was significantly greater than the proportion of late stage larvae in the surface waters, at both high water (14% greater: Tukey's HSD, $p < 0.001$) and the ebb tide (25% greater: Tukey's HSD, $p < 0.001$). The proportional abundance of late stage larvae in the middle depth bin was significantly greater than the proportion of early stage larvae in the middle depth bin on the ebb tide (23% greater: Tukey's HSD, $p < 0.001$), however, there was no significant difference in proportions of early and late stage larvae in the middle depth bin at high water (Tukey's HSD, $p = 0.908$). A significantly greater proportion of late stage larvae were observed near the bed at slack high water than early stage larvae (12% greater: Tukey's HSD, $p < 0.001$), yet on the ebb tide, no differences in proportions of late and early stage larvae were observed in the bin near the bed (Tukey's HSD, $p = 0.959$).

3.4.4 Regional differences

Comparison of the vertical distribution profiles of both larval stages of bivalves collected from the sample site in the English Channel with profiles of larvae collected from the Irish Sea highlighted significant differences. The proportional abundances of

both early- and late-stage larvae relative to the total number of larvae in the water column were significantly different from the Irish Sea vertical for all tidal state/depth bin combinations (Tukey's HSD, $p < 0.001$ for all), apart from the middle depth bin on the ebb tide, where no difference in the proportional abundance between the two populations was found (Tukey's HSD, $p = 0.26$, $p < 0.001$ for all other combinations). Specifically, the proportion of Irish larvae in the surface waters at high water slack was 7% smaller than the proportion of early-stage larvae in the English Channel (Tukey's HSD, $p < 0.001$), but 7% greater than late-stage English Channel larvae. Proportional abundance in the middle water column at high water was greater than the Irish Sea population for both early-stage (mean difference 11%: Tukey's HSD, $p < 0.001$) and late-stage larvae (mean difference 14%: Tukey's HSD, $p < 0.001$), and proportional abundances near the bed at high water were significantly smaller in the English Channel population (early-stage larvae – mean difference 19%: Tukey's HSS, $p <0.001$; late-stage larvae – mean difference 19%: Tukey's HSD, $p <0.001$). During the ebb tide, the English Channel population demonstrated a greater proportional abundance of larvae in the surface waters compared to the Irish Sea – this effect was much more pronounced for early-stage larvae (mean difference 37%: Tukey's HSD, $p < 0.001$) than late-stage larvae (mean difference 12%: Tukey's HSD, $p < 0.001$). Significantly lower proportional abundances were observed near the bed on the ebb tide in the English Channel compared to the Irish Sea (early-stage larvae – mean difference 18%: Tukey's HSD, $p < 0.001$; late-stage larvae – mean difference 19%: Tukey's HSD, $p < 0.001$), and the proportional abundance of early-stage larvae in the middle water column on the ebb tide was significantly smaller than the Irish Sea (mean difference 20%: Tukey's HSD, $p < 0.001$). Distribution profiles of larvae and vertical shifts in the distribution of larvae between high water and ebb tide for early-stage English Channel larvae, late-stage English Channel larvae and Irish larvae are visualised in Fig 3.6.

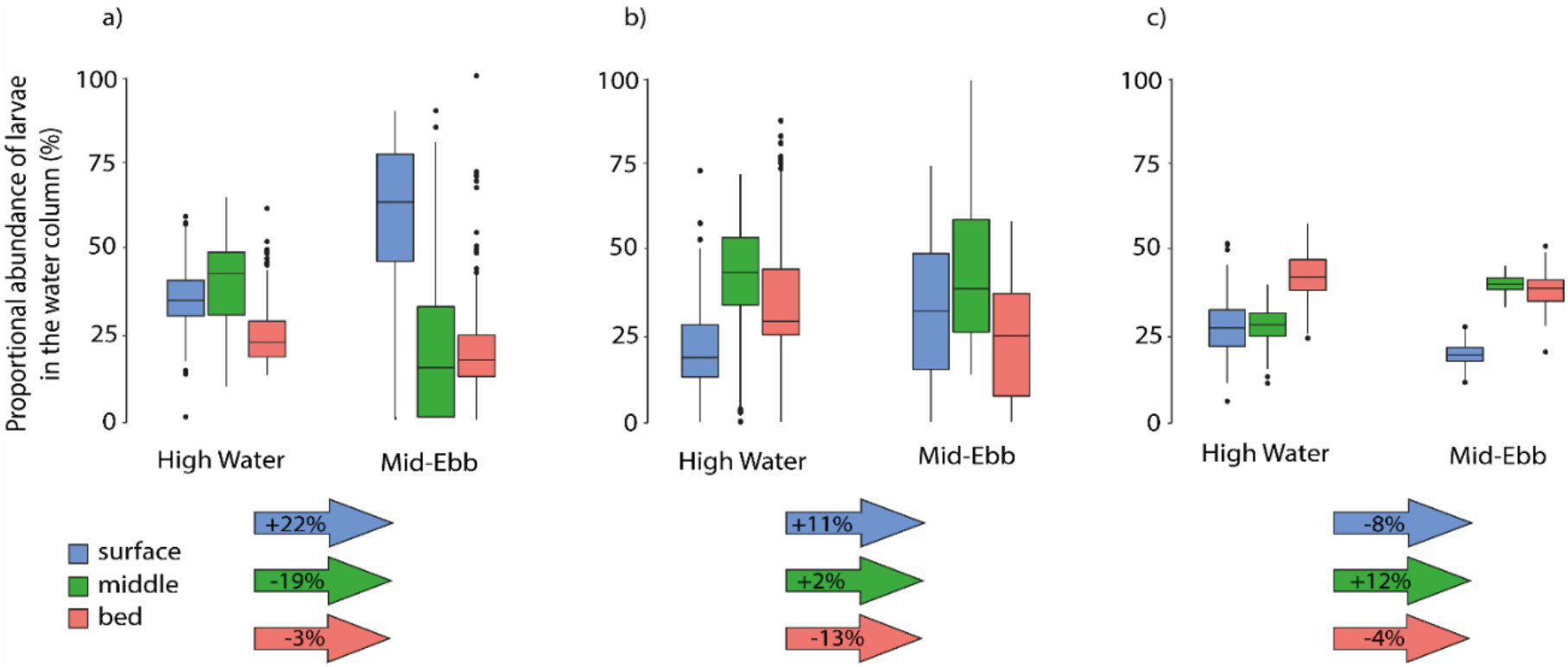

Figure 3.6: Proportional abundances of a) early-stage bivalve larvae collected from the English Channel, b) late-stage bivalve larvae collected from the English Channel and c) Bivalve larvae collected from the Irish Sea (not separated by larval stage as no significant differences observed with ontogeny (Knights et al., 2006) collected +/- 1.5 hour from high water slack (left) and the mid-point of the ebb tide (right). Arrows display the vertical shift in the population required to achieve the change in vertical distribution between high water and ebb tide.

3.4.5 Model fitting to explain larval proportional abundances as a function of their environment

The best fitting-model for both early and late stage larvae included smoothing terms for all tested covariates (Fig 3.7). Model accuracy was increased by fitting thin plate regression splines to all included covariates and was not improved with the removal of any of the covariates. Overall, the best fitting GAMs explained 17.2 % of the variability in proportional abundance of early stage larvae (GCV = 346.57, n = 1350), and 23.9 % of the variability in proportional abundance of late stage larvae (GCV = 290.52, n = 1350) (see Appendix 3). The contribution of the environmental variables to the variance in proportional abundance differed between ontogenetic stages. Eddy diffusivity made the greatest contribution to the variance in proportional abundance of early-stage larvae at 7.84%, followed by water density at 6.83%, then temperature at 2.53% (total variance = 17.2%). In contrast, in late-stage larvae, temperature made the greatest contribution to the variance in proportional abundance at 12.41%, followed by water density at 11.67%, and lastly salinity at 0.09% (total variance = 24%). Although the inclusion of all covariates was deemed necessary to attain the best-fit model in both cases, salinity was shown not to be a contributing factor to the overall variance in proportional abundance of early-stage larvae explained by the model. Similarly, eddy diffusivity did not contribute to the overall variance in proportional abundance of late-stage larvae explained by the model.

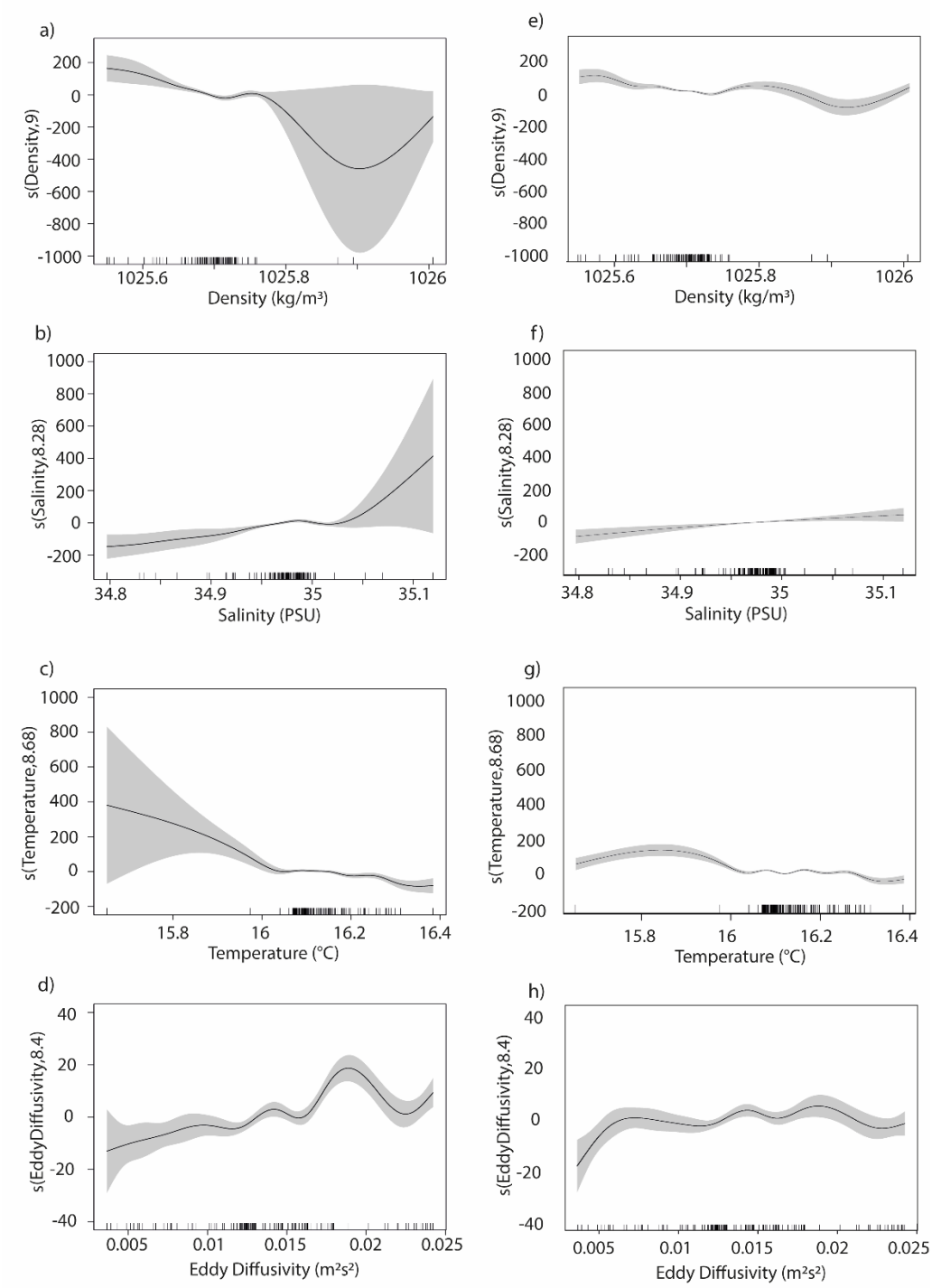

Figure 3.7: Best fit multivariate generalised additive model (GAM) terms displaying the estimated partial effects (smoothed by thin plate regression splines) that density, salinity, temperature, and eddy diffusivity have on the proportional abundance of: early stage (D-veliger) bivalve larvae (a-d), and late stage (pediveliger) bivalve larvae (e-h) in the water column in this study (solid line). 95% confidence intervals are highlighted by grey areas and small lines on the x-axis represent individual data points.

3.5 Discussion

Larval dispersal in marine systems is thought to be influenced by behaviour, resulting in exposure to depth-differentiated current speeds and directions (Knights et al., 2006; North et al., 2008; Shanks, 2009; James et al. 2019). In this paper, we explored how larval vertical distribution profiles change between high water and ebb tide periods and correlate these profiles with environmental features. Here, different vertical distribution profiles were identified in relation to the state of the tide (high water; ebb) and these patterns were dependent on larval ontogenetic stage.

Generalised Additive Models (GAMs) were used to determine larval proportional abundance as a function of the following environmental variables: temperature, density, salinity and eddy diffusivity (i.e. turbulence). All of these factors have been shown to influence larval swimming behaviours in laboratory conditions (Fuchs et al., 2008; North et al., 2008; Podolsky, 1993; Gardener et al., 2004). Here, model compatibility incorporating these factors was generally relatively low, explaining just 17.2% and 23.9% of the variance in proportional abundance of early and late stage larvae respectively. The main factors contributing to the variance were eddy diffusivity at 7.8%, and water density at 6.8% for early stage larvae, and water density at 12.1% and temperature at 11.7% for late stage larvae. Such findings may well be indicative that larval behaviour is governed by many more cues than those tested. Indeed, factors such as light (Ettinger-Epstein et al., 2008; Cisewski et al., 2010; Wahab et al., 2014; Andres-Bragado et al., 2018), conspecific presence (Ettinger Epstein et al., 2008) food availability (Bianco et al., 2011; Fouzai et al., 2015), and soundscapes (Simpson et al., 2011; Lillis et al., 2018) have been shown to influence the directional movement of invertebrate larvae, and coastal topography has been shown to influence vertical

distribution patterns over time (Weinstock et al., 2018). As such, ours GAMs may be limited by the level of included factors.

In coastal environments, stabilising and destabilising forces such as tidal and wind mixing (Hetzel et al., 2015), freshwater runoff (Simpson et al., 1991), the movement of water over heterogeneous topography (Simpson and Hunter, 1974), and surface heating (Simpson and Hunter, 1974) can lead to the stratification and mixing of the water column over a variety of spatial and temporal scales. Indeed, such patterns were observed (albeit weakly) in this study, with the water column becoming stratified over the high-water period and becoming well-mixed during the ebb tide. Discontinuities in both temperature and salinity over depth have been shown in the laboratory to alter the behaviours controlling the vertical movement of larvae in the water column and may act as a barrier to vertical swimming (Daigle and Metaxas, 2011; Lougee et al., 2002; Sameoto and Metaxas, 2008). In this study, gradients in temperature and salinity were small, even when thermo/haloclines had formed (maximum differences over the water column of 0.2°C and 1.2 PSU respectively). Observations of bivalve larvae being unable to cross these features have been shown in the presence of considerably larger gradients (Mann et al., 1991), while being able to freely traverse smaller clines, such that it is unlikely that these gradients would prevent larvae from using active swimming to alter their vertical position in the water column.

The density of the water column contributed to the observed variance in proportional abundance for both early and late stage larvae, however, the mechanism that may be governing this remains unclear. Eddy diffusivity was shown to contribute to the variance observed in the vertical distribution of early stage larvae, but not late-stage larvae, suggesting that larger larvae may have more control over their position in turbulent waters than their smaller counterparts (i.e. Huntley and Zhou, 2004) Bivalve

larvae have been observed in the laboratory to respond to turbulence (Fuchs et al., 2004; Fuchs and DiBaccio, 2011; Wheeler et al., 2013), however, observations have recorded turbulence eliciting a sinking response, with larvae switching from upwards to downwards swimming at a critical turbulence threshold. Larvae in this study increased in the upper water column as the turbulence increased, in contrast to the behaviours predicted by Fuchs suggesting that: a) the critical threshold was not met (unlikely due to the high mixing power in macro-tidal environments like those experienced in the study area); b) larvae are responding to turbulence in a different manner to those observed in a laboratory setting; or c) additional unmeasured variables are acting upon the larvae and influencing their behaviour in-situ that have not been included in laboratory studies of behaviour.

As shown in Knights et al. (2006), the vertical distribution of larvae in this study was highly dependent on the tide, with the proportional abundance of larvae in different depth bins correlating strongly with the state of the tide (Fig. 7). But in contrast to Knights et al. (2006), ontogenetic differences in the vertical distribution profiles of marine bivalve larvae were observed whereby proportional abundances of early-stage larvae in the surface waters are greater than late-stage larvae, regardless of tidal state, and where late-stage larvae show a greater affiliation than early-stage larvae to the middle column during the ebb tide.

There were also significant differences in the overall vertical distribution profiles of larvae collected from the English Channel (this study) and the Irish Sea (Knights et al., 2006). Results suggest that early-stage larvae in the English Channel must migrate from both the bottom and mid-depth waters towards the surface in order to achieve the observed pattern on the ebb tide. Late-stage larvae also appear to exhibit an upwards movement between high water and mid-ebb, however the majority of change for this

population comes from the movement of larvae near the bed (Fig 3.6). In the context of selective Tidal Stream Transport, this is unexpected, as one would assume that late stage larvae to prefer to remain near the bed during the ebbing tide to mitigate their offshore transport and remain in close proximity to suitable habitat (i.e. self-recruitment to a population: Sponaugle et al., 2002). Laboratory experiments suggest a sinking response to strong turbulence by both early and late stage larvae (Fuchs and Dibaccio, 2011), and so it would be expected that larvae experiencing turbulence near the bed would display sinking behaviour. It is possible that larvae near the bed are uplifted by boundary layer turbulence which may overpower their active swimming response (Butman et al., 1988). Recent advances have made studies looking into the impact of turbulent flow on the behaviour of larvae feasible (Fuchs et al., 2013; Wheeler et al., 2013), however the field is still in its infancy. Further work exploring hydrodynamic factors that may act to dampen or prevent larval behavioural responses would definitely provide some useful insights into the mechanisms governing larval vertical distribution patterns.

The net upwards movement of both early and late-stage English Channel larvae differ from the patterns observed in the Irish Sea. In the Irish Sea Study, proportional abundances between high water slack and mid-ebb reduced in both the surface and bottom depth zones and increased in the middle of the water column, suggesting contrasting behavioural responses with depth. Such comparisons between the two populations are anecdotal., as a number of variables such as seasonality (Spring/Summer sampling regime in Knights et al 2006 vs. an Autumnal sampling regime in this study), decadal variation in climate (2005 vs 2019), and local conditions were not controlled for. Both study regions, however, exhibit similar mean current speeds (~0.7ms-1 at the surface: anyTide, National Oceanography Centre), water depth

(25m), and topography, and populations of bivalves, in particular mussels, are ubiquitous in both areas.

Differences in vertical distribution patterns between the two populations suggests either intra-specific or location specific variation in larval behaviours. This has major implications for dispersal studies as it suggests that it may not be appropriate to generalise larval behaviours if models are to present accurate predictions of larval dispersal. We suggest that to achieve the greatest model accuracy, *in-situ* vertical distribution profiles should be collected from the study area prior to analysis of dispersal through modelling, in order to ground-truth local behaviours. Our previous work (James et al., 2019) presents a method by which larval distribution profiles collected from the field can be used to infer behaviours over timescales as small as the sampling regime allows, which can then be applied within modelled environments.

Significant differences in larval densities were observed between tidal states, with a greater number of larvae present in the water column during high water than during the ebb tide. Given the proximity of the study location to the coast, this not surprising, if one was to expect higher densities of larvae off-shore from the observation site. Similar patterns were observed by Knights et al (2006) who suggested that reduced densities on the ebb tide may be due to close association with the sea bed such that larvae are not captured by sampling nets.

This study contributes to already extensive literature showing that vertical distribution profiles of bivalve larvae correspond to the state of the tide (Carriker 1961; Kunkle 1957; Wood and Hargis 1971; Booth 1972; Maru et al. 1973; Andrews 1983; Gregg 2002; Baker and Mann 2003; Knights et al. 2006; Peteiro and Shanks 2015), yet patterns observed differ from previous observations of similar species in a different location (Knights et al., 2006). When attempting to disentangle the drivers of these

profiles, we found that commonly thought-of behavioural cues (i.e. temperature, salinity, density and turbulence) explained relatively little variance in the proportional abundance of larvae observed in the water column at any given time, and as such, these external drivers should be used to determine behavioural 'rules' in biophysical models with great caution. We suggest that, due the complex nature of oceanic environments in which multiple cues are present that have the potential to influence an organism's behaviour at any given time, larval behaviours are likely more idiosyncratic than can be effectively modelled by a 'rule-based' approach, and should instead be considered on a case-by-case basis.

4 A FRAMEWORK FOR ASSESSING THE INFLUENCE OF BEHAVIOURAL PARAMETERISATION ON THE DISPERSION OF LARVAE IN MARINE SYSTEMS

A version of this chapter is currently in preparation as: James, MK, Mayorga-Adame, GC, Knights, AM, Nimmo-Smith, AWM, Howell, KL & Polton, JA A framework for assessing the influence of behavioural parameterisation on the dispersion of larvae in marine systems, for publication in a statistical modelling methodologies research journal, such as Ecological Modelling.

4.1 Abstract

The importance of including behaviour in larval dispersal modelling has gained significant traction, yet, how behaviours are best incorporated to predict patterns in nature remains up for debate. Here, using a coupled three-dimensional hydrodynamic model and a Lagrangian particle tracker, we show how methods of behavioural parameterisation, alongside spatial and temporal hydrodynamic changes, can influence larval dispersal predictions. We compare a novel approach of reverse engineering larval swimming from in-situ observations (REVM behaviours) against simulations adopting passive dispersal (PASSIVE) and particles attributed a tidal vertical migration (TVM) signature. Using statistical models (i.e. LME; GAM and correlation), we test the effects of change in tidal state conditions, season, and planktonic larval duration in conjunction with behavioural parameters on the distance travelled and biogeographic distribution. Our results highlight how the implementation of behaviour within biophysical models can lead to fundamentally different dispersal outcomes, and specifically, that the inclusion of vertical migration behaviour is a mechanism that significantly reduces dispersal distances, but depending on the implementation approach can lead to fundamental differences in dispersal direction. For shorter PLDs (1 day), we find that the inclusion of behaviour does not affect predictions, but for longer PLDs we show that exclusion of behaviour leads to significant overestimates of dispersal, an effect that increases as the PLD increases. Incorrect behavioural parameterisation could lead to mischaracterisation of connectivity and erroneous coastal management strategies.

4.2 Introduction

Many marine species have a bi-phasic life history strategy, whereby they are sessile or display limited movement as adults, while displaying a planktic developmental stage during which they are susceptible to dispersal by ocean currents. This dispersive period

acts to shape patterns of species distribution and governs the connectivity of populations (Levin, 2006; Treml et al., 2012) in a range of taxa including plants (Van der Stocken et al. 2019), fish (Zeng et al. 2019) and invertebrates (Blanco et al. 2019). Yet determining species distribution and population connectivity patterns in the marine environment is often challenging, especially when considering small planktonic organisms due to the obvious difficulties associated with tracking their movement in macro-environments. In contrast to larger organisms, where dispersal studies can be undertaken using visual or GPS tracking (e.g. Olson, 1985), predicting dispersal of micro-organisms requires the use of genetic (Gilg and Hilbish, 2003; Hoey et al., 2020) or geochemical markers (Thorrold et al., 2007), or increasingly, the use of biophysical modelling to predict dispersal based on a combination of hydrodynamics and biological processes (e.g. Levin, 2006; Cowen and Sponaugle, 2009; Swearer et al., 2019).

Biophysical models of larval dispersal can be implemented in a number of ways, adopting relatively simple advection-diffusion models (Hill, 1990; Cowen et al., 2000; Gaylord and Gaines, 2000), or by combining a general ocean circulation model describing local hydrodynamics with an individual particle tracker to incorporate biological traits (e.g. Paris et al., 2013; Schlag and North, 2012; Lett et al., 2008). In recent years, advances in computational power and efficiency have allowed for circulation models to include greater spatial and/or temporal resolution, allowing even complex velocity flow fields over intricate topography to be resolved. Due to this, dispersal modelling using ocean circulation models has become the dominant method of larval dispersal research in order to capture realistic hydrodynamics as experienced by the larvae (Swearer et al., 2019). However, increasingly it is the parameterisation of biological traits assigned to individual particles within the particle-tracking component of the model (traits such as larval duration, mortality and behaviour (Metaxas and

Saunders, 2009) that has received considerable research attention due to the potential of those traits to influence the model predictions (Hill 1990; Cowen et al., 2000; Edwards et al., 2007; Aiken et al., 2007; Phelps et al., 2015; Daigle et al., 2016; Gary et al., 2020) and decouple model predictions from patterns in nature (Marshall et al. 2010, James et al. 2019).

Biological parameterisation has previously relied heavily on the results of laboratory studies and current literature to infer traits, such as planktonic larval duration (Siegal et al., 2003; Aiken et al., 2007; Ross et al., 2016; Munroe et al., 2018) and larval behaviours (North et al., 2008; Daigle et al., 2016; Bode et al., 2019). Typically, larval behaviours such as swimming speed and behavioural triggers are parameterised using directly observed values from the laboratory (North et al., 2008; Robins et al., 2013; Phelps et al., 2015; Daigle et al., 2016; Bode et al., 2019; Gary et al., 2020), or by quantifying swimming speed as a proportion of the critical speed of the organism (again, typically based on laboratory observations of critical swimming speeds). Fifty percent of the critical swimming speed - the maximum speed an organism can actively swim at - is deemed to be a good approximation for the sustainable swimming speed of larvae (Fisher and Wilson, 2004), and has been used to parameterise behaviour by Kobayashi (2006) and Chang et al. (2018). It is argued, however, that this approach may not adequately represent realistic larval behaviours in marine systems, where environmental conditions are more complex than those experienced in controlled laboratory environments. Recent research has endeavoured to bridge the gap between individual larval ability and behavioural manifestation in nature by considering how realistic *in-situ* swimming speeds can best be incorporated within dispersal models (Chapter 2 and in James et al., 2019; Leis, 2020). Results of these studies show that behaviours parameterised through laboratory observations are likely over simplistic and

consequently fail to accurately capture how larvae behave in the field, which in turn can lead to erroneous vertical distribution profiles within the model environment, thus generating under- or overestimations of larval dispersal. It is hypothesised that inaccurate biological parameterisation can lead to a mismatch between estimated dispersal and observed population connectivity (Marshall et al., 2010), and incorrect behavioural assumptions can lead to less accurate predictions of dispersal than models that omit behaviour altogether (Bode et al., 2019).

As biophysical models are frequently used in a range of ecological applications, such as the design of Marine Protected Areas (MPAs), in fisheries management efforts, marine conservation agendas and attempts to minimise the risk of invasive species spread (Botsford et al., 2003; Gaines et al., 2003, 2010; Levin, 2006; Palumbi, 2003), effective decision making relies on model accuracy (Botsford et al., 2009). Accurate descriptors of larval behaviour in dispersal models arguably rely on considering the behaviour of a larvae not as an individual metric but as a product of its environment in any given space and at any given time (Swearer et al., 2019). Studies have clearly demonstrated that larvae can respond to a range of environmental cues (see Kingsford et al., 2002 for a review), and show that larval behaviour is likely a combined response to multiple cues (Morello and Yund, 2016). Thus, the challenge (and limitations) of quantifying larval behaviours in the laboratory becomes 3-fold, namely: (i) recreating the complexity of the natural environment; (ii) determining which cues are being used to govern behavioural manifestation and when, and (iii) identifying the relative importance of each cue to the organism when multiple cues are present. Logically, such challenges can be overcome by studying the larvae in their natural environment.

Although there are logistical challenges associated with inferring larval behaviours from field studies, it is possible through high temporal resolution vertical distribution

sampling regimes (e.g. Dibacco et al., 2001; Knights et al., 2006). In Chapter 2 (and see James et al., 2019), we used *in-situ* observed changes in vertical distribution of mussel larvae *(Mytilus spp.)* from a previous study (Knights et al. 2006) in conjunction with a fine-scale one-dimensional ocean turbulence model (Large Eddy Simulation: Brereton et al., 2019) to infer larval behaviours over the course of a tidal cycle. There, we were able to generate estimates of larval swimming speeds that are not independent of the environmental processes that larvae are exposed to *in-situ* and which allowed replication of vertical distribution patterns in nature. Our conclusion was that the inclusion of swimming behaviours within biophysical model frameworks needs to be more nuanced than adopting a simple 'rules-based approach' if ecological realism is to be achieved (James et al. 2019). For instance, we showed that a change in swimming direction during a tidal state (e.g. during tidal flooding) is needed for models to match *in-situ* patterns; this change would ordinarily not be captured within traditional rules, such as the implementation of a Tidal Vertical Migration (TVM) signature (i.e. upward swimming during flood and downwards swimming during ebb – or vice versa, *sensu* Forward et al., 2003; Kunze et al., 2013). We also identified a 2.5-fold asymmetry in swimming velocities between upward and downward swimming speeds, suggesting differential capacity to utilise vertically stratified horizontal advection for transport (e.g. Knights et al. 2006).

While this earlier study revealed previously undescribed idiosyncrasies in larval swimming over temporal scales ordinarily not considered, the effect(s) of these nuanced 'behaviours' on dispersal predictions have yet to be evaluated i.e. do they actually make a difference to dispersal predictions? Here, we explore how the results of our previous study propagate through larval dispersal estimations made by a biophysical model in relation to behavioural parameterisation determined by both the assumption of passive

particles and a TVM approach based on 'rule-based' behaviours. We achieve this by tracking virtual 'larvae' assigned no swimming behaviour (i.e. passivity) versus larvae assigned one of two swimming behaviours (i.e. TVM and reverse-engineered vertical migration (herein referred to as REVM)) within a hydrodynamic model framework over a 28 day planktonic larval duration period and comparing the influence of time of release (season and tidal state) and behaviour characterisation on the distance travelled by particles, their resultant dispersal kernels and biogeographic dispersal patterns.

4.3 Methods

4.3.1 The study area

The underlying data driving the reverse-engineering approach applied in James et al. (2019) were derived from Knights et al. (2006) and the original *in-situ* data were collected in the southern Irish Sea. Here we assess the implications of behavioural parameterisation in a modelling framework by coupling a particle tracking model to an ocean circulation model of the same region. For this study, a cut-out of the full NEMO AMM7 hydrodynamic model restricted to the Southern Irish Sea (51°N to 55N and 12°W to 2°W) was used (Fig. 4.1). Water depths in this region are typically less than 100 m, although depths can reach up to ~150 m in the central channel and tidal flows typically oscillate in the North-South direction (see Fig. 4.1). The Irish Sea represents a typical semi-enclosed tidally influenced coastal basin with dynamical length scales of 10-1000 km), and as such, the findings of this study are applicable to other analogous ecosystems.

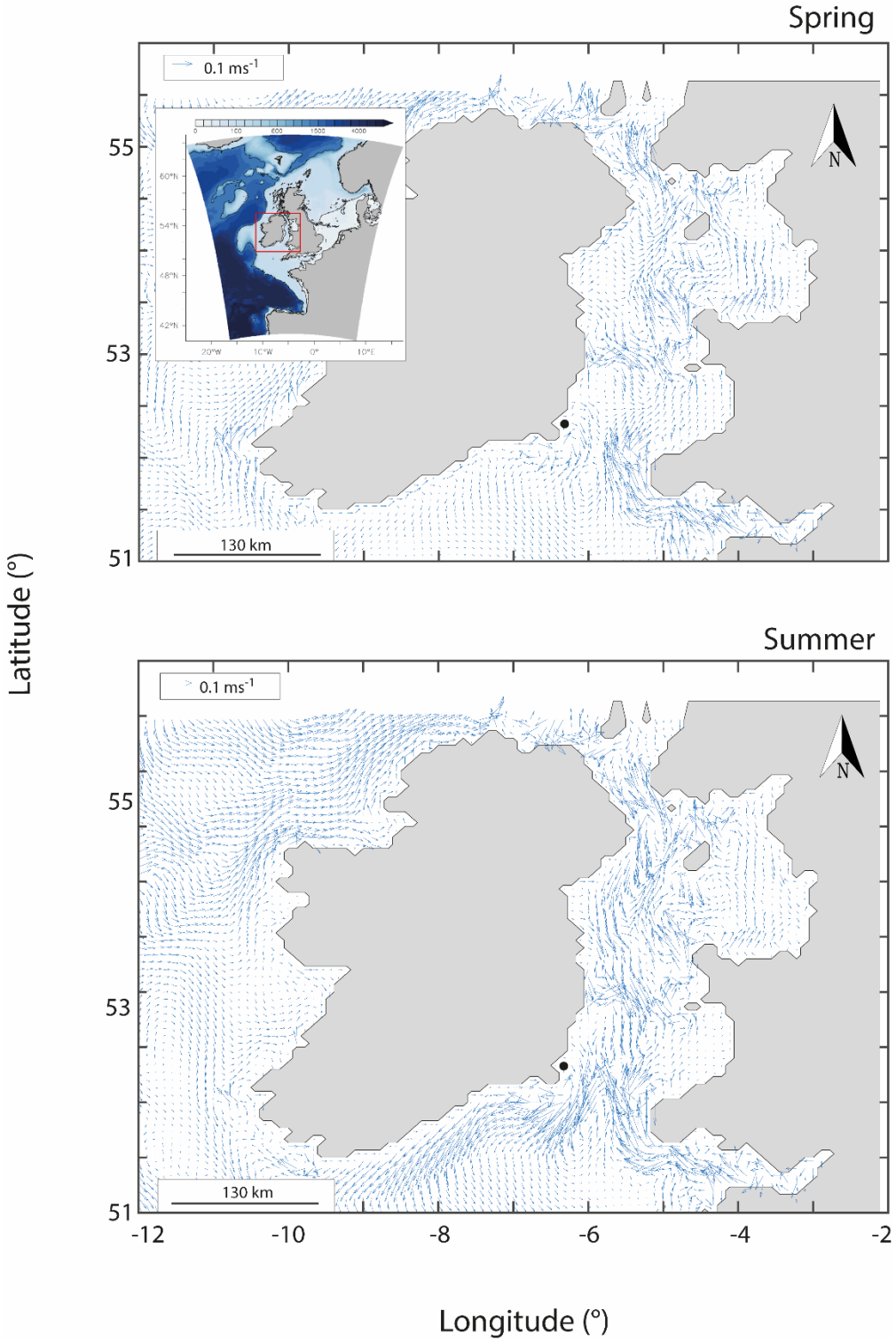

Figure 4.1: Mean tidal flows for Spring 2005 (April 1st – June 30th) and Summer 2005 (July 1st – September 30th) as depicted by NEMO AMM7. Inset shows the domain of the AMM7 configuration of the NEMO hydrodynamic model with bathymetry in metres (colourscale bar) (Taken from Warner et al., 2005). Red box inside inset denotes the location of the model domain cut-out within AMM7. Location of the *insitu* sampling regime undertaken by Knights et al. (2006) on which reverse engineered behaviours were calculated (James et al., 2019) is marked by a black dot. This location was also the location for the seeding of particles within the model.

4.3.2 The hydrodynamic model

The Coastal Ocean Version 5 European North-West shelf configuration (CO5) of the Atlantic Margin 7km Model (AMM7), produced using the Nucleus of European Modelling of the Ocean (NEMO) general ocean circulation modelling framework was used to simulate the hydrodynamics of the Irish Sea (see O'Dea et al. 2017). This model domain encompasses the entire north west European shelf region, though in this study we focus on an Irish Sea subregion. The NEMO AMM7 model was developed by the Met Office in collaboration with the National Oceanography Centre and has been extensively refined and validated against observations for the UK shelf seas region so it is warranted to be a good representation of the coastal ocean for the study region. This model resolves prognostic variables (velocity, turbulence, salinity, temperature) on a curvilinear orthogonal horizontal grid with a horizontal resolution of approximately 7 km, and a vertical grid derived from 51 stretched-σ levels with realistic GEBCO bathymetry (Madec et al., 2016; O'Dea et al., 2017). It includes atmospheric (ERA-interim), tidal (TPXO7.2), and open boundary (ORCA0083) forcing, providing realistic 3-dimensional current velocities.

Model output for the study domain was generated for a 6-month period from 1st April 2005 to 31st September 2005, chosen to coincide with the timeframe of an *in-situ* sampling programme undertaken by Knights et al. (2006). Hourly velocity field outputs were adopted in order to capture the strong tidal flows present in the Irish Sea (Brown et al., 2003).

Two additional variables ('stateid' and 'tchange') were created in MATLAB (v. 2020a) and appended to the NEMO output file. These variables were created in three dimensions (longitude (x), latitude (y) and time (t)). The 'stateid' variable described the state of the tide (x,y,t) using four classification integers: (1) first half flood (low water

slack to mid-point of the flood tide); (2) 2nd half flood (mid-point of the flood tide to high water slack); (3) 1st half ebb (high water slack to the mid-point of the ebb tide) and, (4) 2nd half ebb (mid-point of the ebb tide to low water slack). The 'tchange' variable was used to describe the number of seconds until the tidal state at (x,y,t) was due to change from one 'stateid' classification to another. This was calculated by first calling the hourly sea surface height (SSH) data from the NEMO model output file at (x,y,t-4:t+4), which was then interpolated from hours to minutes, followed by fitting of a cubic spline. Local maxima (high tide) and minima (low tide) were then identified within the interpolated SSH dataset, and midpoints of the flooding and ebbing tide determined as the time-points halfway between the time-points of the slack tides. The resultant variable 'tchange' provided the number of seconds between the model timestep and the next consecutive change in tidal state, so that tidal changes occurring within the 1-hour model output frequencies are accounted for.

4.3.3 The particle tracking model

Particles were tracked using a version of the Lagrangian TRANSport model (LTRANS v.2: Schlag and North, 2012), modified to be forced by the offline output of the NEMO model and larval behaviours governed by the 'stateid' and 'tchange' variables. LTRANS is an offline individual-based particle tracking model that runs with the stored predictions of a 3D hydrodynamic model, tracking the trajectories of particles in three dimensions based on advection, diffusion and individual particle behaviours. The model includes a 4th order Runge-Kutta scheme for the advection of particles and a random walk, scaled by the spatially and temporally variable vertical viscosity coefficient of the underlying hydrodynamic model, to simulate vertical movement due to turbulence at sub-grid scales (Visser et al., 1997; Ross and Sharples, 2004).

Preliminary convergence testing was undertaken to determine the appropriate number of particles to be released within the model. This test was a simple experiment following (Robins et al., 2013). Initially, 100,000 particles were released from a single location point (the *insitu* sampling point of Knights et al., 2006) and the number of particles in each grid cell calculated after 30 days. Following simulations were then undertaken, reducing the number of particles to 50,000, then 10,000, then 5000, and the proportion of the cohort in each grid cell calculated. Simulations were considered significantly different if the proportion of larvae in the grid cells deviated by more than 10% of the original simulation with 100,000 particles. Results indicated that simulations with 10,000 particles were sufficient to capture variation within the population whilst maintaining computational efficiency, with no discernible difference in outcomes between simulations run with 10,000 and 100,000 particles. Other studies in the same domain (e.g. Robins et al., 2013) have used a similar number of particles.

4.3.4 Swimming behaviours

Larval behaviours can be specified within LTRANS via the behaviour sub-routine. Modifications were made to the behavioural sub-routine to test two active swimming behaviours. (1) Applying a tidal vertical migration (TVM) whereby individuals are parameterised to swim up during the flood tide and down during the ebb tide at a fixed rate of $0.001 ms^{-1}$ in alignment with values in the literature (Chia et al. 1984; Sprung, 1984; Young, 1995 and values used by other biophysical modelling studies focussing on bivalves (e.g. Robins et al., 2013; Daigle et al., 2016)). (2) Reverse-engineered swimming behaviour (as described in Chapter 2 and James et al., 2019), in which virtual larvae were configured to swim at a random speed taken from a normal distribution profile fitted over the Modelled Predictive Capability (MPC) for a range of swimming speeds for each tidal state (means and standard deviations of the MPC are given in

Table 4.1). The methodology is discussed in greater detail in Chapter 2 (section 2.3.6: assessing model compatibility) and in James et al. (2019) but briefly, the MPC describes the results of two-way ANOVAs and planned F-test comparisons between the simulated vertical distribution of larvae by the model and in-situ vertical distribution profiles of larvae from Knights et al. (2006). P-values of the interaction term provided a quantifiable continuous measure of compatibility between the observed data and the model outcome - the model predictive capability (MPC) - with values ranging from 0 (complete incompatibility) to 1 (perfect compatibility). The model is considered not significantly different from the observed data at a significance level of 0.01 after Bonferroni correction (James et al. 2019). For the period ranging from high water to mid ebb, where the predictive capability of the model was low across all swimming speeds using the reverse-engineering approach ($p < 0.05$ for all tested swimming speeds), particles were configured to swim downwards at a fixed rate of $0.0011 ms^{-1}$, as to match the lowest total sum of squares of the proportional difference (i.e. our 'best guess') calculated between the field observations of larval vertical distribution and the models run in James et al. (2019). For completeness, the 'active' TVM and REVM behavioural models were compared with passive model simulations with no larval behaviour described.

Table 4.1: Mean and standard deviation of a normal distribution curve fitted to the Model Predictive Capacity after James et al. (2019) for 4 tidal periods: low water slack to mid flood, mid flood to high water slack, high water slack to mid ebb, and mid ebb to low water slack.* denotes a tidal period where the MPC was unresolved for all tested swimming speeds.

Tidal Period	Mean swimming speed (mms^{-1})	Standard Deviation
Low water slack to mid flood	2.06	0.5
Mid flood to high water slack	-0.91	0.2
High water slack to mid ebb	*	*
Mid ebb to low water slack	-0.76	0.07

At each modelled hour, LTRANS was configured to read the variables ‘stateid’ and ‘tchange’ from the underlying hydrodynamic model and larvae were assigned behaviours dependent on the current state of the tide. The ‘tchange’ variable was used so that if a change in the state occurred during the modelled hour, larval behaviour changed at this point, rather than during the consecutive timestep. This approach of quantifying the tidal state in space and time was chosen over simpler methods of determining the tidal state (i.e. using tidal charts and a time counter within the model: *sensu* Daigle et al., 2016), as at a single time-point (e.g. 'Hour 1'), the tidal state could be fundamentally different depending on its position within the study domain (see Figure 4.2) resulting in different behavioural responses in both space and time.

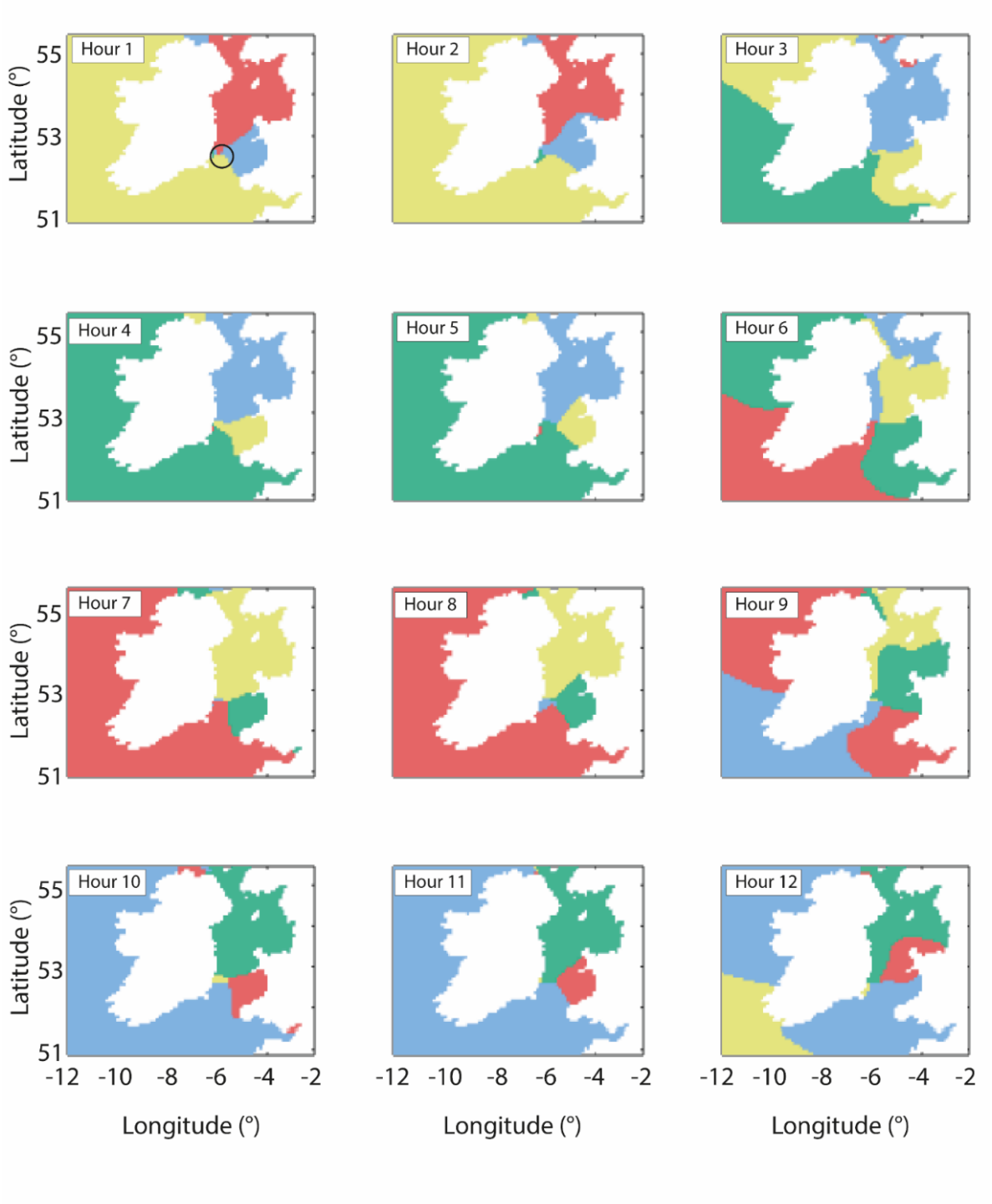

Figure 4.2: An illustration of tide propagation around an amphidromic point (location circled in first plot) in the Irish Sea over a 12-hour window highlighting spatial variation in the tidal period. Four tidal states periods are shown: low water slack to mid flood (blue); mid flood to high water slack (yellow); high water slack to mid ebb (green) and; mid ebb to low water slack (red).

4.3.5 Particle release and tracking

Particles were released within the model at the location of *in-situ* sampling (52.2N, 6.15W; Knights et al., 2006) Particles were released following observed proportional distribution patterns for each tidal state, binned according to the vertical grid of the hydrodynamic model (following the methodology of Daigle et al., 2016), and individual runs were undertaken for each starting profile. Runs simulating each of the three behavioural parameterisation approaches (namely: Passive, Tidal Vertical Migration (TVM), and Reverse-Engineered Vertical Migration (REVM), were simulated during the spring (April) and summer (July) to account for potential differences in dispersal due to seasonal stratification as there is a known frontal system that develops in the Southern Irish Sea (Neill et al., 2012). The full list of all simulations undertaken is shown in Table 4.2. As no difference was observed in the vertical distribution patterns of larvae with respect to tidal phase (i.e. neap vs. spring) in the field (Knights et al., 2006), phase was not considered here. Particles were released on the first spring tide following April 1st (spring) or July 1st (summer). Particles were tracked for a duration of 28 days, which is within the typical range of ciliated larvae (Siegel et al. 2003; Hartnett et al. 2007; Tian et al. 2009). LTRANS was configured to output the location (lat/lon) and depth of each particle every 30 minutes. Output files were then processed in MATLAB (v. 2020a) to calculate (i) radial distance travelled by the particle from its source to its end point, and (ii) the cumulative distance travelled by the particle (i.e. the total path length), every 30 minutes.

Table 4.2: Design of the study capturing starting variation in tidal state, season and larval behaviour in individual simulations in LTRANS.

Simulation ID	Behaviour	Season	Release Tidal State
1.1.1	Passive	Spring	flood tide
1.1.2	Passive	Spring	high water slack
1.1.3	Passive	Spring	ebb tide
1.1.4	Passive	Spring	low water slack
1.2.1	Passive	Summer	flood tide
1.2.2	Passive	Summer	high water slack
1.2.3	Passive	Summer	ebb tide
1.2.4	Passive	Summer	low water slack
2.1.1	TVM	Spring	flood tide
2.1.2	TVM	Spring	high water slack
2.1.3	TVM	Spring	ebb tide
2.1.4	TVM	Spring	low water slack
2.2.1	TVM	Summer	flood tide
2.2.2	TVM	Summer	high water slack
2.2.3	TVM	Summer	ebb tide
2.2.4	TVM	Summer	low water slack
3.1.1	REVM	Spring	flood tide
3.1.2	REVM	Spring	high water slack
3.1.3	REVM	Spring	ebb tide
3.1.4	REVM	Spring	low water slack
3.2.1	REVM	Summer	flood tide
3.2.2	REVM	Summer	high water slack
3.2.3	REVM	Summer	ebb tide
3.2.4	REVM	Summer	low water slack

4.3.6 Statistical Analysis

All analyses were undertaken in R (R Core Team, 2020). A Linear mixed effects (lme) model in the R package 'nlme' (Pinheiro et al. 2020) was used to test the effects of four fixed variables on mean distance travelled by a particle. Model factors were: (1) **Behaviour** (levels: Passive; Tidal Vertical Migration; REVM); (2) **Season** (levels: Spring; Summer); (3) **Tidal State at Release** (levels: flood; low water slack; ebb; high water slack); and (4) **Prediction** (levels: radial distance; cumulative distance). **Time** (days) was included as a random variable, and an autocorrelation structure (AR(1)) applied following identification of temporal/spatial autocorrelation using the auto-correlation function (ACF, package 'nlme'; Pinheiro et al. 2020). A stepwise model reduction approach based on Akaike Information Criterion (AIC; Sakamoto et al. 1986) scores was used to identify the best-fitting model.

We also used Generalised Additive Models (GAMs) to assess relationships between behaviour, tidal state, and season and their effect on radial distance and cumulative distance over a 28-day planktonic larval duration. The GAM modelling incorporated fitting a smooth function to the timestep covariate (days since release) and followed a gamma distribution for each of the response variables. GAM models were fitted using the R package 'mgcv' (Wood, 2011).

Pettitt's test (Pettitt, 1979) was used to estimate the mean time point for a shift in central tendency in radial distance over the time series, using the R package 'trend' (Pohlert, 2020). Pettitt estimates from model simulations were then compared using one-factor ANOVA on a randomised normally distributed sample (n=100 using the rnorm() function in R) of values based on the mean and standard deviations of the Pettitt's test outcome.

Additional descriptive statistics, specifically the mean, median, standard deviation, and interquartile ranges were used also to describe the dispersal kernels of passive, REVM and TVM particles at 1, 7, 14, 21, and 28 days. ANOVA and Tukey post-hoc pairwise comparison tests were used to compare the mean radial distances travelled for each explored timepoint and Mood's Pairwise median tests (Mood, 1954) used to formally compare kernel medians of model outputs.

Lastly, the 'meanm' function was used in MATLAB (v.2020a) to calculate the central tendency of the dispersal cloud as a lat/long coordinate for each season (spring/summer), behaviour (passive/reverse-engineered/TVM) and day (1, 7, 14, 21, 28 days) combination, and the Euclidean distance between central tendencies was calculated in R using the 'sp' package (Pebesma and Bivand, 2005). The 'cor' function in R was used to calculate the correlation between the central tendencies and correlation plots were formally tested using Spearman's rank correlation coefficient (Spearman, 1904).

4.4 Results

4.4.1 LME modelling

There was a significant interaction between behaviour and prediction method ($F_{2,188}$ = 6.162, $p < 0.01$) on mean dispersal distance. No other interactions were significant ($p > 0.05$: Appendix 4). Mean radial and cumulative distances after 28 days were greatest in passive simulations, travelling on average, 79 km from source, and 1359 km along their path, respectively. Reverse-engineered particles travelled considerably shorter distances, travelling a mean radial distance of 33.7 km (2.3× shorter), and a mean cumulative distance of 359 km (3.8× shorter). Notably, mean radial distance of reverse-engineered particles increased by only 1.6 km between 14 and 28 days, with no significant

difference in the radial distances between 14 and 21 days (Tukey's HSD: p = 0.329). TVM particles travelled a mean radial distance of 52 km (+1.5× REVM; -1.5× Passive) after 28 days, and a mean cumulative distance of 1024 km (+2.9× REVM; -1.3× Passive) (Figure 4.3).

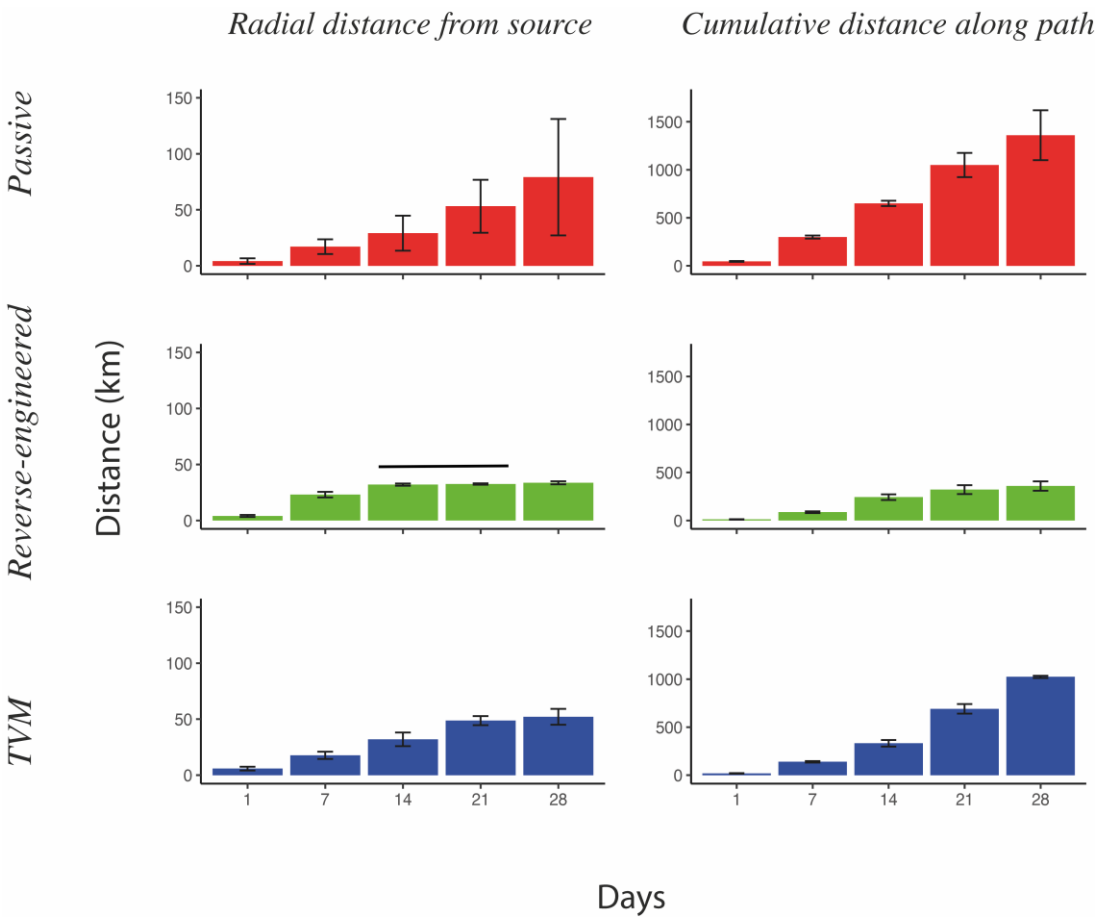

Figure 4.3: **Left**: Comparison of the distance travelled 'as the crow flies' from a single point source location (radial distance ± SD), and **Right**: the mean distance travelled by particles along their dispersal path (cumulative distance ± SD) after 1, 7, 14, 21 and 28 days planktonic duration.

4.4.2 GAM fitting and identifying points of change

In general., GAM models were a good fit, with behaviour, season, and tidal state explaining 75.7% of the deviance in radial distance travelled by particles from their source, and 97% of the deviance in cumulative distance travelled by particles along their

dispersal path (Appendix 5 and 6). All incorporated covariates could significantly predict radial distance travelled from source (Appendix 5). Results demonstrated that both radial distance and cumulative distance path clearly differed with respect to behaviour and season, however, seasonal effects were only apparent in passive model simulations, and not 'behaving' models (Figs 4.4 and 4.5) and significant differences were observed in the estimates among experiments. Additionally, differences were only found between tidal state in the passive model, whereby particles travelled the greatest radial distance from source yet travelled the shortest cumulative distance when released on the ebb tide (Figs 4.4 and 4.5).

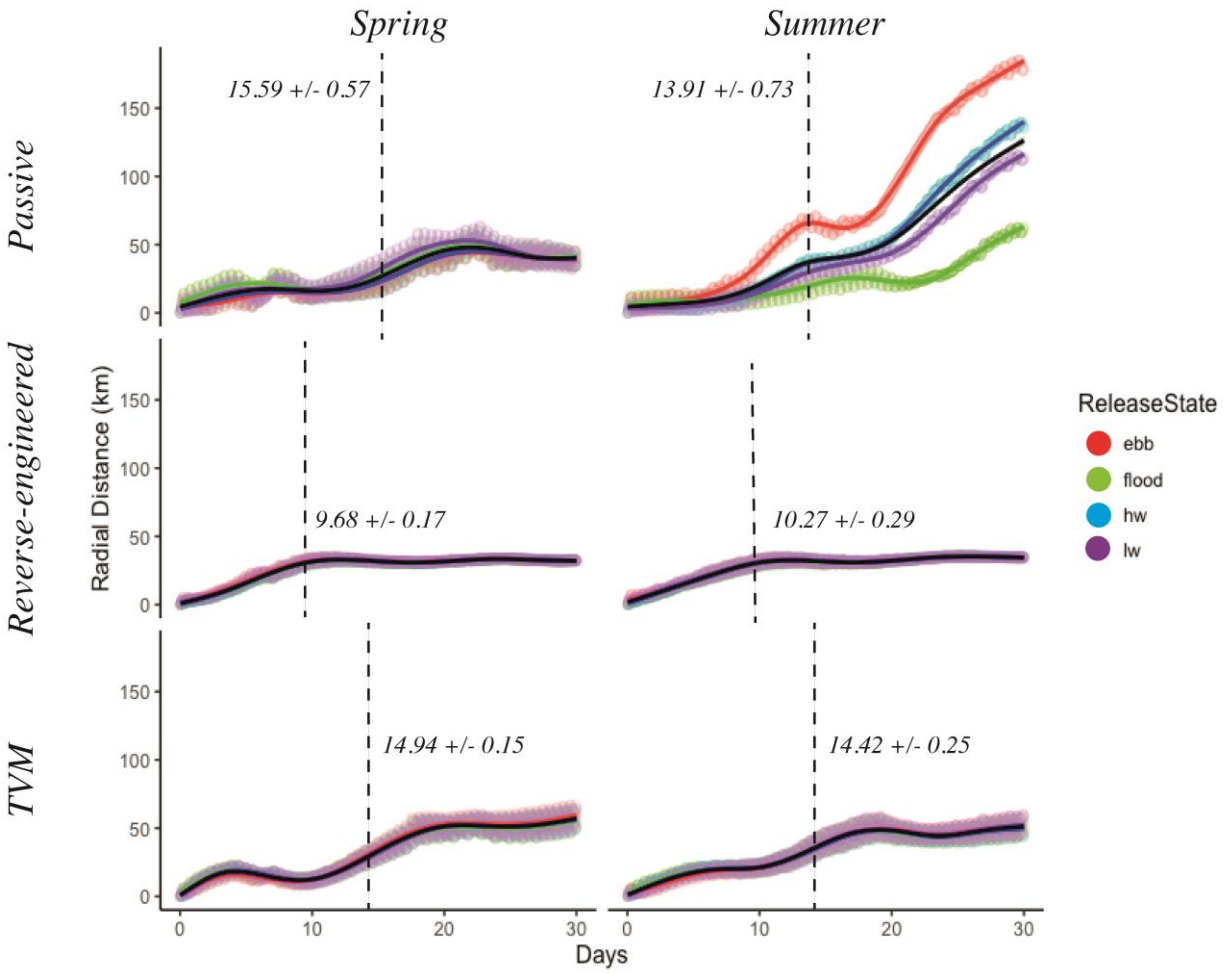

Figure 4.4: Fitted Generalise Additive Model (GAM) of radial distance from source over time (Days) grouped by behavioural modelling (3 levels: passive, reverse engineered, tidal vertical migration), season (2 levels: Spring (April) and Summer (July)) and tidal state at release (4 levels: flood tide, high water, ebb tide, low water) (n = 10,000, N=240,000). The black line is the mean fitted GAM summarising the response for all release states, and colours indicate individual tidal state GAMs. Vertical dashed lines indicate the estimated mean time point for a shift in central tendency of the time series based on Pettitt's test outcomes.

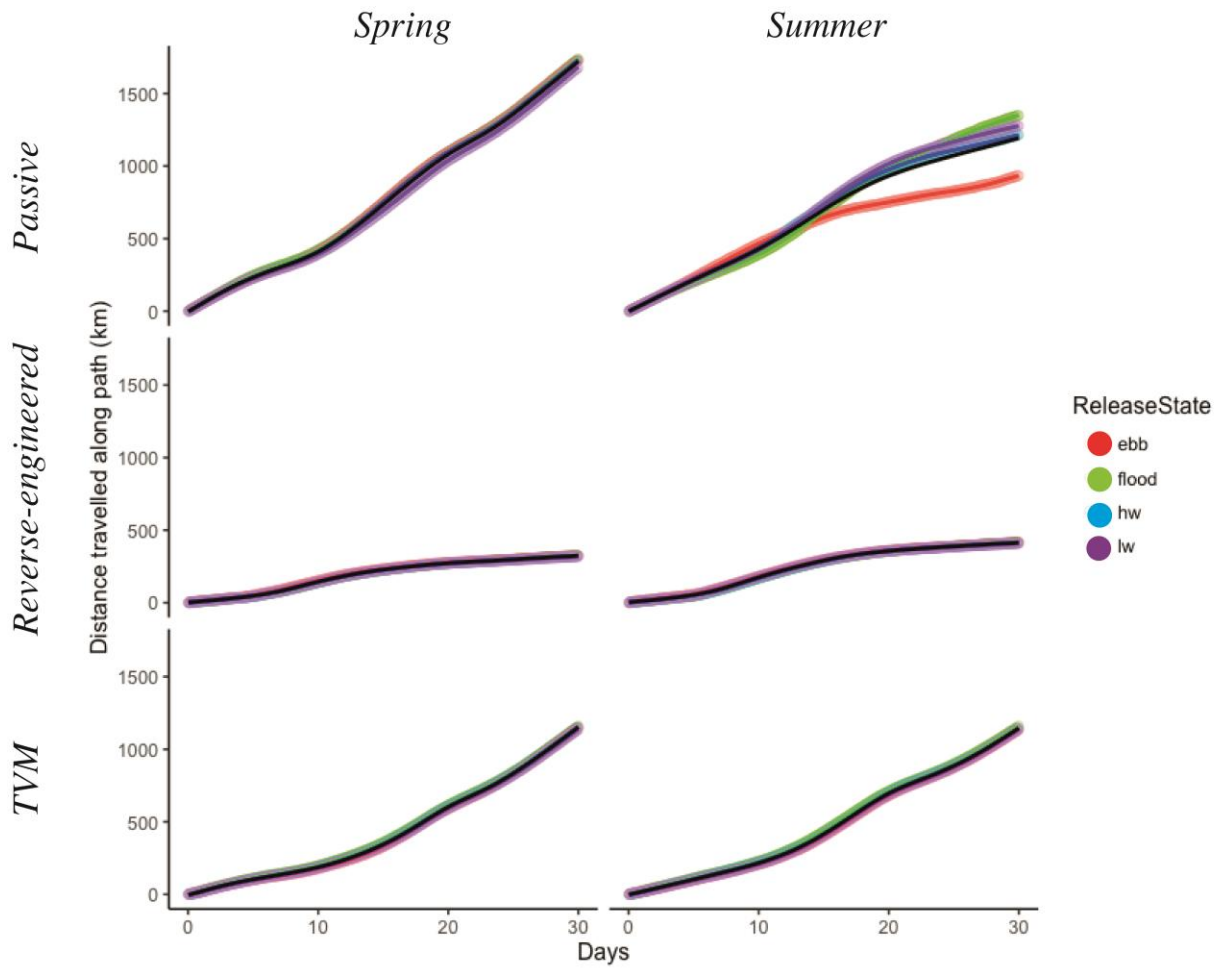

Figure 4.5: Fitted Generalise Additive Model (GAM) of cumulative distance travelled by a particle along its path over time (Days) grouped by behavioural modelling (3 levels: passive, reverse engineered, tidal vertical migration), season (2 levels: Spring (April) and Summer (July)) and tidal state at release (4 levels: flood tide, high water, ebb tide, low water). N = 34584. The black line is the mean fitted GAM summarising the response for all release states, and colours indicate individual tidal state GAMs. Vertical dashed lines indicate the estimated mean time point for a shift in central tendency of the time series based on Pettitt's test outcomes.

Analysis of the estimated mean time point for a shift in central tendency of the time series following Pettitt's test indicated significant differences in the point of change for each behaviour × season interaction combination (Figure 4.6): (Tukey's HSD: $p < 0.001$) for all pairwise comparisons). Passive particles released in the spring exhibited the latest shift, occurring at 15.59 ± 0.57 days, which occurred 1.7 days earlier in the summer (13.91 ± 0.73 days). The shift in central tendency of the TVM model occurred at 14.92 days (± 0.15 days) and 14.42 days (± 0.25 days) in spring and summer, respectively. Reverse-engineered particles exhibited a shift in central tendency after just 9.68 days (± 0.17 days) in spring, but unlike the passive and TVM models, showed an increase to 10.27 days (± 0.29 days) in summer.

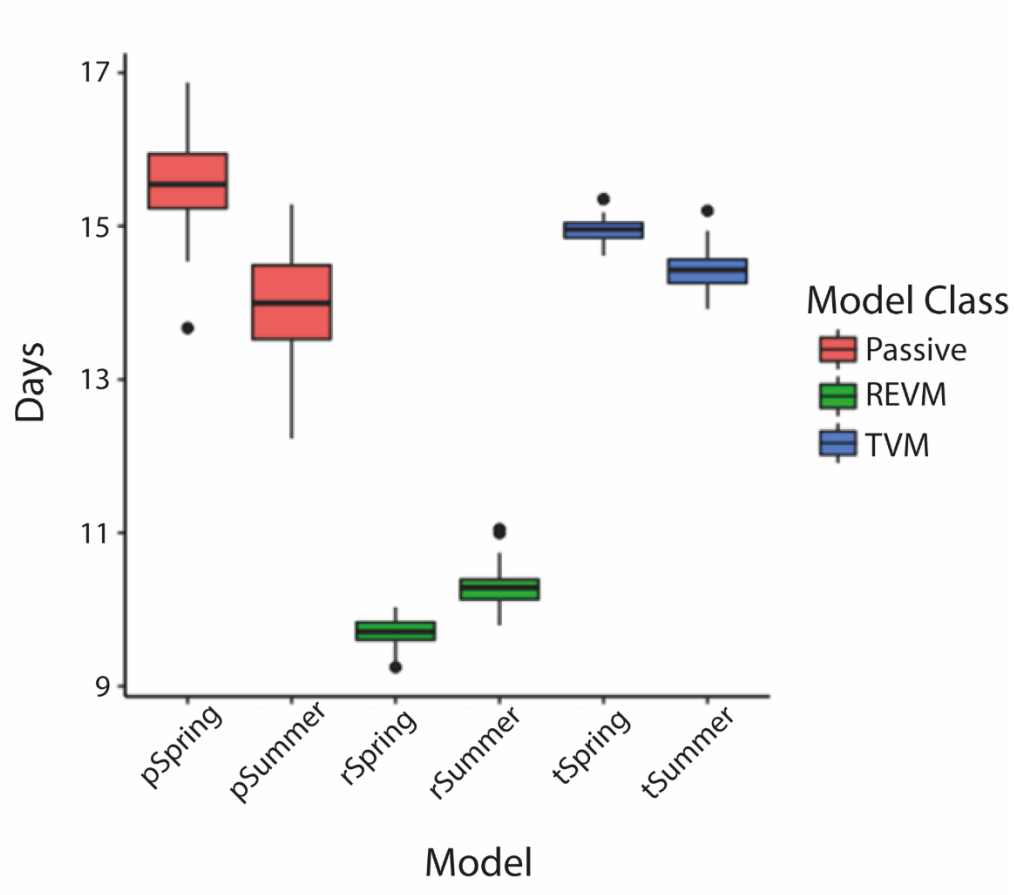

Figure 4.6: Distribution of estimates of shift in central tendency (days) of the time series following Pettitt's test for each of behaviour × season model combination. Random sample distributions (n = 100) generated using the rnorm() function based on estimates of Pettitt mean and standard deviation. All groups significantly different ($p < 0.001$).

4.4.3 Density kernels (probability density functions)

Comparison of the dispersal kernels revealed differences between models over time (Fig. 4.7). After 24 modelled hours, differences in the dispersal distance between behaviours were small. TVM particles travelled 1.8 km farther from source than reverse-engineered particles, and 1.7 km farther from source than passive particles (Table 4.3). The median distance travelled by TVM particles (5.3 km) was 1.4 km and 1.5 km greater than reverse-engineered and passive particles respectively (Figure 4.7: 1 day).

After 1 modelled week, the mean dispersal distance of reverse-engineered particles was significantly greater than passive or TVM models (Tukey's HSD, $p < 0.001$ in all cases) by 5.4 km and 6 km respectively (Table 4.3). Reverse-engineered particles also exhibit a significantly greater median distance at this time point than passive (4.8 km difference: Mood's median test, $p < 0.001$) and TVM (4.9 km difference Pairwise Moods median test, $p < 0.001$). There was no difference in median distance between passive and TVM particles ($p = 0.734$) (Figure 4.7: 7 days)

At 14 days, post-hoc testing showed no difference in the mean dispersal distance of reverse-engineered and TVM particles (Tukey's HSD, $p = 0.774$), however a significant difference of 0.5 km was observed in the median distance travelled (Pairwise Moods median test, $p < 0.001$: Table 4.5). Reverse-engineered particles showed greater radial distance clustering (SD = 5.5 km) in comparison to passive (SD = 16.9 km) and TVM (SD = 9.6 km) simulations. 50% of the population were within 4.3 km of the median, in contrast to the passive (Inter Quartile Range = 13.1 km) and TVM (12.9 km) models. REVM particles continued to become increasingly clustered over time, whereas particles continued to disperse in the passive and TVM experiments (Fig. 4.7).

After a 28-day planktonic larval duration, significant differences were observed in the mean (Tukey's HSD, $p < 0.001$ in all cases) and the median (Pairwise Moods median test, $p < 0.001$ in all cases) radial dispersal distance from the source point. Reverse-engineered particles exhibited the shortest distance travelled (median distance: 32.9 km) and their distribution was the least spread out, with 50% off the population found between 30.5 km and 35.3 km from source. Passive particles had the greatest mean distance at the end of the simulation (79.1 km (Reverse-engineered: 33.7 km, TVM: 52.1 km)), however the median distance travelled by particles after 28 days was greater for TVM particles (54.9 km (passive: 46.4 km)). At this time point, the distribution of passive particles displayed the greatest spread with 50% off the population found between 6.8 km and 86 km from source.

Table 4.3: Descriptive statistics of the dispersal kernels of passive, reverse-engineered (REVM) and TVM assigned particles after 1, 7, 14, 21, and 28 days.

Day	Behaviour	Mean Radial Distance (km)	Standard Deviation	Median Radial Distance (km)	Minimum Radial Distance (km)	Maximum Radial Distance (km)	Inter-quartile Range
1	Passive	4.191	2.523	3.825	0.605	13.272	3.133
1	Reverse-Engineered	4.031	2.196	3.882	0.036	19.411	3.465
1	TVM	5.890	3.442	5.280	0.034	21.897	4.746
7	Passive	17.084	6.953	18.178	3.349	33.707	13.049
7	Reverse-Engineered	23.113	4.858	23.013	0.217	41.096	7.113
7	TVM	17.721	6.653	18.164	0.275	43.410	8.564
14	Passive	29.119	16.940	24.691	1.314	70.976	13.077
14	Reverse-Engineered	32.053	5.514	31.886	2.180	56.133	4.329
14	TVM	32.013	9.601	32.389	0.684	68.771	12.900
21	Passive	53.159	31.286	45.946	0.897	144.819	26.415
21	Reverse-Engineered	32.547	4.786	32.166	4.259	73.335	0.961
21	TVM	48.704	13.623	50.788	0.291	91.736	18.813
28	Passive	79.113	57.362	46.370	0.316	228.177	39.551
28	Reverse-Engineered	33.674	4.468	32.908	1.901	76.504	2.368
28	TVM	52.085	16.972	54.914	0.894	117.524	22.642

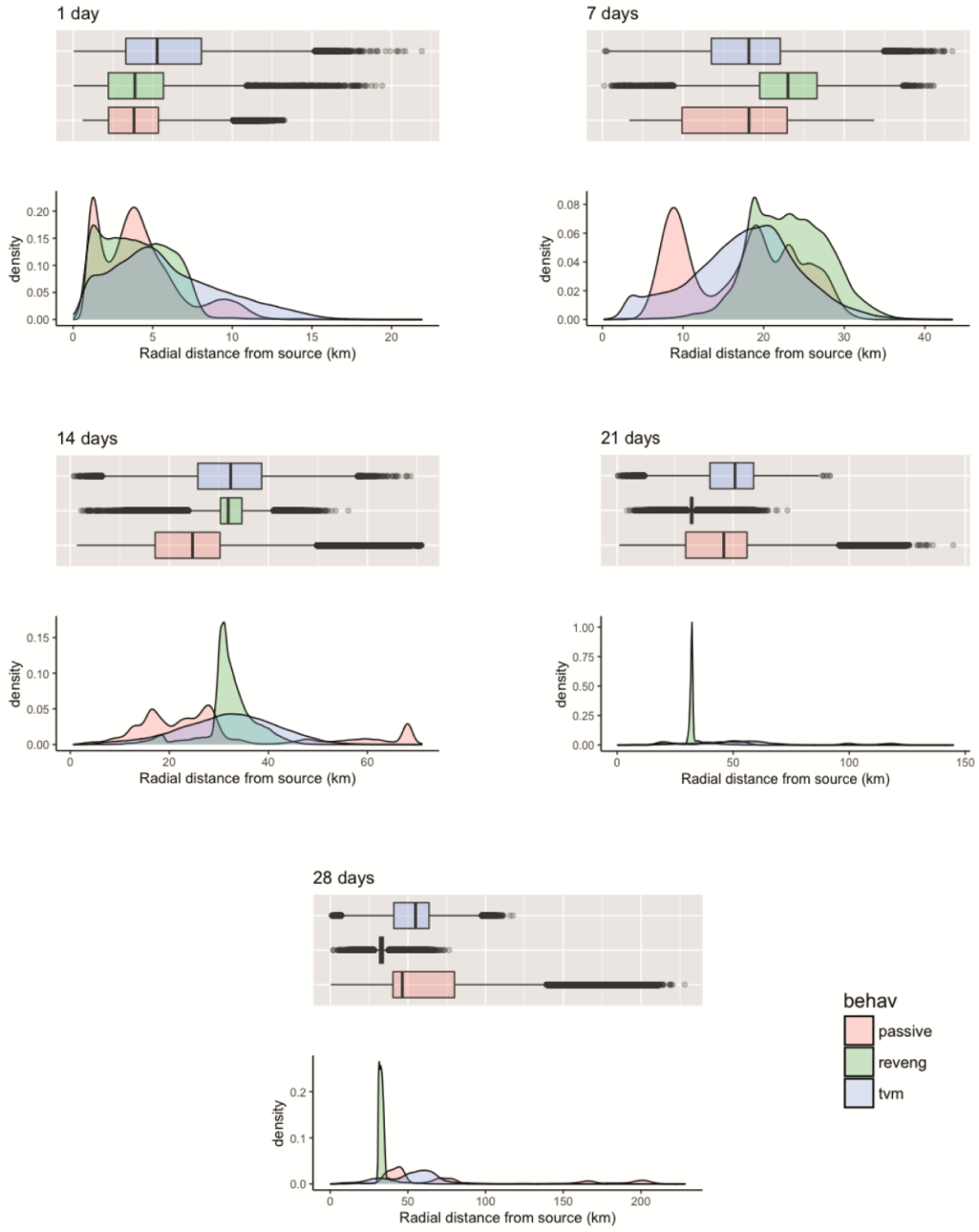

Figure 4.7: Density kernels of the radial distance from source for the population of passive (n = 80,000), reverse-engineered (REVM) (n = 80,000) and TVM (n = 80,000) particles at 1, 7, 14, 21 and 28 days from release.

4.4.4 Biogeography

Mapping the locations of particles at set time points highlighted disjunct biogeographic distributions depending on the behavioural model implemented (Figure 4.8) with clear differences in the centre of gravity of the 2-dimensional cloud and direction of travel (Figs 4.9 & 4.10). REVM model simulations showed a south west mean direction of travel, whereas the TVM model predicted a mean north/north east movement. Passive models followed a similar direction of travel to TVM models in the spring, and a similar direction to REVM models in the summer, albeit with different central tendencies and spread of particles.

After 24 hours, these differences were relatively small, with strong positive correlation between all behavioural comparisons in both seasons (Figures 4.9 & 4.10). TVM and REVM particles displayed the greatest distance between central tendencies at this time point, with 10 km in both spring and summer. Seasonal differences in central tendencies after 1 day were also small: 4 km between spring and summer passive particles, and 3 km between spring and summer TVM particles and spring and summer REVM particles.

After 7 simulation days, differences in the behavioural dispersal clouds became more apparent (Figure 4.8: 7 days). TVM particles followed a north-easterly trajectory, whilst REVM particles travelled south and circumnavigated the coast to the West. This directional trend propagated throughout the simulation (Figure 4.8). In spring, passive particles travelled in a similar direction to TVM particles, however in Summer the cloud of passive particles travelled Southwest (Fig 4.8) The central tendency of REVM particles held a strong positive correlation at 14, 21 and 28 days. In summer after 21 days, the central tendency of passive particles was positively correlated to REVM particles (Fig 4.9) and the central tendencies of the groups were separated by a distance

of 13 km (Fig. 4.10), however the spread of passive particles was much greater (Figs 4.7 & 4.8).

After 28 simulation days, the geographic distances between the central tendencies of the dispersal clouds of each behavioural class were large. In spring, the central tendency of the passive cloud was positioned 41 km from the central tendency of the TVM cloud, and 112 km from the central tendency of the REVM cloud. The central point of the passive cloud was positively correlated to the central point of the TVM cloud, and negatively correlated to the central point of the REVM cloud (Fig. 4.9). The difference in distance between the central tendencies of the TVM and REVM clouds in spring was 107 km and the two points showed strong negative correlation (Fig. 4.9). In summer, after 28 days the central tendency of the passive cloud was 208 km from the central tendency of the TVM cloud, and 105 km from the central tendency of the REVM cloud. In contrast to spring, the central point of the passive cloud was negatively correlated to the central point of the TVM cloud, and positively correlated to the central point of the REVM cloud (Fig. 4.9). The difference in distance between the central tendencies of the TVM and REVM clouds in summer after 28 days was 107 km. These two points again showed negative correlation, but to a weaker extent than observed in the spring (Fig. 4.9).

The seasonal difference between the central tendencies of passive particles increased over time (Fig 4.8 & Fig 4.10), and after 28 days planktonic larval duration the central tendencies of the clouds were separated by a Euclidean distance of 217 km. Behaving particles were less geographically influenced by season (Fig 4.10), and after 28 days seasonal clouds were geographically separated by 9 km and 10 km for TVM and REVM respectively.

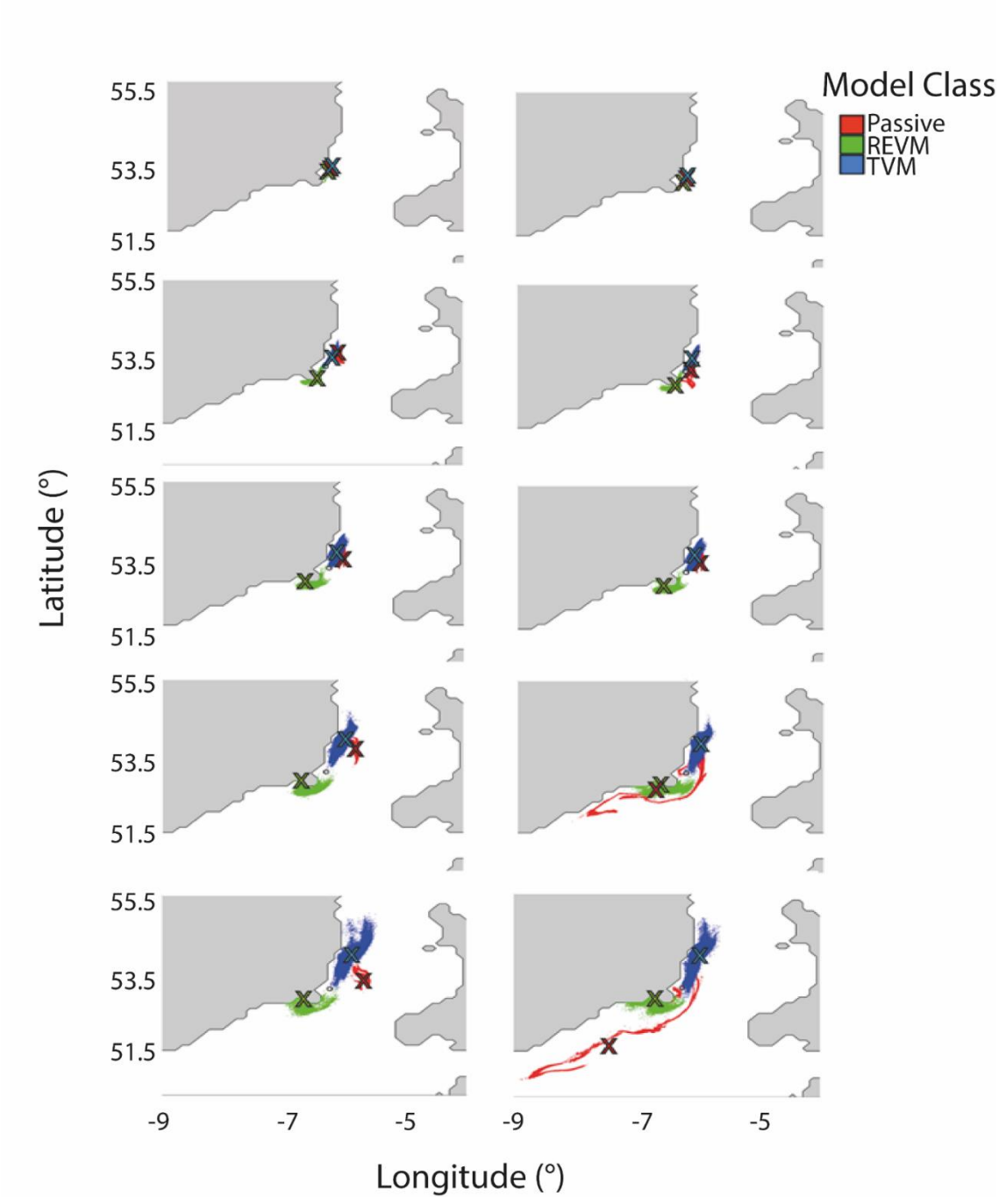

Figure 4.8: Visualisation of the dispersal of virtual larvae in LTRANS v2.0 assigned 3 behavioural regimes (red: passive, green: reverse-engineered (REVM), blue: TVM) from a single-point source location in the Irish Sea. X denotes the centre of gravity of each of the dispersal clouds.

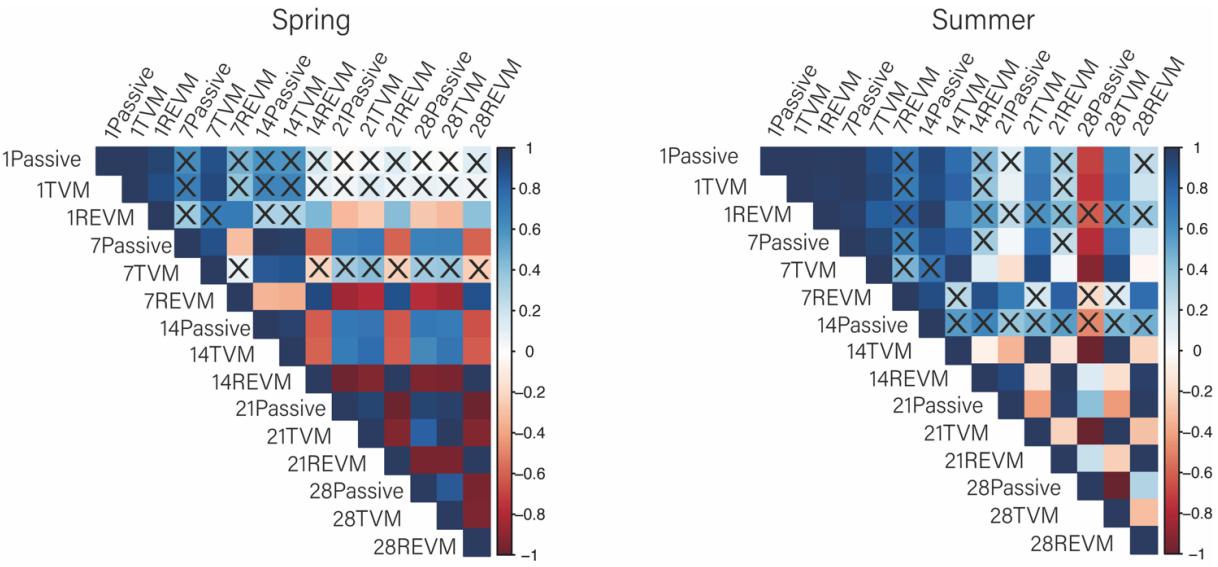

Figure 4.9: Correlation matrix of the distance of centre of gravity of the dispersal clouds for each day × season × behaviour combination. Labels denote the day and the behavioural mode. Pairwise comparisons range from strong positive correlation (close proximity of centre of gravity of dispersal clouds) to strong negative correlation (large distances between centre of gravity of dispersal clouds). Pairs with no significant correlation (Spearman's rank correlation coefficient: $p > 0.05$) denoted by 'X'.

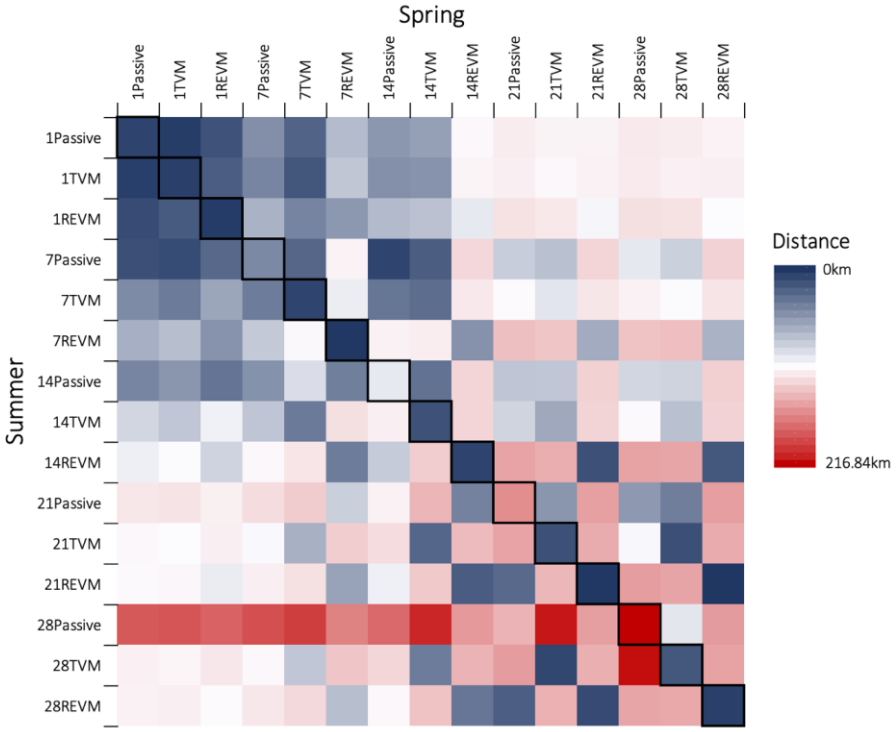

Figure 4.10: Matrix of the Euclidean distances between central tendencies of the dispersal clouds calculated from the lat/lon. Labels denote the day and the behavioural mode. Boxes with thick borders are comparisons between seasons for the same model class (behaviour). Colour scale indicates small (blue) to large (red) distance between the centre of gravity of the clouds.

4.5 Discussion

The capacity of biophysical models to predict dispersal and allow spatial and temporal assessment of connectivity are currently at the forefront of larval dispersal research, and more broadly, central to our efforts to understanding pressing global challenges including climate change (Lett et al., 2010; Andrello et al., 2015; Lacroix et al., 2018; Oldfather et al. 2020) and the impacts of invasive species (Richardson et al., 2016; Lashley et al., 2018). Yet understanding how to parameterise the 'biological component' of these models and the potential effects of inaccurate representation of biological traits on model predictions remains a key challenge (Metaxas and Saunders, 2009). It is largely accepted that larval behaviour plays a key role in larval transport and wider ecological functioning; but despite this recognised importance, many dispersal models still assume passive dispersal (see Swearer et al., 2019 for review). Nevertheless, there is clear recognition of the need to include behaviour in biophysical models (e.g. Garland et al., 2002; Marta-Almeida et al., 2006; Paris et al., 2007; North et al., 2008; Nicolle et al., 2013; Phelps et al., 2015; Daigle et al., 2016; Mayorga-Adame et al., 2017; Bode et al., 2019; James et al. 2019). Here, our results highlight how differential classification of a single behaviour - active larval swimming - within a model framework, can lead to markedly different dispersal outcomes. Notably we show that, at least where coastal circulation has a strong tidal component such as in and around the Irish Sea, inclusion of vertical migration behaviour, a known behavioural phenomena in a range of marine taxa including bivalves (Watters et al., 2001; Knights et al., 2006; Bonicelli et al., 2016), crustaceans, (Zhou and Dorland., 2004; Queiroga and Blanton (2005) and fish (Paris and Cowen, 2004; Irisson et al. 2010; Hawes et al., 2020) can reduce dispersal distance, but that the modification of that simulated vertical migration behaviour greatly influences dispersal distances and direction.

It has been widely recognised that small changes in the vertical position of a larva can greatly influence its dispersal trajectory due to depth-related differences in the magnitude and direction of the current (Largier, 2003; Pringle, 2007; Correll et al., 2012; Torres et al., 2018), and that some organisms actively migrate in the vertical in order to take advantage of favourable currents (i.e. Selective Tidal Stream Transport; Forward et al., 2003; Knights et al., 2006; Kunze et al., 2013; Peterio and Shanks, 2015), avoid predation (i.e. Diel Vertical Migration – Lampbert, 1993; Scheuerell and Schindler, 2003; Gibson et al., 2016; Pinti and Visser, 2019), and access available food sources (Gibson et al., 2016). However, what remains uncertain is the extent to which a larva can manipulate its position *in-situ.* Here, we incorporated a state-of-art assessment of larval swimming behaviour based on statistical models of likelihood (Chapter 2) of match between model simulations and field-derived observations of vertical distribution profiles. We argue that the REVM approach offers a behavioural parameterisation that addresses some of the previous limitations of laboratory observations of behaviour; specifically, their failure to capture 'real-life' interactions between larvae and their environment (Bowler and Benton, 2005) and subsequent expression of a behaviour as movement. Further, there is also mounting evidence that not all larvae are equal (see Toonen and Pawlik, 2001; Marshall et al., 2010 and Nanninga and Berumen, 2014 for a review) with a high degree of intra-specific variability. The REVM method of behavioural parameterisation captures this intra-population variation by stochastically assigning behaviours within the larval cohort based on a range of likely swimming speeds inferred from the field; an approach previously advocated by Fisken et al. (2007). Interestingly, we demonstrate that even with inclusion of intra-population variability in capacity to 'behave', the dispersal of REVM particles displayed the lowest variance and dispersal distances of all three scenarios (e.g. Fig 4.8), travelling considerably shorter distances than passive or TVM equivalents (on average 1000 km

less than passive particles and 665 km less than TVM particles). Our results further reinforce the potential for larval swimming and active behaviours such as selective tidal stream transport or vertical migration (Forward and Tankersley (2001); Knights et al. 2006) to be an effective transport mechanism for even small, relatively slow-swimming organisms despite flow-fields orders of magnitude faster.

Our results suggest that for organisms with short planktonic durations (e.g. 1 day), dispersal predictions were largely the same, suggesting a 'simple' passive dispersal model will provide equally robust predictions of dispersal as a more complex model that incorporates behaviour. Over time, however, we show that the incorporation of (a) behaviour, and parameterisation of the behaviour in the model framework, becomes increasingly important. In Chapter 2, we specifically addressed our concern that inaccurate parameterisation of behaviours would lead to additive errors in model predictions as a function of time. Here, comparison of our REVM and TVM simulations reinforce this concern; after 14 days, the REVM models indicate biogeographic stability and suggest at an effective retention mechanism, whereas the TVM model suggests continued dispersion away from the source (Fig. 4.8; Table 4.3) and supports the hypothesis that larval behaviour acts to reduce dispersal in the marine environment (Shanks et al., 2003; Shanks 2009). However, it is clear that how and when larvae utilise heterogeneous flow regimes can have a stark impact on realised dispersal patterns.

4.5.1 Cohort clustering

Our work showed that our REVM approach resulted in rapid early dispersal followed by high levels of clustering at short distances from the source. Clustering of the larval cohort has ecological pros and cons: it can provide advantages, such as allowing

organisms to evade predation and offer protection through a ‘safety in numbers’ approach, but also it may lead to increased mortality due to intraspecific competition for resources (Hixon and Jones, 2005). Mortality is not considered in our models as its inclusion was beyond the scope of our objectives, however it is a key factor to consider in estimating population dynamics from dispersal models (Treml et al., 2015), and hence the design of connectivity-informed conservation agendas should endeavour to include temporal and spatial species-specific mortality rates (Carr et al., 2017).

4.5.2 Biogeography – the need for a 3D approach

We also draw attention to the importance of choosing relevant metrics to quantify dispersal. In our study, the mean dispersal distance of TVM and REVM larvae after 14 days was not significantly different, however mapping the dispersal cloud identified north-easterly movement of TVM particles, and south-westerly movement of REVM particles. Average distance of dispersal of the larval cohort therefore arguably fails to provide adequate information for spatial management of marine environments. Furthermore, distance travelled from source proved to be an order of magnitude smaller than the distance travelled by particles along their dispersal paths, irrespective of behaviour and timing of release. Such findings support the case for the use of Lagrangian approaches coupling local circulation models with individual based models (Cowen et al., 2006; Rochette et al., 2012) when estimating dispersal as opposed to mean estimates of dispersal distance (Sala et al., 2002; Lockwood et al., 2002; White et al., 2010) or *speed = distance*time* calculations (Shanks et al., 2003; Shanks, 2009).

4.5.3 Implications

Despite the importance of dispersal to the ecological and evolutionary success of both terrestrial and marine organisms, our results continue to highlight our limited

understanding of the role of behaviour in dispersal predictions. Dispersal is a key consideration in estimates of population connectivity and models continue to play a critical theoretical and applied role in science today, whether being used to design Marine Protected Areas (MPAs: Gaines et al., 2003; 2010; Almany et al., 2009; Kaplan et al., 2009; Costello et al., 2010; Krueck et al., 2017), identify pathways of invasion (Viard et al., 2006; Kitchens et al., 2017), or understanding metapopulation dynamics and biogeography (Sanvicente-Añorve et al., 2018). We consider models to be an invaluable tool in these endeavours, but the results here highlight the disproportionate effects that even a single behaviour - larval swimming - can have on model predictions, our understanding of ecosystem functioning, and notably the ecological coherence of marine systems (Jonsson et al., 2020). Although the questions of which behavioural modelling approach is best remain, the results of our REVM model are in broad alignment with the findings of other studies (Woodson and McManus, 2007; Shanks 2009; Sundelöf & Jonsson, 2011) reinforcing our thinking that active larval behaviour does serve as a mechanism to reduce larval dispersal., and that coastal marine systems, even physically dynamic systems like the Irish Sea, can be relatively 'closed' (*sensu* Cowen et al. 2000) and that MPAs and other coherent networks may need to be closer together. Our results suggest that management decisions made on incorrect behavioural assumptions in dispersal models may overestimate the connectivity between local populations (in contention with the suggestions of Costello and Connor, 2019 and Manel et al., 2019) who argue that the spatial scale of marine connectivity is underestimated), leading to a false sense of security in the ecological coherence of protected networks.

Although further work is needed, we suggest that in the meantime, that best estimates of dispersal and specifically, biogeography, requires (i) use of a Lagrangian particle-

tracking approach coupled with localised circulation models, and ii) empirical data of vertical distribution profiles to allow the estimation of larval swimming speeds likely to occur *in-situ.*

5 GENERAL DISCUSSION

5.1 Thesis background and rationale

5.1.1 Larval behaviour in dispersal models

Over the past 40 years, biophysical models that combine a hydrodynamic model and particle tracker that mimics biological traits have become the ‘go-to’ tool for predicting the dispersive trajectories of planktic marine organisms (Swearer et al., 2019). Increasingly, they are used to design Marine Protected Areas (MPAs: Gaines et al., 2003; 2010; Almany et al., 2009; Kaplan et al., 2009; Costello et al., 2010; Krueck et al., 2017), identify pathways of invasion (Viard et al., 2006; Kitchens et al., 2017), and understand metapopulation dynamics and biogeography (Sanvicente-Añorve et al., 2018). Yet, despite this relatively long history of development, continued technological advancement and increased usage, models continue to often fail to predict patterns in nature (James et al., 2019).

As particle trackers coupled with ocean models are able to accurately predict the dispersal trajectories of abiotic particles (Soulsby et al., 2009), the failure of such models to accurately predict dispersal is increasingly argued to be a result of inaccurate parameterisation of the biological traits of organisms rather than failure of the underlying hydrodynamic model to predict ocean processes. Indeed, the concept that larval behaviour can play a significant role in their dispersal has continued to gain significant traction in the field of larval dispersal modelling (e.g. Kingsford et al., 2002; Shanks et al., 2003; Levin, 2006; Knights et al., 2006; Shanks, 2009; James et al., 2019). Particular focus has been placed on characterising active larval movement (swimming), following numerous field studies showing temporal changes in the vertical distribution profiles of marine larvae (e.g. Richter, 1973; Knights et al. 2006; Lloyd et al., 2012; Shulzitski et al., 2017) that cannot be explained by random dispersal trajectories.

Despite the recognised importance of vertical distribution/position to dispersal by advection, especially in smaller organisms, there is currently no general consensus of how, what, and when behaviours can and should be included (Swearer et al., 2019), perhaps because the drivers of larval behaviour are inherently complex (see Figure 5.1), and as yet, not fully understood. Nevertheless, larval behaviour is often represented within dispersal models as an active swimming response (speed/direction) by a model propagule (larvae) to an exogenous (i.e. external stimuli) or endogenous cue (e.g. circadian rhythm). Furthermore, swimming behaviours are often described using laboratory observations of swimming speeds in response to a small number of (often one) cues such as salinity (North et al., 2008), tidal direction (Banas et al., 2009; Daigle et al., 2016), ontogeny (Butler et al., 2011), or daylight (Daigle et al., 2016)). Yet, studies have shown that swimming behaviours observed in lab-based settings can be absent from field observations (Maldonado et al., 2003; 2006), which may be due to the fact that in nature organisms are likely exposed to multiple, rather than single cues, which may cause their behavioural responses to differ from those in these necessarily simplified control experiments.

5.1.2 Getting the vertical position right

A fundamental purpose of including larval behaviours in biophysical models of the planktonic dispersal of invertebrate larvae is to accurately represent the vertical position of larvae in the water column to ensure that they are exposed to the ‘correct’ advective currents. Planktic marine organisms actively migrate across the vertical in order to take advantage of favourable currents (i.e. Selective Tidal Stream Transport; Forward et al., 2003; Knights et al., 2006; Kunze et al., 2013; Peterio and Shanks, 2015), avoid predation (i.e. Diel Vertical Migration – Lampbert, 1993; Scheuerell and Schindler, 2003; Gibson et al., 2016; Pinti and Visser, 2019), and access available food sources

(Gibson et al., 2016). Studies have shown that even relatively small changes in the vertical position of planktic organisms in the water column can have a vast effect on their horizontal trajectories due to exposure to depth-differentiated current speeds and directions influencing dispersal distance, retention, and the degree of connectivity between populations. (Largier, 2003; North et al., 2008; Corell et al., 2012; Robins et al. 2013; Phelps et al., 2015; Daigle et al., 2016; Torres et al., 2018). Therefore, ensuring the correct vertical position of larvae, and consequently the correct exposure to horizontal advective currents in biophysical models, is paramount to accurate predictions of dispersal.

5.2 Thesis objectives

The experiments and observations that make up this thesis were undertaken with two objectives in mind: 1) improving current understanding into how larval behaviours manifest in nature, and 2) development of a framework within biophysical models of dispersal that better reflects vertical distribution patterns observed in the natural environment. To that end, I undertook a multidisciplinary approach, combining novel modelling techniques with field-based observations of larval vertical distribution profiles (see Fig. 5.1). Specifically, I first developed techniques to infer larval swimming speeds (behaviours) from *in-situ* observations of changes in vertical distribution profiles (Chapter 2), then explored whether *in-situ* larval vertical distribution profiles could be described as a function of tidally-influenced environmental signals (Chapter 3). Finally, I assessed the sensitivity of change in within-model behavioural parameterisation on larval dispersal estimates and biogeography within a 3D Lagrangian modelling framework using the Irish Sea as a case study example (Chapter 4).

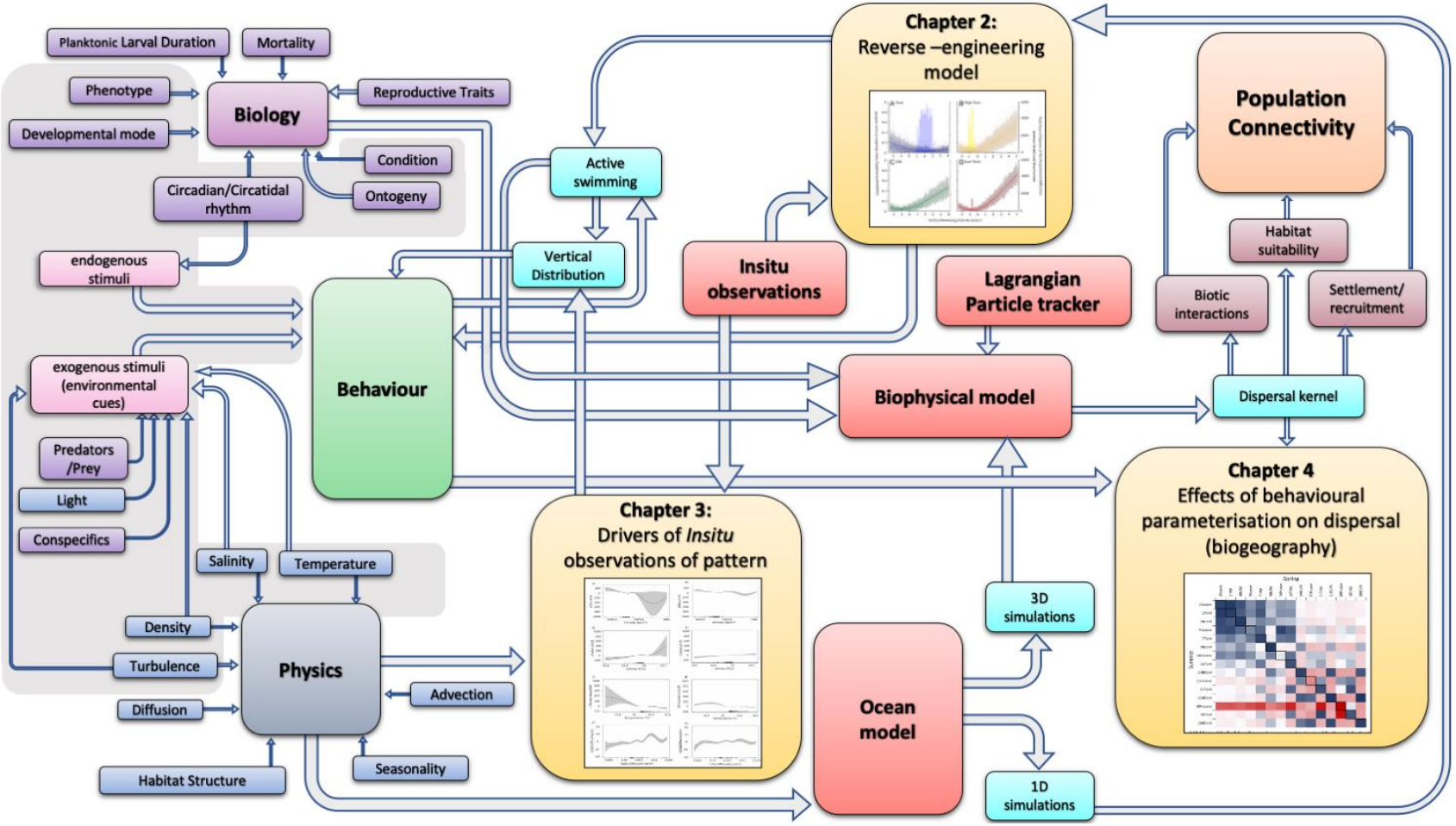

Figure 5.1: General schematic displaying the components required to generate descriptors of dispersal (red), the biological (purple) and physical (dark blue) factors that must be considered when parameterising behaviour based on 'rules', and how the data chapters of this thesis act to improve current understanding of how behaviours manifest in nature (chapters 2 & 3) and the demonstrate the effects of behavioural parameterisation on dispersal predictions (Chapter 4). Grey shaded areas indicated the drivers that are encompassed in descriptions of larval behaviour made by inferring behaviour using the methods outlined in Chapters 2 & 3.

5.3 Synopsis of data chapters

In Chapter 2, I presented a novel approach for modelling larval behaviour (i.e. active swimming) based on *in-situ* observations of larval vertical distribution profiles. The aim of this chapter was to create an amalgamated behavioural function that can be applied in dispersal models that captures all 'behavioural responses' without knowing the individual mechanisms (and thus, individual rules) that govern active swimming. I used a combination of empirical data modelling techniques to explore the active movements that larvae would need to undertake in order to create the patterns observed in nature over the course of a tidal cycle. This was achieved by testing a range of swimming velocities in a model environment and looking for replication of pattern between the modelled and field-derived distribution patterns. The results of this study suggest that active swimming behaviours are inconsistent with previous hypothesised behavioural functions (e.g. TVM). Instead, I showed a need for adaptation of active swimming speed and direction that varies over tidal cycles, but also that, in some instances, we are unable to explain observed vertical patterns using active swimming. Specifically, I showed that in order to match *in-situ* observations, there are two requirements: first, a shift from positive (upward) to negative (downward) movement at mid-points of a circa-tidal cycle (rather than at the turning point between the ebb and flood) is required to best match vertical distribution patterns, and second, different swimming velocities in the upward and downward direction are required (i.e. 2.5× faster when swimming upwards). The approach was not always successful; during the ebb tide, model compatibility was low, suggesting that we do not fully understand the behavioural responses of the larvae and their relationship with the physical characteristics of the ocean during this particular period of the tide. Despite this, I was able to identify the

optimum vertical velocities that give the “best fit” to the observed patterns when larval behaviour is parameterized by constant swimming in one direction.

In Chapter 3 and following the low model compatibility achieved during the ebb tide period, I undertook a high spatial and temporal sampling regime of larval vertical distribution profiles and common physical input parameters of ocean models (i.e. density, temperature, salinity and eddy diffusivity) between high water and low water. The aim was to better resolve behaviours during this period and describe a signal that could be used to parameterise larval behaviour in dispersal modelling studies. I used Generalised Additive Models (GAMs) to reveal the influences of density, temperature, salinity and eddy diffusivity on the observed distribution profiles of bivalve larvae (*Mytilus spp.*). Additionally, I compared the vertical distribution profiles sampled here with profiles from the Irish Sea in 2005 (Knights et al., 2006) to assess whether it is appropriate to generalise vertical patterns over different locations. I demonstrated that of the environmental drivers investigated, they generally explained little difference in vertical distribution patterns, although, some differential use of environmental cues between ontogenetic stages was observed. As shown in Knights et al. (2006), the vertical distribution of larvae displayed a strong correlation to the state of the tide, with marked differences observed between the vertical distribution profiles at high water and mid ebb, however the proportional abundances during each tidal state significantly differed from those observed by Knights et al. (2006) in the Irish Sea.

In Chapter 4, I undertook simulations to predict dispersal pathways using the Irish Sea as a case study, and specifically, explored how vertical distribution profile error may propagate in biophysical larval dispersal predictions. Formal comparisons of three models were made, namely: (1) a passive dispersal model; (2) simulations implementing a tidal vertical migration (TVM) ‘rule-based’ behaviour; and (3)

simulations implementing a reverse-engineered active swimming behaviour (after Chapter 2). The effects of (non) behavioural parameterisation on larval dispersal and biogeography were considered. The results highlight how differences in the method of behaviour characterisation within a biophysical model can lead to fundamentally different dispersal outcomes. Results highlight how differential classification of a single behaviour - active larval swimming - within a model framework, can lead to markedly different dispersal outcomes, reinforcing previous findings that vertical migration behaviour is a mechanism that significantly reduces dispersal distances (e.g. Woodson and McManus, 2007). Specifically, I show that the approach to behavioural parameterisation can lead to fundamental differences in biogeographic dispersal predictions. I show that the inclusion of swimming behaviour (either a 'TVM' or reverse-engineered behavioural signature) reduces the influence of the state of the tide and the season at which particles are released, and highlight that distance travelled from source is a limited metric that can fail to describe the whole picture when comparing dispersal trajectories (dispersal clouds can travel similar distances to different locations). I argue that a 3D approach that incorporates horizontal and vertical spatial components is fundamental to effectively describing biogeographic dispersal. Importantly, I also demonstrate that over short planktonic larval durations ($\leq$ 24 hours), the dispersal trajectories are largely the same irrespective of behavioural parameterisation, but with increasing PLD length, stark differences in both the distance travelled from source and the biogeographic location of the dispersal cloud become increasingly apparent between all behavioural models (passive; TVM; REVM).

5.4 Implications of findings

Dispersal is a key consideration in estimates of population connectivity, and biophysical modelling provides a cost-effective and well-utilised tool to estimate dispersal in the marine environment. These models continue to play a critical theoretical and applied role in science today, however, inaccuracies within these models can misguide those using them, and consequently decisions made off the back of inaccurate model estimations may be ineffective (Botsford et al., 2009a).

The findings of the studies within this thesis highlight the disproportionate effects that even a single behaviour - larval swimming - can have on model predictions, our understanding of ecosystem functioning, and notably the ecological coherence of marine systems (Jonsson et al., 2020). Our results suggest that current methods of behavioural parameterisation used in biophysical modelling studies (i.e. rule-based approaches) are limited in their capacity to match *in-situ* observations of vertical distribution profiles, and consequently fail to place larvae in the 'correct' vertical position in the water column and expose them to the 'correct' advective currents. The 'best-fit' velocities calculated by the model in Chapter 2 fell between the boundaries of larval swimming reported in the literature for *Mytilus* larvae (-2.5mms^{-1} to 5mms^{-1}: Chai et al., 1984; Sprung, 1984; Fuchs and DiBacco, 2001), suggesting that vertical migration is important mechanism for even small, relatively slow-swimming organisms despite flow-fields orders of magnitude faster (Forward and Tankersley, 2001; Knights et al., 2006). However, I demonstrated that active movement changes over the course of the tidal cycle at temporal scales typically not modelled. Specifically, the change in both swimming speed and direction around the midpoint of the flood tide (from upwards swimming at 2.2mm s^{-1} to downwards swimming/sinking at 1mm s^{-1}) necessary to match the *in-situ* profiles observed by Knights et al. (2006) (Chapter 2) is counter to the

theory of Tidal Vertical Migration (TVM) in which organisms swim upwards for the duration of one tidal state and downward during the opposing state (e.g. Civelek et al., 2013), and to Weinstock et al.'s (2018) theory of passive vertical advective movement by tidal straining. Consequently, the implementation of passivity (e.g. Wood et al., 2014; 2016) or TVM (e.g. Robins et al., 2013) in a dispersal model may be ineffective at generating vertical profiles that accurately represent nature, with potential for error in vertical position to generate errors in dispersal predictions that propagate over time (as demonstrated in Chapter 4); for instance, as planktonic duration increases. Given that the larval duration can be dependent on numerous factors including temperature (O'Connor et al., 2007), food (Tupoint et al., 2012), and the physiological condition of the larvae (Phillips, 2004), future work should perhaps also consider the local environment of the organism and consider stochastic larval durations in biophysical models depending on abiotic conditions.

It has long been argued that the length of PLD assigned to a particle can have a significant influence on its dispersal in a biophysical model (e.g. Edwards et al., 2007). The results of Chapter 4 demonstrate that with increasing time (i.e. PLD length), there is increasing divergence between the modelled dispersal outputs of each tested behavioural mode. Our findings show that, for organisms with shorter PLD's (≤ 24 hours), incorporation (or absence) of behaviours within a biophysical model has no effect on predictions. However, as time spent in the plankton increases, there is prediction divergence. Consequently, I argue that when modelling dispersal over short time scales (up to 1 day), the assumption of passivity may well be sufficient and that dispersal models could consider omitting behaviour altogether. However, for species with longer PLD's (> 24 hours), which is common for many taxa including a range of commercially important taxa such as mussels (21 –35 days: Filgueira et al., 2015), oysters (10 –21 days: Yoo et al., 1976), and periwinkles (28 –49 days: Chang et al.,

2011), accurate representation of the vertical position of larvae in the water column may well be fundamental to achieving realistic predictions of dispersal.

When attempting to disentangle the drivers of vertical distribution from the profiles collected from the field in Chapter 3, I discovered that temperature, salinity, density, and turbulence explained relatively little variance in the proportional abundance of larvae observed in the water column at any given time. As such, I argue that these external drivers as determinants of behavioural 'rules' in biophysical models should be used with caution. Additionally, numerous other factors were unexplored in Chapter 3; for instance, light (Ettinger-Epstein et al., 2008; Cisewski et al., 2010; Wahab et al., 2014; de Andres-Bragado et al., 2018), conspecific presence (Ettinger Epstein et al., 2008), food availability (Bianco et al., 2011; Fouzai et al., 2015), and soundscapes (Simpson et al., 2011; Lillis et al., 2016) have also been shown to influence the directional movement of invertebrate larvae in laboratory settings. In reality, it is likely that larval behaviours manifest in nature as a result of interactions between all these (and potentially more) cues (see Fig. 5.1), yet our understanding of larval decision-making in response to multiple cues and their subsequent capacity to effect movement remains unresolved. I suggest that, due the complex nature of oceanic environments in which multiple cues are present that have the potential to influence an organism's behaviour at any given time, larval behaviours are more likely to be locally idiosyncratic such that the success (validation) of 'rule-based' approaches is more a result of luck rather than design.

I also highlighted differences in vertical distribution patterns between the populations of larvae collected in southwest England (Chapter 3) and in the Irish Sea (Knights et al., 2006), signifying either intra-specific or location specific variation in larval behaviours. This suggests that it may not be appropriate to generalise behavioural rules if models

are to present accurate predictions of larval dispersal. In the absence of an in-depth understanding of larval decision-making *in-situ*, I suggest that larval behaviour should be considered in dispersal models on a case-by-case basis, using the methodology provided in Chapter 2 to amalgamate all the potential factors that may influence behaviour into a single movement metric that allows us to get the vertical position of larvae 'right' when the drivers of vertical swimming are unknown. Although the questions of which behavioural modelling approach is best remain, the findings of Chapter 4 emphasize that how we include behaviour in models can have significant effects on our predictions of dispersal. The results of "Reverse-engineered" model predictions of larval swimming support the findings of other studies (Woodson and McManus, 2007; Shanks 2009; Sundelöf & Jonsson, 2011) that argue that active larval behaviour serves as a mechanism to reduce larval dispersal. If this is the case, we may be overestimating connectivity within our oceans and between marine populations, and that efforts to protect connectivity, such as by way of MPAs and creation of 'coherent networks', may need to be designed in a way that ensures populations are closer together.

5.5 Bridging the gap between larvae and their environment: a framework for dispersal modelling studies

The biological and physical drivers of larval dispersal create a complex suite of parameters for consideration in a 'rule-based' approach (Fig. 5.1). Marine invertebrate larvae have been shown to exhibit hierarchal responses to environmental cues (Welch and Forward, 2001; Ettinger-Epstein et al., 2008; Whalan et al., 2008; Teodósio et al., 2016; Verasztó et al., 2018), so effectively capturing behaviours using a 'rule-based' approach requires not only an understanding of decision making in response to cues, but also an understanding of how behaviour is influenced by the interactions between multiple signals. How larvae make decisions in response to multiple cues and how this

effects their active movement, and consequently their dispersal, remains an unanswered and significant question in marine ecology. Swearer et al. (2019) argue that in dispersal models, behaviour exists independently of the physical state of the larva (i.e. behaviour exists without consideration of the influence of the environment on the larva), and that breaking through this 'dualism' will be an important step moving forward. By amalgamating all the potential drivers of larval behaviour into a signal metric representing behavioural manifestation (Figure 5.2), the chapters within this thesis provide a framework for achieving this by connecting larval behaviours in models to larval behavioural manifestation in nature, overcoming the need to rely on descriptors of behaviour derived from observations made under controlled laboratory conditions, which may not be present in the field, (Maldonado et al., 2003; Maldonado, 2006) to reflect the vertical position of larvae in the water column at a given time point.

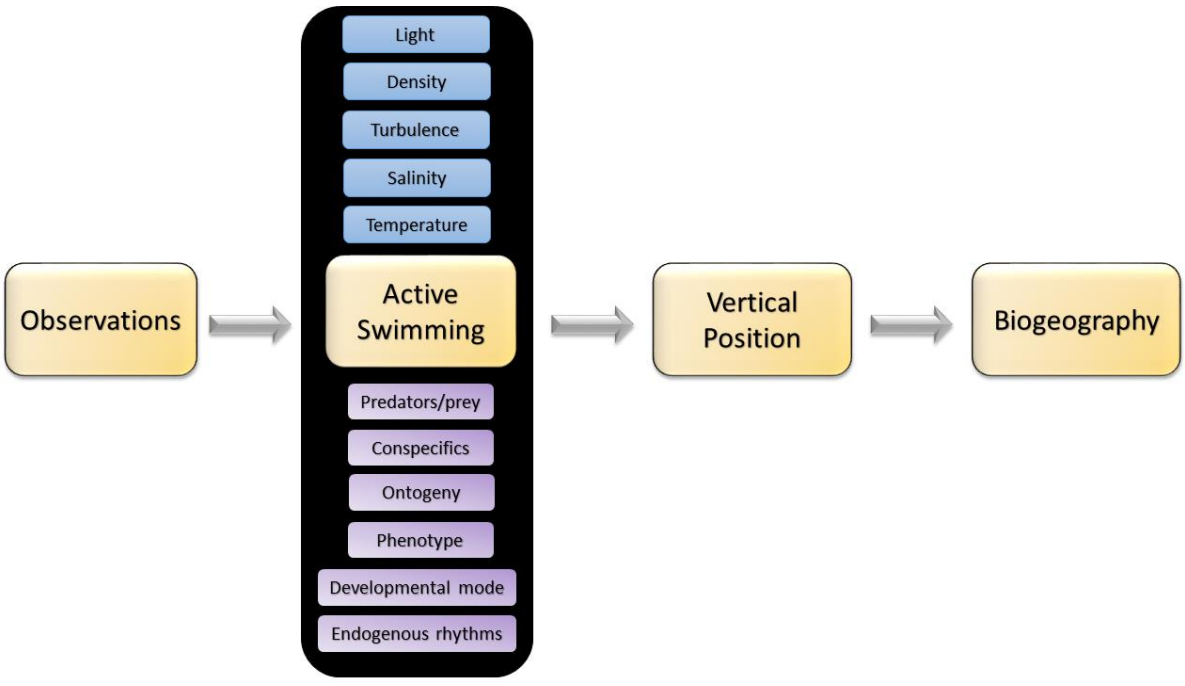

Figure 5.2: Schematic describing the links between larval vertical position in the field and biogeography, showing the drivers of larval movement (active (vertical) swimming) as a 'black box'. The approach proposed in Chapter 2 provides a methodology for amalgamating the behavioural response of larvae to all these cues as a single 'active swimming' behavioural response.

Moving forward, I suggest that dispersal modellers consider the following building blocks in model development in order to generate accurate predictions of larval movement. 1) A well-validated ocean model of sufficient spatial and temporal resolution to capture the hydrodynamics relevant to the scale of the larvae, and 2) a Lagrangian particle tracker in which species-specific behaviours are parameterised using an amalgamated behavioural metric derived from *in-situ* vertical distribution profiles local to the study area, collected using a high spatio-temporal sampling regime (*sensu* Knights et al., 2006). Although it may not be cost and time-effective, extensive sampling currently provides the best means of identifying how larval behaviours manifest in nature in a way that encompasses the entire range of *in-situ* biological and physical drivers that can influence movement (Metaxas and Saunders, 2009). The approaches presented in this thesis provide the framework for converting such observed vertical distribution profiles into behavioural metrics for use in biophysical models, which allow us to make predictions that are arguably more accurate, however validation of the approaches outlined is required to ascertain their effectiveness.

5.6 Future directions

5.6.1 Addressing the limitations of this thesis

"All models are wrong, but some are useful"

In 1976, statistician George Box used the above aphorism in a paper published in the Journal of the American Statistical Association to emphasise that, by nature, models are simplifications of reality applied with the aim of improving our current understanding. But do previous models of larval dispersal improve our understanding, or have they muddied the waters and led us down the garden path? Non-validated biophysical

models have been used to address hypothetical considerations of the influence of varying factors on larval dispersal (Hill, 1990; Marta-Almeida et al., 2006; Aiken, 2007; North et al., 2008; Phelps et al., 2015), however, without validation, the outcomes of such models are purely theoretical., and model outcomes need to be compared to species distributions in the field to justify their findings in an ecological context. The assessments within this thesis were undertaken with the aim of determining if current biophysical modelling approaches do indeed improve our current understanding or if we are being misled by their outcomes, but additional work is required to fully test the validity of the approaches proposed here. For instance, further field studies would be beneficial to assess whether our 1-dimensional model proposed in Chapter 2 is successful in matching *in-situ* observations. Additionally, genetic tools could be used to test the 'goodness of fit' of a model prediction that adopts our reverse-engineered behavioural parameterisation approach (Chapter 4); for instance, using genetic parentage data (e.g. Bode et al., 2019 and see review by Hedgecock et al., 2007) and comparison with other behavioural parameterisation approaches. This method, however, does rely upon knowledge of the genetic structure of potential source populations and adequate genetic differentiation between populations (Hedgecock et al., 2007; Metaxas and Saunders, 2009). The dispersal model outcomes presented in Chapter 4 could also be validated by comparing spatial patterns in dispersal with *in-situ* observations of population dynamics of the study species (i.e. known locations of adult populations Incze and Naimie, 2000; Pfeiffer-Herbert et al., 2007), but this may be overly simplistic as population dynamics are not only governed by dispersal., but also the settlement of larvae at the end of their planktic life-history stage, and post-settlement survival to recruitment into the adult population (Treml et al., 2015). Arguably, we therefore need to incorporate components parameterising settlement, mortality, and recruitment into

models in order to effectively validate their outcomes against observed species distributions patterns (Metaxas and Saunders, 2009).

5.6.2 Linking dispersal and recruitment

In this thesis, I have only considered dispersal and not the recruitment stages of population dynamics. The omission of this crucial life history stage can decouple dispersal predictions with observed species distribution patterns (Marshall et al., 2010; Treml et al., 2015). A logical next step would therefore be to also consider the relationship between dispersal and recruitment in order to provide insights into the likelihood and rate of change in species distribution profiles over time.

5.6.2.1 Settlement

For a larva to settle, it is required to come into contact with suitable habitat during its competency window, and there is evidence that some species are able to delay settlement in the absence of good habitat (e.g. Pechenik, 1990). Settlement on suitable habitat is a biophysically complex process, governed in part by the length of the competency window, the detection of cues that indicate and orientate the larvae towards good habitat, and larval swimming ability (Swearer et al., 2019). Like larval behaviour during dispersal, limited information is available on the drivers of settlement *in-situ* due to the logistical challenges of monitoring the process. It is therefore unsurprising that, despite its importance to population connectivity, habitat detection is seldom incorporated into biophysical models, however advances have been made to probabilistically implement realistic active settlement behaviours within modelling studies (Staaterman & Paris 2014, Treml et al. 2015).

5.6.2.2 Mortality

It is widely accepted that larval mortality can have a significant impact on connectivity (Thorson, 1946; Cowen et al., 2000; Metaxas and Saunders 2009; Vaughn and Allen,

2010; Paris et al., 2007; Treml et al., 2015). Estimates of connectivity therefore should consider the likelihood of larval survival throughout the dispersal process and into subsequent life-history stages (Swearer et al., 2019). Quantifying the mortality rate of the larvae of benthic invertebrates faces logistical challenges as reliable estimates can only be obtained from field studies (White et al., 214), however is assumed to be relatively high, ranging from 0.02% to 1.01% of the population per day (Dahlberg 1979, Houde 1997, Rumrill 1990, Morgan 1995, Vaughn and Allen 2010). The rarity of empirical estimates of mortality from field-based studies, and the uncertainty within the estimates where they are available (ranging more than two orders of magnitude within a single taxon: White et al., 2014) suggest that this is a significant area for future research. Poor fertilisation success, stress, lack of resources, and offshore transport have been found to be major contributors to larval mortality (Rumrill, 1990; Morgan, 1995; Vaughn and Allen, 2010), however predation is believed to be the primary factor of larval and post-larval mortality (Thorson, 1950; Morgan, 1995).

5.6.3 The day/night cycle

Predation is believed to be a factor that drives the vertical distribution of larvae in the marine environment, as larvae of a range of taxa have been observed to synchronise their vertical migratory behaviours to the day/night, occupying the surface waters at night when visibility is low and staying in deeper waters during the day as a predation-avoidance response (Lampert, 1994; Raby et al., 1994; Breckenridge et al., 2011; Romero et al., 2012). The sampling regimes used (Knights et al., 2006) and undertaken (Chapter 3) in this thesis were carried out during daylight hours, and so potential diurnal vertical migration patterns were not explored. It is therefore possible that, even when the reverse-engineering approach is implemented, model outcomes over- or underestimate larval dispersal as I cannot guarantee that the observed patterns used to

'fit' the active swimming metric over the course of the tidal cycle are repeated by larvae during the night. Future research would benefit from sampling programmes that encompass the 24-hour diel cycle in order to encapsulate potential variation in the vertical distribution of larvae as a function of the day/night cycle.

5.7 Final conclusions

Dispersal models play a critical role in theoretical and applied science and can be invaluable tools in these endeavours, but as this thesis highlights, additional focus needs to be placed on the importance of correctly parameterising behaviour in these models in order for their findings to better replicate patterns in nature, and thus patterns of dispersal. I have shown this to be especially important when modelling the dispersal of species with extended planktonic larval durations (> 24 hours), where models using a rule-based approach lead to marked differences in dispersal and larval biogeography.

This thesis makes significant steps towards improving the parameterisation of behaviour within dispersal models by considering larval movement as a manifestation of behaviour influenced by the larva's *in-situ* environment. The methodologies and analytical techniques designed and applied within the data chapters can be applied to any species with a planktonic dispersal phase in any location, and provide an important step towards improving the biological 'realism' of behavioural parameterisation in dispersal models in the absence of an understanding of the complex drivers of active larval movement.

REFERENCES

Adams DK & Mullineaux LS (2008) Supply of gastropod larvae to hydrothermal vents reflects transport from local larval sources. *Limnology and Oceanography*. 53(5):1945-55.

Aiken CM, Navarrete SA & Pelegrí JL (2011) Potential changes in larval dispersal and alongshore connectivity on the central Chilean coast due to an altered wind climate. *Journal of Geophysical Research: Biogeosciences.* 116(G4).

Aiken CM, Navarrete SA, Castillo MI & Castilla JC (2007) Along-shore larval dispersal kernels in a numerical ocean model of the central Chilean coast. *Marine Ecology Progress Series*. 339: 13-24.

Allain, G, Petitgas, P, Lazure, P & Grellier, P (2007) Biophysical modelling of larval drift, growth and survival for the prediction of anchovy *(Engraulis encrasicolus)* recruitment in the Bay of Biscay (NE Atlantic). *Fisheries Oceanography.* 16 (6): 489-505.

Almany GR, Connolly SR, Heath DD, Hogan JD, Jones GP, McCook LJ, Mills M, Pressey RL & Williamson DH (2009) Connectivity, biodiversity conservation and the design of marine reserve networks for coral reefs. *Coral Reefs*. 28(2): 339-51.

Andrello M, Mouillot D, Beuvier J, Albouy C, Thuiller W & Manel S (2013) Low connectivity between Mediterranean marine protected areas: a biophysical modeling approach for the dusky grouper *Epinephelus marginatus. PLoS One.* 8(7):e68564.

Andrello M, Mouillot D, Somot S, Thuiller W & Manel S (2015) Additive effects of climate change on connectivity between marine protected areas and larval supply to fished areas. *Diversity and Distributions*. 21(2):139-50.

Andrews JD (1983) transport of bivalve larvae in James River, Virginia. *Journal of Shellfish Research.* 3:29-40.

Assis J, Zupan M, Nicastro KR, Zardi GI, McQuaid CD & Serrao EA (2015) Oceanographic conditions limit the spread of a marine invader along southern African shores. *PLoS One.* 10(6).

Awaji T, Imasato N & Kunishi H (1980) Tidal exchange through a strait: a numerical experiment using a simple model basin. *Journal of Physical Oceanography*. 10 (10):1499-1508.

Baker P & Mann R (2003) Late stage bivalve larvae in a well-mixed estuary are not inert particles. *Estuaries*. 26(4):837-45.

Banas, NS, McDonald PS & Armstrong DA (2009) Green crab larval retention in Willapa Bay, Washington: An intensive lagrangian modelling approach. *Estuaries Coast.* 32, 893–905.

Barber PH, Palumbi SR, Erdmann MV & Moosa MK (2002) Sharp genetic breaks among populations *of Haptosquilla pulchella (Stomatopoda)* indicate limits to larval transport: patterns, causes, and consequences. *Molecular Ecology*. 11(4):659-74.

Becker BJ, Levin LA, Fodrie FJ & McMillan PA (2007). Complex larval connectivity patterns among marine invertebrate populations. *Proceedings of the National Academy of Sciences*. 104 (9): 3267-3272.

Berenshtein I, Paris CB, Gildor H, Fredj E, Amitai Y, Lapidot O & Kiflawi M (2018) Auto-correlated directional swimming can enhance settlement success and connectivity in fish larvae. *Journal of Theoretical Biology*. 439:76-85.

Bernhardt JR & Leslie HM (2013) Resilience to climate change in coastal marine ecosystems. *Annual Review of Marine Science.* 5: 371-392.

Bianco IH, Kampff AR & Engert F (2011) Prey capture behavior evoked by simple visual stimuli in larval zebrafish. *Frontiers in Systems Neuroscience*. 5:101.

Blanco, M, Ospina-Álvarez, A, Navarrete, SA & Fernández, M (2019) Influence of larval traits on dispersal and connectivity patterns of two exploited marine invertebrates in central Chile. *Marine Ecology Progress Series*. *612*: 43-64.

Blanke B & Raynaud S (1997) Kinematics of the Pacific equatorial undercurrent: An Eulerian and Lagrangian approach from GCM results. *Journal of Physical Oceanography*. 27(6):1038-53.

Bleck R, Rooth C, Hu D & Smith LT (1992) Salinity-driven thermocline transients in a wind and thermohaline-forced isopycnic coordinate model of the North Atlantic. *Journal of Physical Oceanography*. 22: 1486–1505.

Blumberg AF & Mellor GL (1987) A description of a three-dimensional coastal ocean circulation model. In: Heaps, N (Ed.) Three-Dimensional Coastal Ocean Models, 208. *American Geophysical Union.*

Bode M, Leis JM, Mason LB, Williamson DH, Harrison HB, Choukroun S & Jones GP (2019) Successful validation of a larval dispersal model using genetic parentage data. *PloS Biology*. 17(7): e3000380.

Bonicelli J, Tyburczy J, Tapia FJ, Finke GR, Parragué M, Dudas S, Menge BA & Navarrete SA (2016) Diel vertical migration and cross-shore distribution of barnacle and bivalve larvae in the central Chile inner-shelf. *Journal of Experimental Marine Biology & Ecology.* 485, 35-46.

Booth JD (1972) Studies on New Zealand Bivalve Larvae, with Observations on the Adults, and on the Hydrology of Bay of Islands and Wellington Harbour. *PhD thesis.* Victoria University of Wellington, *NZ.*

Botsford L, Micheli F & Hastings A (2003) Principles for the design of marine reserves. *Ecological Applications.* 13, S25–S31.

Botsford LW, Brumbaugh DR, Grimes C, Kellner JB, Largier J, O'Farrell MR, Ralston S, Soulanille E & Wespestad V(2009a) Connectivity, sustainability, and yield: bridging the gap between conventional fisheries management and marine protected areas. *Reviews in Fish Biology and Fisheries*. 19(1):69-95.

Botsford LW, White JW, Coffroth MA, Paris CB, Planes S, Shearer TL, Thorrold SR & Jones GP (2009b) Connectivity & resilience of coral reef metapopulations in marine protected areas: matching empirical efforts to predictive needs. *Coral Reefs.* 28, 327-337.

Bowler, DE, & Benton, TG (2005) Causes and consequences of animal dispersal strategies: relating individual behaviour to spatial dynamics. *Biological Review of the Cambridge Philosophical Society*. 80, 205–225.

Box, GEP (1976) Science and statistics. *Journal of the American Statistical Association.* 71 (356): 791–799.

Bradley CJ, Strickler JR, Buskey, EJ & Lenz PH (2013) Swimming & escape behavior in two species of calanoid copepods from nauplius to adult. *Journal of Plankton Research*. 35: 49–65.

Breckenridge JK & Bollens SM (2011) Vertical distribution and migration of decapod larvae in relation to light and tides in Willapa Bay, Washington. *Estauries & Coasts.* 34: 1255-1261.

Brereton A, Tejada-Martínez AE, Palmer MR & Polton JA (2019) The perturbation method-A novel large-eddy simulation technique to model realistic turbulence: Application to tidal flow. *Ocean Modelling.* 135: 31-9.

Brickman, D and Frank KT (2000) Modelling the dispersal and mortality of Browns Bank egg and larval haddock (*Melanogrammus aeglefinus*). *Canadian Journal of Fisheries and Aquatic Sciences*. 57(12): 2519-2535.

Britto FB, Schmidt AJ, Carvalho AM, Vasconcelos CC, Farias AM, Bentzen P & Diniz FM (2018) Population connectivity and larval dispersal of the exploited mangrove crab *Ucides cordatus* along the Brazilian coast. *PeerJ.* 6: e4702.

Brown J, Carrillo L, Fernand L, Horsburgh KJ, Hill AE, Young EF & Medler, KJ (2003) Observations of the physical structure & seasonal jet-like circulation of the Celtic Sea & St. George's Channel of the Irish Sea. *Continental Shelf Research*. 23: 533–561.

Bryan K (1969) A numerical method for the study of the circulation of the world ocean. *Journal of Computational Physics*. 4(3): 347-376.

Buonaccorsi VP, Westerman M, Stannard J, Kimbrell C, Lynn E & Vetter RD (2004) Molecular genetic structure suggests limited larval dispersal in grass rockfish, *Sebastes rastrelliger*. *Marine Biology*. 145(4): 779-88.

Burrows MT, Schoeman DS, Buckley LB, Moore P, Poloczanska ES, Brander KM, Brown C, Bruno JF, Duarte CM, Halpern BS & Holding J (2011) The pace of shifting climate in marine and terrestrial ecosystems. *Science*. 334 (6056): 652-655.

Butler IV MJ, Paris CB, Goldstein JS, Matsuda H & Cowen RK (2011) Behavior constrains the dispersal of long-lived spiny lobster larvae. *Marine Ecology Progress Series*. 422:223-37.

Butman CA, Grassle JP & Webb CM (1988) Substrate choices made by marine larvae settling in still water and in a flume flow. *Nature.* 333(6175): 771-773.

Carlson DF, Suaria G, Aliani S, Fredj E, Fortibuoni T, Griffa A, Russo A & Melli V (2017) Combining litter observations with a regional ocean model to identify sources and sinks of floating debris in a semi-enclosed basin: the Adriatic Sea. *Frontiers in Marine Science*. 4:78.

Carr MH, Robinson SP, Wahle C, Davis G, Kroll S, Murray S, Schumacker EJ & Williams M (2017) The central importance of ecological spatial connectivity to effective coastal marine protected areas and to meeting the challenges of climate change in the marine environment. *Aquatic Conservation: Marine and Freshwater Ecosystems.* 27:6-29.

Carriker MR (1951) Ecological observations on the distribution of oyster larvae in New Jersey estuaries. *Ecological Monographs*. 21(1):19-38.

Carriker MR (1961) Interrelation of functional morphology, behavior, and autecology in early stages of the bivalve *Mercenaria mercenaria. Journal of the Elisha Mitchell Scientific Society.* 77(2):168-241.

Carter MI, Russell DJ, Embling CB, Blight CJ, Thompson D, Hosegood PJ & Bennett KA (2017) Intrinsic and extrinsic factors drive ontogeny of early-life at-sea behaviour in a marine top predator. *Scientific Reports*. 7 (1): 1-14.

Chang AL., Blakeslee AM, Miller AW & Ruiz GM (2011) Establishment failure in biological invasions: a case history of *Littorina littorea* in California, USA. *PLoS One*. 6(1):e16035.

Chang YL, Miller MJ, Tsukamoto K & Miyazawa Y (2018) Effect of larval swimming in the western North Pacific subtropical gyre on the recruitment success of the Japanese eel. *PloS one.* 13(12):e0208704.

Chen C, Liu H & Beardsley RC (2003) An unstructured grid, finite-volume, three-dimensional., primitive equations ocean model: application to coastal ocean and estuaries. *Journal of Atmospheric and Oceanic Technology*. *20* (1): 159-186.

Chia F-S, Buckland-Nicks J & Young CM (1984) Locomotion of marine invertebrate larvae: a review. *Canadian Journal of Zoology.* 62, 1205-1222.

Christie MR, Meirmans PG, Gaggiotti OE, Toonen RJ & White C (2017) Disentangling the relative merits and disadvantages of parentage analysis and assignment tests for inferring population connectivity. *ICES Journal of Marine Science*. 74(6):1749-62.

Christie MR, Tissot BN, Albins MA, Beets JP, Jia Y, Ortiz DM, Thompson SE & Hixon MA (2010) Larval connectivity in an effective network of marine protected areas. *PloS one*. 5(12):e15715.

Cisewski B, Strass VH, Rhein M & Krägefsky S (2010) Seasonal variation of diel vertical migration of zooplankton from ADCP backscatter time series data in the Lazarev Sea, Antarctica. *Deep Sea Research Part I: Oceanographic Research Papers*. 57(1):78-94.

Civelek CV, Daigle RM & Metaxas A (2013) Effects of temperature on larval swimming patterns regulate vertical distribution relative to thermoclines in *Asterias rubens*. *Journal of Experimental Marine Biology & Ecology.* 445, 1–12.

Cleve PT (1900) The seasonal distribution of Atlantic plankton organisms. *Goteborg.*

Cleve-Euler A (1928) Per Theodore Cleve. *Conseil Permenant International pour l'Exploration de la Mer. Rapports et Proces-verbaux.* 47: 35-38.

Clobert J, Danchin E, Dhont AA and Nichols JD (2001) Dispersal. Oxford University Press. *Oxford.*

Cohen JH, Hanson CK, Dittel AI, Miller DC & Tilburg CE (2015) The ontogeny of larval swimming behavior in the crab *Hemigrapsus sanguineus*: implications for larval transport. *Journal of Experimental Marine Biology and Ecology*. 462:20-8.

Cohen, J. (2013) Statistical power analysis for the behavioural sciences: Revised Edition. Academic press. *London*

Comblen R, Blaise S, Legat V, Remacle JF, Deleersnijder E & Lambrechts J (2010) A discontinuous finite element baroclinic marine model on unstructured prismatic meshes. *Ocean Dynamics*. 60(6): 1395-1414.

Conway DV (2012a) Marine Zooplankton of Southern Britain-Part 1: Radiolaria, Heliozoa, Foraminifera, Ciliophora, Cnidaria, Ctenophora, Platyhelminthes, Nemertea, Rotifera and Mollusca. *Occasional Publication of the Marine Biological Association 25.*

Conway DV (2012b) Marine Zooplankton of Southern Britain-Part 2: Arachnida, Pycnogonida, Cladocera, Facetotecta, Cirripedia and Copepoda. *Occasional Publication of the Marine Biological Association 26*.

Corell H & Nissling A (2019) Modelling of larval dispersal of Baltic flounder (*Platichthys solemdali*) revealed drifting depth as a major factor determining opportunities for local retention vs large-scale connectivity. *Fisheries Research.* 1(218): 127-37.

Corell H, Moksnes PO, Engqvist A, Döös K & Jonsson PR (2012) Depth distribution of larvae critically affects their dispersal and the efficiency of marine protected areas. *Marine Ecology Progress Series*. 467: 29-46.

Costello C, Rassweiler A, Siegel D, De Leo G, Micheli F & Rosenberg A (2010) The value of spatial information in MPA network design. *Proceedings of the National Academy of Sciences*.107(43):18294-9.

Costello MJ & Connor DW (2019) Connectivity is generally not important for marine reserve planning. *Trends in Ecology & Evolutiom.* 34 (8): 686-688.

Cowen RK & Sponaugle S (2009) Larval Dispersal & Marine Population Connectivity. *Annual Review of Marine Sciences.* 1, 443–466.

Cowen RK, Lwiza KM, Sponaugle S, Paris CB & Olson DB (2000) Connectivity of marine populations: open or closed? *Science*. 287 (5454): 857-859.

Cowen RK, Paris CB, Olson DB & Fortuna JL (2003) The role of long distance dispersal versus local retention in replenishing marine populations. *Gulf and Caribbean Research*. 14(2):129-37.

Cox SL, Miller PI, Embling CB, Scales KL, Bicknell AWJ, Hosegood PJ, Morgan G, Ingram SN & Votier SC (2016) Seabird diving behaviour reveals the functional significance of shelf-sea fronts as foraging hotspots. *Royal Society Open Science*. 3 (9): 160317.

Criales MM, Chérubin L, Gandy R, Garavelli L, Ghannami MA & Crowley C (2019) Blue crab larval dispersal highlights population connectivity and implications for fishery management. *Marine Ecology Progress Series.* 625:53-70.

Criales MM, Robblee MB, Browder, JA, Cardenas H & Jackson TL (2011) Field Observations on Selective Tidal-Stream Transport for Postlarval & Juvenile Pink Shrimp in Florida Bay. *Journal of Crustacean Biology*. 31, 26–33.

Crosbie T, Wright DW, Oppedal F, Johnsen IA, Samsing F & Dempster T (2019) Effects of step salinity gradients on salmon lice larvae behaviour and dispersal. *Aquaculture Environment Interactions*. 11:181-90.

Dabrowski K & Tsukamoto K (1986) Tetracycline tagging in coregonid embryos and larvae. *Journal of Fish Biology*. 29 (6): 691-698.

Dahlberg MD (1979) A review of survival rates of fish eggs and larvae in relation to impact assessments. *Marine Fisheries Review.* 41(3):1-2.

Daigle RM & Metaxas A (2011) Vertical distribution of marine invertebrate larvae in response to thermal stratification in the laboratory. *Journal of Experimental Marine Biology & Ecology.* 409, 89-98.

Daigle RM, Chassé J & Metaxas A (2016) The relative effect of behaviour in larval dispersal in a low energy embayment. *Progress in Oceanography*. 144:93-117.

de Andres-Bragado L, Mazza C, Senn W & Sprecher SG (2018) Statistical modelling of navigational decisions based on intensity versus directionality in Drosophila larval phototaxis. *Scientific Reports*. 8(1):1-2.

de Boor C (1978) A Practical Guide to Splines. Springer-Verlag. *New York.*

de Oliveira Sodré E & Bozelli RL (2019) How planktonic microcrustaceans respond to environment and affect ecosystem: a functional trait perspective. *International Aquatic Research.* 1:1-7.

Delandmeter P & van Sebille E (2019) The Parcels v2.0 Lagrangian framework: new field interpolation schemes. *Geoscientific Model Development*. 12: 3571–3584.

DiBacco C & Levin LA (2000) Development and application of elemental fingerprinting to track the dispersal of marine invertebrate larvae. *Limnology and Oceanography*. 45 (4): 871-880.

DiBacco C, Fuchs HL, Pineda J & Helfrich K (2011) Swimming behavior and velocities of barnacle cyprids in a downwelling flume. *Marine Ecology Progress Series*. 433:131-48.

DiBacco C, Sutton D & McConnico L (2001) Vertical migration behavior and horizontal distribution of brachyuran larvae in a low-inflow estuary: implications for bay-ocean exchange. *Marine Ecology Progress Series*. 217: 191-206.

Doak DF & Morris WF (2010) Demographic compensation and tipping points in climate-induced range shifts. *Nature*. 467(7318):959-62.

Doherty PD, Baxter JM, Godley BJ, Graham RT, Hall G, Hall J, Hawkes LA, Henderson SM, Johnson L, Speedie C & Witt MJ (2019) Seasonal changes in basking shark vertical space use in the north-east Atlantic. *Marine Biology*. *166* (10): 129.

Donahue MJ, Karnauskas M, Toews C & Paris CB (2015) Location isn't everything: timing of spawning aggregations optimizes larval replenishment. *PLoS One*. 10(6).

Drijfhout SS, Maier-Reimer E & Mikolajewicz U (1996) Tracing the conveyor belt in the Hamburg large-scale geostrophic ocean general circulation model. *Journal of Geophysical Research: Oceans.* 101(C10):22563-75.

Dronkers J (1986) Tidal asymmetry & estuarine morphology. *Netherlands Journal of Sea Research.* 20: 117-131.

Dumas P, Tiavouane J, Senia J, Willam A, Dick L & Fauvelot C (2014) Evidence of early chemotaxis contributing to active habitat selection by the sessile giant clam *Tridacna maxima. Journal of Experimental Marine Biology and Ecology*. 452:63-9.

Edwards KP, Hare JA, Werner FE & Seim H (2007) Using 2-dimensional dispersal kernels to identify the dominant influences on larval dispersal on continental shelves. *Marine Ecology Progress Series*. 352: 77-87.

Eggleston DB, Lillis A & Bohnenstiehl D (2016) Soundscapes and larval settlement: larval bivalve responses to habitat-associated underwater sounds. In: The Effects of Noise on Aquatic Life II. Popper AN & Hawkins A (Eds.) *Springer*, New York, NY. 255-263

Ekman VW (1905) On the influence of the Earth's rotation on ocean currents. *Archive of Mathematical and Astronomical Physics.* 2: 1-52.

Elith J (2017) Predicting distributions of invasive species. In: Invasive species: Risk assessment and management. Robinson, AP, Walshe, T, Burgman, MA, & Nunn, M (Eds). *Cambridge University Press*. 93-129.

Ellein C, Thiebaut É, Barnay AS, Dauvin JC, Gentil LF & Salomon JC (2000) The influence of variability in larval dispersal on the dynamics of a marine metapopulation in the eastern Channel. *Oceanologica Acta*. *23* (4): 423-442.

Eloire D, Somerfield PJ, Conway DV, Halsband-Lenk C, Harris R & Bonnet D (2010) Temporal variability and community composition of zooplankton at station L4 in the Western Channel: 20 years of sampling. *Journal of Plankton Research*. 32(5):657-79.

Endler JA (1977) Geographic variation, speciation, and clines. 10. *Princeton University*

Ettinger-Epstein P, Whalan S, Battershill CN & de Nys R (2008) A hierarchy of settlement cues influences larval behaviour in a coral reef sponge. *Marine Ecology Progress Series.* 365, 103–113.

Fiksen Ø, Jørgensen C, Kristiansen T, Vikebø F & Huse G (2007) Linking behavioural ecology and oceanography: larval behaviour determines growth, mortality and dispersal. *Marine Ecology Progress Series*. 347:195-205.

Filgueira R, Brown MS, Comeau LA & Grant J (2015) Predicting the timing of the pediveliger stage of *Mytilus edulis* based on ocean temperature. *Journal of Molluscan Studies*. 81(2):269-73.

Firth LB, Harris D, Blaze JA, Marzloff MP, Boyé A, Miller PI, Curd A, Nunn JD, O'Connor NE, Power AM, Mieszkowska N, O'Riordan RM, Burrows MT, Bricheno LM, Knights, AM, Nunes FLD, Bordeyne F, Bush LE, Byers JE, David C, Davies AJ, Dubois SF, Edwards, H, Foggo A, Grant L, Green, JAM, Gribben P, Lima FP, McGrath D, Noël LMLJ, Seabra R, Simkanin C, Vasquez M, Hawkins S (in review) Specific niche requirements underpin multidecadal range edge stability but introduce barriers for climate change adaptation. *Submitted to Diversity and Distributions*

Firth LB, Knights AM, Bridger D, Evans AJ, Mieszkowska N, Moore PJ, O'Connor NE, Sheehan EV, Thompson RC & Hawkins SJ (2016) Ocean Sprawl: Challenges & opportunities for biodiversity management in a changing world. *Oceanography and Marine Biology: Annual Review.* 193–269.

Fisher R & Leis JM (2009) Swimming performance in larval fishes: from escaping predators to the potential for long distance migration. In: Fish locomotion: an etho-ecological approach. Domenici P, Kapoor BG (Eds.). *Science Publishers*. Enfield, NH. 333−373

Fisher R & Wilson SK (2004) Maximum sustainable swimming speeds of late-stage larvae of nine species of reef fishes. *Journal of Experimental Marine Biology and Ecology*. 312(1):171-86.

Forward Jr RB (1974) Negative phototaxis in crustacean larvae: possible functional significance. *Journal of Experimental Marine Biology and Ecology*. 16(1):11-7.

Forward RB & Tankersley RA (2001) Selective tidal-stream transport of marine animals. . *Oceanography and Marine Biology: Annual Review.* 39, 305-353.

Forward RB, Tankersley RA & Welch JM (2003) Selective tidal-stream transport of the blue crab *Callinectes sapidus*: an overview. *Bulletin of Marine Science*. 72(2): 347-65.

Fouzai N, Opdal AF, Jørgensen C & Fiksen Ø (2015) Effects of temperature and food availability on larval cod survival: a model for behaviour in vertical gradients. *Marine Ecology Progress Series*. 529:199-212.

Fredj E, Carlson DF, Amitai Y, Gozolchiani A & Gildor H. The particle tracking and analysis toolbox (PaTATO) for Matlab. *Limnology and Oceanography: Methods*.;14(9):586-99.

Fuchs HL & DiBacco C (2011) Mussel larval responses to turbulence are unaltered by larval age or light conditions: Mussel larval behaviour in turbulence. *Limnology & Oceanography: Fluids & Environments*. 1, 120-134.

Fuchs HL, Hunter EJ, Schmitt EL & Guazzo RA (2013) Active downward propulsion by oyster larvae in turbulence. *Journal of Experimental Biology.* 216, 1458-1469.

Fuchs HL, Mullineaux LS & Solow AR (2004) Sinking behavior of gastropod larvae *(Ilyanassa obsoleta)* in turbulence. *Limnology and Oceanography*. 49(6):1937-48.

Fuchs HL, Solow AR & Mullineaux LS (2010). Larval responses to turbulence and temperature in a tidal inlet: habitat selection by dispersing gastropods? *Journal of Marine Research.* 68(1):153-88.

Gaines SD, Gaylord B, Largier JL (2003) Avoiding current oversights in marine reserve design. *Ecological Applications*. 13(sp1):32-46.

Gaines SD, White C, Carr MH & Palumbi SR (2010) Designing marine reserve networks for both conservation and fisheries management. *Proceedings of the National Academy of Sciences*. 107(43):18286-93.

Gardner C, Maguire GB & Williams H (2004) Effects of water temperature and thermoclines on larval behaviour and development in the giant crab *Pseudocarcinus gigas (Lamarck). Journal of Plankton Research*. 26(4):393-402.

Garland ED, Zimmer CA & Lentz SJ (2002). Larval distributions in inner-shelf waters: The roles of wind-driven cross-shelf currents and diel vertical migrations. *Limnology and Oceanography*. 47(3): 803-17.

Garrison L (1999). Vertical migration behavior and larval transport in brachyuran crabs. *Marine Ecology Progress Series*. 176:103-13.

Gary SF, Fox AD, Biastoch A, Roberts JM & Cunningham SA (2020) Larval behaviour, dispersal and population connectivity in the deep sea. *Scientific reports*. 10(1):1-2.

Gaylord B & Gaines SD (2000) Temperature or transport? Range limits in marine species mediated solely by flow. *The American Naturalist*. *155* (6): 769-789.

Gibson RN (2003) Go with the flow: tidal migration in marine animals. *Hydrobiologia*. 503, 153–161.

Gibson RN, Atkinson RJ & Gordon JD (2016) Zooplankton diel vertical migration—a review of proximate control. *Oceanography and Marine Biology: An Annual Review*. 47: 77-110.

Gilg MR & Hilbish TJ (2003) The geography of marine larval dispersal: coupling genetics with fine-scale physical oceanography. *Ecology*. 84(11):2989-98.

Gilpin W, Prakash VN & Prakash M (2017) Vortex arrays and ciliary tangles underlie the feeding–swimming trade-off in starfish larvae. *Nature Physics*. 13(4):380-6.

Gran HH (1902) Das Plankton des Norwegischen Nordmeeres. *Report on Norwegian Fishery and Marine Investigations.* 2(5).

Gravinese PM (2018) Vertical swimming behavior in larvae of the Florida stone crab, *Menippe mercenaria*. *Journal of Plankton Research*. 40(6):643-54.

Greenland S, Senn SJ, Rothman KJ, Carlin JB, Poole C, Goodman SN & Altman DG (2016) Statistical tests, P values, confidence intervals and power; a guide to misinterpretations. *European Journal of Epidemiology.* 31,337-350.

Gregg CS (2002) Effects of biological and physical processes on the vertical distribution and horizontal transport of bivalve larvae in an estuarine inlet. *PhD thesis.* Rutgers University, New Brunswick, NJ.

Harding GC & Trites RW (1988) Dispersal of *Homarus americanus* larvae in the Gulf of Maine from Browns Bank. *Canadian Journal of Fisheries and Aquatic Sciences* 45 (3): 416-425.

Hare JA, Wuenschel MJ & Kimball ME (2012) Projecting range limits with coupled thermal tolerance-climate change models: an example based on gray snapper (*Lutjanus griseus*) along the US east coast. *PLoS One*. 7(12): e52294

Hartnett M, Berry A, Tully O, Dabrowski T (2007) Investigations into the transport and pathways of scallop larvae—the use of numerical models for managing fish stocks. *Journal of Environmental Monitoring.* 9(5):403-10.

Hasumi, H (2015) CCSR ocean component model (COCO). *CCSR Report*. 13: 68.

Hawes S, Miskiewicz T, Garcia V & Figueira W (2020). Size and stage-dependent vertical migration patterns in reef-associated fish larvae off the eastern coast of Australia. *Deep Sea Research Part I: Oceanographic Research Papers.* 103362.

Hayes DR, Dobricic S, Gildor H & Matsikaris A (2019) Operational assimilation of glider temperature and salinity for an improved description of the Cyprus eddy. *Deep Sea Research Part II: Topical Studies in Oceanography.* 164:41-53.

Haza AC, Özgökmen TM & Hogan P (2016) Impact of submesoscales on surface material distribution in a gulf of Mexico mesoscale eddy. *Ocean Modelling*. 107: 28–47.

Hedgecock D, Barber PH & Edmands S (2007) Genetic approaches to measuring connectivity. *Oceanography.* 20 (3): 70-79.

Hellberg ME (2007) Footprints on water: the genetic wake of dispersal among reefs. *Coral Reefs.* 26 (3): 463-473.

Hellberg ME, Burton RS, Neigel JE & Palumbi SR (2002) Genetic assessment of connectivity among marine populations. *Bulletin of marine science*. 70 (1): 273-290.

Hetzel Y, Pattiaratchi C, Lowe R & Hofmeister R (2015) Wind and tidal mixing controls on stratification and dense water outflows in a large hypersaline bay. *Journal of Geophysical Research: Oceans*. 120(9):6034-56.

Hiddink JG, Burrows MT & García Molinos J (2015) Temperature tracking by North Sea benthic invertebrates in response to climate change. *Global Change Biology*. 21(1): 117-129.

Hill AE (1990) Pelagic dispersal of Norway lobster *Nephrops norvegicus* larvae examined using an advection-diffusion-mortality model. *Marine Ecology Progress Series. 64* (3):.217-226.

Hill D (2007) Tidal modeling of glacier bay, alaska-methodology, results, and applications. Department of Civil, Environmental Engineering, *Pennsylvania State University.* Technical Report

Hirase S, Tezuka A, Nagano AJ, Kikuchi K & Iwasaki W (2020) Genetic isolation by distance in the yellowfin goby populations revealed by RAD sequencing. *Ichthyological Research.* 67 (1): 98-104

Hixon MA & Jones GP (2005) Competition, predation, and density-dependent mortality in demersal marine fishes. *Ecology*. 86(11):2847-59.

Hjort, J (1926) Fluctuations in the year classes of important food fishes. *Conseil Permanent International pour l'Exploration de la Mer*. 1:5-38.

Hoey JA, Fodrie FJ, Walker QA, Hilton EJ, Kellison GT, Targett TE, Taylor JC, Able KW & Pinsky ML (2020) Using multiple natural tags provides evidence for extensive larval dispersal across space and through time in summer flounder. *Molecular Ecology*. 29(8).

Houde ED (1997) Patterns and trends in larval-stage growth and mortality of teleost fish. *Journal of Fish Biology*. 51: 52-83.

Hsiung KM, Kimura S, Han YS, Takeshige A & Iizuka Y (2018) Effect of ENSO events on larval and juvenile duration and transport of Japanese eel *(Anguilla japonica). PloS one*. 13(4):e0195544.

Huebert KB, Cowen RK & Sponaugle S. (2011) Vertical migrations of reef fish larvae in the Straits of Florida and effects on larval transport. *Limnology and Oceanography*. 56(5):1653-66.

Huijbers CM, Nagelkerken I, Lössbroek PA, Schulten IE, Siegenthaler A, Holderied MW & Simpson SD (2012) A test of the senses: fish select novel habitats by responding to multiple cues. *Ecology*. 93(1):46-55.

Huntley ME & Zhou M (2004) Influence of animals on turbulence in the sea. *Marine Ecology Progress Series.* 273, 65–79.

Iida M, Zenimoto K, Watanabe S, Kimura S & Tsukamoto K (2010) Larval transport of the amphidromous goby *Sicyopterus japonicus* by the Kuroshio Current. *Coastal and Marine Science*. 34:42-6.

Imasato N, Awaji T & Kunishi H (1980) Tidal exchange through naruto, akashi and kitan straits. *Journal of the Oceanographic Society of Japan.*36 (3): 151-162.

Incze LS & Naimie CE (2000) Modelling the transport of lobster (*Homarus americanus*) larvae and postlarvae in the Gulf of Maine. *Fisheries Oceanography*. 9(1): 99-113.

Irisson JO, Paris CB, Guigand C & Planes S (2010) Vertical distribution and ontogenetic migration in coral reef fish larvae. *Limnology and Oceanography*.; 55(2):909-19.

Jalon-Rojas I, Wangw XH, Liao F & Fredj E (2019) A new 3D model for tracking plastic marine debris: impact of particle physical properties and behaviour on microplastics fate. *Geophysical Research Abstracts*. 21.

James MK, Polton JA, Brereton AR, Howell KL, Nimmo-Smith WA & Knights AM (2019) Reverse engineering field-derived vertical distribution profiles to infer larval swimming behaviors. *Proceedings of the National Academy of Sciences*. 116(24): 11818-23.

Jékely G, Colombelli J, Hausen H, Guy K, Stelzer E, Nédélec F & Arendt D (2008) Mechanism of phototaxis in marine zooplankton. *Nature*. 456(7220):395-9.

Johnson MW (1939) The correlation of water movements and dispersal of pelagic larval stages of certain littoral animals, especially the sand crab, *Emerita. Journal of Marine Research.* 2(3): .236-245.

Jones JE (2002) Coastal and shelf-sea modelling in the European context. *Oceanography and Marine Biology: An Annual Review*. 40: 37–141.

Jonsson PR, André C & Lindegarth M (1991) Swimming behaviour of marine bivalve larvae in a flume boundary-layer flow: evidence for near-bottom confinement. *Marine Ecology Progress Series.* 79, 67-76.

Jonsson PR, Moksnes PO, Corell H, Bonsdorff E & Nilsson Jacobi M (2020) Ecological coherence of Marine Protected Areas: New tools applied to the Baltic Sea network. *Aquatic Conservation: Marine and Freshwater Ecosystems*. 30(4):743-60.

Jutzeler M, Marsh R, Carey RJ, White JDL, Talling PJ & Karlstrom L (2014) On the fate of pumice rafts formed during the 2012 Havre submarine eruption. *Nature Communications.* 5: 3660.

Kaplan DM, Botsford LW, O'Farrell MR, Gaines SD & Jorgensen S (2009) Model-based assessment of persistence in proposed marine protected area designs. *Ecological Applications*. 19(2):433-48.

Kasai A, Komatsu K, Sassa C & Konishi Y (2008) Transport and survival processes of eggs and larvae of jack mackerel *Trachurus japonicus* in the East China Sea. *Fisheries Science*. 74(1):8-18.

Kim CK, Park K, Powers SP, Graham WM & Bayha KM (2010) Oyster larval transport in coastal Alabama: Dominance of physical transport over biological behavior in a shallow estuary. *Journal of Geophysical Research: Oceans*. 115(C10).

Kimball ME, Miller JM, Whitfield PE & Hare JA (2004) Thermal tolerance and potential distribution of invasive lionfish (*Pterois volitans*) on the east coast of the United States. *Marine Ecology Progress Series.* 283: 269-278.

Kimmerer WJ, Burau JR & Bennett WA (1998) Tidally oriented vertical migration & position maintenance of zooplankton in a temperate estuary. *Limnology & Oceanography*. 43, 1697–1709.

Kimmerer WJ, Gross ES & MacWilliams ML (2014) Tidal migration and retention of estuarine zooplankton investigated using a particle-tracking model. *Limnology and Oceanography.* 59(3):901-16.

Kingsford MJ, Leis JM, Shanks A, Lindeman KC, Morgan SG & Pineda J (2002) Sensory environments, larval abilities & local self-recruitment. *Bulletin of Marine Science.*. 70, 309-340.

Kinlan BP & Gaines SD (2003) Propagule dispersal in marine and terrestrial environments: a community perspective. *Ecology*. 84 (8): 2007-2020.

Kitchens LL, Paris CB, Vaz AC, Ditty JG, Cornic M, Cowan JH & Rooker JR (2017) Occurrence of invasive lionfish (*Pterois volitans*) larvae in the northern Gulf of Mexico: characterization of dispersal pathways and spawning areas. *Biological Invasions*. 19(7):1971-9.

Knights AM, Crowe TP & Burnell G (2006) Mechanisms of larval transport: vertical distribution of bivalve larvae varies with tidal conditions. *Marine Ecology Progress Series.* 326, 167–174.

Kobayashi DR (2006) Colonization of the Hawaiian Archipelago via Johnston Atoll: a characterization of oceanographic transport corridors for pelagic larvae using computer simulation. *Coral Reefs*. 25(3):407-17.

Krueck NC, Ahmadia GN, Green A, Jones GP, Possingham HP, Riginos C, Treml EA & Mumby PJ (2017) Incorporating larval dispersal into MPA design for both conservation and fisheries. *Ecological Applications.* 27(3):925-41.

Krumme U & Liang TH (2004) Tidal-induced changes in a copepod-dominated zooplankton community in a macrotidal mangrove channel in northern Brazil. *Zoological Studies*. 43(2):404-14.

Kuhn M (2008) Caret package. *Journal of Statistical Software*. 28 (5).

Kunkle DE (1957) The vertical distribution of oyster larvae in Delaware Bay. *Proceedings of the National Shellfish Association*. 48: 90-91.

Kunze HB, Morgan SG & Lwiza KM (2013) Field test of the behavioral regulation of larval transport. *Marine Ecology Progress Series.*487:71-87.

Lacroix G, Barbut L & Volckaert FA (2018) Complex effect of projected sea temperature and wind change on flatfish dispersal. *Global Change Biology*. 24(1):85-100.

Lampert, W (1994) Ultimate causes of diel vertical migration of zooplankton: New evidence for the predator-avoidance hypothesis. *Ergebnisse der Limnologie*. 39, 79-88.

Largier JL (2003) Considerations in estimating larval dispersal distances from oceanographic data. *Ecological Applications*. 13(sp1): 71-89.

Lashley MA, Jordan HR, Tomberlin JK & Barton BT (2018) Indirect effects of larval dispersal following mass mortality events. *Ecology.* 99(2):491-3.

Laubier L (2001) Climatic changes and Mediterranean marine invertebrates: observation network and ecophysiology. *Proceedings of the Italian Association for Oceanology and Limnology*. 14: 15–23.

Le Gouvello DZ, Hart-Davis MG, Backeberg BC & Nel R (2020) Effects of swimming behaviour and oceanography on sea turtle hatchling dispersal at the intersection of two ocean current systems. *Ecological Modelling.* 431:109130.

Le Quesne WJ & Codling EA (2009) Managing mobile species with MPAs: the effects of mobility, larval dispersal., and fishing mortality on closure size. *ICES Journal of Marine Science*: 66(1):122-31.

Lebreton LM, Greer SD & Borrero JC (2012) Numerical modelling of floating debris in the world's oceans. *Marine Pollution Bulletin*. 64(3):653-61.

Leis JM (2020) Measurement of swimming ability in larval marine fishes: comparison of critical speed with in situ speed. *Marine Ecology Progress Series*. LFCav4.

Leitão P, Mateus M, Braunschweig L, Fernandes L & Neves R (2008) Modelling coastal systems: the MOHID Water numerical lab. *Perspectives on Integrated Coastal Zone Management in South America*. 77-88.

Lenoir J, Gégout JC, Guisan A, Vittoz P, Wohlgemuth T, Zimmermann NE, Dullinger S, Pauli H, Willner W & Svenning JC (2010) Going against the flow: potential mechanisms for unexpected downslope range shifts in a warming climate. *Ecography*. 33(2):295-303.

Lessios HA (1988) Mass mortality of *Diadema antillarum* in the Caribbean: what have we learned? *Annual Review of Ecology and Systematics*. 19(1):371-93.

Lett C, Ayata SD, Huret M & Irisson JO (2010) Biophysical modelling to investigate the effects of climate change on marine population dispersal and connectivity. *Progress in Oceanography*. 1(4):106-13.

Lett C, Verley P, Mullon C, Parada C, Brochier T, Penven P & Blanke B (2008) A Lagrangian tool for modelling ichthyoplankton dynamics. *Environmental Modelling & Software.* 23(9): 1210-4.

Leuttich RA, Westerink JJ & Scheffner NW (1992) ADCIRC: an advanced three-dimensional circulation model for shelves, coasts, and estuaries. *Report 1, Theory and methodology of ADCIRC-2DD1 and ADCIRC-3DL.*

Levin LA (2006) Recent progress in understanding larval dispersal: new directions & digressions. *Integrated Computational Biology.* 46, 282–297.

Lillis A, Bohnenstiehl D, Peters JW & Eggleston D (2016) Variation in habitat soundscape characteristics influences settlement of a reef-building coral. *PeerJ.* 4:e2557.

Lloyd MJ, Metaxas A & deYoung B (2012) Patterns in vertical distribution and their potential effects on transport of larval benthic invertebrates in a shallow embayment. *Marine Ecology Progress Series.* 469:37-52.

Lockwood DR, Hastings A & Botsford LW (2002) The effects of dispersal patterns on marine reserves: does the tail wag the dog? *Theoretical Population Biology.* 61(3):297-309.

Lockwood JL, Cassey P & Blackburn T (2005) The role of propagule pressure in explaining species invasions. *Trends in Ecology & Evolution*. 20 (5): 223-228.

López-Duarte PC & Tankersley RA (2007) Circatidal swimming behavior of brachyuran crab zoea larvae: implications for ebb-tide transport. *Marine Biology*. 151(6):2037-51.

Lougee LA, Bollens SM & Avent SR (2002) The effects of haloclines on the vertical distribution and migration of zooplankton. *Journal of Experimental Marine Biology & Ecology.* 278,111-134

Lowe WH & McPeek MA (2014) Is dispersal neutral? *Trends in Ecology and Evolution.* 29 (8): 444-450.

Ludsin SA, DeVanna KM & Smith RE (2014) Physical–biological coupling and the challenge of understanding fish recruitment in freshwater lakes. *Canadian Journal of Fisheries and Aquatic Sciences*. 71 (5): 775-794.

Lutz RA & Kennish MJ (1992) Ecology and morphology of larval and early postlarval mussels. In: The mussel *Mytilus*: ecology, physiology, genetics and culture. Gosling EM (Ed.) *Elsevier,* Amsterdam. 53-85.

Luyten P, Andreu-Burillo I, Norro A, Ponsar S. & Proctor R (2006) A new version of the European public domain code COHERENS. *European Operational Oceanography: Present and Future*. *474*.

Luyten PJ, Jones JE, Proctor A (1999) COHERENS-A coupled hydrodynamical ecological model for regional and shelf seas: User Documentation. *MUMM Report,* Management Unit of the Mathematical Models of the North Sea. 911.

Madec G (2008) the NEMO team: NEMO ocean engine. Note du Pôle de modélisation, Institut Pierre-Simon Laplace (IPSL), *France.* 27: 1288-619.

Maier-Reimer E, Müller D, Olbers D, Willebrand J & Hasselmann KF (1982) An ocean circulation model for climate variability studies. *Hamburg: Max-Planck-Institut für Meteorologie. (Umweltforschungsplan des Bundesministers des Innern - Entwicklung von Klimamodellen;* FB 104 02 612).

Maldonado M (2006) The ecology of the sponge larva. *Canadian Journal of Zoology*. 194: 175–194.

Maldonado M, Durfort M, McCarthy DA & Young CM (2003) The cellular basis of photobehavior in the tufted parenchymella larva of demosponges. *Marine Biology*. 143(3):427-41.

Manel S, Loiseau N & Puebla O (2019) Long-Distance Marine Connectivity: Poorly Understood but Potentially Important. *Trends in Ecology & Evolution*. 34 (8): 688-689.

Mann KH & Kazier JRN (2006) Dynamics of Marine Ecosystems: Biological-Physical Interactions in the Ocean. 3rd edition. *Wiley*. 512.

Mann R, Campos BM & Luckenbach MW (1991) Swimming rate and responses of larvae of three mactrid bivalves to salinity discontinuities. *Marine Ecology Progress Series.* 3:257-69.

Marsh R, Ivchenko VO, Skliris N, Alderson S, Bigg GR, Madec G, Blaker AT, Aksenov Y, Sinha B, Coward AC, Le Sommer J, Merino N & Zalesny VB (2015) NEMO–ICB (v1.0): interactive icebergs in the NEMO ocean model globally configured at eddy-permitting resolution. *Geoscientific Model Development*. 8 (5): 1547-1562.

Marshall DJ, Monro K, Bode M, Keough MJ & Swearer S (2010) Phenotype–environment mismatches reduce connectivity in the sea. *Ecology Letters.* 13, 128–140.

Marshall J, Adcroft A, Hill C, Perelman L & Heisey C (1997). "A finite-volume, incompressible Navier Stokes model for studies of the ocean on parallel computers". *Journal of Geophysical Research: Oceans*. 102 (C3): 5753–5766

Marta-Almeida M, Dubert J, Peliz Á & Queiroga H (2006) Influence of vertical migration pattern on retention of crab larvae in a seasonal upwelling system. *Marine Ecology Progress Series*.307: 1-9.

Maru K, Obara A, Kikuchi K & Okesaku H (1973) Studies on the ecology of the scallop, *Patinopecten yessoensis (Jay)*: On the diurnal vertical distribution of scallop larvae. *Scientific Reports of the Hokkaido Fisheries Experimental Station*. 15:33-52.

Mayorga-Adame CG, Batchelder HP & Spitz Y (2017b) Modeling larval connectivity of coral reef organisms in the Kenya-Tanzania region. *Frontiers in Marine Science*. 4: 92.

Mayorga-Adame CG, Polton J, Holt J, Graham J & Henry LA (2017a) Dispersal patterns in the North Sea, insights from a high resolution model. *EGUGA*. 1376.

Mayr E (1963) Animal species and evolution. *Animal species and evolution.*

McIntyre BA, McPhee-Shaw EE, Hatch MB, Arellano SM (2020) Location matters: passive and active factors affect the vertical distribution of Olympia oyster (*Ostrea lurida*) larvae. *Estuaries and Coasts*. 16:1-5.

McManus MA & Woodson CB (2012) Plankton distribution & ocean dispersal. *Journal of Experimental Biology*. 215, 1008–1016.

McManus MC, Ullman DS, Rutherford SD & Kincaid C (2020) Northern quahog *(Mercenaria mercenaria)* larval transport and settlement modeled for a temperate estuary. *Limnology and Oceanography*. 65(2):289-303.

McVeigh DM, Eggleston DB, Todd AC, Young CM & He R (2017) The influence of larval migration and dispersal depth on potential larval trajectories of a deep-sea bivalve. *Deep Sea Research Part I: Oceanographic Research Papers.* 127:57-64.

Metaxas A & Saunders M (2009) Quantifying the "bio-" components in biophysical models of larval transport in marine benthic invertebrates: advances & pitfalls. *Biological Bulletin.* 216, 257–272.

Metaxas A (2001) Behaviour in flow: perspectives on the distribution & dispersion of meroplanktonic larvae in the water column. *Canadian Journal of Fisheries & Aquatic Sciences.* 58, 86-98.

Michalec FG, Souissi S. & Holzner M (2015) Turbulence triggers vigorous swimming but hinders motion strategy in planktonic copepods. *Journal of the Royal Society Interface*. 12, 150-158.

Mileikovsky SA (1971) Types of larval development in marine bottom invertebrates, their distribution and ecological significance: A re-evaluation. *Marine Biology*. 10 (3):193–213.

Moksnes PO and Jonsson PR (2020) Larval connectivity and marine protected area networks. In: The Natural History of the Crustacea: Developmental Biology and Larval Ecology. Anger K, Harzsch S & Theil M (Eds.). *Oxford University Press, Oxford.* (7) 408.

Moksnes PO, Corell H, Tryman K, Hordoir R & Jonsson PR (2014) Larval behavior and dispersal mechanisms in shore crab larvae (*Carcinus maenas*): Local adaptations to different tidal environments?. *Limnology and Oceanography*. 59(2): 588-602.

Møller OS, Olesen J & Waloszek D (2007) Swimming and cleaning in the free-swimming phase of Argulus larvae (*crustacea, branchiura*)—Appendage adaptation and functional morphology. *Journal of Morphology.* 268(1):1-1.

Mood (1954) On the asymptotic efficiency of certain nonparametric two sample tests. *Annual of Mathematics and Statistics.* 25: 514-522

Moore RD, Wolf J, Souza AJ & Flint SS (2009) Morphological evolution of the Dee Estuary, Eastern Irish Sea, UK: a tidal asymmetry approach. *Geomorphology*. 103, 588-596.

Morello SL & Yund PO (2016) Response of competent blue mussel (*Mytilus edulis*) larvae to positive and negative settlement cues. *Journal of Experimental Marine Biology and Ecology. 480:8-16.*

Morgan LE & Botsford LW (2001) Managing with reserves: modeling uncertainty in larval dispersal for a sea urchin fishery. Spatial processes and management of marine populations. *Alaska Sea Grant College Program, Fairbanks, Alaska*.

Morgan SG (1995) Life and death in the plankton: larval mortality and adaptation. *Ecology of Marine Invertebrate Larvae*. 1:279-322.

Morin PA, Martien KK & Taylor BL (2009) Assessing statistical power of SNPs for population structure and conservation studies. *Molecular Ecology Resources*. 9 (1): 66-73.

Munroe DM, Haidvogel D, Caracappa JC, Klinck JM, Powell EN, Hofmann EE, Shank BV & Hart DR (2018) Modeling larval dispersal and connectivity for Atlantic sea scallop (*Placopecten magellanicus*) in the Middle Atlantic Bight. *Fisheries Research*. 208: 7-15.

Nathan R, Klein EK, Robledo-Arnuncio JJ & Revilla E (2012) Dispersal kernels. in Dispersal ecology and evolution. Baguete M, Benton TG & Bullock JM (Eds.). *Oxford University Press.* 187-210.

Neil C, Cunningham A, McKee D & Polton JA (2012) Remote sensing of seasonal stratification dynamics in the southern Irish Sea. *Remote Sensing of Environment.* 127: 288-97.

Neubert MG & Caswell H (2000) Demography and dispersal: calculation and sensitivity analysis of invasion speed for structured populations. *Ecology.* 81: 1613-28.

Neumann H, de Boois I, Kröncke I & Reiss H (2013) Climate change facilitated range expansion of the non-native angular crab *Goneplax rhomboides* into the North Sea. *Marine Ecology Progress Series.* 484: 143-153.

Newell GE, & Newell RC (1977) Marine plankton: a practical guide, 206 pp. *Hutchinson Educational Editions*, University of London, London

Nicolle A, Dumas F, Foveau A, Foucher E & Thiebaut E (2013) Modelling larval dispersal of the king scallop (*Pecten maximus*) in the English Channel: examples from the bay of Saint-Brieuc & the bay of Seine. *Ocean Dyn.* 63, 661–678.

North EW, Gallego A & Petitgas P (2009) Manual of recommended practices for modelling physical–biological interactions during fish early life. *ICES Cooperative Research Report*. 295: 111.

North EW, Schlag Z, Hood RR, Li M, Zhong L, Gross T & Kennedy VS (2008) Vertical swimming behavior influences the dispersal of simulated oyster larvae in a coupled particle-tracking and hydrodynamic model of Chesapeake Bay. *Marine Ecology Progress Series*. 359: 99-115.

O'Dea E, Furner R, Wakelin S, Siddorn J, While J, Sykes P, King R, Holt J & Hewitt H (2017) The CO5 configuration of the 7 km Atlantic Margin Model: large-scale biases and sensitivity to forcing, physics options and vertical resolution. *Geoscientific Model Development*. 10(8): 2947.

Oberhuber JM (1993) The OPYC ocean general circulation model. *World Data Center for Climate (WDCC) at DKRZ.*

Occhipinti-Ambrogi A (2007) Global change and marine communities: alien species and climate change. *Marine Pollution Bulletin.* 55 (7-9): 342-352.

O'Connor MI, Bruno JF, Gaines SD, Halpern BS, Lester SE, Kinlan BP & Weiss JM (2007) Temperature control of larval dispersal and the implications for marine ecology,

evolution, and conservation. *Proceedings of the National Academy of Sciences*. 104(4): 1266-1271.

Oldfather MF, Kling MM, Sheth SN, Emery NC & Ackerly DD (2010) Range edges in heterogeneous landscapes: Integrating geographic scale and climate complexity into range dynamics. *Global Change Biology*. 26(3):1055-67.

Olson RR (1985) The consequences of short-distance larval dispersal in a sessile marine invertebrate. *Ecology*. 66(1): 30-9.

Oteiza P, Odstrcil I, Lauder G, Portugues R & Engert F (2017) A novel mechanism for mechanosensory-based rheotaxis in larval zebrafish. *Nature.* 547, 445-448.

Pacanowski RC, Dixon K & Rosati A (1991) The GFDL modular ocean model users guide. *GFDL Ocean Group Technical Reports*. 2:142.

Palumbi S. (2003) Population genetics, demographic connectivity & the design of marine reserves. *Ecological Applications*. 13, S146–S158.

Paris CB & Cowen RK (2004) Direct evidence of a biophysical retention mechanism for coral reef fish larvae. *Limnology and Oceanography*. 49(6):1964-79.

Paris CB, Cherubin LM, & Cowen RK (2007) Surfing, spinning or diving: effects on population connectivity. *Marine Ecology Progress Series.* 347, 285-300.

Paris CB, Helgers J, Van Sebille E & Srinivasan A (2013) Connectivity Modeling System: A probabilistic modeling tool for the multi-scale tracking of biotic and abiotic variability in the ocean. *Environmental Modelling & Software*. 42: 47-54.

Paris CB, Le Hénaff M, Aman ZM, Subramaniam A, Helgers J, Wang D-P, Kourafalou VH & Srinivasan A (2012) Evolution of the Macondo well blowout: simulating the effects of the circulation and synthetic dispersants on the subsea oil transport. *Environmental Science and Technology.* 42: 47-54

Parmesan C & Yohe G (2003) A globally coherent fingerprint of climate change impacts across natural systems. *Nature*. 421 (6918): 37-42.

Pebesma, EJ & Bivand, RS (2005) Classes and methods for spatial data in R. *R News.* 5(2)

Pechenik J (1999) On the advantages and disadvantages of larval stages in benthic marine invertebrate life cycles. *Marine Ecology Progress Series.* 177: 269-297.

Pechenik JA (1990) Delayed metamorphosis by larvae of benthic marine invertebrates: does it occur? Is there a price to pay? *Ophelia*. 32(1-2):63-94.

Peteiro LG & Shanks AL (2015) Up and down or how to stay in the bay: retentive strategies of Olympia oyster larvae in a shallow estuary. *Marine Ecology Progress Series*. 530:103-17.

Pettitt AN (1979) A non-parametric approach to the change-point problem. *Applied Statistics.* 28: 126–135

Pfeiffer-Herbert AS, McManus MA, Raimondi PT, Chao Y & Chai F (2007) Dispersal of barnacle larvae along the central California coast: a modeling study. *Limnology and Oceanography*. 52(4): 1559-69.

Phelps J, Polton J, Souza A, & Robinson L (2015) Behaviour influences larval dispersal in shelf sea gyres: *Nephrops norvegicus* in the Irish Sea. *Marine Ecology Progress Series.* 518: 177–191.

Phillips NA (1956) The general circulation of the atmosphere: A numerical experiment. *Quarterly Journal of the Royal Meteorological Society*. *82* (352): 123-164.

Phillips NE (2004) Variable timing of larval food has consequences for early juvenile performance in a marine mussel. *Ecology.* 85(8):2341-6.

Piñeda J, Hare JA & Sponaugle SU (2007) Larval transport and dispersal in the coastal ocean and consequences for population connectivity. *Oceanography*. 20 (3): 22-39.

Pingree RD & Griffiths, DK (1979) Transport paths around the British Isles resulting from M2 & M4 tidal interactions. *Journal of the Marine Biological Association of the United Kingdom.* 59, 497-513.

Pinheiro J, Bates D, DebRoy S, Sarkar D, R Core Team (2020)_lme: Linear and Nonlinear Mixed Effects Models. R package version 3.1-148.

Pinsky ML, Saenz-Agudelo P, Salles OC, Almany GR, Bode M, Berumen ML, Andréfouët S, Thorrold SR, Jones GP & Planes S (2017) Marine dispersal scales are congruent over evolutionary and ecological time. *Current Biology*. 27 (1): 149-154.

Pinti J & Visser AW (2019) Predator-prey games in multiple habitats reveal mixed strategies in diel vertical migration. *The American Naturalist*. 193(3): e65-77.

Pinto L, Mateus M & Silva A (2016) Modeling the transport pathways of harmful algal blooms in the Iberian coast. *Harmful Algae*. 53:8-16.

Podolsky RD & Emlet RB (1993) Separating the effects of temperature and viscosity on swimming and water movement by sand dollar larvae *(Dendraster excentricus). Journal of Experimental Biology.* 176(1):207-22.

Pohlert, T (2020). Trend: Non-Parametric Trend Tests and Change-Point Detection. R package version 1.1.2.

Polton JA, Lenn, Y-D, Elipot S, Chereskin TK & Sprintall J (2013a) Can Drake Passage observations match Ekman's classic theory. *Journal of Physical Oceanography*. 48, 1733-1740.

Polton JA, Palmer, MR & Howarth MJ (2013b) The vertical structure of time-mean estuarine circulation in a shallow, rotating, semi-enclosed coastal bay: A Liverpool Bay case study with application for monitoring. *Continental Shelf Research*. 59, 115-126.

Porch C (1998) A theoretical comparison of the contributions of random swimming and turbulence to absolute dispersal in the sea. *Bulletin of Marine Science*. 62, 31–44.

Pringle JM (2007) Turbulence avoidance and the wind-driven transport of plankton in the surface Ekman layer. *Continental Shelf Research.* 27(5): 670-8.

Puckett BJ, Eggleston DB, Kerr PC & Luettich Jr RA (2014) Larval dispersal and population connectivity among a network of marine reserves. *Fisheries Oceanography*. 23(4):342-61.

Queiroga H & Blanton J (2005) Interactions between behaviour and physical forcing in the control of horizontal transport of decapod crustacean larvae. *Advances in Marine Biology*. 47:107-214.

R Core Team (2020) R: A language and environment for statistical computing. R Foundation for Statistical Computing, Vienna, Austria. URL: https://www.R-project.org/.

Raby D, Lagadeuc Y, Dodson JJ & Mingelbier M (1994) Relationship between feeding and vertical distribution of bivalve larvae in stratified and mixed waters. *Marine Ecology Progress Series.* 103: 275-284.

Richards SA, Possingham HP & Noye J (1996) Diel vertical migration: modelling light-mediated mechanisms. *Journal of Plankton Research*. 18(12): 2199-2222.

Richardson MF, Sherman CD, Lee RS, Bott NJ & Hirst AJ (2016) Multiple dispersal vectors drive range expansion in an invasive marine species. *Molecular Ecology*. 25(20):5001-14.

Richter G (1973) Field and laboratory observations on the diurnal vertical migration of marine gastropod larvae. *Netherlands Journal of Sea Research*.7:126-34.

Rittschof D, Forward Jr RB, Cannon G, Welch JM, McClary Jr M, Holm ER, Clare AS, Conova S, McKelvey LM, Bryan P & Van Dover CL (1998) Cues and context: larval responses to physical and chemical cues. *Biofouling*. 12(1-3): 31-44.

Rius M, Branch GM, Griffiths CL & Turon X (2010) Larval settlement behaviour in six gregarious ascidians in relation to adult distribution. *Marine Ecology Progress Series*. 418:151-63.

Robins PE, Neill SP & Giménez L (2012) A numerical study of marine larval dispersal in the presence of an axial convergent front. *Estuarine, Coastal and Shelf Science.* 100, 172-185.

Robins PE, Neill SP, Giménez L, Jenkins SR & Malham SK (2013) Physical and biological controls on larval dispersal and connectivity in a highly energetic shelf sea. *Limnology and Oceanography*. 58(2): 505-24.

Rocha LA, Robertson DR, Rocha CR, Van Tassell JL, Craig MT & Bowen BW (2005) Recent invasion of the tropical Atlantic by an Indo-Pacific coral reef fish. Molecular *Ecology*. 14(13):3921-8.

Rochette S, Huret M, Rivot E & Le Pape O (2012) Coupling hydrodynamic and individual-based models to simulate long-term larval supply to coastal nursery areas. *Fisheries Oceanography*. 21(4):229-42.

Rohlf FJ & Schnell GD. (1971) An investigation of the isolation-by-distance model. *The American Naturalist.* 105 (944): 295-324.

Romero MR, Walker KM, Cortez CJ, Sanchez Y, Nelson KJ, Ortega DC, Smick SL, Hoese WJ & Zacherl DC (2012) Larval diel vertical migration of the marine gastropod *Kelletia kelletii* (Forbes, 1850). *Journal of Marine Biology*.

Ross ON & Sharples J (2004) Recipe for 1-D Lagrangian particle tracking models in space-varying diffusivity. *Limnology and Oceanography: Methods.* 2(9): 289-302.

Ross RE, Nimmo-Smith AW & Howell KL (2017) Towards 'ecological coherence': Assessing larval dispersal within a network of existing Marine Protected Areas. *Deep Sea Research Part I: Oceanography Research Papers. 126, 128-138.*

Ross RE, Nimmo-Smith WA & Howell KL (2016) Increasing the depth of current understanding: Sensitivity testing of deep-sea larval dispersal models for ecologists. *PloS one*. 11(8):e0161220.

Ross RE, Nimmo-Smith WA, Torres R, Howell KL (2020) Comparing deep-sea larval dispersal models: a cautionary tale for ecology and conservation. *Frontiers in Marine Science*.7:431.

Ross, ON & Sharples J (2004) Recipe for 1-D Lagrangian particle tracking models in space-varying diffusivity. *Limnology & Oceanography: Methods*. 2, 289–302.

Rowe MD, Anderson EJ, Wynne TT, Stumpf RP, Fanslow DL, Kijanka K, Vanderploeg HA, Strickler JR & Davis TW (2016) Vertical distribution of buoyant *Microcystis* blooms in a Lagrangian particle tracking model for short-term forecasts in Lake Erie. *Journal of Geophysical Research: Oceans.* 121(7):5296-314.

Rowe PM & Epifanio CE (1994) Tidal stream transport of weakfish larvae in Delaware Bay, USA. *Marine Ecology-Progress Series*. 110:105-105.

Roy A, Metaxas A & Ross T (2012) Swimming patterns of larval *Strongylocentrotus droebachiensis* in turbulence in the laboratory. *Marine Ecology Progress Series*. 453:117-27.

Rumrill SS (1990) Natural mortality of marine invertebrate larvae. *Ophelia.* 32(1-2):163-98.

Sakamoto, Y, Ishiguro, M & Kitagawa, G (1986) Akaike information criterion statistics. *D. Reidel.* Dordrecht, The Netherlands. *81*

Sala E, Aburto-Oropeza O, Paredes G, Parra I, Barrera JC & Dayton PK (2002) A general model for designing networks of marine reserves. *Science.* 298(5600): 1991-3.

Sameoto JA & Metaxas A (2008) Interactive effects of haloclines and food patches on the vertical distribution of 3 species of temperate invertebrate larvae. *Journal of Experimental Marine Biology and Ecology.* 367(2):131-41.

Sanvicente-Añorve L, Zavala-Hidalgo J, Allende-Arandía E & Hermoso-Salazar M (2018) Larval dispersal in three coral reef decapod species: Influence of larval duration on the metapopulation structure. *PloS one*.13(3):e0193457.

Savina M, Lacroix G & Ruddick K (2010) Modelling the transport of common sole larvae in the southern North Sea: influence of hydrodynamics and larval vertical movements. *Journal of Marine Systems*. 81(1-2):86-98.

Scheuerell MD & Schindler DE (2003) Diel vertical migration by juvenile sockeye salmon: empirical evidence for the antipredation window. *Ecology*. 84(7):1713-20.

Schlag ZR & North EW (2012) Lagrangian TRANSport model (LTRANS v. 2) User's Guide, University of Maryland Center for Environmental Science, Horn Point Laboratory, *Cambridge,* MD. USA, Tech. rep., 183 pp.

Schuech R & Menden-Deuer S (2014) Going ballistic in the plankton: anisotropic swimming behavior of marine protists. *Limnology and Oceanography: Fluids and Environments*. 4(1):1-6.

Shanks AL & Brink L (2005) Upwelling, downwelling, and cross-shelf transport of bivalve larvae: test of a hypothesis. *Marine Ecology Progress Series*. 302:1-2.

Shanks AL (2009) Pelagic larval duration and dispersal distance revisited. *The Biological Bulletin.* 216 (3): 373-385.

Shanks AL, Grantham BA & Carr MH (2003) Propagule dispersal distance and the size and spacing of marine reserves. *Ecological Applications*. 13(sp1):159-69

Shchepetkin AF & McWilliams JC (2005) The Regional Ocean Modeling System: A split-explicit, free-surface, topography-following-coordinate ocean model. *University of California at Los Angeles: Institute of Geophysics and Planetary Physics*. Los Angeles, California

Shulzitski K, Sponaugle S, Hauff M, Walter KD, D'Alessandro EK & Cowen RK (2017) Patterns in larval reef fish distributions and assemblages, with implications for local retention in mesoscale eddies. *Canadian Journal of Fisheries and Aquatic Sciences.*

Siegel DA, Kinlan BP, Gaylord B & Gaines SD (2003) Lagrangian descriptions of marine larval dispersion. *Marine Ecology Progress Series*. 260:83-96.

Silliman K (2019) Population structure, genetic connectivity, and adaptation in the Olympia oyster (*Ostrea lurida*) along the west coast of North America. *Evolutionary applications.* 12 (5): 923-939.

Silva CN, Villacorta-Rath C, Woodings LN, Murphy NP, Green BS, Hartmann K, Gardner C, Bell JJ & Strugnell JM (2019) Advancing our understanding of the connectivity, evolution and management of marine lobsters through genetics. *Reviews in Fish Biology and Fisheries*.1-19.

Simpson JH & Hunter JR (1974) Fronts in the Irish Sea. *Nature*. 250(5465): 404-6.

Simpson JH, Sharples J & Rippeth TP (1991) A prescriptive model of stratification induced by freshwater runoff. *Estuarine, Coastal and Shelf Science.* 33(1):23-35.

Simpson SD, Munday PL, Wittenrich ML, Manassa R, Dixson DL, Gagliano M & Yan HY (2011) Ocean acidification erodes crucial auditory behaviour in a marine fish. *Biology Letters*. 7(6):917-20.

Smith R, Jones P, Briegleb B, Bryan F, Danabasoglu G, Dennis J, Dukowicz J, Eden C, Fox-Kemper B, Gent P & Hecht M (2010) The parallel ocean program (POP) reference manual: ocean component of the community climate system model (CCSM) and community earth system model (CESM). *LAUR-01853*. 141:1-140.

Sokal R & Rohlf F (1995) Biometry. W.H. Freeman & Co. *New York.*

Soulsby RL, Mead CT & Wild BR (2007) A model for simulating the dispersal tracks of sand grains in coastal areas - "SandTrack". In: Balson PS, Collins MB (Eds.) Coastal and Shelf Sediment Transport. Book 274. *Geological Society Special Publications.*

Spaulding ML (2017) State of the art review and future directions in oil spill modeling. *Marine Pollution Bulletin.* 115(1-2): 7-19.

Spearman C (1904) The proof and measurement of association between two things. *American Journal of Psychology*. 15 (1): 72–101

Sponaugle S, Cowen RK, Shanks A, Morgan SG, Leis JM, Pineda J, Boehlert GW, Kingsford MJ, Lindeman KC, Grimes C & Munro JL (2002) Predicting self-recruitment in marine populations: biophysical correlates and mechanisms. *Bulletin of Marine Science*. 70(1):341-75.

Sprong PA, Fofonova V, Wiltshire KH, Neuhaus S, Ludwichowski KU, Käse L, Androsov A & Metfies K (2020) Spatial dynamics of eukaryotic microbial communities in the German Bight. *Journal of Sea Research*. 163:101914.

Sprung M (1984) Physiological energetics of mussel larvae (*Mytilus edulis*). III. Respiration. *Marine Ecology Progress Series.* 171–178.

Staaterman E & Paris CB (2014) Modelling larval fish navigation: the way forward. *ICES Journal of Marine Science.* 71(4):918-24.

Stanley R, Snelgrove PV, Deyoung B & Gregory RS (2012) Dispersal patterns, active behaviour, and flow environment during early life history of coastal cold water fishes. *PloS one*. 7(9):e46266.

Stouffer SA, Suchman EA, DeVinney LC, Star SA & Williams RM Jr. (1949) The American Soldier, Vol. 1: Adjustment during Army Life. Princeton University Press, *Princeton.*

Strathmann RR & Grünbaum D (2006) Good eaters, poor swimmers: compromises in larval form. *Integrative and Comparative Biology.* 46(3):312-22.

Strathmann RR (1985) Feeding and non-feeding larval development and life-history evolution in marine invertebrates. *Annual Review of Ecology, Evolution and Systematics*. 16: 339-36.

Sundelöf A & Jonsson PR (2012) Larval dispersal and vertical migration behaviour–a simulation study for short dispersal times. *Marine Ecology*. 33(2):183-93.

Swearer SE, Treml EA, & Shima JS (2019) A review of biophysical models of marine larval dispersal. In: *Oceanography and Marine Biology: An Annual Review.* Hawkins SJ, Allcock AL., Bates AE, Firth LB, Smith IP, Swearer SE & Todd PA (Eds.) *Taylor and Francis.*

Szmant AM & Meadows MG (2006) Developmental changes in coral larval buoyancy and vertical swimming behavior: implications for dispersal and connectivity. In: *Proceedings of the 10th International Coral Reef Symposium*. 1: 431-437.

Tang EE (2010) Physical factors affecting larval transport in Mission Bay, California. *Masters Thesis.* UC San Diego

Teodósio MA & Garel E (2015) Linking hydrodynamics and fish larvae retention in estuarine nursery areas from an ecohydrological perspective. *Ecohydrology & Hydrobiology*. 15(4):182-91.

Teodosio MA, Paris CB, Wolankski E & Morias P (2016) Biophysical processes leading to the ingress of temperate fish larvae into estuarine nursery areas: a review. *Estuaries, Coasts Shelf Science.* 183, 187-202.

Thornhill DJ, Mahon AR, Norenburg JL & Halanych KM (2008) Open-ocean barriers to dispersal: a test case with the Antarctic Polar Front and the ribbon *worm Parborlasia corrugatus (Nemertea: Lineidae). Molecular Ecology*. 17(23):5104-17.

Thorpe S (2005) The Turbulent Ocean. *Cambridge University Press.* Cambridge.

Thorrold SR, Zacherl DC & Levin LA (2007) Population connectivity and larval dispersal: using geochemical signatures in calcified structures. *Oceanography*. 20(3): 80-9.

Thorson G (1946) Reproduction and larval development of Danish marine bottom invertebrates, with special reference to the planktonic larvae in the Sound (Øresund). *Meddelelser fra Kommissionen for Danmarks Fiskeri- Og Havundersögelser, Serie: Plankton.* 4, 1-523.

Thorson G. (1950) Reproductive and larval ecology of marine bottom invertebrates. *Biological Reviews*. 25 (1): 1-45.

Tian RC, Chen C, Stokesbury KD, Rothschild BJ, Xu Q, Hu S, Cowles G, Harris BP, Marino II MC (2009) Sensitivity analysis of sea scallop (*Placopecten magellanicus*) larvae trajectories to hydrodynamic model configuration on Georges Bank and adjacent coastal regions. *Fisheries Oceanography*. 2009. 18(3):173-84.

Toonen, RJ & Pawlik, JR (2001) Foundations of gregariousness: a dispersal polymorphism among the planktonic larvae of a marine invertebrate. *Evolution*. 55, 2439–2454.

Torres AP, Reglero P, Hidalgo M, Abelló P, Simão DS, Alemany F, Massutí E & Dos Santos A (2018) Contrasting patterns in the vertical distribution of decapod crustaceans throughout ontogeny. *Hydrobiologia.* 808(1): 137-52.

Tosches MA, Bucher D, Vopalensky P & Arendt D (2014) Melatonin signaling controls circadian swimming behavior in marine zooplankton. *Cell.* 159(1):46-57.

Toupoint N, Gilmore-Solomon L, Bourque F, Myrand B, Pernet F, Olivier F & Tremblay R. (2012) Match/mismatch between the *Mytilus edulis* larval supply and seston quality: effect on recruitment. *Ecology.* 93(8):1922-34.

Treml EA & Halpin PN (2015) Marine population connectivity identifies ecological neighbors for conservation planning in the Coral Triangle. *Conservation Letters.* 5: 441–449.

Treml EA, Ford JR, Black KP & Swearer SE (2015) Identifying the key biophysical drivers, connectivity outcomes, and metapopulation consequences of larval dispersal in the sea. *Movement Ecology*. 3(1):17.

Treml EA, Halpin PN, Urban DL & Pratson LF (2008) Modeling population connectivity by ocean currents, a graph-theoretic approach for marine conservation. *Landscape Ecology*. *23* (1): 19-36.

Treml EA, Roberts JJ, Chao Y, Halpin PN, Possingham HP & Riginos C (2012) Reproductive output and duration of the pelagic larval stage determine seascape-wide connectivity of marine populations. *Integrative and Comparative Biology.* 52(4): 525-537.

Troost K, Veldhuizen R, Stamhuis EJ & Wolff WJ (2008) Can bivalve veligers escape feeding currents of adult bivalves? *Journal of Experimental Marine Biology and Ecology.* 358(2):185-96.

Ueda H, Kuwatani M & Suzuki KW (2010) Tidal vertical migration of two estuarine copepods: naupliar migration & position-dependent migration. *Journal of Plankton Research.* 32, 1557–1572.

Uncles RJ & Stephens JA (1990) Salinity stratification and vertical shear transport in an estuary. In: Residual Currents and Long-term Transport. Cheng RT (Ed.) *Springer,* New York, NY. pp 137-150.

Van der Stocken, T, Carroll, D, Menemenlis, D, Simard, M. & Koedam, N (2019) Global-scale dispersal and connectivity in mangroves. *Proceedings of the National Academy of Sciences*, *116*(3):.915-922.

van Sebille E, Griffies SM, Abernathey R, Adams TP, Berloff P, Biastoch A, Blanke B, Chassignet EP, Cheng Y, Cotter CJ & Deleersnijder E (2018) Lagrangian ocean analysis: Fundamentals and practices. *Ocean Modelling*. 121: 49–75.

Van Wyngaarden M, Snelgrove PV, DiBacco C, Hamilton LC, Rodríguez-Ezpeleta N, Jeffery NW, Stanley RR & Bradbury IR (2017) Identifying patterns of dispersal., connectivity and selection in the sea scallop, *Placopecten magellanicus*, using RAD seq-derived SNPs. *Evolutionary Applications.* 10 (1): 102-117.

Vaughn D & Allen JD (2010) The peril of the plankton. I*ntegrative and Comparative Biology.* 50(4):552-70.

Verasztó C, Gühmann M, Jia H, Rajan VB, Bezares-Calderón LA, Piñeiro-Lopez C, Randel N, Shahidi R, Michiels NK, Yokoyama S & Tessmar-Raible K (2018) Ciliary and rhabdomeric photoreceptor-cell circuits form a spectral depth gauge in marine zooplankton. *Elife.* 7:e36440.

Viard F, Ellien C & Dupont L (2006) Dispersal ability and invasion success of Crepidulafornicata in a single gulf: insights from genetic markers and larval-dispersal model. *Helgoland Marine Research*; 60(2):144-52.

Vieira MLC, Santini L, Diniz AL & Munhoz CDF (2016) Microsatellite markers: what they mean and why they are so useful. *Genetics and molecular biology*. 39 (3): 312-328.

Visser AW (1997) Using random walk models to simulate the vertical distribution of particles in a turbulent water column. *Marine Ecology Progress Series*. 158: 275-81.

Volk EC, Schroder SL & Grimm JJ (1999) Otolith thermal marking. *Fisheries Research.* 43 (1-3): 205-219.

Wagner P, Rühs S, Schwarzkopf FU, Koszalka IM & Biastoch A (2019) Can Lagrangian tracking simulate tracer spreading in a high-resolution Ocean General Circulation Model? *Journal of Physical Oceanography*. 49(5): 1141-57.

Wahab MA, de Nys R & Whalan S (2011) Larval behaviour and settlement cues of a brooding coral reef sponge. *Coral Reefs*. 30(2):451-60.

Wahab MA, de Nys R, Webster N & Whalan S (2014) Larval behaviours and their contribution to the distribution of the intertidal coral reef sponge *Carteriospongia foliascens. PloS one*.9:1-3.

Walford LA (1938) Effect of Currents on Distribution and Survival of the Eggs and Larvae of the Haddock (*Melanogrammius Aeglefinus*) on Georges Bank (No. 29). *US Government Printing Office.*

Walker G (2004) Swimming speeds of the larval stages of the parasitic barnacle, *Heterosaccus lunatus* (Crustacea: Cirripedia: Rhizocephala). Marine Biological Association of the United Kingdom. *Journal of the Marine Biological Association of the United Kingdom.* 84(4):737.

Wallcraft AJ, Metzger EJ & Carroll SN (2009) Software design description for the hybrid coordinate ocean model (HYCOM), Version 2.2 (No. NRL/MR/7320--09-9166). *Naval Research Lab, Stennis Space Centre, MC Oceanography Division.*

Wang Q, Danilov S, Sidorenko D, Timmermann R, Wekerle C, Wang X, Jung T, & Schröter J (2014) The Finite Element Sea Ice-Ocean Model (FESOM) v.1.4: formulation of an ocean general circulation model. *Geoscientific Model Development* 7: 663–693.

Wang WX & Widdows J (1991) Physiological responses of mussel larvae *Mytilus edulis* to environmental hypoxia and anoxia. Marine Ecology Progress Series. 70(3):223-36.

Warner, JC, Sherwood, CR, Arango, HG & Signell, RP (2005) Performance of four turbulence closure models implemented using a generic length scale method. *Ocean Modelling*. 8, 81-115

Waters JM, King TM, O'loughlin PM & Spencer HG (2005) Phylogeographical disjunction in abundant high-dispersal littoral gastropods. *Molecular Ecology.* 14(9):2789-802.

Watters GT, O'Dee SH & Chordas III S (2001) Patterns of vertical migration in freshwater mussels (Bivalvia: Unionoida). *Journal of Freshwater Ecology*. 16(4):541-9.

Weinstock JB, Morello SL, Conlon LM, Xue H & Yund PO (2018) Tidal shifts in the vertical distribution of bivalve larvae: vertical advection vs. active behaviour. *Limnology & Oceanography.* 63.

Welch J & Forward R (2001) Flood tide transport of blue crab, *Callinectes sapidus*, postlarvae: behavioural responses to salinity & turbulence. *Marine Biology.* 139, 911–918.

Werner FE, Cowen RK & Paris CB (2007) Coupled biological and physical models: present capabilities and necessary developments for future studies of population connectivity. *Oceanography*. 20(3).54-69.

Whalan S, Ettinger-Epstein P, Battershill C & de Nys R (2008) Larval vertical migration and hierarchical selectivity of settlement in a brooding marine sponge. *Marine Ecology Progress Series.* 368:145-54.

Wheeler JD, Chan KY, Anderson EJ & Mullineaux LS (2016) Ontogenetic changes in larval swimming and orientation of pre-competent sea urchin *Arbacia punctulata* in turbulence. *Journal of Experimental Biology*. 219(9):1303-10.

Wheeler JD, Helfrich KR, Anderson EJ, McGann B, Staats P, Wargula AE, Wilt K & Mullineaux LS (2013) Upward swimming of competent oyster larvae Crassostrea virginica persists in highly turbulent flow as detected by PIV flow subtraction. *Marine Ecology Progress Series*. 488:171-85.

White JW, Botsford LW, Hastings A & Largier JL (2010) Population persistence in marine reserve networks: incorporating spatial heterogeneities in larval dispersal. *Marine Ecology Progress Series.* 398:49-67

White JW, Morgan SG & Fisher JL (2014) Planktonic larval mortality rates are lower than widely expected. *Ecology.* 95(12):3344-53.

Whomersley P, Van der Molen J, Holt D, Trundle C, Clark S, & Fletcher D (2018) Modeling the dispersal of spiny lobster (*Palinurus elephas*) larvae: Implications for future fisheries management and conservation measures. *Frontiers in Marine Science*. 5:58.

Wilderbuer T, Duffy-Anderson JT, Stabeno P, Hermann A (2016) Differential patterns of divergence in ocean drifters: Implications for larval flatfish advection and recruitment. *Journal of Sea Research.*111:11-24.

Wilson LJ, Fulton CJ, Hogg AM, Joyce KE, Radford BT & Fraser CI (2016) Climate-driven changes to ocean circulation and their inferred impacts on marine dispersal patterns. *Global Ecology and Biogeography.* 25 (8): 923-939.

Wolff JO, Maier-Reimer E & Legutke S (1997) *The Hamburg ocean primitive equation model*. DKRZ.

Wood LH & Hargis WJ (1971) Transport of bivalve larvae in a tidal estuary. *Cambridge University Press*

Wood S, Baums IB, Paris CB, Ridgwell A, Kessler WS & Hendy EJ (2016) El Niño and coral larval dispersal across the eastern Pacific marine barrier. *Nature Communications.* 7(1): 1-1.

Wood S, Paris CB, Ridgwell A & Hendy EJ (2014) Modelling dispersal and connectivity of broadcast spawning corals at the global scale. *Global Ecology and Biogeography*. 23(1):1-1.

Wood, SN (2011) Fast stable restricted maximum likelihood and marginal likelihood estimation of semiparametric generalized linear models. *Journal of the Royal Statistical Society (B).* 73(1):3-36

Woodson CB & McManus MA (2007) Foraging behavior can influence dispersal of marine organisms. *Limnology and Oceanography*. 52(6):2701-9.

Wright S (1943) "Isolation by Distance". *Genetics*. 28: 114–38.

Wright S. The genetical structure of populations (1949) *Annals of Eugenics*. 15(1):323-54.

Yamazaki H & Squires KD (1996) Comparison of oceanic turbulence and copepod swimming. *Marine Ecology Progress Series.*144:299-301.

Yoo SK (1976) Growth of transplanted Pacific oyster *Crassostrea gigas*. *Bulletin of National Fisheries (Natural Sciences).* 16 (2) 42-48.

Young CM. (1995) Behavior and locomotion during the dispersal phase of larval life. *Ecology of Marine Invertebrate Larvae*. 249: 278.

Zeng, X, Adams, A, Roffer, M & He, R (2019) Potential connectivity among spatially distinct management zones for Bonefish (*Albula vulpes*) via larval dispersal. *Environmental Biology of Fishes*, *102*(2): 233-252.

Zhou, M & Dorland, RD (2004) Aggregation and vertical migration behavior of *Euphausia superba*. *Deep Sea Research Part II: Topical Studies in Oceanography*. 51(17-19):.2119-2137.

PUBLICATIONS

James MK, Polton JA, Brereton AR, Howell KL, Nimmo-Smith WA & Knights AM (2019) Reverse engineering field-derived vertical distribution profiles to infer larval swimming behaviors. Proceedings of the National Academy of Sciences. 116(24): 11818-23.

PNAS

Reverse engineering field-derived vertical distribution profiles to infer larval swimming behaviors

M. K. James[a,1], J. A. Polton[b], A. R. Brereton[b], K. L. Howell[a], W. A. M. Nimmo-Smith[a], and A. M. Knights[a]

[a]School of Biological and Marine Sciences, University of Plymouth, PL4 8AA Plymouth, United Kingdom; and [b]Marine Systems Modelling Group, National Oceanography Centre, L3 5DA Liverpool, United Kingdom

Edited by Alan Hastings, University of California, Davis, CA, and approved May 3, 2019 (received for review January 11, 2019)

Biophysical models are well-used tools for predicting the dispersal of marine larvae. Larval behavior has been shown to influence dispersal, but how to incorporate behavior effectively within dispersal models remains a challenge. Mechanisms of behavior are often derived from laboratory-based studies and therefore, may not reflect behavior in situ. Here, using state-of-the-art models, we explore the movements that larvae must undertake to achieve the vertical distribution patterns observed in nature. Results suggest that behaviors are not consistent with those described under the tidally synchronized vertical migration (TVM) hypothesis. Instead, we show (*i*) a need for swimming speed and direction to vary over the tidal cycle and (*ii*) that, in some instances, larval swimming cannot explain observed vertical patterns. We argue that current methods of behavioral parameterization are limited in their capacity to replicate in situ observations of vertical distribution, which may cause dispersal error to propagate over time, due to advective differences over depth and demonstrate an alternative to laboratory-based behavioral parameterization that encompasses the range of environmental cues that may be acting on planktic organisms.

larval behavior | vertical migration | larval swimming | reverse engineering | biophysical modeling

Larval dispersal is a primary factor shaping the distribution of marine species and influencing the structure of marine communities (1). Understanding mechanisms of dispersal is, therefore, imperative to predicting species distributions (2). Biophysical modeling—the tracking of particles assigned biological parameters ("behaviors") within ocean models—has become a ubiquitous tool for predicting propagule dispersal in the marine environment (3–5). Models have become increasingly complex to enhance "realism," yet despite these efforts, simulation outcomes often do not match the patterns observed in nature identified by genetic studies (6). As biophysical models are able to accurately predict the trajectories of abiotic particles (7), the decoupling of modeled and observed distributions is frequently attributed to poorly defined larval behavior mechanisms and a limited understanding of how to incorporate behaviors within dispersal models (6, 8).

In the context of biophysical modeling, behavior refers to applying an active swimming response, typically in the z dimension, to a model propagule (larvae). Planktic organisms generally swim at relatively slow speeds (millimeters to centimeters second^{-1}) in comparison with horizontal currents, which can be orders of magnitude faster (i.e., meters second^{-1}). As such, active horizontal movement, especially for the early life history stages of many marine organisms (which tend to be small), can be assumed to be passive. Swimming speeds can, however, exceed the vertical mixing velocities in the ocean (9), providing individuals with a mechanism by which they can alter their vertical position in the water column. When considered in conjunction with depth-related differences in horizontal velocity, vertical migration is argued to provide a mechanism through which weak-swimming individuals can manipulate their horizontal trajectory (10, 11). Such depth-related differences can be generated by Ekman processes, which can be significant in both tidal (12) and open ocean environments (13), and tidally induced vertical shear (14).

Vertical swimming is often modeled in response to exogenous (i.e., external stimuli) or endogenous cues (e.g., circadian rhythm) (3, 15). This seems sensible, as laboratory studies have clearly shown that larvae can exhibit behavioral responses and directed movement in response to stimuli (16). In nature, however, organisms are likely exposed to multiple rather than single cues, which may alter their responses (17). Moreover, the scale and/or intensity of cues may be masked in nature such that behaviors observed in a laboratory are not always expressed in the field (18). As such, laboratory-observed behaviors in response to a single stimulus in a controlled environment may not be reflective of the in situ movements of larvae.

A number of field-based studies have highlighted changes in larval vertical distribution patterns that correlate with the tidal cycle: for instance, where larvae occupy surface waters during the flooding tide and remain in close proximity to the seabed during the ebbing tide or vice versa. Such tidally synchronized vertical migration (TVM) has been documented for a range of taxa (11, 19–21) across a range of larval ages (15, 22), and observations have been made in both estuarine (23, 24) and coastal (11, 25) environments. Active occupation of different depths during alternate tidal states (flood/ebb), often referred to as selective tidal stream transport (STST) (20, 26), allows organisms to exploit depth-related current differences. These observations are often interpreted as evidence of larval behavior and specifically, an energy-efficient tactic to facilitate migration over long distances or promote retention close to coastal areas. However, the mechanisms that govern tidally timed movements of marine larvae remain poorly resolved (26). Synchronization of movement with the

Significance

Estimating the dispersal of propagules in terrestrial, freshwater, and marine ecosystems has been of primary research interest for many years, yet efforts to accurately predict dispersal, especially in marine ecosystems, have remained a significant and unresolved challenge. A common approach is to use a biophysical model, but field studies and genetic tools reveal that these models can overestimate dispersal range, often attributed to inaccurate behavioral parameterization. This study reverse engineers a biophysical model in an effort to describe larval behavior. The approach demonstrated, which can be applied to any species with a larval phase, provides a method for assessing in situ larval behavior that negates the need for a mechanistic understanding of behavioral responses to cues.

Author contributions: M.K.J., J.A.P., K.L.H., W.A.M.N.-S., and A.M.K. designed research; M.K.J. performed research; J.A.P., A.R.B., and A.M.K. contributed new reagents/analytic tools; M.K.J. analyzed data; and M.K.J. wrote the paper.

The authors declare no conflict of interest.

This article is a PNAS Direct Submission.

[1]To whom correspondence may be addressed. Email: molly.james@plymouth.ac.uk.

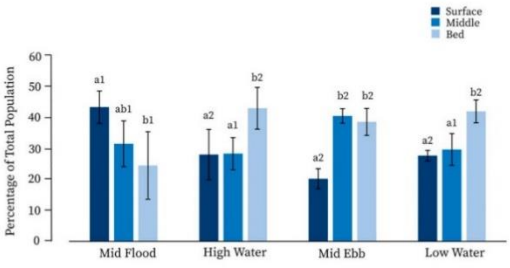

Fig. 1. Observed proportional abundance (percentage ± SD) of *Mytilus* spp. larvae within each depth zone during four tidal states (midflood, high water, midebb, and low water). Multiple comparison outcomes are shown above each bar, where different letters and numbers indicate a significant difference ($P < 0.05$) in (a and b) larval proportions between depth zones within a tidal state and (1 and 2) between tidal states within a depth zone (Tukey's honestly significant difference test).

tide suggests the presence of (*i*) cue(s) and (*ii*) behavioral decision making (27).

Research has suggested that salinity gradients may act as a cue to vertical migration (15). Salinity gradients associated with tidal state would be expected in estuaries; however, in coastal environments where tidally correlated distribution profiles have also been observed, these signals would be much weaker and thus, more difficult for larvae to detect. At coastal sites, one could assume that there would be an absence of strong tidal signals, except in velocity (28). It was recently shown that some larval fish can detect flow velocity using their lateral line, providing a navigational signal in the absence of visual or chemical cues, but it is unclear if nonfish larvae can perceive changes in the magnitude and direction of the current due to their small size and the lack of focal points in the marine environment (29). There is, however, increasing evidence to suggest that they can respond to turbulence (17), either acting as a cue for larval behavior (30, 31) or alternatively, hindering a larva's motion strategy (32) due to disorientation preventing expression of a behavioral response (33). Weinstock et al. (25) suggest that TVM patterns may be passive and caused by vertical advection resulting from the tidal flow over a sloping shelf; however, Knights et al. (11) observed a shift in abundance from the surface waters during the flood tide to deeper waters at high water (Fig. 1) that contradicts this theory. It was suggested that larvae may be responding to tidal conditions to facilitate transport, but the exact mechanism could not be resolved.

Larval behavior can be applied in biophysical models through the application of simple "rules" [e.g., TVM can be simulated by programming "larvae" to swim up during the flood and down during the ebb (or vice versa)]. This approach has been implemented in numerous studies (15, 34, 35). However, is it appropriate to apply these rules, and if so, does our current understanding of larval movement allow accurate replication of in situ patterns? Although distribution profiles in ref. 11 correlated to tidal state, the patterns observed were not analogous STST theory in which larval abundances would be expected to be greatest in the surface waters during midflood and high water to promote advection toward the coast and greatest near the bed during midebb and low water to limit offshore transport (26). Instead, larvae were most closely associated with the sea bed during both slack water periods and with the middle and bed during the ebb tide (11). Despite these observations (11), it has been heavily cited as evidence of STST and specifically used as justification for TVM in dispersal models (35). We argue that this inaccurate and will lead to erroneous predictions of dispersal. Here, using a combination of empirical data and state-of-the-art modeling, we explore the active movements that bivalve larvae would need to undertake to create the patterns observed in nature over the course of a tidal cycle. We test a range of swimming velocities within a model environment to examine if vertical swimming could feasibly be the mechanism that facilitates the patterns observed in situ given what we know about the swimming speed of early life history stages of bivalves.

Methods

Observations of Vertical Distribution Profiles. To determine the extent of vertical migration in a coastal environment, we used data collected for a previous study (11) from two 100 × 100-m sites (site 1: 52° 19.542′ N, 6° 15.538′ W; site 2: 52° 20.036′ N, 6° 15.344′ W) within a 4-km^2 area with a mean depth of 24 m in the Southern Irish Sea off the coast of County Wexford, Ireland. The waters at this location are well mixed (36) with mean horizontal advection of up to 1 ms^{-1} (11) and vertical mixing at rates of up to 0.1 m^2 s^{-1} (Fig. 2), which can result in turbulent velocities that are orders of magnitude greater than the swimming speeds of larvae. These conditions, therefore, provide a challenging test for the effectiveness of larval behavior (e.g., swimming) to influence vertical distribution. Replicate samples ($n = 5$) were collected from three depth zones (surface, 0–8 m; midwater, 8–16 m; bottom, 16–24 m) during four consecutive tidal states (low-water slack, flood, high-water slack, ebb) over a full tidal cycle (12.1 h). Replicate sampling was undertaken in May/June and July/August to capture early- and late-stage larvae, respectively, and to encompass variation associated with differences in the tidal amplitude cycle (spring/neap). Previous analyses of the data have shown that larval vertical distribution profiles correlate to a change in the tidal state (flood, high-water slack, ebb, low-water slack) but not the tidal phase (spring/neap), ontogenetic larval stage, or sampling location. In this study, we take a numerical approach using a realistic modeled hydrodynamic environment to explore whether vertical swimming could feasibly be the mechanism that facilitates the observed changes in distribution over a tidal cycle.

The Hydrodynamic Model. A large-eddy simulation (LES) of an unstratified tidal boundary layer was used to generate a time- and depth-varying diffusivity coefficient. The purpose of the LES was to create a diffusivity matrix that represented the hydrodynamic environment at the time/location of sampling. The LES configuration was set up to be forced by time series profiles of "filtered" horizontal velocities obtained from an acoustic doppler current profiler record and solved for the turbulent "perturbation" flow (37). The LES domain was nominally 50 × 50 × 25 m, with a lateral grid size of 0.4 m and stretched vertical grid sizes of 0.07–0.17 m. This method is validated against independent measurements of turbulence dissipation. The advantage of this method over a direct three-dimensional (3D) turbulent simulation of particles comes from the fact that online Lagrangian simulations are computationally demanding. This method undertakes trajectory analysis offline using the output from the LES, reducing the computational demand

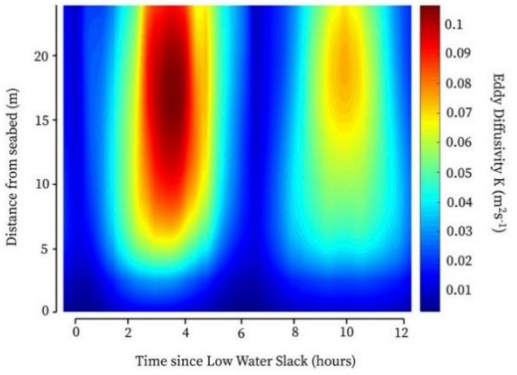

Fig. 2. Visualization of the eddy diffusivity field (K) created by the LES over a 12.1-h tidal period from low-water slack$_1$ to low-water slack$_2$ forced by time series profiles of "filtered" horizontal velocities and solved for the turbulent "perturbation" flow. Ref. 37 has full details.

of the simulation and allowing many experiments to be run to seek statistical convergence (*The Particle-Tracking Model*). In this simulation, the background tidal flow, U, was assumed to be oscillating in one direction. The direction of the flow had no influence on the resultant diffusivity coefficient. From these resolved turbulent fluctuations, an effective eddy diffusivity (Fig. 2) can be derived from the following relationship:

$$K = \frac{<u'w'>}{\frac{\partial U}{\partial z}} \mathrm{Pr}_t,$$

where K is the eddy diffusivity (in meters^2 second^{-1}), $<u'w'>$ is a resolved Reynolds stress averaged horizontally over the domain (calculated by the LES), $\frac{\partial U}{\partial z}$ is the prescribed vertical mean (tidal) shear, and Pr_t is the turbulent Prandtl number of seawater, which is taken as one. As this statistic is not well defined when the vertical mean is near zero, a cubic spline was used to smooth K in time with 2-min intervals (38). This has no discernable effect on K away from the slack tide.

A velocity depth profile was fitted assuming a log-layer approximation with a roughness length of $z_0 = 0.001$ m, although eddy diffusivity was not sensitive to the choice of z_0. As the Irish Sea tends to be well mixed with no known hydrographic features during the spring and summer months when field samples were collected (36), it was deemed appropriate to use a constant density LES. The midpoints of the flood and ebb tide were determined from the depth-averaged current velocities when maximum positive and maximum negative flows occurred. Similarly, the slack tide midpoints were identified as the times when the associated depth-averaged current velocities were nearest to zero.

It should be noted that, as is the case with all models, the parameterized diffusivity output of the LES may not necessarily be a perfect match for what the real organisms experienced in the field. However, direct calculation of the diffusivities using an LES seems preferable to simply taking a constant value or estimating diffusivity from either a hydrostatic model or scaling arguments. Furthermore, the LES is validated to simulate realistic levels of dissipation (which represents processes at the scale of the organisms) (39). As such, it was considered an appropriate tradeoff between hydrodynamic complexity and physical accuracy while also permitting investigation into larval movement through offline particle tracking.

The Particle-Tracking Model. To test the potential of larvae to undergo vertical migration, a 1D Lagrangian particle-tracking algorithm was built in MATLAB (version 2017b) to follow the vertical trajectories of virtual larvae within the filtered eddy diffusivity flow field as generated by the LES. The 1D definition of the particle tracker is due to the exclusion of horizontal movement within the simulation (i.e., eddy diffusivity can only move particles upward or downward). Preliminary tests using 100, 10,000, and 100,000 seed particles indicated convergence of the relative vertical distribution profiles. As such, it was deemed appropriate to use 100 particles in each simulation to minimize computational effort without influencing results.

The hydrodynamic environment was prescribed using the horizontally averaged output of the LES,K, which was coupled with a particle movement component implemented using a random walk approach (as described in ref. 40) and larval active swimming (ω) behavior (described in detail below). The model timestep, δt, was set at 60 s. This was deemed sufficiently small enough so that the diffusivity profile was locally well approximated by the first-order Taylor expansion. Particle movement was calculated for δt by

$$z_{n+1} = z_n + K'(z_n)\delta t + R\left[\frac{2K\left(z_n + \frac{1}{2}K'(z_n)\delta t\right)\delta t}{r}\right]^{0.5} + \omega_n \delta t,$$

where z_n is the depth of a particle at the nth timestep, K' is the diffusivity gradient at the particle location ($\delta K/\delta z$), R is a random number from a continuous distribution between 1 and −1 (with variance $r = 0.33$), and ω_n is the vertical swimming velocity of a particle at timestep n.

A Mersenne–Twister algorithm was applied to the random number generator to ensure that values of R were sufficiently random. The inclusion of the deterministic component $K'(z_n)\delta t$ ensures that particles are always advected in the direction of higher diffusivity, thus preventing artificial accumulation in low-diffusion areas. It was assumed that the rate of larval diffusivity was equal to the rate of eddy diffusivity calculated by the LES. This was considered appropriate, as larval transport by eddies is not affected by inertial and crossing trajectories effects due to their small size (40).

Larval vertical movement was explored from each tidal state to the next consecutive state (flood to high water, high water to ebb, ebb to low water, low water to flood) using a "mixed model" approach. Before each simulation, the model water column was seeded with particles in a probabilistic vertical distribution profile based on the observed vertical distribution for the defined starting tidal state. To achieve this, the model particles ($n = 100$) were distributed so that the percentage of particles in each bin matched the percentage of the total population of larvae observed in the field for that bin/tidal state. Additionally, particles were randomly assigned depths within each depth bin using a random number generator. Particles were then assigned "behavioral rules," which are explained in additional detail below.

Parameterizing Swimming Behavior. To assess the influence of larval swimming on vertical distribution profiles, multiple simulations were run using a range of swimming velocities ($n = 2{,}525$). Although bivalve larvae have been observed to swim in a helical pattern (41), swimming in the model was confined to one dimension, and as such, swimming velocities represent the absolute swimming velocity (the vertical distance traveled by an organism) rather than the linear velocity (the velocity of a larva along its swimming path). Swimming velocities explored ranged from −2.5 to 5 mm s^{-1}, justified by an in-depth literature review (30, 42). Particles were considered neutrally buoyant (i.e., downward movement was an active response) and swam constantly at the swimming velocity given by the model parameters.

Each simulation ran from the midpoint of the defined starting tidal state to the midpoint of the next consecutive state. Simulation duration was variable: 174 model minutes between low water and midflood, 176 min between midflood and high water, 198 min between high water and midebb, and 182 min between midebb and low water. Variation matched that at the survey location, where local bathymetry can act to distort the pattern of the tide, generating tidal asymmetry (43). Furthermore, around the British Isles, the M_2 and M_4 tides can combine to give differences in the flood and ebb tidal streams (44). Tidal asymmetry has been demonstrated in the Irish Sea (45) and was observed by Knights et al. (11) at the study site. Such patterns were replicated by the LES.

After each simulation, the proportional abundance of particles within each depth bin was calculated (where the proportion is the number of particles in each bin divided by the total number of seeded model particles) and compared with the observed proportional abundance of particles for the end tidal state of the model run.

Larval Vertical Velocity as a Predictor of in Situ Distribution Profiles. A bootstrap approach was used to assess the error between the modeled and observed profiles for each tested vertical velocity at each tidal state given the variation in the sampled (modeled and observed) populations. We generated 100 estimates of the observed distribution profile using the mean and SD of the observed proportional abundances in each depth bin ($n = 5$). We then used the same method to bootstrap 100 distribution profiles for each tested swimming velocity using the modeled proportional abundances in each depth bin as the sample data ($n = 25$). Pairwise comparisons were used to determine the sum of squares of the proportional difference between the simulated and observed profiles for each depth bin, and the overall difference between the observed and simulated profiles was demonstrated by the total of the sum of squares of the difference for all three bins (SS_{total}). The mean square error (MSE) and 95% confidence intervals were calculated for each tested velocity. SS_{total} ($n = 7{,}600$ for each tidal period: 100 pairwise comparisons × 76 tested swimming velocities) and MSE ($n = 76$) were plotted against swimming velocity. Best-fitting curves were constructed in R using ANOVA to justify the order of the polynomial. The equation of each curve was then solved for the smallest value of y to determine the swimming velocity where the likelihood of difference between the simulated and observed profiles was lowest and as such, the quality of that velocity as a predictor of in situ distribution patterns was greatest.

Assessing Model Compatibility. Two-way ANOVA and planned F-test comparisons were used to compare proportions of larvae recorded from in situ observations ($n = 5$) and proportions of virtual larvae from model simulations ($n = 5$) (46). For each tested velocity, the number of simulation runs was fixed to match the number of replicates observed. As proportional distribution data were in percentages, data were transformed by the angular (arcsine of square root) transformation before statistical analysis to satisfy the assumptions of the ANOVA. The simulation was replicated five times for each scenario to generate variance estimates around the mean diffusivity based on the random walk. Stouffer's transformed z method (47) was used to combine the P values of the interaction term of the five independently run tests to provide a quantifiable continuous measure of compatibility between the observed data and the model outcome—model predictive capability (MPC)—ranging from zero (complete incompatibility) to one (perfect compatibility) (48). In addition to the continuous measure of compatibility, the combined P value was used at the significance level of 0.01 (Bonferroni

correction: α = 0.05/5 tests) to accept or reject the null hypothesis that there was no difference between the simulated and observed distribution profiles

Results

The success of the model at predicting the distribution profiles observed in nature was highly variable and dependent on tidal period modeled and swimming velocity assigned to the particles as demonstrated by the MPC (Fig. 3, bars). When particles were passive, the modeled distribution profile was significantly different from the observed profile for all tidal states (Stouffer's $P < 0.01$). On the flood tide, modeled distribution profiles did not significantly differ from those observed in nature when particles were assigned swimming velocities ranging from 0.8 to 3.3 mm s^{-1} (Stouffer's $P > 0.01$), and maximum MPC (MPC_{max}) was achieved at 2.2 mm s^{-1} (Stouffer's $P = 0.997$) (Fig. 3*A*). MPC_{max} at high water was achieved when particles were assigned a swimming velocity of −0.8 mm s^{-1} (Stouffer's $P = 0.883$), and velocities between −0.4 and −1.5 mm s^{-1} produced profiles that did not significantly differ from the observations (Stouffer's $P > 0.01$), with the exception of −1.4 mm s^{-1} (Stouffer's $P < 0.01$) (Fig. 3*B*). The model predicted distributions were not significantly different from those observed at low water when particles were assigned swimming velocities of −0.7, −0.8, and −1 mm s^{-1} tide (Stouffer's $P > 0.01$), with MPC_{max} at −0.7 and −0.8 mm s^{-1} tide (Stouffer's $P = 0.23$ for both) (Fig. 3*D*). Combined *P* values suggest significant differences between the modeled and observed distribution profiles on the ebb tide for all tested swimming velocities (Fig. 3*C*), and therefore, a value for MPC_{max} on the ebb tide could not be determined.

Minimum SS_{total}, as predicted by the fitted curves, correlated well to MPC_{max} (Fig. 3), with the lowest values predicted within 2 mm s^{-1} of the swimming velocities related to MPC_{max} for the flood tide ($Velocity_{Min.SStotal}$ = 2.4 mm s^{-1}; MPC_{max} = 2.2 mm s^{-1}) (Fig. 3*A*), high water ($Velocity_{Min.SStotal}$ = −1 mm s^{-1}; MPC_{max} = −0.8 mm s^{-1}) (Fig. 3*B*), and low water ($Velocity_{Min.SStotal}$ = −0.8 mm s^{-1}; MPC_{max} = −0.7/−0.8 mm s^{-1}) (Fig. 3*D*). The velocity at which the lowest SS_{total} was predicted on the ebb tide was −1.1 mm s^{-1} (Fig. 3*C*).

Discussion

Behavior is often included in biophysical models using relatively simple rules based on laboratory-based observations of larval responses to cues (15, 35). Here, we argue that this approach may not be appropriate. Our results suggest that current methods of behavioral parameterization used in biophysical modeling studies are limited in their capacity to "match" in situ observations of vertical distribution profiles. Using a bootstrap approach, we identified the swimming velocities that best reduced the likelihood of difference between observed distributions and those predicted by the model, even in instances where the MPC was low (i.e., the ebb tide).

We simulated change in the vertical distribution of virtual larvae by assigning "behaviors" to particles within a high-resolution tidal boundary-layer Lagrangian model. To our knowledge, there is no study that has attempted to reverse engineer model simulations to determine larval behavioral parameters in this way. In addition to showing that the likelihood of difference between model and nature is reduced when particles are assigned some sort of active movement compared with passive particles, our results indicate when larvae change their swimming "behavior" in response to changes in tidal state. We showed that a shift from positive (upward) to negative (downward) movement around the midflood point of the circatidal cycle was necessary for larvae to achieve the distribution patterns observed in nature (11). This is counter to the STST hypothesis, which argues that organisms swim upward for the duration of one tidal state and downward during the opposing state (49), and it contradicts the theory of Weinstock et al. (25) of passive vertical advective movement by tidal straining, as this mechanism would result in the direction of vertical movement being consistent during the flooding tide. Consequently, the implementation of TVM in a dispersal model using this "rule" (35) may be ineffective at generating vertical profiles that accurately represent nature. Even over relatively short time periods, such as the 3-h period between midflood and high water, inaccurate vertical distributions in biophysical models will influence dispersal estimates, and such errors will accumulate and propagate over time (consider species with long planktic larval durations). This effect was recently hypothesized by Firth et al. (50). Looking forward, future research should explore how the results of this study propagate through the larval dispersal estimated by a biophysical model and how behavioral parameters derived from the reverse engineering of in situ vertical distribution profiles influence both dispersal and connectivity predictions compared with estimates

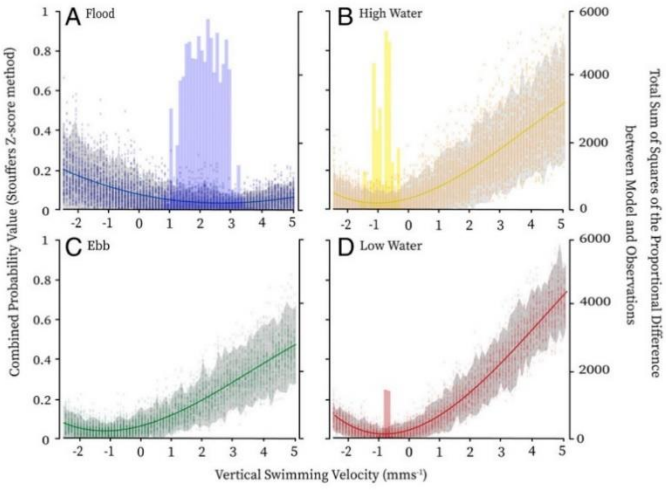

Fig. 3. Compatibility of the model with predicting the distribution profiles observed in nature during (*A*) the flood tide, (*B*) high-water slack, (*C*) the ebb tide, and (*D*) low-water slack after an ∼3-h simulation period and the quality of vertical swimming velocity as an estimator of observed profiles. Vertical swimming velocity (millimeters $second^{-1}$) is shown against MPC (Stouffer's combined *P* value; colored bars; left axis) and total sum of squares of the difference between 100 pairwise comparisons of modeled and observed distribution profiles generated using a bootstrap approach (right axis). Data points indicate individual pairwise comparisons (n = 7,600), and gray bands demonstrate 95% confidence intervals. MSE is represented by colored lines. Curves of best fit are calculated using third-order polynomials. (*A*) Flood: $y = -1.18x^3 + 43x^2 - 193.16x + 448.48$; r^2 = 0.39 (SS_{total}); r^2 = 0.97 (MSE). (*B*) High water: $y = -9.95x^3 + 122.25x^2 + 276.62x + 363.19$; r^2 = 0.75 (SS_{total}); r^2 = 0.99 (MSE). (*C*) Ebb: $y = -9.05x^3 + 91.61x^2 + 252.34x + 379.60$; r^2 = 0.82 (SS_{total}); r^2 = 0.99 (MSE). (*D*) Low water: $y = -13.49x^3 + 170.38x^2 + 335.67x + 251.78$; r^2 = 0.93 (SS_{total}); r^2 = 0.99 (MSE).

made using alternative approaches to vertical distribution [i.e., "rule-based" behaviors (35)] and/or probabilistic larval vertical distribution profiles (51).

All velocities resulting in the smallest error between model and observations fell between the boundaries of larval swimming reported in the literature, suggesting that swimming is an important mechanism. Reported swimming speeds and sinking velocity estimates are typically highly variable both within and across taxa, although they are typically in the range of 1–10 mm s^{-1} and rarely exceed 20 mm s^{-1} (4.2 cm s^{-1} in *Cancer magister* megalopa) (52). Our study showed that, for our data, upward swimming must be 2.5× faster than downward swimming to best match the observed profiles. This demonstrates the need for swimming speed to be a variable parameter in dispersal modeling studies and highlights that the speeds of upward and downward movements are not always consistent; however, we acknowledge that any difference in optimum swimming speed among tidal states will be most marked in slower swimming species, such as bivalves, and effects will likely be less pronounced for stronger swimmers (53).

The model-generated distribution profiles on the ebb tide were significantly different from those observed for all tested velocities, leading to low model compatibility (high water to midebb; midebb to low water). This is in marked contrast to the flood tide, where compatibility was high. Our approach was able to identify the optimum vertical velocities that give the "best fit" to the observed patterns when larval behavior is parameterized by constant swimming in one direction; however, the low compatibility between the modeled data and observed profiles suggests that we do not fully understand the behavioral responses of the larvae and their relationship with the physical characteristics of the ocean during this particular tidal state. For instance, it is possible that spatially and/or temporally inconsistent behavioral responses in situ may cause larval swimming to differ among depths over even shorter timescales. One possible solution to this problem might be to use higher spatiotemporal resolution in situ sampling coupled with a short model internal timestep in an effort to improve model compatibility. This process alone may provide further insights into the relationship between manifestation of larval behaviors in response to their environment while simultaneously supporting improved model compatibility and better characterization of larval behavior within model frameworks.

Due to the sampling regime of the original study, our model was only able to reverse engineer optimum swimming speeds during daylight hours. Diel vertical migration (DVM) occurs when organisms synchronize their vertical movement to the day/night cycle. Such behavior, thought to be a predation avoidance response (54), has been documented for a number of taxa (55–57). Whether bivalve larvae exhibit DVM remains unclear; there is conflicting evidence in the literature (57, 58), and differences may well be location specific. Future research would benefit from sampling programs that encompass the 24-h diel cycle to encapsulate potential variation in the vertical distribution of larvae within the study domain due to the day/night cycle.

The model system of this study assumes a well-mixed open coastal environment with a flat bathymetry and laterally homogenous spatially averaged velocities. Given this and the fact that the LES model could be directly forced by observed velocities suggest that the LES data broadly described the hydrodynamic conditions that the larvae would experience throughout the study domain. It must be noted, however, that, in environments with high spatial heterogeneity (for example, over sloping bathymetry or across lateral or vertical frontal systems), differential vertical mixing may influence larval ability to regulate depth as expected. Stratification of the water column has been shown to alter the vertical migration of marine organisms (57, 59) by acting as a barrier to vertical movement (60). Should our approach be undertaken to infer larval swimming in a more heterogeneous environment, such as an estuary, the underlying hydrodynamic model should be designed as to adequately represent realistic conditions.

The cues that govern larval swimming responses in situ remain unclear and were beyond the scope of this study. It has been previously suggested that some larvae may respond to a hierarchy of cues; indeed, many have the sensory ability to do so (16, 28). Hierarchical responses to stimuli have been shown to influence the vertical migration of a range of taxa, including the larvae of sponges (18) and fish (61), and therefore, it is possible that a similar response exists in other organisms: for example, bivalves. If cues do influence the vertical migration of larvae in a hierarchical manner, their order of importance to the organism must be determined if behaviors are to be parameterized using a rule-based approach in dispersal models so that behaviors accurately depict responses in nature. This order may change over space and time and in relation to other cues, and therefore, rule-based models must account for this. Failure to do so could greatly contribute to model error.

With this in mind, accurately parameterizing larval behavior using a rule-based approach is clearly a complex endeavor that requires an in-depth understanding of a multitude of potential drivers of larval movement and knowledge of how these drivers influence both larvae and each other. Using field-derived vertical distribution data to set the goal posts, our approach allows larval behavior to be based on real-life changes in the vertical distribution patterns of larvae. By focusing on the active movements particles would be required to undertake within the model domain to achieve a distribution profile that is the least different from that observed in nature, we effectively bypass the need for a complex understanding of the mechanisms of planktic swimming and larval responses to behavioral stimuli, instead, we focus on the end goal: achieving a modeled distribution profile that accurately replicates nature.

Dispersal is a key mechanism that shapes the distribution of marine species, and thus, an understanding of how and why species disperse is imperative to the success of marine conservation agendas, fisheries management efforts, and attempts to minimize the risk of invasive species spread (2, 62, 63). Biophysical modeling provides a cost-effective tool to estimate dispersal in the marine environment; however, inaccuracies within these models can misguide those using them, and consequently, decisions made off the back of inaccurate model estimations may be ineffective (64). This study demonstrates that active movement changes over the course of the tidal cycle at temporal scales typically not modeled. Our approach has reverse engineered model simulations to identify the larval swimming speeds and directions that generate the smallest error between modeled and observed distribution patterns. These estimates are not perfect, but as error is reduced compared with the passive model when particles are given active movement, we can conclude that larval swimming is an important mechanism in accurate depictions of vertical distribution. This approach will allow future research to determine the best-fitting behaviors of a range of taxa, where in situ vertical distribution data are/can be made available.

This study highlights that, over a period as short as 12 h, differences in behavior (i.e., speed/direction) required to replicate observed vertical distribution profiles are great. Our results indicate that current "rule-based" approaches to behavioral parameterization [for example, assigning a constant swimming speed to particles and/or assuming vertical direction with respect to tidal direction (35)] may lead to significant over- or underestimates of dispersal. For larvae swimming outside optimum speeds, modeled predictions of dispersal will become increasingly divergent over time in terms of match to in situ observations due to depth-related differences in current velocity, especially for species with planktonic larval durations longer than 1 d. This study offers an alternative

method of behavioral parameterization where behavior is inferred from the field rather than the laboratory, which will aid in minimizing the error associated with inaccurate vertical distribution profiles in biophysical models.

ACKNOWLEDGMENTS. This research was supported by an internal grant from the University of Plymouth (to K.L.H., W.A.M.N.-S., and A.M.K.). We thank the handling editor and two anonymous reviewers for their constructive and insightful comments and suggestions that helped to strengthen this manuscript.

1. R. K. Cowen, S. Sponaugle, Larval dispersal and marine population connectivity. *Annu. Rev. Mar. Sci.* **1**, 443–466 (2009).
2. L. A. Levin, Recent progress in understanding larval dispersal: New directions and digressions. *Integr. Comp. Biol.* **46**, 282–297 (2006).
3. N. S. Banas, P. S. McDonald, D. A. Armstrong, Green crab larval retention in Willapa Bay, Washington: An intensive Lagrangian modeling approach. *Estuaries Coasts* **32**, 893–905 (2009).
4. A. Nicolle, F. Dumas, A. Foveau, E. Foucher, E. Thiebaut, Modelling larval dispersal of the king scallop (Pecten maximus) in the English channel: Examples from the bay of Saint-Brieuc & the bay of Seine. *Ocean Dyn.* **63**, 661–678 (2013).
5. R. E. Ross, A. W. Nimmo-Smith, K. L. Howell, Towards 'ecological coherence': Assessing larval dispersal within a network of existing marine protected areas. *Deep Sea Res. Part I Oceanogr. Res. Pap.* **126**, 128–138 (2017).
6. D. J. Marshall, K. Monro, M. Bode, M. J. Keough, S. Swearer, Phenotype-environment mismatches reduce connectivity in the sea. *Ecol. Lett.* **13**, 128–140 (2010).
7. R. L. Soulsby, C. T. Mead, B. R. Wild, "A model for simulating the dispersal tracks of sand grains in coastal areas–"SandTrack" in *Coastal and Shelf Sediment Transport*, P. S. Balson, M. B. Collins, Eds. (Geological Society Special Publications, 2007), Book 274, pp. 65–72.
8. A. Metaxas, M. Saunders, Quantifying the "bio-" components in biophysical models of larval transport in marine benthic invertebrates: Advances and pitfalls. *Biol. Bull.* **216**, 257–272 (2009).
9. S. Thorpe, *The Turbulent Ocean* (Cambridge University Press, Cambridge, 2005).
10. C. Porch, A theoretical comparison of the contributions of random swimming & turbulence to absolute dispersal in the sea. *Bull. Mar. Sci.* **62**, 31–44 (1998).
11. A. M. Knights, T. P. Crowe, G. Burnell, Mechanisms of larval transport: Vertical distribution of bivalve larvae varies with tidal conditions. *Mar. Ecol. Prog. Ser.* **326**, 167–174 (2006).
12. J. A. Polton, M. R. Palmer, M. J. Howarth, The vertical structure of time-mean estuarine circulation in a shallow, rotating, semi-enclosed coastal bay: A Liverpool Bay case study with application for monitoring. *Cont. Shelf Res.* **59**, 115–126 (2013).
13. J. A. Polton, Y.-D. Lenn, S. Elipot, T. K. Chereskin, J. Sprintall, Can Drake Passage observations match Ekman's classic theory. *J. Phys. Oceanogr.* **48**, 1733–1740 (2013).
14. R. J. Uncles, J. A. Stephens, The structure of vertical current profiles in a macrotidal partly-mixed estuary. *Estuaries* **13**, 349–361 (1990).
15. E. W. North *et al*., Vertical swimming behavior influences the dispersal of simulated oyster larvae in a coupled particle-tracking & hydrodynamic model of Chesamide Bay. *Mar. Ecol. Prog. Ser.* **359**, 99–115 (2008).
16. M. J. Kingsford *et al*., Sensory environments, larval abilities & local self-recruitment. *Bull. Mar. Sci.* **70**, 309–340 (2002).
17. J. Welch, R. Forward, Flood tide transport of blue crab, Callinectes sapidus, postlarvae: Behavioral responses to salinity & turbulence. *Mar. Biol.* **139**, 911–918 (2001).
18. P. Ettinger-Epstein, S. Whalan, C. N. Battershill, R. de Nys, A hierarchy of settlement cues influences larval behaviour in a coral reef sponge. *Mar. Ecol. Prog. Ser.* **365**, 103–113 (2008).
19. W. J. Kimmerer, J. R. Burau, W. A. Bennett, Tidally oriented vertical migration & position maintenance of zooplankton in a temperate estuary. *Limnol. Oceanogr.* **43**, 1697–1709 (1998).
20. M. M. Criales, M. B. Robblee, J. A. Browder, H. Cardenas, T. L. Jackson, Field observations on selective tidal-stream transport for postlarval & Juvenile Pink Shrimp in Florida Bay. *J. Crustac. Biol.* **31**, 26–33 (2011).
21. H. Ueda, M. Kuwatani, K. W. Suzuki, Tidal vertical migration of two estuarine copepods: Naupliar migration & position-dependent migration. *J. Plankton Res.* **32**, 1557–1572 (2010).
22. R. A. Lutz, M. J. Kennish, "Ecology and morphology of larval and early larval post-larval mussels" in *The Mussel Mytilus: Ecology, Physiology, Genetics and Culture*, E. M. Gosling, Ed. (Developments in Aquaculture and Fisheries Science, no. 25, Elsevier Science Publishers, Amsterdam, 1992), pp. 53–85.
23. H. B. Kunze, S. G. Morgan, M. L. Kamazima, Field test of the behavioural regulation of larval transport. *Mar. Ecol. Prog. Ser.* **487**, 71–87 (2013).
24. L. G. Peteiro, A. L. Shanks, Up and down or how to stay in the bay: Retentive strategies of Olympia oyster larvae in a shallow estuary. *Mar. Ecol. Prog. Ser.* **530**, 103–117 (2015).
25. J. B. Weinstock, S. L. Morello, L. M. Conlon, H. Xue, P. O. Yund, Tidal shifts in the vertical distribution of bivalve larvae: Vertical advection vs. active behaviour. *Limnol. Oceanogr.* **63**, 2681–2694 (2018).
26. R. B. Forward, R. A. Tankersley, Selective tidal-stream transport of marine animals. *Oceanogr. Mar. Biol. Annu. Rev.* **39**, 305–353 (2001).
27. R. N. Gibson, Go with the flow: Tidal migration in marine animals. *Hydrobiol.* **503**, 153–161 (2003).
28. P. Oteiza, I. Odstrcil, G. Lauder, R. Portugues, F. Engert, A novel mechanism for mechanosensory-based rheotaxis in larval zebrafish. *Nature* **547**, 445–448 (2017).
29. M. A. McManus, C. B. Woodson, Plankton distribution and ocean dispersal. *J. Exp. Biol.* **215**, 1008–1016 (2012).
30. H. L. Fuchs, C. DiBacco, Mussel larval responses to turbulence are unaltered by larval age or light conditions. *Limnol. Oceanogr. Fluids Environ.* **1**, 120–134 (2011).
31. H. L. Fuchs, E. J. Hunter, E. L. Schmitt, R. A. Guazzo, Active downward propulsion by oyster larvae in turbulence. *J. Exp. Biol.* **216**, 1458–1469 (2013).
32. F. G. Michalec, S. Souissi, M. Holzner, Turbulence triggers vigorous swimming but hinders motion strategy in planktonic copepods. *J. R. Soc. Interface* **12**, 150–158 (2015).
33. C. J. Bradley, J. R. Strickler, E. J. Buskey, P. H. Lenz, Swimming and escape behavior in two species of calanoid copepods from nauplius to adult. *J. Plankton Res.* **35**, 49–65 (2013).
34. C. B. Paris, J. B. Helgers, E. van Sebille, A. Srinivasan, Connectivity modeling system: A probabilistic modeling tool for the multi-scale tracking of biotic & abiotic variability in the ocean. *Environ. Model. Softw.* **42**, 47–54 (2013).
35. P. E. Robins, S. P. Neill, L. Giménez, A numerical study of marine larval dispersal in the presence of an axial convergent front. *Estuar. Coast. Shelf Sci.* **100**, 172–185 (2012).
36. J. Brown *et al*., Observations of the physical structure & seasonal jet-like circulation of the Celtic Sea & St. George's channel of the Irish Sea. *Cont. Shelf Res.* **23**, 533–561 (2003).
37. A. R. Brereton, A. Tejada-Martinez, M. R. Palmer, J. A. Polton, The perturbation method–A novel large-eddy simulation technique to model realistic turbulence: Application to tidal flow. *Ocean Model.* **135**, 31–39 (2019).
38. C. de Boor, *A Practical Guide to Splines* (Springer-Verlag, New York, 1978).
39. A. Metaxas, Behaviour in flow: Perspectives on the distribution & dispersion of meroplanktonic larvae in the water column. *Can. J. Fish. Aquat. Sci.* **58**, 86–98 (2001).
40. O. N. Ross, J. Sharples, Recipe for 1-D Lagrangian particle tracking models in space-varying diffusivity. *Limnol. Oceanogr. Methods* **2**, 289–302 (2004).
41. P. R. Jonsson, C. André, M. Lindegarth, Swimming behaviour of marine bivalve larvae in a flume boundary-layer flow: Evidence for near-bottom confinement. *Mar. Ecol. Prog. Ser.* **79**, 67–76 (1991).
42. M. Sprung, Physiological energetics of mussel larvae (Mytiius edulis). III. Respiration. *Mar. Ecol. Prog. Ser.* **18**, 171–178 (1984).
43. J. Dronkers, Tidal asymmetry & estuarine morphology. *Neth. J. Sea Res.* **20**, 117–131 (1986).
44. R. D. Pingree, D. K. Griffiths, S& transport paths around the British Isles resulting from M2 & M4 tidal interactions. *J. Mar. Biol. Assoc. U. K.* **59**, 497–513 (1979).
45. R. D. Moore, J. Wolf, A. J. Souza, S. S. Flint, Morphological evolution of the Dee Estuary, Eastern Irish sea, UK: A tidal asymmetry approach. *Geomorphology* **103**, 588–596 (2009).
46. R. Sokal, F. Rohlf, *Biometry* (W. H. Freeman & Co., New York, 1995).
47. S. A. Stouffer, E. A. Suchman, L. C. DeVinney, S. A. Star, R. M. Williams Jr, *The American Soldier, Vol. 1: Adjustment During Army Life* (Princeton University Press, Princeton, 1949).
48. S. Greenland *et al*., Statistical tests, P values, confidence intervals, and power: A guide to misinterpretations. *Eur. J. Epidemiol.* **31**, 337–350 (2016).
49. C. V. Civelek, R. M. Daigle, A. Metaxas, Effects of temperature on larval swimming patterns regulate vertical distribution relative to thermoclines in Asterias rubens. *J. Exp. Mar. Biol. Ecol.* **445**, 1–12 (2013).
50. L. B. Firth *et al*., Ocean sprawl: Challenges and opportunities for biodiversity management in a changing world. *Oceanogr. Mar. Biol. Annu. Rev.* **54**, 193–269 (2016).
51. C. B. Paris, L. M. Cherubin, R. K. Cowen, Surfing, spinning or diving: Effects on population connectivity. *Mar. Ecol. Prog. Ser.* **347**, 285–300 (2007).
52. F.-S. Chia, J. Buckland-Nicks, C. M. Young, Locomotion of marine invertebrate larvae: A review. *Can. J. Zool.* **62**, 1205–1222 (1984).
53. M. E. Huntley, M. Zhou, Influence of animals on turbulence in the sea. *Mar. Ecol. Prog. Ser.* **273**, 65–79 (2004).
54. W. Lampert, Ultimate causes of diel vertical migration of zooplankton: New evidence for the predator-avoidance hypothesis. *Ergebnisse Limnol.* **39**, 79–88 (1993).
55. M. R. Romero *et al*., Larval diel vertical migration of the marine gastropod Kelletia kelletii (Forbes, 1850). *J. Mar. Biol.* **2012**, 1–9 (2012).
56. J. K. Breckenridge, S. M. Bollens, Vertical distribution and migration of decapod larvae in relation to light and tides in Willapa Bay, Washington. *Estuaries Coasts* **34**, 1255–1261 (2011).
57. D. Raby, Y. Lagadeuc, J. J. Dodson, M. Mingelbier, Relationship between feeding and vertical distribution of bivalve larvae in stratified and mixed waters. *Mar. Ecol. Prog. Ser.* **103**, 275–284 (1994).
58. J. Bonicelli *et al*., Diel vertical migration and cross-shore distribution of barnacle and bivalve larvae in the central Chile inner-shelf. *J. Exp. Mar. Biol. Ecol.* **485**, 35–46 (2016).
59. L. A. Lougee, S. M. Bollens, S. R. Avent, The effects of halodines on the vertical distribution and migration of zooplankton. *J. Exp. Mar. Biol. Ecol.* **278**, 111–134 (2002).
60. R. M. Daigle, A. Metaxas, Vertical distribution of marine invertebrate larvae in response to thermal stratification in the laboratory. *J. Exp. Mar. Biol. Ecol.* **409**, 89–98 (2011).
61. M. A. Teodosio, C. B. Paris, E. Wolankski, P. Morias, Biophysical processes leading to the ingress of temperate fish larvae into estuarine nursery areas: A review. *Estuar. Coast. Shelf Sci.* **183**, 187–202 (2016).
62. L. Botsford, F. Micheli, A. Hastings, Principles for the design of marine reserves. *Ecol. Appl.* **13**, S25–S31 (2003).
63. S. Palumbi, Population genetics, demographic connectivity & the design of marine reserves. *Ecol. Appl.* **13**, S146–S158 (2003).
64. L. W. Botsford *et al*., Connectivity and resilience of coral reef metapopulations in marine protected areas: Matching empirical efforts to predictive needs. *Coral Reefs* **28**, 327–337 (2009).

APPENDICES

Appendix 1: MATLAB code for the 1D particle tracker (Chapter 2)

```
%%===== ANOVA MODULE ==========


%2 way anova to compare modelled and observed data


%organise the distribution replicates so that they are in the same
format as the observational data (rows = TMB; columns = reps)

%transpose the matrix
drep = distribution_rep';
%flip the matrix so is reads TMB not BMT
dflip = flipud(drep);
%remove the top line of 0s
distro_rep(:,:,modelrun) = dflip(2:end,:);

%#########################################################
%convert the data to decimal percentages
distro_decimal = distro_rep/100;
% arcsin square root tranform the data
distro_transform = asin(sqrt(distro_decimal));

clear dep;
clear dflip;
clear distro_decimal;

%original ANOVA (raw percentages)
%create a matrix with 2 columns (modelled and observed) and
(reps*depthbins) rows

%populate the observed column

if strcmp(endpoint,'flood')
        %top depth bin
        anova_data(1:5,2) = obs_data(1,:);
        %mid depth bin
        anova_data(6:10,2) = obs_data(2,:);
        %bottom depth bin
        anova_data(11:15,2) = obs_data(3,:);
elseif strcmp(endpoint,'hws')
    %top depth bin
    anova_data(1:5,2) = obs_data(5,:);
    %mid depth bin
    anova_data(6:10,2) = obs_data(6,:);
    %bottom depth bin
    anova_data(11:15,2) = obs_data(7,:);

elseif strcmp(endpoint,'ebb')
    %top depth bin
    anova_data(1:5,2) = obs_data(9,:);
    %mid depth bin
    anova_data(6:10,2) = obs_data(10,:);
    %bottom depth bin
    anova_data(11:15,2) = obs_data(11,:);

elseif strcmp(endpoint,'lws')
```

```
    %top depth bin
    anova_data(1:5,2) = obs_data(13,:);
    %mid depth bin
    anova_data(6:10,2) = obs_data(14,:);
    %bottom depth bin
    anova_data(11:15,2) = obs_data(15,:);
end

%populate the modelled column
anova_data(1:5,1) = distro_rep(1,:,modelrun);
anova_data(6:10,1) = distro_rep(2,:,modelrun);
anova_data(11:15,1) = distro_rep(3,:,modelrun);

anova_data;


anova_labels =
['modelled';'modelled';'modelled';'modelled';'modelled';'observed';'ob
served';'observed';'observed';'observed'];

[p,tbl,stats] = anova2(anova_data,5,'off');
%top_data(1:5,1) = anova_data(1:5,1);
%top_data(6:10,1) = anova_data(1:5,2);

%mid_data(1:5,1) = anova_data(6:10,1);
%mid_data(6:10,1) = anova_data(6:10,2);

%bottom_data(1:5,1) = anova_data(11:15,1);
%bottom_data(6:10,1) = anova_data(11:15,2);


p_interaction = p(3)


% ANOVA - transformed data

%create a matrix with 2 columns (modelled and observed) and
(reps*depthbins) rows

%populate the observed column

if strcmp(endpoint,'flood')
        %top depth bin
        anova_data(1:5,2) = obs_transform(1,:);
        %mid depth bin
        anova_data(6:10,2) = obs_transform(2,:);
        %bottom depth bin
        anova_data(11:15,2) = obs_transform(3,:);
elseif strcmp(endpoint,'hws')
    %top depth bin
    anova_data(1:5,2) = obs_transform(5,:);
    %mid depth bin
    anova_data(6:10,2) = obs_transform(6,:);
    %bottom depth bin
    anova_data(11:15,2) = obs_transform(7,:);

elseif strcmp(endpoint,'ebb')
    %top depth bin
    anova_data(1:5,2) = obs_transform(9,:);
    %mid depth bin
    anova_data(6:10,2) = obs_transform(10,:);
    %bottom depth bin
    anova_data(11:15,2) = obs_transform(11,:);
```

```
elseif strcmp(endpoint,'lws')
    %top depth bin
    anova_data(1:5,2) = obs_transform(13,:);
    %mid depth bin
    anova_data(6:10,2) = obs_transform(14,:);
    %bottom depth bin
    anova_data(11:15,2) = obs_transform(15,:);
end

%populate the modelled column
anova_data(1:5,1) = distro_transform(1,:,modelrun);
anova_data(6:10,1) = distro_transform(2,:,modelrun);
anova_data(11:15,1) = distro_transform(3,:,modelrun);

anova_data;


anova_labels =
['modelled';'modelled';'modelled';'modelled';'modelled';'observed';'ob
served';'observed';'observed';'observed'];

[p,tbl,stats] = anova2(anova_data,5,'off');
%top_data(1:5,1) = anova_data(1:5,1);
%top_data(6:10,1) = anova_data(1:5,2);

%mid_data(1:5,1) = anova_data(6:10,1);
%mid_data(6:10,1) = anova_data(6:10,2);

%bottom_data(1:5,1) = anova_data(11:15,1);
%bottom_data(6:10,1) = anova_data(11:15,2);


p_transform(modelrun) = p(3)




%=================================================================

%%===== AVERAGES MODULE ==========



%calculates the mean proportion of articles in each depth bin from all
replicate model runs


mean_top = mean(distribution_rep(:,3))
se_top = std(distribution_rep(:,3))/(sqrt(replicates))
mean_middle = mean(distribution_rep(:,2))
se_middle = std(distribution_rep(:,2))/(sqrt(replicates))
mean_bottom = mean(distribution_rep(:,1))
se_bottom = std(distribution_rep(:,1))/(sqrt(replicates))

if strcmp(mean_histogram,'on')
mean_bar = [mean_top hist_Z_percent_end(3); mean_middle
hist_Z_percent_end(2); mean_bottom hist_Z_percent_end(1)];

se_bar = [se_top standard_error_observed(3); se_middle
standard_error_observed(2); se_bottom standard_error_observed(1)];
```

```
figure (1)
hold on
bar(mean_bar);
title('Modelled vs observed vertical distribution')
ylim([0 100]);
ylabel('Percent of total population')
xticks([1 2 3])
xticklabels({'Top (0.8m)','Middle (8-16m)','Bottom (16-24m)'});

ngroups = size(mean_bar,1);
nbars = size(mean_bar,2);
groupwidth = min(0.8, nbars/(nbars + 1.5));
for i = 1:nbars
x = (1:ngroups) - (groupwidth/2) + (2*i-1) * (groupwidth / (2*nbars));
  errorbar(x, mean_bar(:,i), se_bar(:,i), 'k', 'linestyle', 'none');
end
legend('labels',({'Modelled','Observed'}))
end
```

```
%=================================================================

%===== BOUNDARY CONDITIONS MODULE ==========
%particles stick to the boundaries if they are rigid

if strcmp(boundary,'rigid')
if Z_new(i) >H
Z_new(i) = H -0.0001;
elseif Z_new(i) < 0
Z_new(i) = 0.0001;
end

%particles are reflected back into the water column at a distance
equal to that of which they traversed the boundary
elseif strcmp(boundary,'reflective')
if Z_new(i) >H
Z_new(i) = H-(Z_new(i) - H);
elseif Z_new(i) < 0
Z_new(i) = abs(Z_new(i));
end
end
```

```
%=================================================================

%========== HYDRODYNAMIC MODULE============

%LES smoothing and interpolating module

depth_interval = 0.01; %depth interval in metres
 H = 24; %water depth (m)

 interp_method = 'spline'; %interpolation method
 Prt = 1; %Turbulent Prandtl number
 LES_scale = 1; %to explore different magnitides of K
```

```
 %external timestep
 LES_ts = 2;

 load('Eddy_Vis.mat') %matrix containing nxn K profile generated by
the LES
 [EV, ~, ~, ~, ~] =filloutliers(eddy_vis,interp_method,2);
 EVsmooth = smoothdata(EV,2);
 EVsmooth = smoothdata(EVsmooth,1);
 EV=EVsmooth;
 clear EVsmooth
 clear eddy_vis
 zq = 0:depth_interval:z(end);
 EV_interp = zeros(length(zq),length(time));

 for tidx = 1:length(time) %loops through each timestep
   y = EV(:,tidx) ; % selects the EV values for all depths for the
timestep
   y_interp = interp1(z,y,zq,interp_method); %interpolates the EV
values for the queried z points (zq)
   EV_interp(:,tidx) = y_interp; %populates the column relating to the
timestep with the interpolated values
end

 EV = EV_interp;
 z = zq;

 clear y
 clear y_interp
 clear EV_interp
 clear  zq

 clear y
 clear y_interp
 clear EV_interp
 clear  zq


 %extend the time scale
for xx = 345:380
time(1,xx) = time(1,xx-1)+0.0333333333;
end

p = polyfit(time(:,1:344),tide_5m,4);
x1 = time(1,1):0.0333333333:time(end);
y1 = polyval(p,x1);


%attach extrapolated values to tide_5m
 tide_5m(:,345:380) = y1(:,345:380);
clear xx

%Cut dataset to water column height (H)
[~,hidx] = min(abs(z-H),[],2);
 zH = z(1:hidx);
 z = zH;
 clear zH
 EVH = EV(1:hidx,:);
 EV = EVH;
 clear EVH

%extend the EV dataset with blank values to fill

EV(:,344:380) = zeros;
```

```
%find the cumulative eddy viscosity to plot the tide
EVsum = sum(EV(:,1:380));

%reflect the tide between hws and ebb overlay anomoly values and
extrapolate data
EV_reflect = fliplr(EV(:,194:286));
EV(:,288:380) = EV_reflect;

clear EV_reflect
clear extrap_method
clear EVsum


K = EV*Prt;
meanK = mean(K);

%extend the time dataset to start at 0 hours
time_new = 0:0.033333333:1.966666667;
%add the original time series to the new time series
time_new(1,61:440) = time;

%extend the tide dataset to match the new time dataset
tide5m_new(1,61:440) = tide_5m;
tide5m_new(1,1:60) = NaN;

tide_reflect = fliplr(tide5m_new(1,140:278));
tide5m_new(1,1:139) = tide_reflect;

clear tide_reflect
time = time_new;
tide_5m = tide5m_new;
clear tide5m_new
clear time_new

%extend K inline with tide and time
K_new(:,61:440) = K;
K_new(:,1:60) = 0;
K_reflect = fliplr(K_new(:,244:319));
K_new(:,1:76) = K_reflect;
K_new(:,67:105) = smoothdata(K_new(:,67:105),2);
K = K_new;
meanK = mean(K);

%find points marking tidal states (Achieved by manually searching the
dataset)
lws1_idx = 52;
midflood = 139;
hws_idx = 227;
midebb = 326;
lws_idx = 417;


%Calulate the diffusivity gradient between depth bins
 Kprime = zeros(size(K));
 Kprime(1,:) = (K(2,:)- K(1,:)) / ((z(2)) - (z(1)));
 Kprime(end,:) = (K(end,:) - K(end-1,:)) / (z(end) - z(end-1));
for kk = 2:length(z)-1
 Kprime(kk,:) = (K(kk+1,:) - K(kk-1,:)) / (z(kk+1) - z(kk-1));
end


%Calculate the second derivative of K with respect to z
```

```
Kdev = zeros(size(K));
Kdev(1,:) = ((K(2,:) - K(1,:)).^2) / ((z(2)^2) - (z(1)^2));
Kdev(end,:) = ((K(end,:) - K(end-1,:)).^2) / ((z(end)^2) - (z(end-
1)^2));

for kk = 2:length(z)-1
        Kdev(kk,:) = ((K(kk+1,:) - K(kk-1,:)).^2) / ((z(kk+1)^2) -
(z(kk-1)^2));
end

minKdev = min(Kdev(:));
min_ts = 1/minKdev;

clear interp_method
 clear Prt
 clear tidx
 clear EV
 clear kk




%=================================================================

%=====OUTPUT MODULE ============
%saves data into an array

data_array = cell(41,6);

if strcmp(startpoint,'flood')
data_array(1,1) = cellstr('HWS');
elseif strcmp(startpoint,'hws')
data_array(1,1) = cellstr('Ebb');
elseif strcmp(startpoint,'ebb')
data_array(1,1) = cellstr('LWS');
elseif strcmp(startpoint,'lws')
data_array(1,1) = cellstr('Flood');
end

 datalabels = ["MeanSurf", "MeanMid", "MeanBed", "SESurf", "SEMid",
"SEBed"];
data_array(2,1) = cellstr(datalabels(1));
data_array(2,2) = cellstr(datalabels(2));
data_array(2,3) = cellstr(datalabels(3));
data_array(2,4) = cellstr(datalabels(4));
data_array(2,5) = cellstr(datalabels(5));
data_array(2,6) = cellstr(datalabels(6));


data_array(3,1) = num2cell(mean_top);
data_array(3,2) = num2cell(mean_middle);
data_array(3,3) = num2cell(mean_bottom);
data_array(3,4) = num2cell(se_top);
data_array(3,5) = num2cell(se_middle);
data_array(3,6) = num2cell(se_bottom);

anovalabels = ["2Way ANOVA", "1Way ANOVA: Surface", "1Way ANOVA:
Middle"," 1Way ANOVA: Bed"];

data_array(5,1) = cellstr(anovalabels);
data_array(6:11,1:6) = tbl;
```

```
data_array(32,2) = cellstr('Modelled');
data_array(32,3) = cellstr('Observed');
data_array(32,4) = cellstr('Difference');

data_array(33,1) = cellstr('Surface (0-8m)');
data_array(34,1) = cellstr('Middle (8-16m)');
data_array(35,1) = cellstr('Bed (16-24m)');

mean_bar_cell = num2cell(mean_bar);
data_array(33:35,2:3) = mean_bar_cell;

data_array(37,1) = cellstr('Standard Error');
data_array(37,2) = cellstr('Modelled');
data_array(37,3) = cellstr('Observed');

data_array(38,1) = cellstr('Surface (0-8m)');
data_array(39,1) = cellstr('Middle (8-16m)');
data_array(40,1) = cellstr('Bed (16-24m)');

se_bar_cell = num2cell(se_bar);
data_array(38:40,2:3) = se_bar_cell;




%=================================================================
%=======START==========

%runs the model

%load in hydrodynamic data
hydrodynamic_module

%load in variables
variables_module

for modelrun = 1:5
swimloop = 0;
for swimspeed = -0.0025:0.0001:0.005
    swimloop = swimloop + 1;

    for rep = 1:replicates

%~~~STARTING DISTRIBUTION OF PARTICLES BASED ON OBSERVATIONAL DATA
~~~~%

        if strcmp(startpoint,'flood')
            top = 43.61;
            middle = 31.72;
            bottom = 24.67;
        elseif strcmp(startpoint,'hws')
            top = 28.23;
            middle = 28.51;
            bottom = 43.27;
        elseif strcmp(startpoint,'ebb')
            top = 20.36;
            middle = 40.79;
            bottom = 38.85;
        elseif strcmp(startpoint,'lws')
            top = 27.86;
            middle = 29.88;
```

```
            bottom = 42.26;
        end


    top_no = N/(100/top);
    middle_no = N/(100/middle);
    bottom_no = N/(100/bottom);

    step = 0;
    %~~~ RANDOMLY ASSIGN PARTICLE DEPTHS WITHIN EACH DEPTH BIN ~~~%

        for i = 1:N
            if i < top_no
                Z(i) = ((H/3)*2) + (H-((H/3)*2)).*rand; %random
distribution of particles in top depth bin
            elseif  i > top_no && i < (top_no+middle_no)
                Z(i) = (H/3) + (((H/3)*2)-(H/3)).*rand; %random
distribution of particles in mid depth bin
            elseif i > (top_no+middle_no) && i <= N
                Z(i) = 0 + ((H/3)-0).*rand; %random distribution of
particles in bottom depth bin
            end
        end % particle loop

        %~~~VERTICAL DISPLACEMENT~~~%

        for ts = ts_start:ts_end

            %counter
            timestep_count= ['Timestep counter: ',num2str(ts),' out of
',num2str(ts_end), ' Behaviour: ',behaviour,' ',startpoint, ' to
',endpoint, ' (Replicate ',num2str(rep),];
            disp(timestep_count)
            disp(modelrun)
            disp(swimspeed)

            for its = 1:nested_ts %internal timestep loop

                step = step + 1; %internal timestep counter

                vertical_displacement_module

                if strcmp (show_particles, 'on')
                    figure (1)
                    hold off
                    scatter(x,Z,60,'k')
                    set(gca, 'XLim', [0 N], 'YLim', [0 24])
                    title('1D water column')
                    xlabel('')
                    set(gca,'xtick',[])
                    ylabel('Depth (m)')
                    hold on
                    pause (0.0005)
                end

            end %end internal timestep loop
        end % end external timestep loop



        %Number of particles in each depth bin
        hist_Z = histc(Z,edges);
```

```
        %histogram as a percentage of population
        hist_Z_percent = 100 ./ (N./hist_Z);
        modelled__distribution = hist_Z_percent;
        observed__distribution = hist_Z_percent_end;

        %store distribution results for replicate in a matrix
        distribution_rep(rep,:) = hist_Z_percent;

    end



    anova_module
    averages_module

    output_module
    disp completed



    for i = 1:5
      xlswrite([num2str(swimspeed),'.xls'],distro_rep(:,:,i),i)
    end

    xlswrite('p-values',swimspeed,1,['A' num2str(swimloop)])
    range = ['B', num2str(swimloop), ':', 'F', num2str(swimloop)];
    xlswrite('p-values',p_transform,1,range)


end



%=====================================================================
%========= SWIM CAPACITY MODULE ==========
%this module gives the option to suppress swimming behavour as a
function of a vaiable (default is a critical level of K)

if strcmp(swimming_performance, 'con')

        L(i) = 1;

elseif strcmp(swimming_performance,'pass')

    L(i) = 0;

elseif strcmp(swimming_performance,'lambda')

    if K(zidx(i),ts) < Kcrit
    L(i) = 1;
    elseif K(zidx(i),ts)  >= Kcrit
    L(i) = 0;
    end


end
```

```
%================================================================
%==========VARIABLES MODULE==============


N = 25; %number of particles
dt =120; %internal timestep (s)
replicates =5;
behaviour  = 'active'; % active or passive
time_swimming = 1;
 %time spent swimming (cruising and escaping) as a decimal percentage

time_escape = 0;
 % of total swimming time spent escaping as a decimal percentage

 if time_escape > 0;
     escspeed =0.03; %in ms-1
 end

%Kcrit = 1; %optional. see swimming performance module


loop = 0;
figpath = 'pwd';
swimming_performance = 'con';
%options:
%'con': constant: lambda = 1
%'lamdba': lambda is a function of K
%'pass': passiveL lambda = 0

startpoint = 'ebb';
endpoint = 'lws';

if strcmp(startpoint,'lws')
    ts_start = lws1_idx;
elseif strcmp(startpoint,'flood')
    ts_start = midflood;
elseif strcmp (startpoint, 'hws')
    ts_start = hws_idx;
elseif strcmp(startpoint,'ebb')
    ts_start = midebb;
end

if strcmp(endpoint,'flood')
    ts_end = midflood;
elseif strcmp(endpoint,'hws')
    ts_end = hws_idx;
elseif strcmp(endpoint,'ebb')
    ts_end = midebb;
elseif strcmp(endpoint,'lws')
    ts_end = lws_idx;
end


show_particles =''; % 'on' displays a visualisation of particle
movement in the water column
show_histogram = 'on'; % 'on' shows a bar chart comparing the modelled
and oserved distribution profiles
mean_histogram = 'on'; % 'on' generates a bar chart showing the mean
observed distribution profile and the mean modelled distribution
profile over all replicate model runs (default 5)
```

```
boundary = 'reflective';

%nested timestep (number of internal timesteps in model timestep
nested_ts = (LES_ts*60) / dt;

%read in the observational percentage data
obs_data = xlsread("obs_data.xlsx");

%convert obs data to decimal
obsdata_decimal = obs_data/100;
% arcsin square root transform the obs data to anova
obs_transform = asin(sqrt(obsdata_decimal));
clear obsdata_decimal;


%calculate the mean percentage of particles in each depth bin from the
replicates
mean_obs = mean(obs_data,2);

%calcuate the SD for each mean
sd_obs = std(obs_data,0,2);

%calculate the SE for each mean
obs_repcount = size (obs_data,2);
se_obs = sd_obs/sqrt(obs_repcount);

%ebb tide vertical distribution

if strcmp(endpoint,'flood')
hist_Z_percent_end = [mean_obs(3) mean_obs(2) mean_obs(1)];
standard_error_observed = [se_obs(3) se_obs(2) se_obs(1)];
elseif strcmp(endpoint,'hws')
hist_Z_percent_end = [mean_obs(7) mean_obs(6) mean_obs(5)];
standard_error_observed = [se_obs(7) se_obs(6) se_obs(5)];
elseif strcmp(endpoint,'ebb')
hist_Z_percent_end = [mean_obs(11) mean_obs(10) mean_obs(9)];
standard_error_observed = [se_obs(11) se_obs(10) se_obs(9)];
elseif strcmp(endpoint,'lws')
hist_Z_percent_end = [mean_obs(15) mean_obs(14) mean_obs(13)];
standard_error_observed = [se_obs(15) se_obs(14) se_obs(13)];
end

for i = 1:N
if i < hist_Z_percent_end(3)
Z_obs(i) = ((H/3)*2) + (H-((H/3)*2)).*rand; %random distribution of
particles in top depth bin
elseif  i > hist_Z_percent_end(3) && i <
(hist_Z_percent_end(3)+hist_Z_percent_end(2))
Z_obs(i) = (H/3) + (((H/3)*2)-(H/3)).*rand; %random distribution of
particles in mid depth bin
elseif i > (hist_Z_percent_end(3)+hist_Z_percent_end(2)) && i <= N
Z_obs(i) = 0 + ((H/3)-0).*rand; %random distribution of particles in
bottom depth bin
end
end %end particle loop

%binned data
numbins = 3; %number of bins in the histogram
binsize = H/numbins; % size of each depth bin in metres
edges= 0:H/numbins:H; %edges of the bins

%x position of particles (fixed - no horizontal advection)
x= 1 + (N-1)*rand(1,N);
```

```
%multiply K by lES scaler
K = K*LES_scale;

swimloop = 0;

%Mersenne twister random number generator
twister = RandStream('mt19937ar','Seed',1);
RandStream.setGlobalStream(twister);

%Pre allocated arrays and comment strings
Z = zeros(1,N); %particle depths
w = zeros(1,N); %particle swimming speeds
R = zeros(1,N); % Random walk factor
L = zeros(1,N); %swimming ability of particles
Z_new = zeros(1,N); % new particle locations
zidx = zeros(1,N); %depth index of particle loop iteration
Z_offset=zeros(1,N); %offset depth
Ki=zeros(1,N); % Kprime (dt^2/d^2z)




%============================================================
%===========VERTICAL DISPLACEMENT MODULE================

for i =1:N %particle loop

%Random number between -1 and 1
%normal distribution
R(i) = -1 + 2.*rand;

 %swimspeed
w(i) = swimspeed;


%find the location of the particle
%local index of z nearest to the depth of the particle
zidx(i) = knnsearch(z'',Z(i));

%find the diffusivity gradient at the particles location
Ki(i) = Kprime(zidx(i),ts);

%offset the particles location at a distance of 1/2K''dt
Z_offset(i) = Z(i) + ((Ki(i)/2)*dt);
%find the depth index for the offset particle
offset_zidx(i) = knnsearch(z'', Z_offset(i));

swimming_capacity_module

%GENERATE A MATRIX OF THE SWIMMING SPEEDS OF EACH PARTICLE DURING EACH
TIMESTEP
swim_matrix(i,step,rep) = w(i) * L(i);

Kstep(i,step) = K(zidx(i),ts);

KRWstep(i,step) = Kstep(i,step) * R(i);
```

```
%calculate particle vertical displacement
%using the equation Z(n+1) = Zn + K''(Zn)dt + (R((2K(Zn +
1/2K''dt)dt)/r)^0.5) + (w*l)dt (Visser,1997)

if strcmp(behaviour,'active')

Z_new(i) = Z(i)  + (Ki(i)*dt) + R(i)
*((2*K(offset_zidx(i),ts)*dt)/(1/3))^0.5 +((w(i)*L(i))*dt);


elseif strcmp(behaviour,'passive')
Z_new(i) = Z(i)  + (Ki(i)*dt) + R(i)
*((2*K(offset_zidx(i),ts)*dt)/(1/3))^0.5;
end
boundary_conditions_module

% New particle Location
Z(i) = Z_new(i);

end
```

Appendix 2: Sensitivity analysis of the 1D particle tracking model (Chapter 2)

Number of Particles	Replicate	Top (%)	Mid (%)	Bed (%)
100	1	45.4	29.8	24.8
100	2	41.6	33.8	24.6
100	3	45	32.8	22.2
100	4	41.4	33.6	25
100	5	45.2	33.8	21
100,000	1	43.24	32.86	23.9
100,000	2	42.88	33.06	23.9
100,000	3	43.18	33.8	24.06
100,000	4	42.52	32.32	23.02
100,000	5	43.32	33.24	25.16

```
> mod <- aov(data = sanalysis, mod ~ Top+Mid+Bed)
> summary(mod)

             Df   Sum Sq  Mean Sq    F value Pr(>F)
Top           1 1.645e+09 1.645e+09   0.427  0.538
Mid           1 4.344e+05 4.344e+05   0.000  0.992
Bed           1 1.935e+08 1.935e+08   0.050  0.830
Residuals     6 2.311e+10 3.852e+09
```

Appendix 3: GAM model summaries (Chapter 3)

```
summary(earlybiv.gam)

Family: gaussian
Link function: identity

Formula:
BivalvePropAbun_e ~ s(Temperature) + s(Salinity) + s(Density) +
    s(EddyDiffusivity)

Parametric coefficients:
            Estimate Std. Error t value Pr(>|t|)
(Intercept) 0.351843   0.005717   61.55   <2e-16 ***
---
Signif. codes:  0 ‘***’ 0.001 ‘**’ 0.01 ‘*’ 0.05 ‘.’ 0.1 ‘ ’ 1

Approximate significance of smooth terms:
                    edf Ref.df      F  p-value
s(Temperature)     8.680  8.940  5.942 3.96e-08 ***
s(Salinity)        8.388  8.805  4.999 2.50e-06 ***
s(Density)         9.000  9.000  8.342 3.38e-12 ***
s(EddyDiffusivity) 8.461  8.885 10.995 1.45e-13 ***
---
Signif. codes:  0 ‘***’ 0.001 ‘**’ 0.01 ‘*’ 0.05 ‘.’ 0.1 ‘ ’ 1

R-sq.(adj) =   0.17
Deviance explained = 17.2%
GCV = 346.57
n = 1350


summary(latebiv.gam)

Family: gaussian
Link function: identity

Formula:
BivalvePropAbun_l ~ s(Temperature) + s(Salinity) + s(Density) +
    s(EddyDiffusivity)

Parametric coefficients:
            Estimate Std. Error t value Pr(>|t|)
(Intercept) 0.350163   0.005306      66   <2e-16 ***
---
Signif. codes:  0 ‘***’ 0.001 ‘**’ 0.01 ‘*’ 0.05 ‘.’ 0.1 ‘ ’ 1

Approximate significance of smooth terms:
                    edf Ref.df      F  p-value
s(Temperature)     6.832  7.776  6.898 1.48e-08 ***
s(Salinity)        3.334  4.109  0.503    0.728
s(Density)         2.722  3.412  1.009    0.375
s(EddyDiffusivity) 8.791  8.978 39.713  < 2e-16 ***
---
Signif. codes:  0 ‘***’ 0.001 ‘**’ 0.01 ‘*’ 0.05 ‘.’ 0.1 ‘ ’ 1

R-sq.(adj) =  0.239
Deviance explained = 23.9%
GCV = 290.52
n = 1350
```

Appendix 4: ANOVA of the best fit linear mixed-effects model (sqrt(meandist) ~ ReleaseState*Season*Behaviour*method, random=~1|days, correlation=corAR1()) (Chapter 4)

	Num D.F	DEN D.F.	F-Value	p-value
Intercept	1	188	19.849	<0.0001
State	3	188	0.02	0.996
Season	1	188	1.322	0.252
Behaviour	2	188	206.705	<0.001
Distance metric	1	188	94.079	<0.001
State : Season	3	188	0.403	0.751
State : Behaviour	6	188	0.157	0.988
Season : Behaviour	2	188	2.038	0.133
State : Distance metric	3	188	0.19	0.903
Season : Distance metric	1	188	1.712	0.192
Behaviour : Distance metric	2	188	6.162	0.003
State : Season : Behaviour	6	188	0.107	0.996
State : Season : Distance metric	3	188	0.182	0.909
State : Behaviour : Distance metric	6	188	0.109	0.995
Season : Behaviour : Distance metric	2	188	0.219	0.803
State : Season : Behaviour : Distance metric	6	188	0.192	0.978

Appendix 5: Summary of the GAM log(RadialDistance + 1) ~ s(Days) + Behaviour + Season + TidalState (Chapter 4)

Parametric Coefficients	Estimate	Std. Error	T value	Pr (>|t|)
(Intercept)	3.318387	0.005069	654.54	<2e-16 ***
Behaviourreveng	-0.053756	0.004693	-11.45	<2e-16 ***
Behaviourtvm	0.062178	0.004693	13.25	<2e-16 ***
Seasonsummer	0.085295	0.003832	22.26	<2e-16 ***
TidalStateflood	0.120265	0.005419	-22.19	<2e-16 ***
TidalStatehw	-0.085168	0.005419	-15.72	<2e-16 ***
TidalStatelw	-0.071867	0.005419	-13.26	<2e-16 ***

Smooth Terms	Edf	Ref.df	F	p-value
S(Days)	8.95	8.999	11815	<2e-16 ***

Significance codes : 0 ‘***’ 0.001 ‘**’ 0.01 ‘*’ 0.05

Appendix 6: Summary of the GAM log(PathTravelled + 1) ~ s(Days) + Behaviour + Season + TidalState (Chapter 4)

Parametric Coefficients	Estimate	Std. Error	T value	Pr (>|t|)
(Intercept)	6.2108180	0.0029394	2112.935	<2e-16 ***
Behaviourreveng	-1.2002112	0.0027214	-441.03	<2e-16 ***
Behaviourtvm	-0.5749442	0.0027214	-221.269	<2e-16 ***
Seasonsummer	0.0585558	0.0022220	26.353	<2e-16 ***
TidalStateflood	0.187068	0.0031424	5.953	2.66e-09 ***
TidalStatehw	0.0040826	0.0031424	1.229	0.194
TidalStatelw	0.0005868	0.0031424	0.187	0.852

Smooth Terms	Edf	Ref.df	F	p-value
S(Days)	8.997	9	102768	<2e-16 ***

Significance codes : 0 ‘***’ 0.001 ‘**’ 0.01 ‘*’ 0.05